Negative growth regulatory role of *PTPN11*/SHP2 in breast epithelial tumorigenesis

A thesis

submitted in partial fulfillment of the requirements

of the degree of

Doctor of Philosophy

By

Madhumita Chakladar

Roll No. /ID: 20143312

INDIAN INSTITUTE OF SCIENCE EDUCATION AND RESEARCH

(IISER), PUNE

2020

Dedicated to my beloved uncle

Late Sri Susanta Chakladar

Certificate

Certified that the work incorporated in the thesis entitled "Negative growth regulatory role of *PTPN11*/SHP2 in breast epithelial tumorigenesis" submitted by Madhumita Chakladar was carried out by the candidate, under my supervision. The work presented here or any part of it has not been included in any other thesis submitted previously for the award of any degree or diploma from any other university or institution.

Date: 27-05-2020

(Supervisor)

Prof. L S Shashidhara

Declaration

I declare that this written submission represents my ideas in my own words and where others' ideas have been included, I have adequately cited and referenced the original sources. I also declare that I have adhered to all principles of academic honesty and integrity and have not misrepresented or fabricated or falsified any idea/data/fact/source in my submission. I understand that violation of the above will be cause for disciplinary action by the Institute and can also evoke penal action from the sources which have thus not been properly cited or from whom proper permission has not been taken when needed.

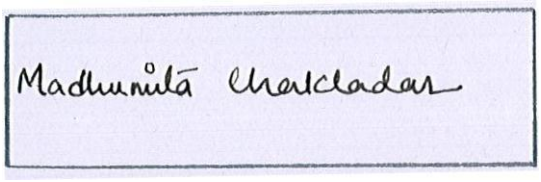

Date: 27-05-2020

Madhumita Chakladar

Roll No. 20143312

Acknowledgment

I would like to extend my sincere gratitude to my Ph.D. supervisor, Prof. L S Shashidhara for supporting my work. He has been constant guidance showing me a path in every up and down of my research career. It is said Ph.D. is like the character development in itself and Shashi has been a father-like figure who has shaped my ideas, scientific aptitude, scientific temperament, and most importantly gave me freedom and confidence for completing my work. Even though I was initially skeptical, I am thankful to Shashi for introducing me to data science and even more for making me enjoy doing bioinformatics as much as I enjoyed mammalian cell culture work. It is he who taught me it's ok to make mistakes and have made me learn to enjoy troubleshooting to find answers rather than see mistakes as more tasks. His guidance urged me to think and to have honesty towards my work. Every discussion with him has been insightful and has helped me find answers to most of the scientific problems I dealt with during my doctoral journey.

I would also like to thank my collaborators Prof. Stephen Cohen, UCPH, Denmark, and Dr. T S Sridhar, SJRI, Bangalore for guiding me through my bioinformatics work and clinical work. The cell culture work was partially done in SJRI, Bangalore and I would like to extend my regards to Dr. Jyothi S Prabhu and Dr. Madhumathy G Nair for providing me with lab space, reagents, and protocols. I am thankful to Dr. Devaki Kelkar, PCCM/IISER, Pune for analysing the TCGA and METABRIC data with me and Dr. Madhura Kulkarni, PCCM/IISER, Pune providing me with the premade 48 hours pQCXIH virus used in this study for YAP1 overexpression and also thank them both for helping me with writing the thesis.

This work has been shaped over the last four years under the guidance of my RAC members at IISER Pune. I am thankful to Dr. Mayurika Lahiri for her guidance and her generosity in providing me with the MCF10A cell line used in this study. I would also like to thank Dr. Kundan Sengupta and Dr. Siddhesh Kamat for directing my project on the right path during my RACs. I am happy to be a part of the IISER Pune scientific community and for being nurtured under the open lab facility and learning to share ideas and resources.

I would express my gratefulness to Prof. Sanjeev Galande and Dr. Nagaraj Balasubramaniun for accommodating me with cell culture resources and facilities whenever needed without a delay.

Most importantly I would like to extend my appreciation to the IISER Pune Biomanager, IISER Pune microscopy facility, IISER Pune Flow cytometry facility, IISER Pune Perkin Elmer facility, and IISER Pune Bio-Administration for their co-operation and support.

I would like to express my joy in sharing the lab space with the most cordial lab mates, colleagues, and friends at IISER Pune. I would also take this opportunity to extend my love and gratefulness to my parents, Mr. Prasanta Chakladar and Mrs. Swapna Chakladar, my sister Ms. Moumita Chakladar and my husband Mr. Rajdip Thakur for being supportive and encouraging towards my research career.

I would also extend my sincere gratitude to my little daughter, Ridhima for being part of the doctoral journey in a special way. This little wonder has been my biggest positive influence during completion of this beautiful journey and have shared my work load of early morning experiments and late-night thesis writing.

Table of Contents

Abstract

Drosophila model system has played a pivotal role in the identification of genes involved at all stages of tumorigenesis. An RNAi mediated screen of the *Drosophila* genome conducted in our laboratory identified putative negative regulators of growth in Epidermal Growth Factor Receptor (EGFR) and Yorkie (Yki) driven tumors. In this study, human orthologues of the RNAi mediated screen were subjected to detailed network analyses. Enrichment of the protein-protein interaction network among these putative growth regulators (in humans) identified major signaling pathways like the Hippo pathway and the mitogen-activated protein kinase (MAPK) signaling pathway to be involved in driving both EGFR and the Yes-associated protein 1 (YAP1) (a mammalian ortholog of Yki) mediated tumorigenesis. One of the identified negative growth regulators in the Yki screen but not a positive in the EGFR screen was corkscrew (Csw), a non-receptor protein tyrosine phosphatase. Tyrosine-protein phosphatase type 11 (*PTPN11*) encoding the Src Homology Phosphatase 2 (SHP2) protein is one of the closest human orthologs of Csw and it is reported to be a bonafide oncogene in EGFR driven neoplasia. However, our clinical metadata analysis showed *PTPN11*/SHP2 functions as a putative tumor suppressor in breast adenocarcinoma (BRCA). Our analysis of dataset availed by the Molecular Taxonomy of Breast cancer International Consortium (METABRIC), 2012 showed *PTPN11*/SHP2 copy number loss in Luminal A subtype of breast cancer patient correlated to poor 4 years disease-specific survival (DSS) and late-stage cancer at diagnosis. Furthermore, our analysis of The Cancer Genome Atlas (TCGA) BRCA level 4 protein data showed low expression levels of active phospho SHP2-Y542 associated with larger tumor size and more lymph node positivity in Luminal A subtype of patients at diagnosis.

We experimentally investigated the possible role of *PTPN11*/SHP2 as a tumor suppressor in breast cancer. Knockdown of *PTPN11*/SHP2 in MCF10A, a non-transformed breast epithelial cell line, showed increased migration and cell shape changes to mesenchymal morphology, although there was no change in the rate of cell proliferation. Besides, the treatment of *PTPN11*/SHP2 knockdown cells with epirubicin (chemotherapeutic drug) showed better survival and reduced apoptosis. However, we did not observe any change in the levels of Bcl associated X protein (BAX), a global pro-apoptotic molecule. *PTPN11*/SHP2 may interact with other apoptotic effectors, which needs to be further investigated.

In the context of YAP1 driven neoplasia, we analyzed the METABRIC dataset. Cohorts that had high levels of YAP1 and copy number loss of *PTPN11*/SHP2 correlated to grade 3 tumors at diagnosis and poor 4 years DSS. We examined this relationship in YAP1 overexpressing MCF10A cells. Knockdown of *PTPN11*/SHP2 in the background of over-expressed YAP1 did not change the proliferation rate, which was already at higher levels when wild type YAP1 alone was over-expressed. In summary, we conclude, the tumor suppressor role of *PTPN11*/SHP2 in breast tumorigenesis may use a pathway independent of YAP1.

Molecules like *PTPN11*/SHP2, YAP1, and P53 among many others which show dual specificity in tumorigenesis in the same tissue depending on the upstream signaling cues present challenges in the field of targeted drug therapy. This study puts forth the importance of understanding the contexts and behavior of such dual molecules depending on upstream signaling cues to allow effective cancer treatment.

Chapter 1: Introduction

Organism's growth is a concerted action of multiple signaling pathways that maintain the balance of cellular proliferation and death. Yorkie (Yki), the primary effector of the hippo signaling kinase cascade, Warts (Wts), Salvador (Sav), and Hippo (Hpo), is involved in upregulating proliferation and inhibiting cell death, plays an important role in organism's growth (Ciriello et al. 2015)(D. Pan 2010) (Figure 1.1). Deregulation of signaling pathways either because of hyperactivation of growth promoters like the Yki, Epidermal Growth Factor Receptor (EGFR), and Phosphatidylinositol 3 kinase (PI3K) protein kinase B (AKT) or downregulation of negative growth regulators like P53 and Hpo often leads to tumor formation and neoplastic transformations (Hanahan and Weinberg 2011; Moroishi, Hansen, and Guan 2015).

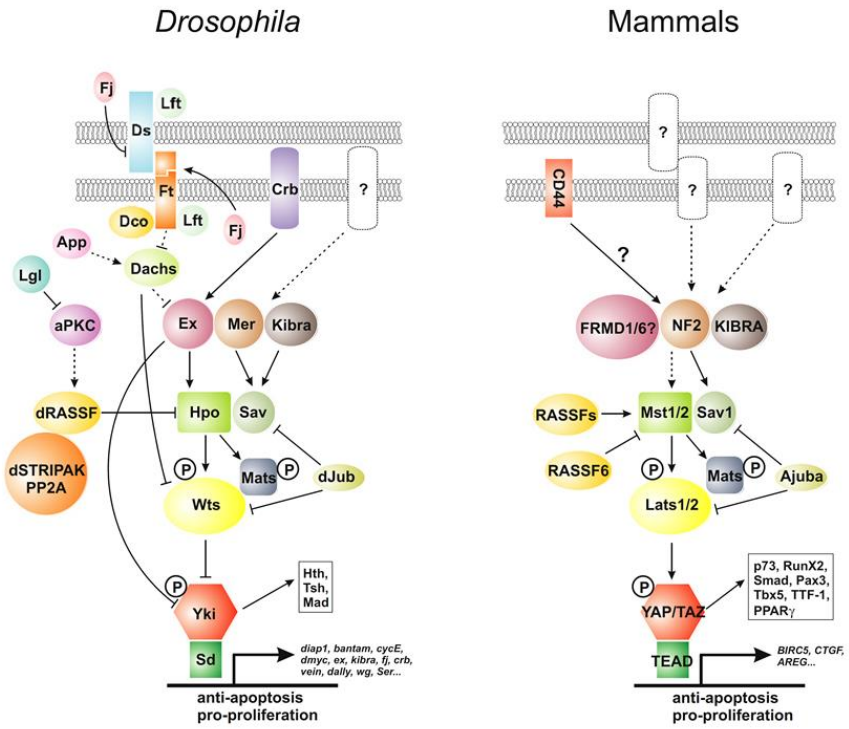

Figure 1.1: Schematic representation of the Yki/Yes Associated Protein 1 (YAP1) pathway in *Drosophila* and humans. Hippo pathway is conserved from flies to humans and plays important role in controlling growth and proliferation processes. Image reproduced from D. Pan 2010.

Tumor development and cancer progression is a multistep process constituting ten major hallmarks. A tumor typically goes through uninhibited growth due to sustained proliferative signaling, decreased cell death, an increase in angiogenesis to support the growing tumor mass, epithelial to mesenchymal transformations, and metastasis, the final stage wherein tumor cells invade into neighbouring lymph nodes and organs (Hanahan and Weinberg 2011). During this process, the cells lose their cellular identity, become clonally populated, show intra-tumor heterogeneity, and adjacent stromal cells further help in tumor dissemination and metastatic colonization (Lambert et al., 2017). Progressive accumulation of mutations in these tumor cells including mutations in DNA repair genes leads to further genomic instability and neoplastic tumor growth (McGranahan and Swanton 2017; Tubbs and Nussenzweig 2017). Comprehensive sequencing of tumor samples has identified a total of 140 driver mutations, of which a minimum of two to a maximum of eight driver mutations are reported to be involved in the neoplastic transformation of solid tumors (Vogelstein et al. 2013).

Using a fly model system, co-operativity of growth regulatory pathways involving a minimum of two driver mutations allowed further understanding of the process of tumorigenesis and metastasis *in-vivo* (Miles, Dyson, and Walker 2011; Washburn and Washburn 2013). Oncogenic mutation of Ras^{v12} and loss of function of Scribbled, a known tumor suppressor, causes metastatic lesions in the eye antennal disc of *Drosophila* through paracrine Janus kinase (JNK) signaling (Wu, Pastor-Pareja, and Xu 2010). Furthermore, cooperative interaction has been reported between the Suppressor of cytokine signaling 36E (Socs36E) and EGFR to promote EGFR driven tumorigenesis through Bantam miRNA in the wing imaginal disc of *Drosophila* larvae (Herranz et al. 2012). A follow-up study to understand co-operativity in EGFR driven neoplasia, identified Perlecan expression in EGFR overexpressing epithelial cells and promotes the expansion of mesenchymal cells by upregulating Wnt signaling in epithelial cells and Bone Morphogenetic Proteins (BMP) signaling pathway in mesenchymal cells (Herranz, Weng, and Cohen 2014). Moreover, an RNAi mediated screen of the *Drosophila* genome conducted in our laboratory identified context-specific negative growth regulators in EGFR driven and Yki driven neoplasia (Groth et al. 2019). Phenotypic observation showed, oncogenic overexpression of Yki or EGFR gave a small overgrowth of the wing disc while RNAi mediated knockdown of genes in Yki/EGFR overexpressing discs that gave larger overgrowth of the wing disc, a giant larval phenotype, inhibited pupariation of the larvae and in some cases lead to metastatic lesions across the body of

larvae at least across two biological replicates were recorded as putative negative regulators of growth (referred to as positive candidates). The screen identified 74 and 905 fly genes whose depletion drives the neoplastic transformation of EGFR and Yki overexpressing wing imaginal discs of *Drosophila*. An independent screen in this study also identified 32 fly genes whose suppression limits EGFR overexpressing tumor growth in the SOCs RNAi background. This study includes the identification of orthologs of all positives from three independent RNAi mediated screen of the *Drosophila* genome and enlists the major pathways involved in EGFR and Yki/YAP1 driven neoplasia. The specificity of the screen and our analysis is reflected from the identification of tumor suppressors like p53 and Hpo and known growth regulatory pathways like Mitogen-Activated Protein Kinase (MAPK) and PI3K-AKT that co-operate in EGFR and Yki driven cancer.

Interestingly, many of our identified candidates from the screen are already classified as oncogenes by the cosmic cancer gene census. We tried to identify these molecules that might have a dual role in tumorigenesis, functioning both as an oncogene and as a tumor suppressor depending on the upstream cues/signaling context. One such molecule we selected for our study was corkscrew (Csw) a non-receptor protein tyrosine phosphatase that was identified from the genome-wide RNAi screen to function as a negative growth regulator exclusively in Yki driven cancer. We examined the tumor suppressor role (if any) of Csw ortholog, Tyrosine-protein phosphatase non-receptor type 11 (*PTPN11*), also known as, Src homology phosphatase (SHP2) from literature mining, clinical metadata analysis, and validated our hypothesis using cell culture techniques.

Csw and its ortholog, *PTPN11*/SHP2 consists of two N-terminal SH2 domain (N-SH2 and C-SH2), a classic phosphatase domain split by cysteine and serine-rich inserts, a C terminal tail with Y-542 required for its activation, and a proline-rich motif in the C terminal end to bind to SH3 domain-containing protein (Neel, Gu, and Pao 2003) (Figure 1.2). Csw has two human orthologs, *PTPN6* and *PTPN11* (https://www.flyrnai.org/cgi-bin/DRSC_orthologs.pl). *PTPN11*/SHP2 primarily helps in sustained growth factor signaling and promotes cellular proliferation and migration (Neel, Gu, and Pao 2003) (Figure 1.3).

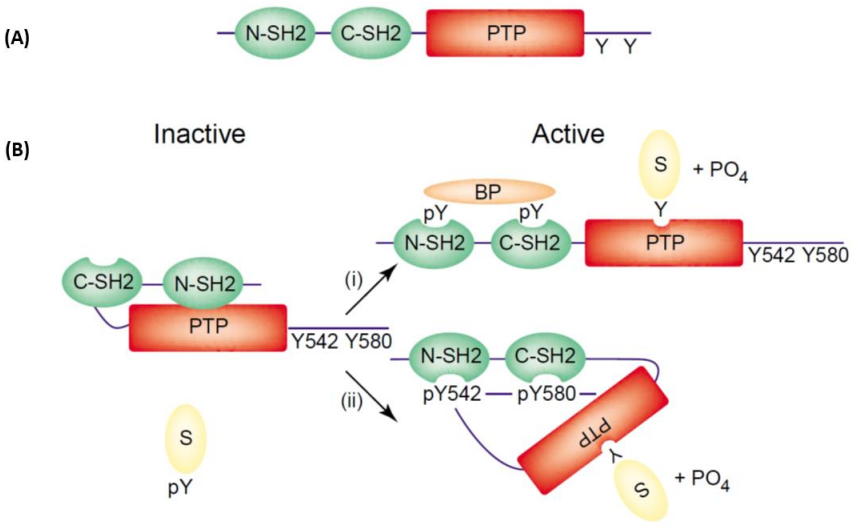

Figure 1.2: (A) shows *PTPN11*/SHP2 in open conformation with N terminal N-SH2 and C-SH2 domains, a classic phosphatase domain, and a c terminal tail with tyrosine residues. (B) shows activation of the closed-loop conformation of *PTPN11*/SHP2 by binding protein (BP) or auto-activation by phosphorylated tyrosine in C terminal tail. Image reproduced from Neel, Gu, and Pao 2003.

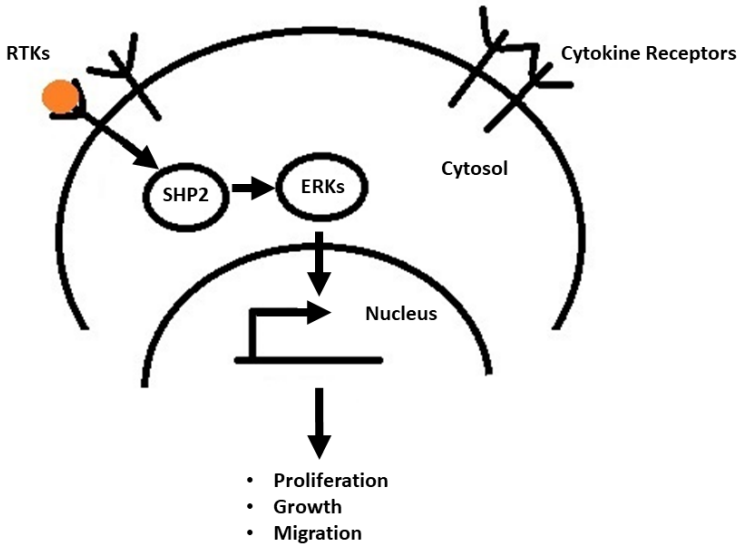

Figure 1.3: Schematic showing *PTPN11*/SHP2 participates in downstream signaling of receptor tyrosine kinases (RTKs) and cytokine receptors and activates the MAPK pathway to control

proliferation, growth, and migration. Image adapted from (Aceto et al. 2012; Neel, Gu, and Pao 2003).

PTPN11/SHP2 is the first identified phosphatase to have an oncogenic function and plays a crucial role in positive feedback signaling of the EGFR pathway (Aceto et al. 2012). The dual-specificity of a molecule in tumorigenesis is not a new concept in the field of cancer research. Previous studies have reported molecules to have a dual role in tumorigenesis. The two variants of the P53 molecule, TP53 variant with the transactivation domain functions as a tumor suppressor and activate cell cycle arrest genes, apoptosis, and maintains genomic stability while the ΔNP53 (without the N terminal transactivation domain) variant has oncogenic functions and helps in cellular survival and self-renewal of stem/progenitor cells (Candi et al. 2014). Similar to P53, its paralogs P63 and P73 also show dual behaviour where ΔNP63 and ΔNP73 variant overexpression induces tumorigenicity in the liver and skin respectively (Costanzo et al. 2014a). In addition to P53, YAP1, a known oncogene in solid tumors is also reported to have a tumor suppressor role. Nuclear YAP1 binds and stabilizes TP73 and induce apoptosis by the Ras association domain family 1 isoform A (RASSF1A) (Strano and Blandino 2007). YAP1 is also known to be phosphorylated by cellular homolog of Abelson murine Leukaemia (ABL) Kinase (c-Abl) at tyrosine 357 upon DNA damage and stabilize P73 thereby preventing its degradation by ITCH (a ubiquitin ligase) (Keshet et al. 2014). *PTPN11*/SHP2, the molecule of our interest in this study, is also reported to function as an oncogene potentially by activation of Ras/MAPK pathway in breast cancer (Patel et al. 2016), colorectal cancer (Prahallad et al. 2015), lung cancer (Schneeberger et al. 2015), glioblastoma (Feng et al. 2012), prostate cancer (K. Zhang et al. 2016), and hematologic malignancies (Richine et al. 2016). Contrarily, *PTPN11*/SHP2 has also been reported to have a tissue-specific role and to function as a tumor suppressor in Hepatocellular Carcinoma (HCC) and Esophageal Squamous Cell Carcinoma (ESCC) (Bard-Chapeau et al. 2011; Qi et al. 2017). *PTPN11*/SHP2 is also reported to mediate Retinoblastoma(Rb)/ Elongation factor 2 (E2F) associated apoptotic response (Morales et al. 2014)

In our study, we tried to investigate the dual role of *PTPN11*/SHP2 in a specified tissue and examined the context of its dual role, if any, in solid tumors, with a major focus on breast epithelial cancer. Breast cancer affects nearly 2.1 million women each year and accounts for nearly 15% of deaths among women (WHO,2020, http://www.who.int). Breast cancer is highly heterogeneous and is clinically classified as Hormone receptor-positive, Human Epidermal growth factor

Receptor 2 (HER2) positive, and Triple Negative Breast Cancer (TNBC) each with a specific outcome and therapeutic targets (Perou et al. 2000). We looked into breast cancer clinical cohorts availed by The Cancer Genome Atlas (TCGA) and the Molecular Taxonomy of Breast Cancer International Consortium (METABRIC) and also looked into solid tumors like lung adenocarcinoma, ovarian cancer, prostate cancer, and colorectal cancer availed by TCGA. Phosphoprotein data for *PTPN11*/SHP2 was availed only for breast cancer by TCGA. Hence, we limited our study to breast cancer, validated our retrospective analysis across to datasets, and correlated clinical parameters to copy number status in METABRIC data and both copy number status and phosphoprotein expression of *PTPN11*/SHP2 in TCGA to identify *PTPN11*/SHP2's role in breast tumorigenesis. Furthermore, *PTPN11*/SHP2 ortholog was reported to function as a tumor suppressor in the Yki screen but not in the EGFR screen in our laboratory. This is intuitive as *PTPN11*/SHP2 is a positive regulator of EGFR signaling. This was indeed interesting as the tumor suppressor role of *PTPN11*/SHP2 in YAP1 driven breast cancer is still nascent and was investigated in our study.

Chapter 2: Biological Interactome Study

2.1: Introduction

Tumorigenesis is a multistep process that enables cells to gain a proliferative advantage, avert death or immune response, evolve, and invade into the adjacent organs, a process referred to as metastasis (Hanahan and Weinberg 2011). With the advent of data science, large scale genomics/transcriptomics/proteomics data from several patients or cancer cells could be compared and subjected to multifactorial analyses. The advantage of developing such interactome is, one could identify multiple causative factors, all of which together orchestrate tumorigenesis. Genetic approaches and sequencing efforts on genome landscapes have identified major driver mutations affecting one or more signaling pathways driving cancer (Vogelstein et al. 2013). Insights into these signaling networks have further progressed our understanding of previously unidentified "silent players" in cancer which neither shows high mutational frequency nor shows differential expression profiles; however plays an essential role in the biological interactome affecting major cancer-related pathways (Ruffalo, Koyutürk, and Sharan 2015).

Protein-Protein interaction network (PPIN) studies in yeast have largely helped in the understanding of structural and functional modules of genes and reflect their essentiality (Kim et al. 2012; Lu et al. 2010). Although highly controversial, the role of hub genes in large interactome has shown to follow the centrality lethality rule wherein a higher degree of interaction tends to make these genes essential for the organism and lethal if these are deleted (Jeong et al. 2001; Khuri and Wuchty 2015). Hubs genes identified in yeast mostly tend to either exist as structural complexes or participate in overlapping functional processes (He and Zhang 2006; Lu et al. 2010; Ning et al. 2010). Non-clustered-non-co expressed genes in hubs form connecting and organizing modules and deletion mutation of these genes are not lethal, unlike the clustered-co-expressed hub genes that are necessary to form protein complexes important for biological processes (Pang, Sheng, and Ma 2010).

A genome-wide RNAi mediated screen using a wing imaginal disc of *Drosophila* as a model was conducted in our laboratory to study epithelial tumorigenesis. This study identified hundreds of negative regulators whose suppression co-operates to enhance Yki driven neoplasia and less than a hundred negative regulators to be involved in EGFR driven neoplasia. We also report from an independent screen, potential candidate genes that suppress EGFR driven neoplasia. The larger number of positives identified in the Yki screen could reflect a higher sensitivity of Yki and its interacting partners or low specificity of the screen resulting in a larger number of false positives (Groth et al. 2019; Vissers et al. 2016). Understanding these negative and positive regulators in a functional network module would allow us a detailed understanding of the pathways involved in EGFR and Yki driven neoplasia. The screen identified a vast repertoire of potential context-specific negative growth regulators that co-operate exclusively with Yki or EGFR in cancer progression. This screen identified previously known targets and a myriad of new context-specific tumor suppressors that could have potential prognostic value in human cancer research. This study involves identifying the essential genes responsible for Yki and EGFR driven neoplasia and identify their closest human orthologs that play a significant role in major growth regulatory pathways. These orthologs could have diverged considerably in sequence homology however functionally possibly remain part of similar protein complexes and participate in similar pathways. Such evolutionary conserved pathways are important and need to be identified to help our understanding of cancer which is highly evolving and heterogeneous.

2.2: Experimental approach

2.2:1: Identification of human orthologs of RNAi mediated *Drosophila* screen

Vienna Drosophila Resource Center (VDRC), https://stockcenter.vdrc.at/control/main, which provides the KK RNAi used for the RNAi screen of *Drosophila* genome in our laboratory, is predicted to have many non-specific targets. VDRC site provides information on whether an RNAi used had any non-specific target or only a specific target. To rule out any spurious results, we sorted only KK RNAi with one specific target for all our analyses of human orthologs. Prediction of human orthologs of selected candidates was performed using the *Drosophila* RNAi Screening Center (DRSC) integrative ortholog prediction tool (DIOPT). DIOPT is a human ortholog prediction tool. Orthology predictions were based on the integration of all twelve

prediction tools including phylogeny-based orthology prediction tools, orthology prediction from genome-wide sequence-based prediction tools, and protein-protein interaction network-based prediction tool and each tool assigning a score of 1 to *Drosophila* orthologs in humans; A scale of 2-11 score was used for selecting all orthologs of the candidate genes in our analysis.

2.2.2: Network Analysis

Search Tool for the Retrieval of Interacting Genes/Proteins (STRING 10) is a PPIN database that integrates knowledge obtained from other PPIN databases such as Molecular INTeraction (MINT), Human Protein Reference Database (HPRD), Biological General Repository for Interaction Database (BioGRID), Database of Interacting proteins (DIP) and Reactome, etc (https://string-db.org/). STRING 10, the most updated version since 2000, allows prediction of protein-protein interactions in a query organism by transferring the interaction observed in one organism to the query organism; STRING 10 build a network from information available not only in primary databases to which it is integrated but also from curated databases with experimental evidence for a protein pair interaction and from text mining evidence from full-text articles using an algorithm that uses part of speech tagging, chunking grammar, and co-occurrence of name of protein pairs within paragraphs and sentences (von Mering et al. 2003, 2005). STRING 10 also uses the information of co-occurrence, co-expression, gene neighbourhood, gene fusion, and does sequence similarity search to predict functional interaction between proteins (Szklarczyk et al. 2015). Each predicted interaction is benchmarked to the Kyoto Encyclopedia of Genes and Genomes (KEGG) database; interacting proteins in the same KEGG map are accounted as positives, if not, they are accounted as false positives (von Mering et al. 2003). Each protein in the network appears as a node and interaction between proteins forms the edges of the network (Szklarczyk et al. 2017). All string 10 maps were built with a high confidence strength (0.7) supported by evidence from co-expression, experimental evidence, and evidence from co-occurrence, gene neighbourhood, gene fusion, curated database, pre-computed orthology predictions and text mining evidence, and Markov Clustering (MCL) clustering coefficient of 0.2 was used for robust clustering of the interactome (Brohée and van Helden 2006).

2.2.3: Pathway enrichment analysis:

STRING 10 allows the user to understand statistically enriched biological functions in a network. We used String 10 to identify the Gene Ontology (GO) molecular processes and KEGG pathways

enriched for the positives on the screen. Significantly enriched groups were given as <0.05 false discovery rate (FDR) values.

2.3: Results

2.3.1: Identification of Human orthologs

Previous work in our laboratory screened 9032 and 9137 RNAi lines to identify negative growth regulators whose suppression co-operates in Yki and EGFR driven neoplasia. 9335 RNAi lines were screened independently in our laboratory to identify positive regulators of growth co-operating in UAS-EGFR+ SOCS36E RNAi tumors. The summary of the identified candidates is provided in Table 1. Details of the list of the candidates are available in the Appendix (Table 2.3.1). We identified 1514 and 129 human orthologs of the 904 and 73 confirmed positives in Yki and EGFR screen respectively from our analysis using DIOPT. We predicted many of these candidates to play a putative tumor suppressor role in the context of YAP1 and EGFR driven human epithelial cancer. We observed less than 1% overlap in the identified tumor suppressor between Yki and EGFR screen candidates with most of the identified positives being context-specific and co-operating specifically in YAP1 or EGFR driven neoplasia. In the SOCs screen, we identified 66 putative genes that co-operate to promote EGFR driven neoplasia.

	UAS-Yki	**UAS-EGFR**	**UAS-EGFR+ SOCS36E RNAi**
Confirmed Positives	904	73	32
Confirmed positives with human orthologs	611	46	31
No of Human orthologs	1514	129	66
Overlap	20		
Overlap with orthologs	11		

Table 1: Summary of analysis of genome-wide RNAi mediated screen of *Drosophila* genome to identify positive and negative regulators of growth co-operating with EGFR and Yki. The screen

was conducted in the wing imaginal disc of *Drosophila* larvae (Larval stage 3/L3), as an epithelial model system to study co-operativity in tumorigenesis and identification of context-specific putative tumor suppressors. The table is adapted from Groth et al., 2019.

2.3:2: String interactome of growth regulators identified in flies

We analysed a stringv10 map of identified positives in flies as shown in figure 2.3.2. We observed 904 positives in the Yki screen and were part of biological interactome with Protein-Protein Interaction (PPI) enrichment of 1.14E-06. KEGG enrichment analysis to identify the pathways involved in Yki driven neoplasia for all 904 positives did not enrich for any significant biological pathway (Figure 2.3.2.A). However, KEGG analysis of only the 228 positives that constituted the large hub among other Yki positives with PPI enrichment of <1.0E-16 showed enrichment of hippo signaling, autophagy, apoptosis, metabolism, and ubiquitin (Ub) mediated proteolysis as major pathways that could be co-operating in Yki driven neoplasia (Figure 2.3.2.B). Details of GO and KEGG enrichment pathways of Yki positives are provided in Appendix Table 2.3.2.1 and Table 2.3.2.4. Analysis of the string v10 map of 73 positives of the EGFR screen does not show any major large hub but small clusters of genes with PPI enrichment of 0.000482. The positives identified in the EGFR screen were enriched in hippo signaling and autophagy processes (Figure 2.3.2.C). Details of GO and KEGG enrichment pathways of EGFR positives are provided in Appendix Table 2.3.2.2 and Table 2.3.2.5. Hippo pathway and autophagy were overlapping pathways that we report to co-operate with both EGFR and Yki driven neoplasia. Moreover, the 32 positives identified in the UAS-EGFR+SOCS RNAi screen show small clusters with PPI enrichment of 0.0122, and KEGG analysis show enrichment of pathways involved in RNA and protein turnover and mammalian target of rapamycin (mTOR) signaling (Figure 2.3.2D). One of the candidate genes *csw*, positive only in the Yki screen was located in the center of the hub, Figure 2.3.2.B, the relevance of which we would be discussing in the later chapters. Details of GO and KEGG enrichment pathways of SOCs positives are provided in Appendix Table 2.3.2.3 and Table 2.3.2.6.

(A) (B)

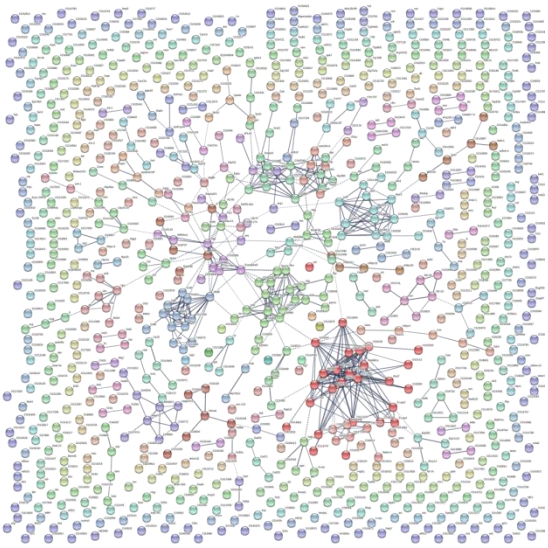

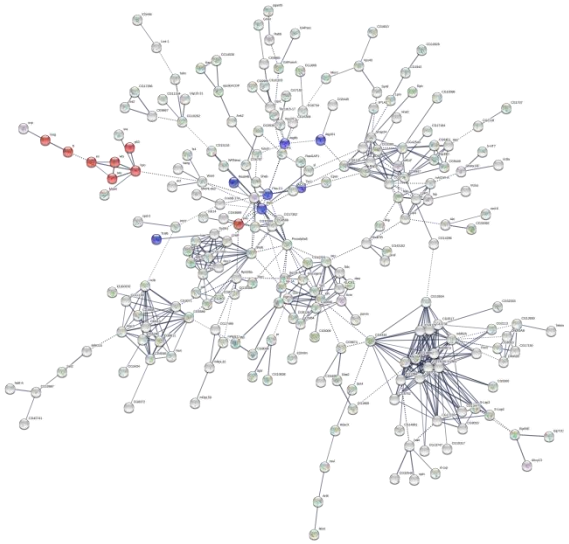

(C) (D)

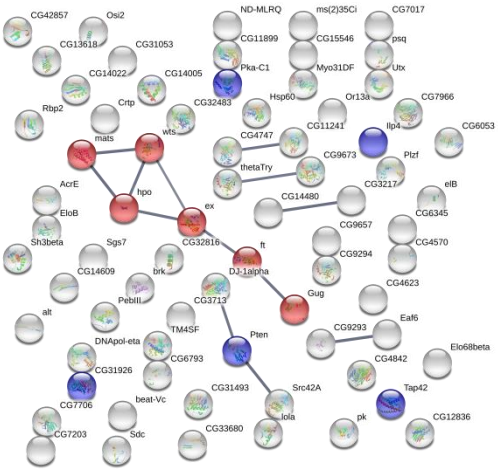

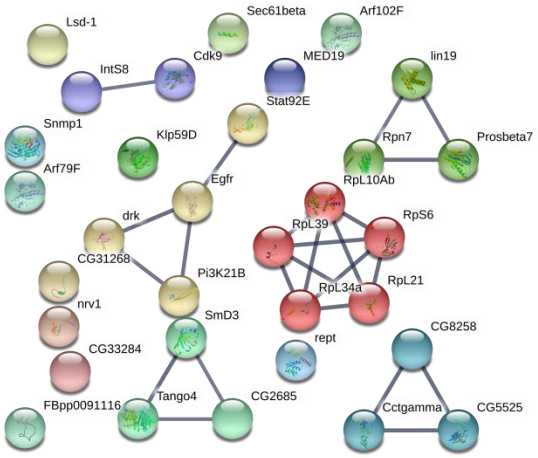

Figure 2.3.2: (A) shows the analysis of the stringv10 map of all 904 positives of the Yki screen. (B) 228 of the 904 positives in the Yki screen formed a single large hub enriched in KEGG pathways including hippo signaling (red nodes) and autophagy (blue nodes). (C) Analysis of 73 positives of the EGFR screen forms many small clusters and are enriched in KEGG pathways like

hippo signaling (red nodes) and autophagy (blue nodes). (D) Stringv10 analysis of all 32 positives identified in the UAS-EGFR+SOCS RNAi screen also shows small clusters and no major large hub, details of pathway analysis reported in the appendix table.

2.3:3: String interactome of human orthologs of the growth regulators identified in flies

Stringv10 analysis of corresponding human orthologs identified using DIOPT of all candidate *Drosophila* genes from the three independent screens is shown in figure 2.3.3.1514 human orthologs of the candidates identified in the Yki screen formed a large biological interactome with PPI enrichment of 1.0E-16. KEGG enrichment analysis identified the pathways involved in YAP1 driven neoplasia for all 1514 positives which included MAPK signaling, autophagy, Hippo signaling, metabolic pathways, and PI3K-AKT among many others (Figure 2.3.3A). However, KEGG analysis of only the 731 hub genes among other YAP1 positives with PPI enrichment of <1.0E-16 showed enrichment of MAPK signaling, autophagy, Hippo signaling, metabolic pathways, PI3K-AKT, and genes of the cell cycle to co-operate in YAP1 driven neoplasia (Figure 2.3.3B). Details of GO and KEGG enrichment pathways of YAP1 positives are provided in Appendix Table 2.3.3.1, Table 2.3.3.2, Table 2.3.3.5, Table 2.3.3.6. String v10 analysis of 129 positives of the EGFR screen did not show us any major large hubs but two small hubs of genes with PPI enrichment of <1.0E-16. The human orthologs of positives identified in the EGFR screen were also enriched for hippo signaling, MAPK signaling, and metabolism among other major pathways (Figure 2.3.3). Details of GO and KEGG enrichment pathways of EGFR positives are provided in Appendix Table 2.3.3.3 and Table 2.3.3.7. We report from our string analysis and GO/KEGG enrichment study, Hippo pathway and MAPK pathway are the major overlapping pathways that co-operate with both EGFR and YAP1 driven neoplasia in humans. 66 positives we identified in the UAS-EGFR+SOCS RNAi screen showed one large hub and several small clusters with PPI enrichment of <1.0E-16. KEGG analysis of these 66 confirmed orthologs shows enrichment of pathways involved in RNA and protein turnover and mTOR signaling (Figure 2.1D). Csw ortholog *PTPN11*/SHP2 like in the fly hub was located in the center of the human biological hub, interacted with cell cycle-related genes, and the MAPK signaling components, the relevance of which will discuss in later chapters. Details of GO and KEGG enrichment pathways of the UAS-EGFR+SOCS RNAi screen are provided in Appendix Table 2.3.3.4 and Table 2.3.3.8.

(A) (B)

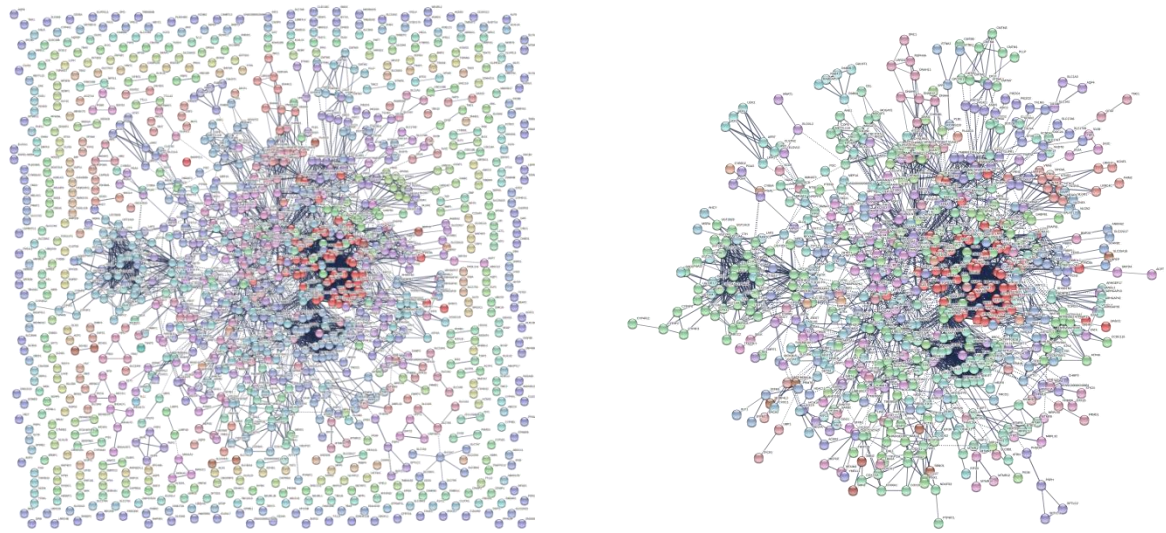

(C) (D)

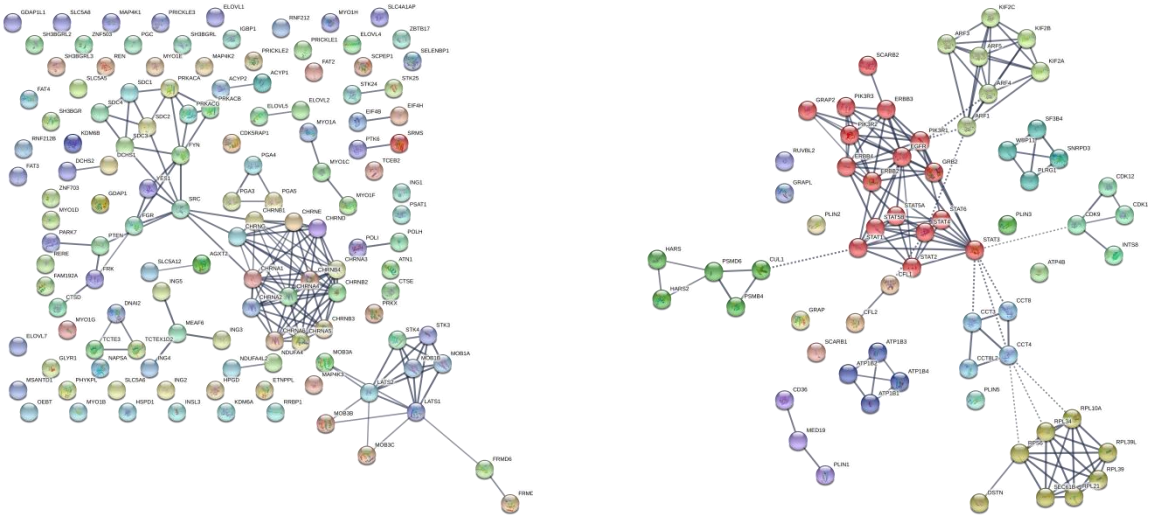

Figure 2.3.3: Stringv10 analysis of all 1514 human orthologs of positives of Yki screen. KEGG analysis shows enrichment of metabolic pathways, genes involved in proteoglycans in cancer (not shown in the figure). Details of all pathways are available in Appendix Table 2.3.3.1, Table 2.3.3.2, Table 2.3.3.5, Table 2.3.3.6. (A) shows 731 of 1514 genes were observed to form a single large hub and enriched in KEGG pathways like Hippo signaling, mTOR signaling, several metabolic pathways, PI3k-AKT, MAPK, Ras signaling pathways. (B) shows the hub separately.

(C) shows 129 human orthologs of positives of the EGFR screen were observed to form two small hubs and were also enriched in KEGG pathways like hippo signaling, MAPK, and Hedgehog signaling and autophagy. (D) shows Stringv10 map of all 66 positives identified in the UAS-EGFR+SOCS RNAi screen shows small clusters and one major large hub enriched in JAK-STAT, ERbB signaling pathways among others.

2.4: Discussion

The screen identified 904 and 73 candidate genes to co-operate with Yki and EGFR driven tumorigenesis respectively. Our analysis suggested 570 candidates out of 904 positives identified in the Yki screen had one or more human orthologs mapping to a total of 611 human genes. 46 of the 73 EGFR positives could be mapped to 50 human genes. While 32 of the SOCs positive candidates could be mapped to 31 human genes.

We report the positives identified in the Yki screen formed a distinct large hub from our network analysis using Stringv10 as observed among the fly genes and their corresponding human orthologs. We do not have similar findings among positives identified in EGFR driven neoplasia. We also found many of the hub genes in the Yki screen were conserved in the hub of the human growth network. These included p53, Shaggy (sgg), PRKC group of genes, *csw*, MAPKs, wnts, and many protein turnovers related genes. Interestingly, we also identified many lipid metabolic genes to be conserved in the biological hub in Yki driven cancer. Most of these evolutionarily conserved genes were also among the largest interactors in the hub. Human orthologs among these essential genes based on the largest number of interactors in Yki driven tumorigenesis had 71 or fewer interactors.

The large interactome co-operating in Yki driven cancer in our analysis suggests, hippo signaling functions as a single most contributing factor controlling many growth-related pathways such as cell cycle, DNA damage, metabolism, death, and proliferation. Our observation confirms the previously reported role of Yki/YAP in biological processes including proliferation, death, metabolism, and DNA damage (Moroishi, Hansen, and Guan 2015). Hippo pathway has been previously reported to interact with EGFR (Herranz et al. 2012), we also report a similar finding and identify the hippo pathway to be sufficient to drive EGFR driven tumors. Furthermore, our findings suggest, the fat/hippo pathway and autophagy process play a relevant role in both Yki and EGFR driven cancers and these pathways are highly conserved in humans. We identify

exclusively, protein turnover to be among other important processes that regulate growth in Yki driven tumorigenesis but not in EGFR driven tumorigenesis. We also report autophagy and hippo pathway to be conserved and important from Yki driven tumors. This study is in coherence with the already reported literature on the role of YAP1 in growth control via Ub related pathways and autophagy related pathways. YAP1 has been reported to control proliferation via autophagy (Pavel et al. 2018), and while Ub protein, ITCH is reported to promote lats degradation and YAP1 activity (Salah and Aqeilan 2011). In summary, a larger interactome observed in Yki driven cancer and with the hippo pathway being a major contributor of EGFR driven tumorigenesis puts the Hippo pathway as a rate-limiting biological pathway that modulates the balance between homeostatic growth and cancer.

Although, Yki and EGFR further seem to merge and employ in the course of evolution similar signaling pathways including MAPK, estrogen, wnt, hedgehog signaling pathways, proteoglycans in cancer to control biological processes like cell cycle and cell death in initiating tumorigenesis. Contrarily, estrogen signaling, MAPK signaling, autophagy, proteoglycans in cancer seems to function as a double-edged sword. These pathways seem to function in a context-specific manner and might be cue driven as we observe suppression of candidates of these pathways co-operate with EGFR driven neoplasia and alternatively helps in the suppression of EGFR overexpressing and SOCs suppressed tumors.

Understanding the molecular cues in the perspective of cancer becomes more challenging with the vulnerability of dual roles of signaling pathways. One of the prominent candidates from the Yki screen, Csw, a non-receptor protein tyrosine phosphatase was interesting in the perspective of molecular duality and role in tumorigenesis. Csw human ortholog *PTPN11*/SHP2 was a prominent oncogene in solid tumors and hematologic malignancies (Sondka et al. 2018). In the human interactome map, *PTPN11*/SHP2 appears to be part of the main hub connecting multiple pathways. Interestingly, it was negative in EGFR and EGFR+SOCs RNAi screen but positive in the Yki screen. Although *PTPN11*/SHP2 participates in positive feedback signaling of the EGFR pathway (Patel et al. 2016), it might not be essential to this pathway. Indeed, its suppression does not rescue EGFR+SOCs RNAi driven tumors. This puts forth the question of whether *PTPN11*/SHP2 is a context-specific molecule and would be interesting to speculate its tumor suppressor role in YAP1 driven epithelial cancers, which is studied in more detail and reported in the subsequent chapters.

Chapter 3: Clinical Relevance of Csw ortholog *PTPN11*/SHP2 in Breast cancer

3.1: Introduction

Breast cancer is the most heterogeneous among solid tumors (Polyak 2011). Molecularly it is categorized into hormone receptor-positive subtype (ER/PR), i.e. Estrogen receptor (ER) and Progesterone receptor (PR) positive, Human Epidermal growth factor Receptor 2 (HER2) driven subtype, and Triple Negative Breast Cancer (TNBC) subtype lacking the ER, PR, and HER2 oncogenic receptors, each of which has different expression pattern of genes (Perou et al. 2000). A minimum of 50 genes set from 1906 "intrinsic" genes analysed by hierarchical clustering further classify breast cancer into Luminal A (ER/PR+, Ki67 low), Luminal B (ER/PR+, Ki67 high), HER2+, and Basal subgroup, referred to as the Predictive analysis of microarray (PAM 50) subset and is often used to evaluate the risk of disease and prognosis (Bernard et al. 2009).

With the advent of molecular techniques, a combined analysis of copy number changes and gene expression patterns of 2000 primary breast tumor specimens with long term follow up of patients (the METABRIC dataset) further helped identify novel subgroups (Curtis et al. 2012). Furthermore, integration of several platforms ranging from whole-genome sequencing, miRNAs sequencing, RNA sequencing, copy number arrays, and reverse-phase protein arrays (RPPA) in the TCGA dataset has helped in better understanding of the molecular complexity of breast cancer in the recent past (Ciriello et al. 2015). Whole-genome sequencing of 560 breast cancer patients identified driver mutational signatures and categorized 93 mutated cancer genes (Nik-Zainal et al. 2016). Quantification of phosphoprotein and protein expressions of 171 cancer genes across 403 breast tumor samples stratified breast cancer into seven subgroups of which overexpression of EGFR and HER2 correlates well with their corresponding phosphorylated tyrosine residues in these RPPA defined HER2 enriched subgroup (Ciriello et al. 2015). This study aimed to identify additional therapeutically important subsets of breast cancer. We performed a retrospective analysis of clinical metadata to find how driver genes like *csw* ortholog *PTPN11*/SHP2 associate with the prognostic status of breast cancer patients and whether *PTPN11*/SHP2 plays a dual role in the genesis of the disease.

PTPN11/SHP2 the human ortholog of Csw is a bonafide oncogene as categorized by the cosmic cancer gene census (Sondka et al. 2018). *PTPN11*/SHP2 knockdown reduces the invasiveness of HER2 overexpressing MCF10A cells while its expression allows activation of v-myc and zeb1 to induce invasive behaviour of HER2 overexpressing MCF10A cells (Aceto et al. 2012). *PTPN11*/SHP2 has been reported to be an independent predictor of poor overall survival of Luminal A and Luminal B/HER2 subtypes as observed in 1401 breast cancer specimens, 46% of which showed a positive correlation of *PTPN11*/SHP2 expression to the aggressive clinical parameters (Muenst et al. 2013). *PTPN11*/SHP2 is also reported to promote BASAL like tumorigenesis possibly by regulating expression and signaling of RTKs like EGFR, Fibroblast Growth Factor Receptor (FGFR), and c-Met in the basal-like and triple-negative breast cancer (BTBC) cell line (Matalkah et al. 2016). We also wanted to study the ambiguous role of *PTPN11*/SHP2 in breast cancer subtypes, validate our findings of the Yki screen, and evaluate the negative growth regulatory role of Csw ortholog *PTPN11*/SHP2 in breast cancer. We examined clinical metadata including METABRIC 2012 and TCGA 2015 and analysed the correlation of *PTPN11* copy number aberration and SHP2 phosphoprotein expression to clinical parameters to understand its clinical relevance and find its dual role, if any, in breast cancer.

3.2: Methods

For all analyses, data from METBRIC 2012 and TCGA 2015 was used. METABRIC data was downloaded from cbioportal (Cerami et al. 2012) and TCGA GRCh38 data from the Genomic Data Commons (GDC) data portal using the GDC R tool (Morgan M, Davis S (2019).

GenomicDataCommons:NIH/NCIGenomicDataCommonsAccess.
(https://bioconductor.org/packages/GenomicDataCommons,
http://github.com/Bioconductor/GenomicDataCommons.).

The TCGA RPPA level 4 data was downloaded from FireBrowse (firebrowse.org). The clinical metadata analysis was performed using R (version 3.6.1, platform x86_64-w64-mingw32/x64). Packages used for analysis include survminer_0.4.6, ggpubr_0.2.3, magrittr_1.5, survival_2.44-1.1, forcats_0.4.0, stringr_1.4.0, purrr_0.3.3 8, readr_1.3.1, tidyr_1.0.0, tibble_2.1.3, ggplot2_3.2.1, tidyverse_1.2.1, dplyr_0.8.3. For TCGA RPPA data analysis additional packages Hmisc_4.2-0, Formula_1.2-3, lattice_0.20-38 were used. Kruskal-Wallis, Wilcoxon, and log-rank test were used for statistical analysis, $p<0.05$ was considered significant.

3.3: Results

3.3.1A: Correlation of *PTPN11*/SHP2 copy number changes and clinical parameters of METABRIC 2012 breast cancer patient cohort

3.3.1A.1: Correlation of *PTPN11*/SHP2 copy number changes and clinical parameter of patients at diagnosis:

We examined the statistical association of *PTPN11*/SHP2 copy number loss to clinical parameters in breast cancer to understand its oncogenic or tumor suppressor nature by loss of function genetics. All analyses include associations of *PTPN11*/SHP2 GISTIC scores to clinical parameters like age, stage, lymph node status, the grade of the tumor, and tumor size availed from the METABRIC data set (Tables S3.3.1A.1). There was only one instance of homozygous deletion and 3 instances of homozygous duplication (GISTIC -2 and +2 respectively) which were therefore not analysed separately from the heterogeneous changes (GISTIC score of -1 and +1 respectively). There were a few cases with claudin low status without any PAM50 classification and hence were excluded from the analysis. We confirmed *PTPN11*/SHP2 gene expression correlated well with its corresponding copy number changes in METABRIC patients (A). From our analysis, we observe *PTPN11*/SHP2 copy number loss correlated to early onset of disease with a mean age of 59.1±13.8 years (B), larger tumor size (28.2±19.2 mm) (C), significantly increased grade 3 tumors (D), and increased late-stage cancer (E) at diagnosis and no changes in lymph node positivity (F) as compared to patients with wild type copy number or copy number gain of *PTPN11*/SHP2.

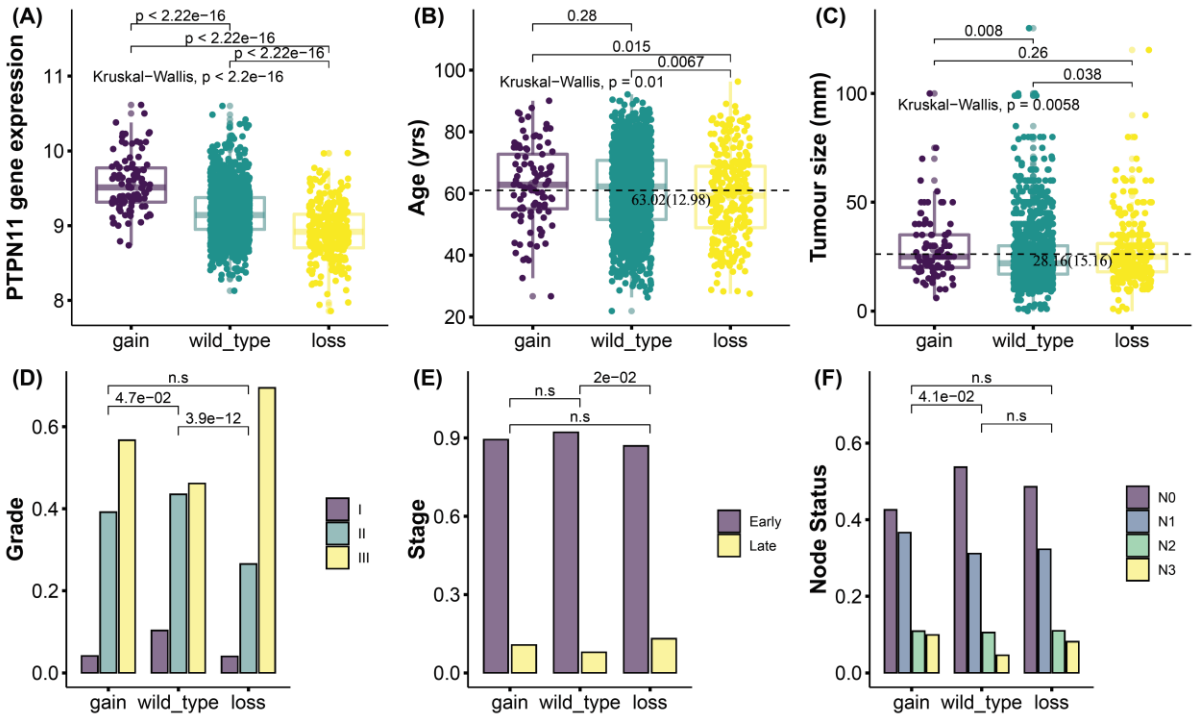

Figure 3.3.1A.1: (A) shows *PTPN11*/SHP2 copy number changes significantly correlate to the *PTPN11* gene expression pattern. (B) shows loss of *PTPN11*/SHP2 correlates with early onset of disease with a mean age of 59.1±13.8 years as compared to patients with wild type (WT) copy number (61.3 ±128) or copy number gain (62.9±13) of *PTPN11*/SHP2. (C) shows patients with *PTPN11*/SHP2 copy number loss associates with a significantly larger tumor size of 28.2±19.2 mm compared to patients with WT copy number (25.6±14.6 mm) but not different from patients with copy number gain (28.7±14.6 mm). (D) shows patients with loss of *PTPN11*/SHP2 has significantly increased grade 3 tumors than patients with WT copy of *PTPN11*/SHP2 and no difference in the grade of tumors of patients with copy number gain. (E) shows with *PTPN11*/SHP2 copy number loss associates with increased late-stage cancer at diagnosis as compared to patients with WT copy of *PTPN11*/SHP2. (F) shows patients with copy number gain of *PTPN11*/SHP2 have increased lymph node metastasis as compared to WT. Y-axis of D, E, F shows the fraction of patients.

3.3.1A.2: Clinical Correlation of *PTPN11*/SHP2 copy number changes and molecular parameters at diagnosis:

We examined the correlation of *PTPN11*/SHP2 copy changes to the molecular subtype of breast cancer patients and gene expression of reported oncogenes Estrogen receptor 1 (ESR1), HER2, and YAP1. Copy number loss of *PTPN11*/SHP2 correlates to low ESR1 expression (A) and higher YAP1 expression (C) however there was no change in HER2 expression (B). Patients with copy number loss of *PTPN11*/SHP2 negatively associates to ER status (E) and positively to HER2 status (D) and have a higher tendency to belong to TNBC (F) or the Basal subtype (G). We also see similar associations alternatively, as patients diagnosed with ER/PR subtype and Luminal A subtype negatively correlates to patients with copy number loss of *PTPN11*/SHP2 (H, I). While patients in the TNBC subtype and Basal subtype shows a positive correlation to patients with copy number loss of *PTPN11*/SHP2 (J, K). Details of the analysis are provided in Table 3.3.1A.2. Taken together, we observe copy number loss of *PTPN11*/SHP2 associates to the most aggressive TNBC/Basal molecular subtype.

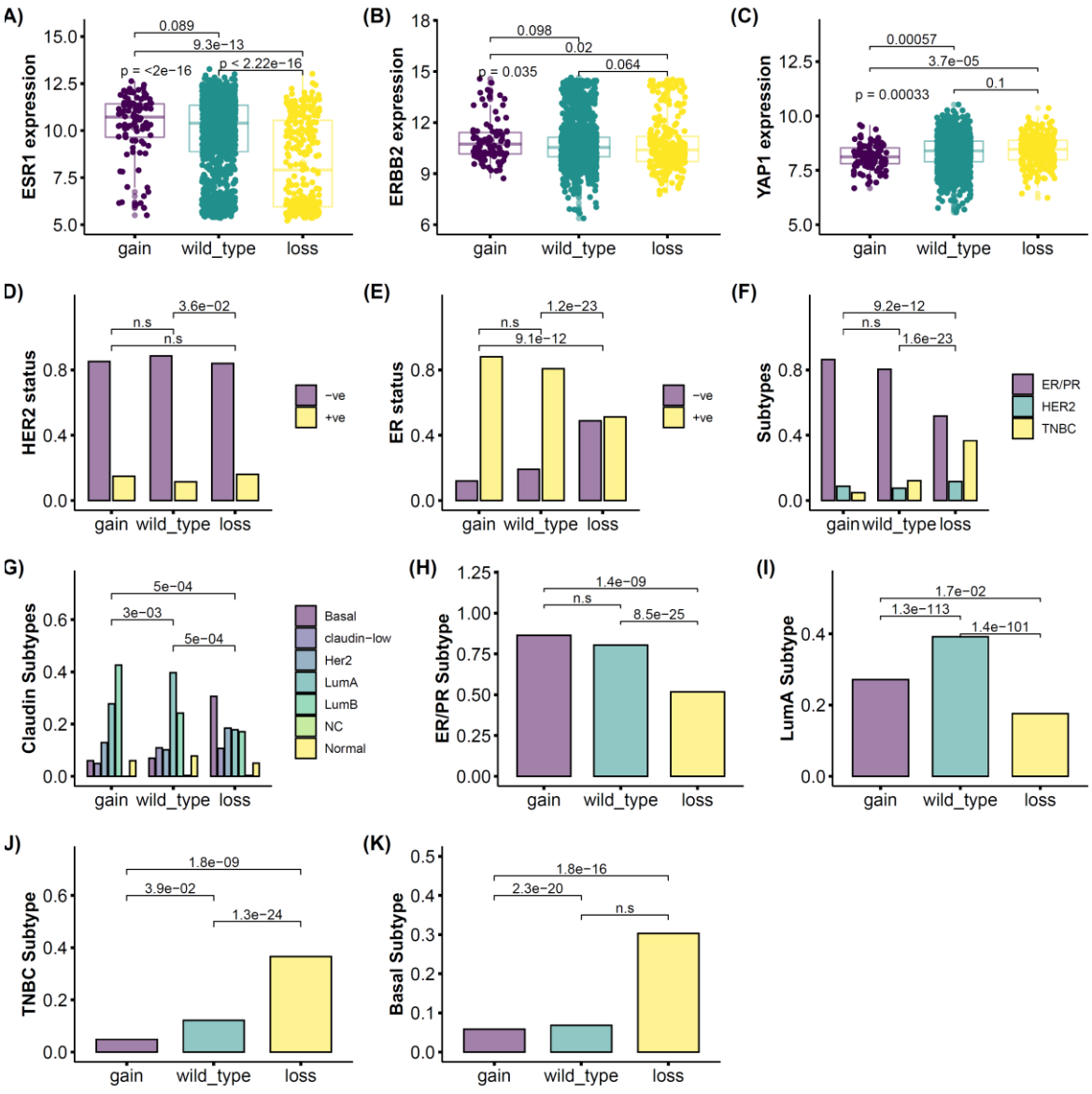

Figure 3.3.1A.2: (A) shows *PTPN11*/SHP2 copy number loss associate with lower ESR1 expression (in comparison to gain and WT copy). (B) shows there is no association of *PTPN11* copy number changes to HER2 expression. (C) shows *PTPN11*/SHP2 loss associates with higher YAP1 expression as compared to either gain of *PTPN11*/SHP2. (D) shows *PTPN11*/SHP2 copy number loss associates with HER2 status and (E) shows *PTPN11*/SHP2 copy number loss associates negatively associate with ER status. (F) and (G) shows *PTPN11*/SHP2 copy number loss has strong associations with TNBC molecular subtype and claudin Basal subtype. The Y-axis shows the fraction subtype in each group. (H) shows *PTPN11*/SHP2 copy number gain correlates to higher ER-positive breast cancer patients and (I) shows a correlation to Luminal (Lum) A

subtype as compared to patients with WT or loss of *PTPN11*/SHP2. (J) and (K) shows patients who are TNBC or Basal subtype positively associates with patients with *PTPN11*/SHP2 copy number loss. The Y-axis of D-K shows the fraction of patients.

3.3.1A.3: Clinical Correlation of *PTPN11*/SHP2 copy number change and survival outcome

We also investigated the influence of *PTPN11*/SHP2 copy number changes on survival outcomes. We examined both overall survival (OS) and disease-specific survival (DSS) at 5 years and 4 years post-diagnosis to *PTPN11*/SHP2 copy number changes. In overall survival, death due to any cause was taken as an event, while in disease-specific survival, only death due to disease was considered an event. The patients who survived post 5 years or 4 years were included in the study but censored at the respective endpoint.

We observed patients with *PTPN11*/SHP2 copy number loss correlated to poor overall and disease-specific 5years survival as compared to wild type (A, D). There was no difference in survival, both OS and DSS of patients with *PTPN11*/SHP2 wild type copy number and copy number gain (B, E) or in patients with copy number loss and copy number gain (C, F). We observe a similar trend even at 4 years, for patients with *PTPN11*/SHP2 loss correlated to poor 4 years OS and DSS as compared to patients with wild type of the gene (G, J). There was no significant change in 4 years of survival both OS and DSS in patients with wild type copy numbers and patients with copy number gain (H, K). Interestingly, at 4 years endpoint, the patients with *PTPN11*/SHP2 copy number loss had better DSS but not OS than patients with copy number gain of *PTPN11*/SHP2 (I, L).

Five years of survival

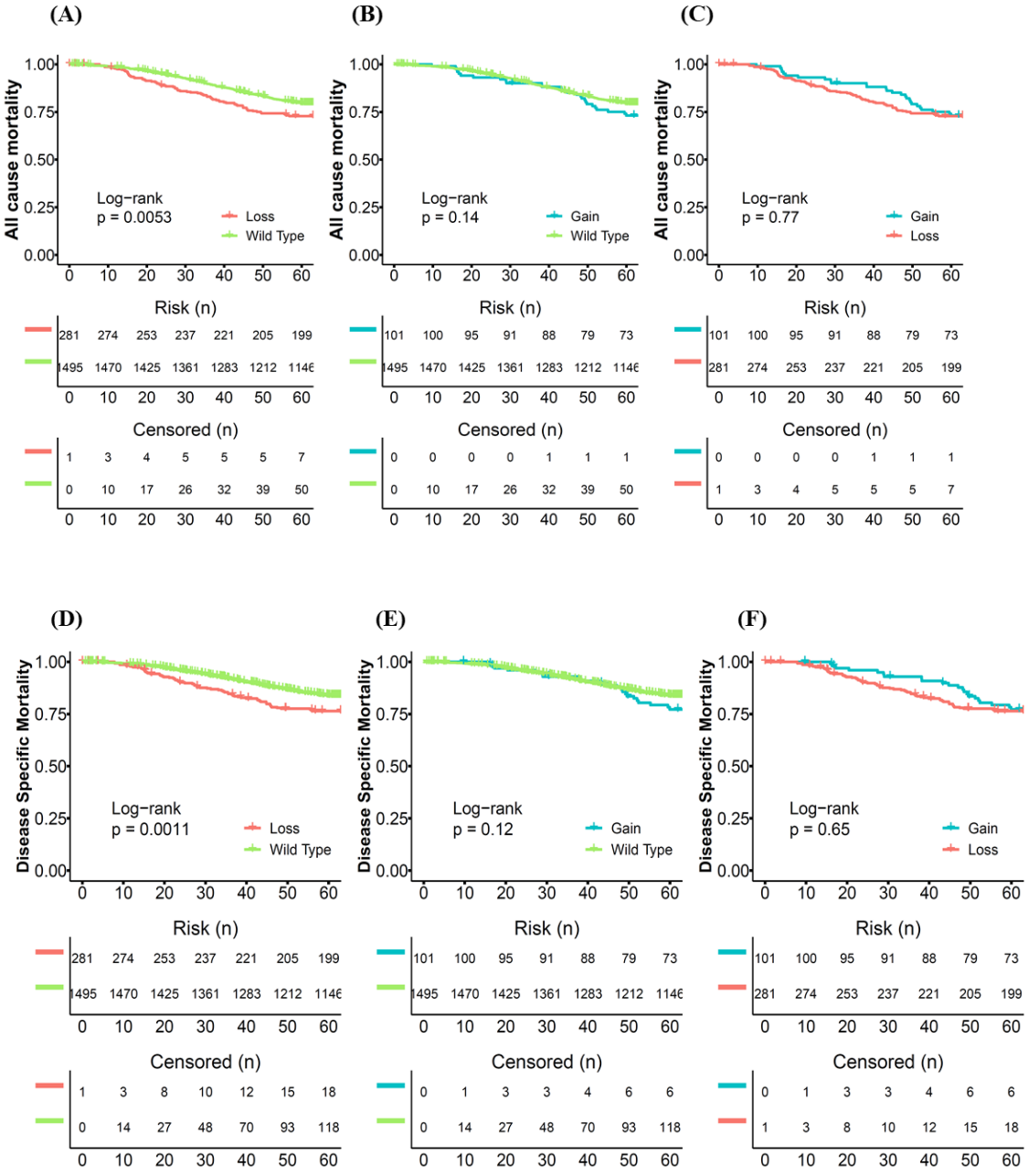

Four years of survival

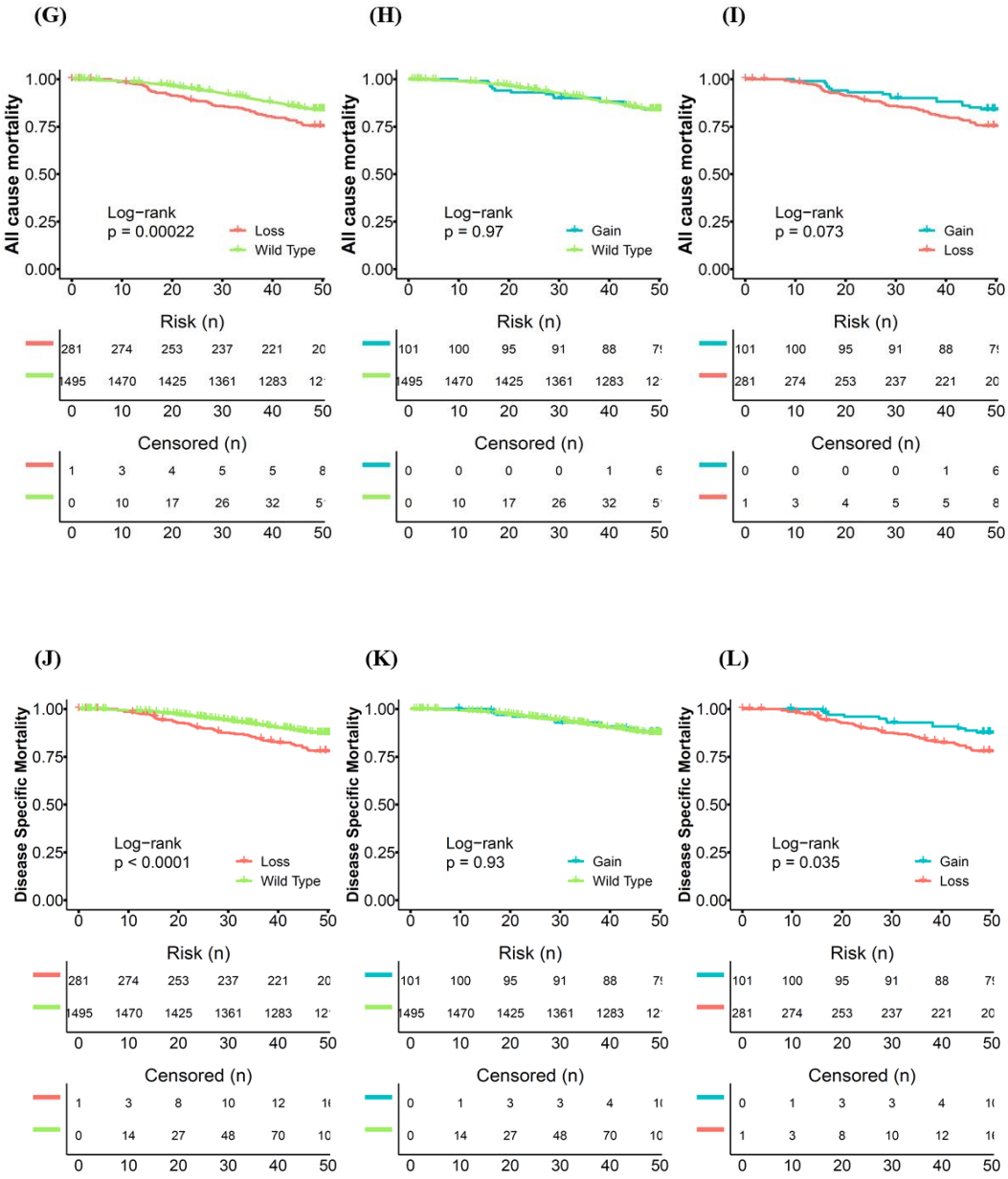

Figure 3.3.1A.3: (A) shows patients with *PTPN11*/SHP2 copy number loss have 5 years of poor OS than patients with *PTPN11*/SHP2 copy number gain. (B) shows there was no difference in 5 years OS of patients with either *PTPN11*/SHP2 copy number gain or wild type copy number. (C)

shows there was no difference in 5 years OS of patients with *PTPN11*/SHP2 copy number gain or patients with copy number loss. (D) shows 5 years DSS shows patients with *PTPN11*/SHP2 wild type copy numbers have a better prognosis than patients with *PTPN11*/SHP2 copy number loss. (E) shows there was no significant difference in 5 years DSS of patients with either copy number gain and wild type copy number. (F) shows no significant difference in DSS between patients with copy number loss and copy number gain. (G) and (J) shows at 4 years endpoint of survival, patients with *PTPN11*/SHP2 copy number loss have a poor OS and DSS than patients with wild type copy number. (I) and (L) shows patients with *PTPN11*/SHP2 copy number loss have poor OSS and DSS than patients with copy number gain at 4 years endpoint. (H) and (K) shows there was no difference in OS or DSS even at 4 years between patients with *PTPN11*/SHP2 wild type copy number and copy number gain.

3.3.1B: Clinical Correlation of *PTPN11*/SHP2 copy number changes in Luminal A Subtype:

From section 3.3.1A.2, we observed copy number gain of *PTPN11*/SHP2 positively correlates to the claudin Luminal subtype. We examined the correlation of *PTPN11* copy number status with clinical parameters within the Luminal subtype to identify if *PTPN11*/SHP2 has any specific (oncogenic or tumor suppressor) role. We also checked the association of *PTPN11*/SHP2 to the disease-specific survival for 4 years in this subset. There was no significant association between *PTPN11*/SHP2 copy number and age of patients at diagnosis (A), or their tumor size (B) and grade (C) in the luminal A subtype of patients. However, we report patients diagnosed with *PTPN11*/SHP2 copy number loss correlated to late-stage cancer (D), more nodal positivity, and poor DSS. Details of the analysis are provided in table 3.3.1B. To summarise, *PTPN11*/SHP2 copy number loss associates with the aggressive stage of Luminal A cancer with poor 4 years DSS in patients.

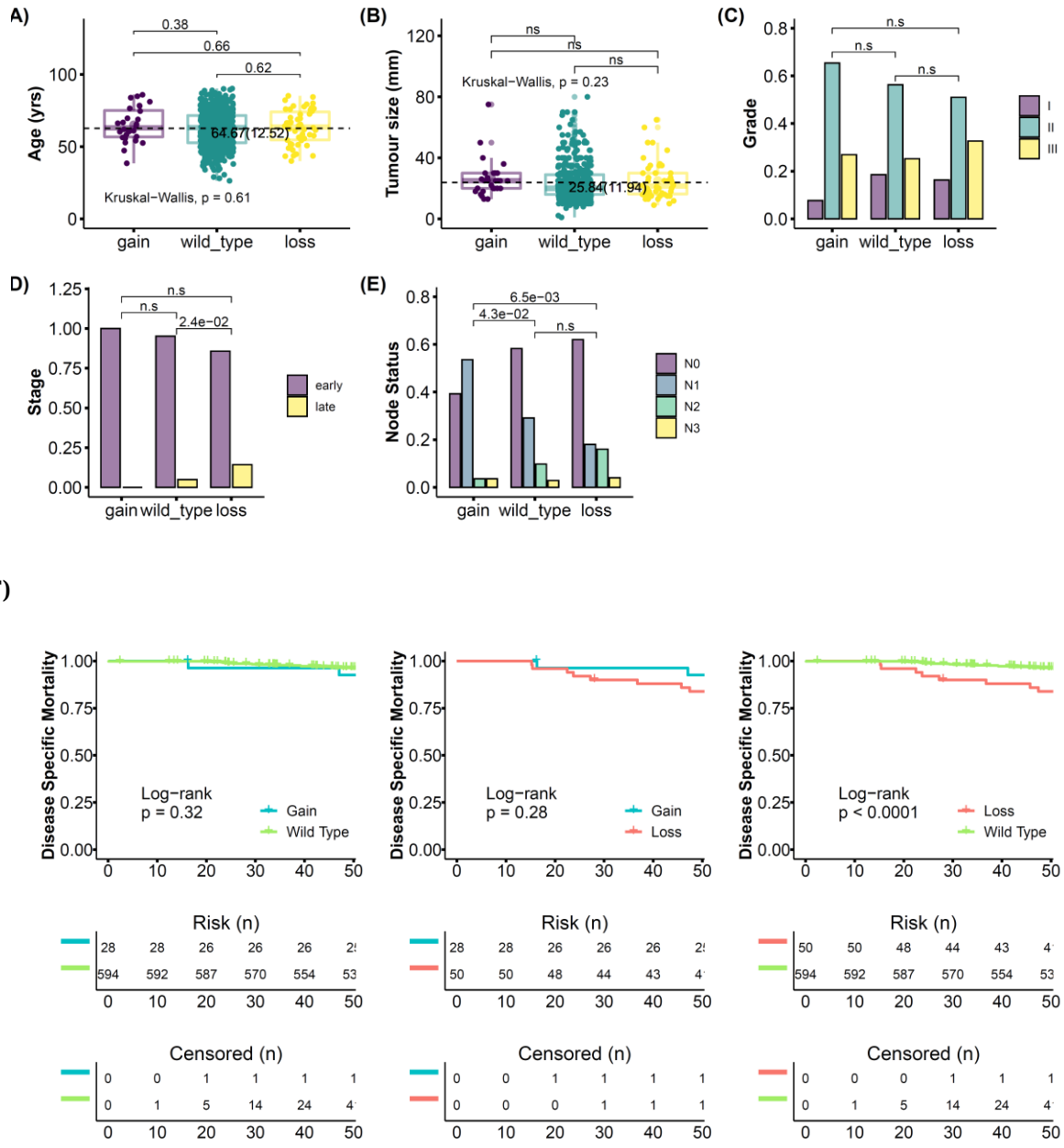

Figure 3.3.1B: In the Luminal A subtype, *PTPN11*/SHP2 copy number changes do not correlate to (A) age, (B) tumor size, and (C) grade of patients at diagnosis. (D) shows copy number loss of *PTPN11*/SHP2 associates with late-stage cancer at diagnosis as compared to patients with wild type copy number while there was no difference in stage of cancer between patients with copy number gain to patients with wild type copy number or copy number loss. (E) shows patients with copy number gain of *PTPN11*/SHP2 also associates with more LN1 positivity and less LN2 than patients with copy number loss or patients with wild type copy numbers of *PTPN11*/SHP2; Patients with the wild type copy number of *PTPN11*/SHP2 had more LN0 but also more LN2 than

patients with copy number gain of *PTPN11*/SHP2 at diagnosis. (F) shows loss of *PTPN11*/SHP2 further associated with poorer DSS as compared to wild type while there is no significant association to survival between patients with copy number gain and copy number loss or wild type copy number. Y-axis of C, D, E shows the fraction of patients.

3.3.1C: Clinical Correlation of *PTPN11*/SHP2 copy number changes in Luminal B subtype:

PTPN11/SHP2 copy number changes were also correlated to clinical parameters in the Luminal B+ subtype to study the association of (oncogenic and tumor suppressor) role of *PTPN11*/SHP2 in the luminal B subtype. The Luminal B group is characterized by HER2±, ER/PR+, and ki67 high. We do not observe a significant correlation between *PTPN11*/SHP2 copy number changes to any clinical parameters including age (A), tumor size (B), grade (C), stage (D) except Nodal positivity in the luminal B subtype of METABRIC cohort. Patients with copy number loss of *PTPN11*/SHP2 correlates to less lymph node positivity than patients with wild type copy number (E). We also do not observe a significant correlation of *PTPN11*/SHP2 copy number variations to the prognosis of the luminal B subtype of patients (F). Details of the analysis are provided in table 3.3.1C.

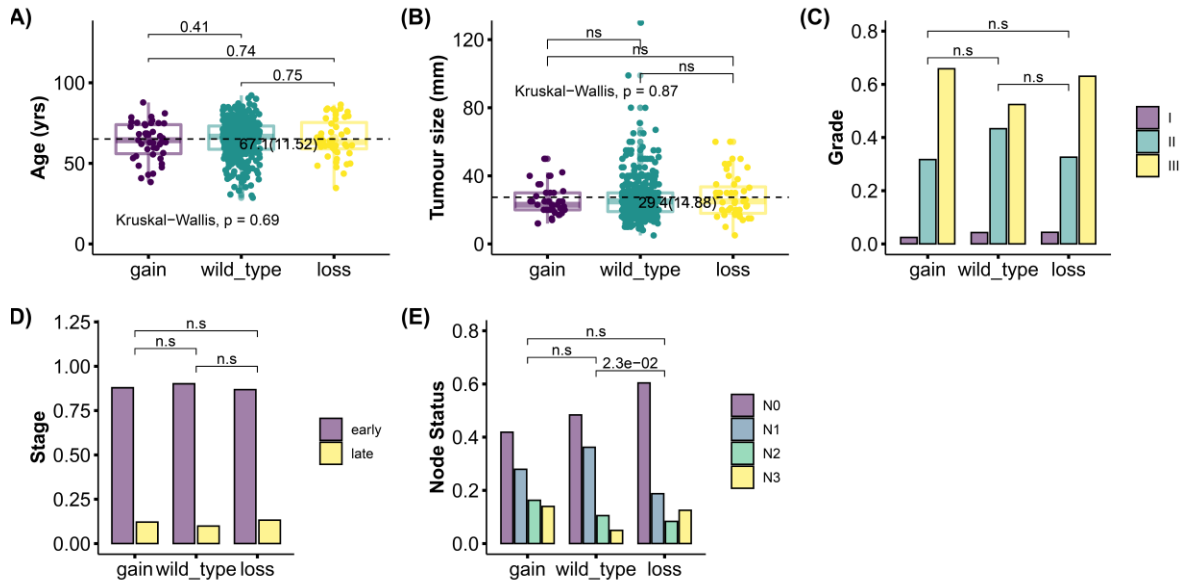

(F)

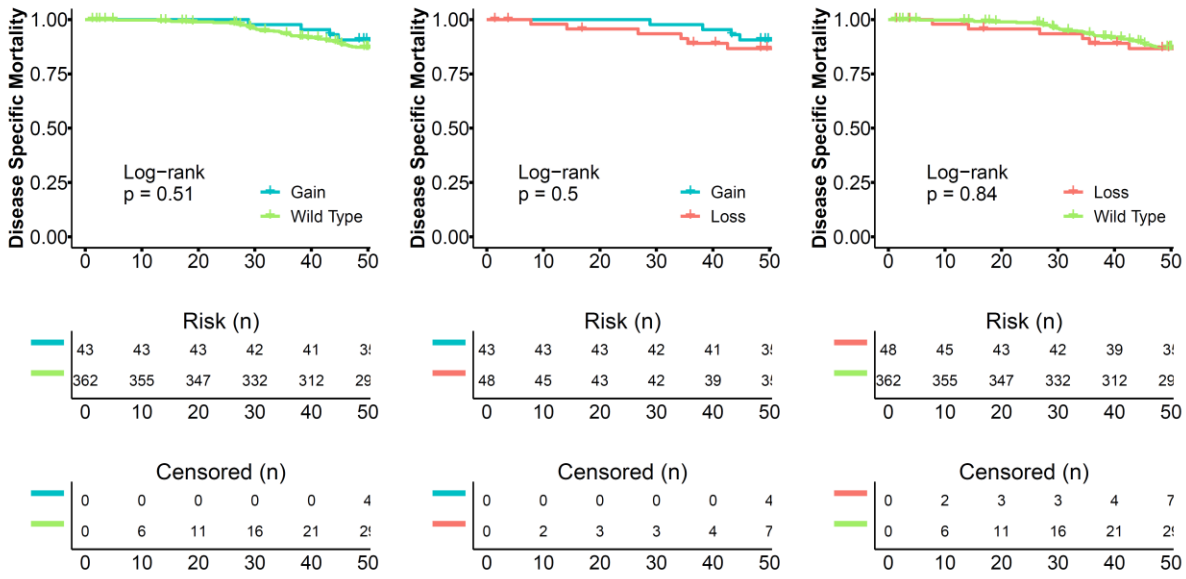

Figure 3.3.1C: In the Luminal B subtype, copy number changes of *PTPN11*/SHP2 does not associate with any clinicopathological phenotype including (A) age, (B) tumor size, (C) grade, (D) stage, or (F) DSS except (E) lymph node status where patients with *PTPN11*/SHP2 loss has more LN0 than the patients with wildtype copy of *PTPN11*/SHP2. Y-axis of C, D, E shows the fraction of patients.

3.3.1D: Clinical Correlation of *PTPN11*/SHP2 copy number changes in HER2 Subtype:

Although in section 3.3.1A.2, *PTPN11*/SHP2 copy number changes do not correlate to HER2 status, *PTPN11*/SHP2 being a positive regulator of EGFR signaling (Agazie and Hayman 2003) were correlated to clinical parameters in the HER2 subtype. We do not observe a significant correlation of *PTPN11*/SHP2 copy number variations to clinical parameters of HER2 subtype including age (A), tumor size (B), grade (C), stage (D), node status (E), and disease-specific mortality (F) in METABRIC cohort. Details of analysis provided in table 3.3.1D.

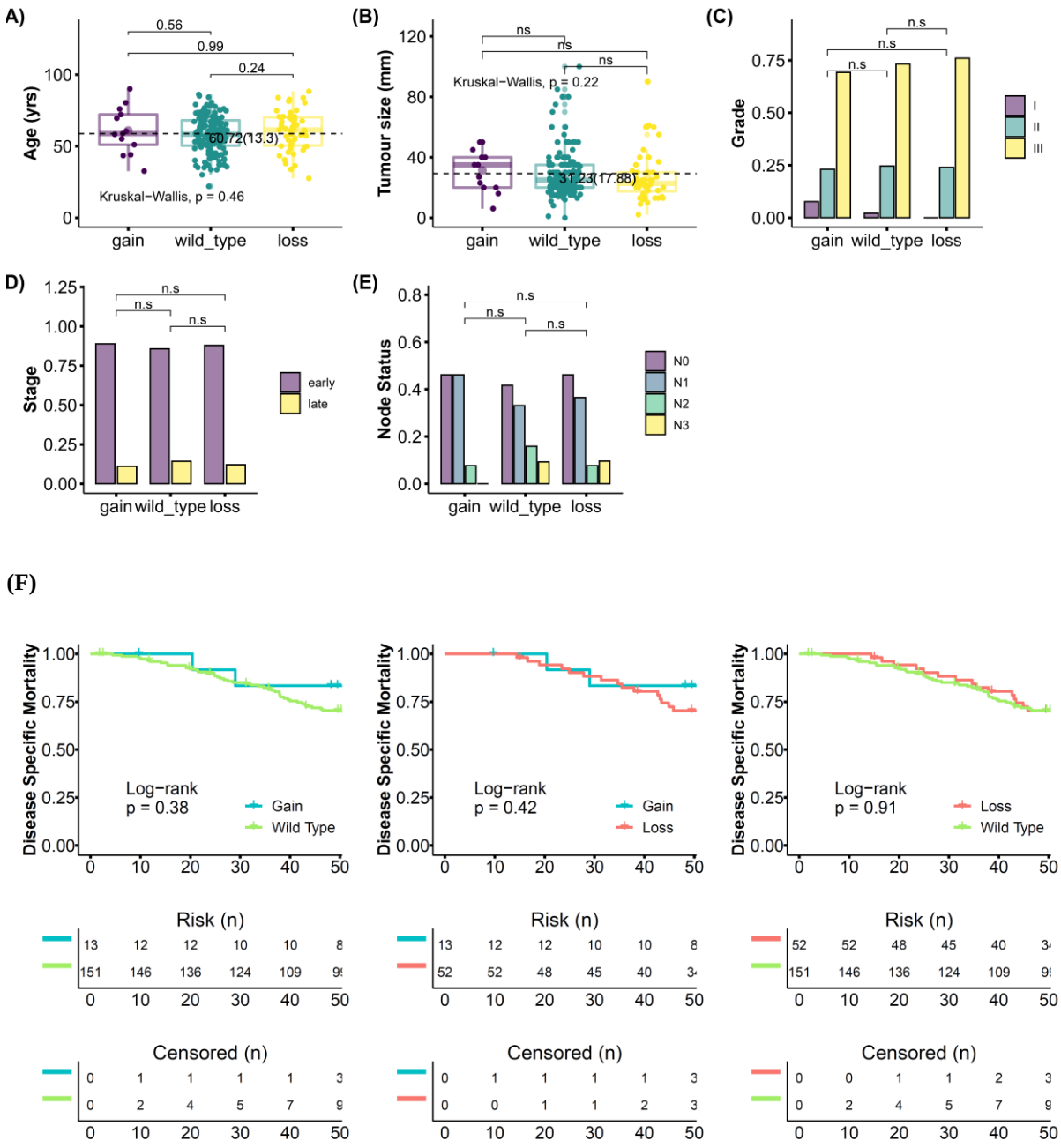

Figure 3.3.1D: In HER2 subtype, copy number changes of *PTPN11*/SHP2 do not associate with any clinicopathological phenotype including (A) age, (B) tumor size, (C) grade, (D) stage**,** (E) lymph node status, and (F) DSS.Y axis of C, D, E shows the fraction of patients.

3.3.1E: Clinical Correlation of *PTPN11*/SHP2 copy number changes in Basal Subtype:

In section 3.3.1A.2, *PTPN11*/SHP2 copy number loss positively correlated to the Basal subtype. Alternatively, *PTPN11*/SHP2 has been reported to help in the expression of receptor tyrosine kinases to promote the tumorigenic potential of BTBC (Matalkah et al. 2016). We analyzed if *PTPN11*/SHP2 copy number loss can function as a prognostic marker in the basal subtype. We do not observe a significant correlation between *PTPN11*/SHP2 copy number variations and clinical parameters within basal subtype including age (A), tumor size (B), grade (C), stage (D), Node status (E), and 4 years disease-specific prognosis (F) in METABRIC cohort. Details of the analysis are provided in table 3.3.1E.

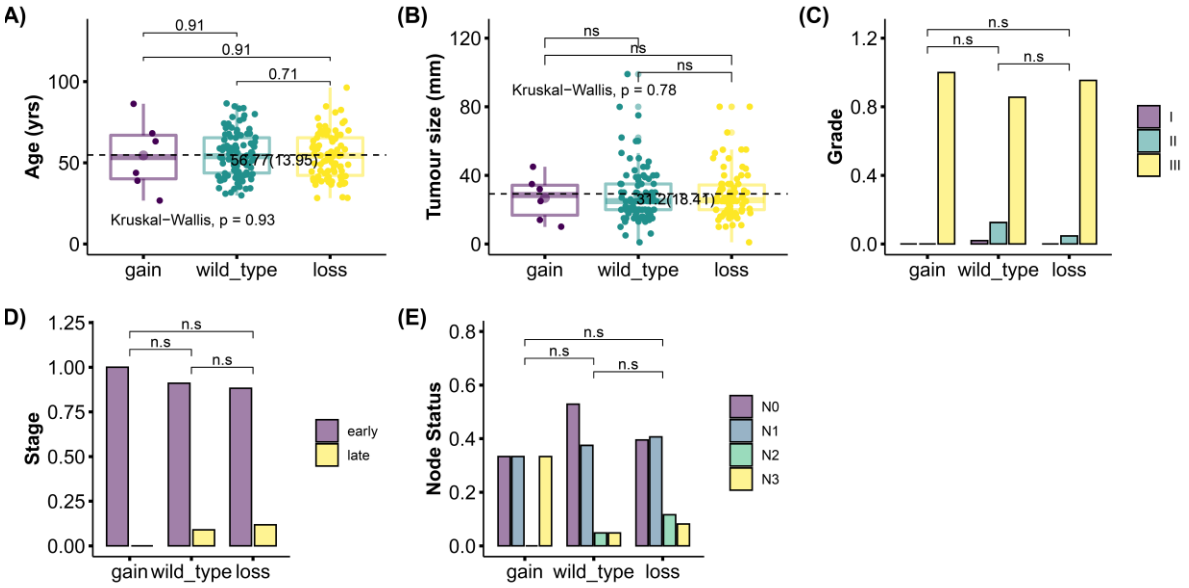

(F)

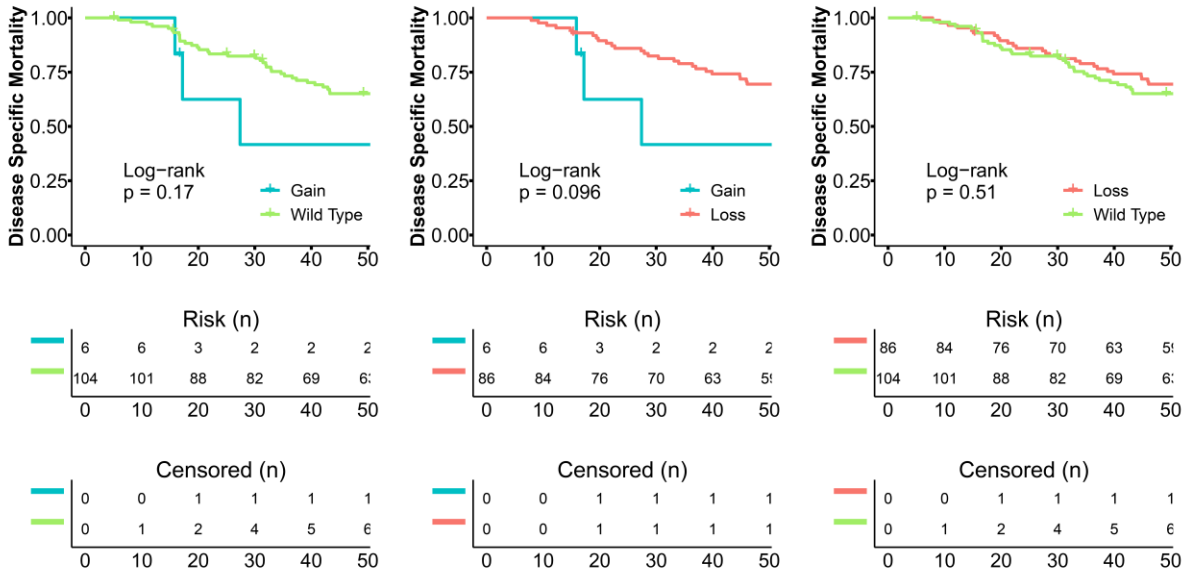

Figure 3.3.1E: In Basal subtype copy number changes of *PTPN11*/SHP2 do not associate to any clinicopathological phenotype including (A) age, (B) tumor size, (C) grade, (D) stage, (E) lymph node status, and (F) DSS. Y-axis of C, D, E shows the fraction of patients.

3.3.1F: Clinical Correlation of *PTPN11*/SHP2 copy number changes in *YAP1* high expression group of patients:

METABRIC cohort was divided into *YAP1* gene expression status to confirm observation from the *Drosophila* screen (Chapter 2). We grouped patients with *YAP1* gene expression above the 3rd quartile as *YAP1* high expressing group. Within *YAP1* high expressing patient group, *PTPN11*/SHP2 copy number changes were correlated to clinical parameters to understand the effect of *PTPN11*/SHP2 in *YAP1* driven breast cancers. There were no correlations regarding *PTPN11*/SHP2 copy number changes and age (A), tumor size (B), stage (D), node status (E). However, patients with *PTPN11*/SHP2 copy number loss correlated to grade 3 tumors at diagnosis (C) and 4 years DSS (F) in the *YAP1* high subset of the METABRIC cohort. Details of the analysis are provided in table 3.3.1F.

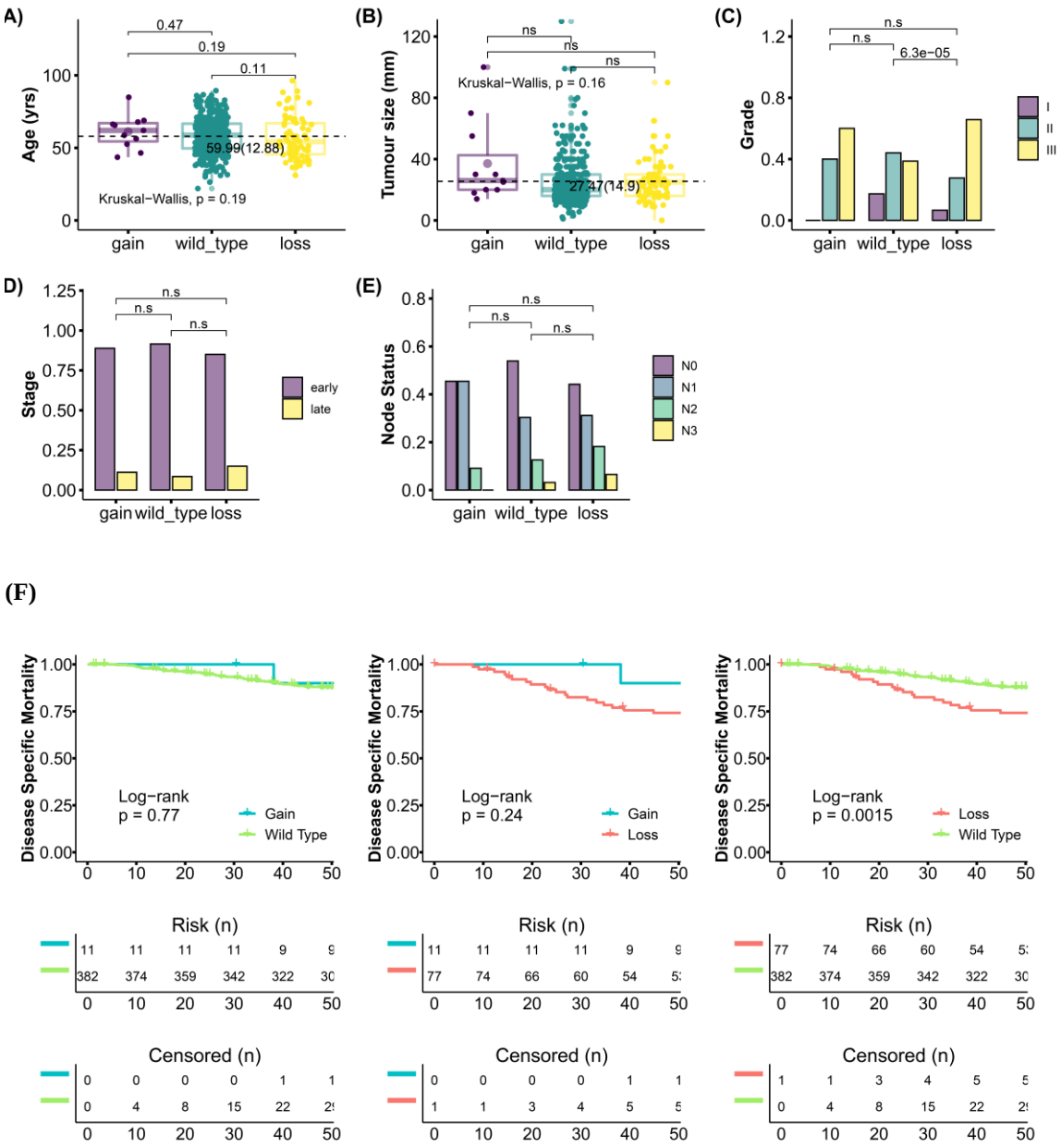

Figure 3.3.1F: In *YAP1* overexpressing breast cancer patients, we do not observe a significant correlation between *PTPN11*/SHP2 copy number variations and (A) age, (B) tumor size, (D) stage, (E) Node status. However, (C) we observe *PTPN11*/SHP2 copy number loss correlates to grade 3 tumors and (F) poor 4 years DSS. Y-axis of C, D, E shows the fraction of patients.

3.3.2A: Correlation of *PTPN11*/SHP2 copy number changes and clinical parameters of TCGA 2015 breast cancer patient cohort

3.3.2A.1: Clinical Correlation of *PTPN11*/SHP2 copy number changes and clinical parameters of patients at diagnosis:

Similar to the METABRIC cohort, we examined the statistical association of *PTPN11*/SHP2 copy number changes and clinical parameters in the TCGA BRCA cohort. We looked at correlations to age, tumor size, lymph node status, and stage to identify the tumorigenic role of *PTPN11*/SHP2 in breast cancer. We did not look at the survival of the TCGA BRCA cohort because of poor follow up data in the TCGA cohort.

Our analysis suggests, *PTPN11*/SHP2 copy number changes significantly correlate to its gene expression pattern (A). However, we do not observe a significant association between *PTPN11*/SHP2 copy number variations and clinical parameters including age (B), tumor size (C), node status (D), and stage (E) of BRCA TCGA cohort. Details of analysis provided in table 3.3.2A.1.

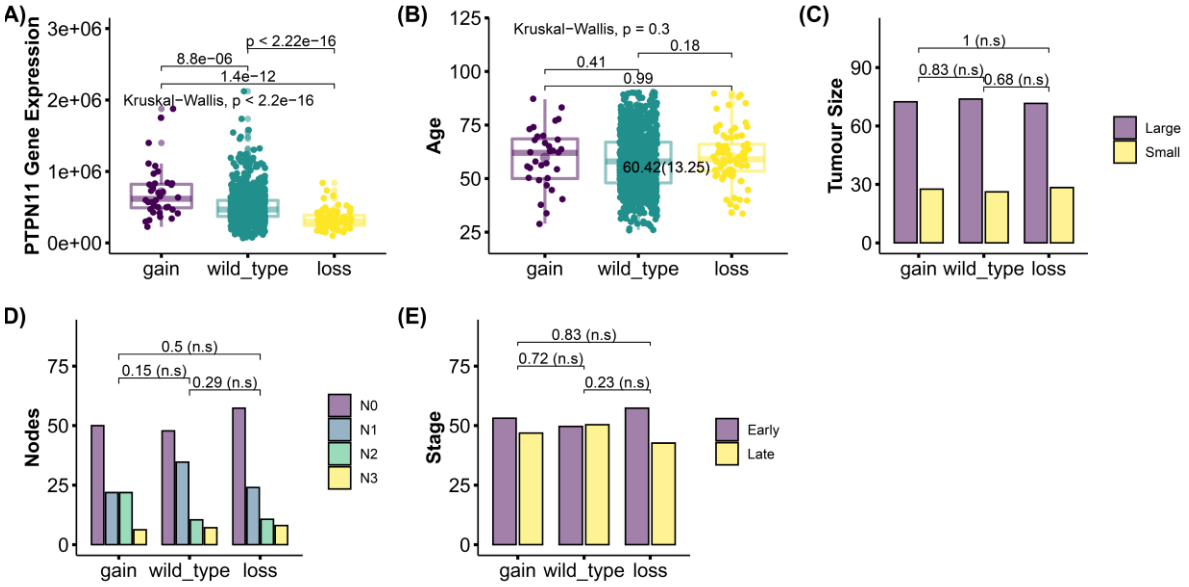

Figure 3.3.2A.1: (A) shows *PTPN11*/SHP2 copy number changes significantly correlate to the *PTPN11* gene expression pattern as obtained from RNA-seq data. Copy number changes of

PTPN11/SHP2 does not associate with any clinicopathological parameter including (B) age, (C) tumor size, (D) node, (E) stage in total TCGA 2015.

3.3.2A.2: Clinical Correlation of *PTPN11*/SHP2 copy number chansssges and molecular subtype of patients at diagnosis:

We verified if *PTPN11*/SHP2 copy number variations correlate to any particular subtype like in the METABRIC cohort. We do not observe any significant associations between *PTPN11*/SHP2 copy number variations to ESR1 expression (A), however, we see *PTPN11*/SHP2 copy number loss correlate to low YAP1 expression (B). There was no association of *PTPN11*/SHP2 copy number variations to any other PAM50 subtype (C) in the TCGA cohort. Alternatively, there was no association of Luminal A (D) or Luminal B (E) HER2 (F), and Basal (G) subtype to *PTPN11*/SHP2 copy number changes. Details of analysis provided in table 3.3.2A.2.

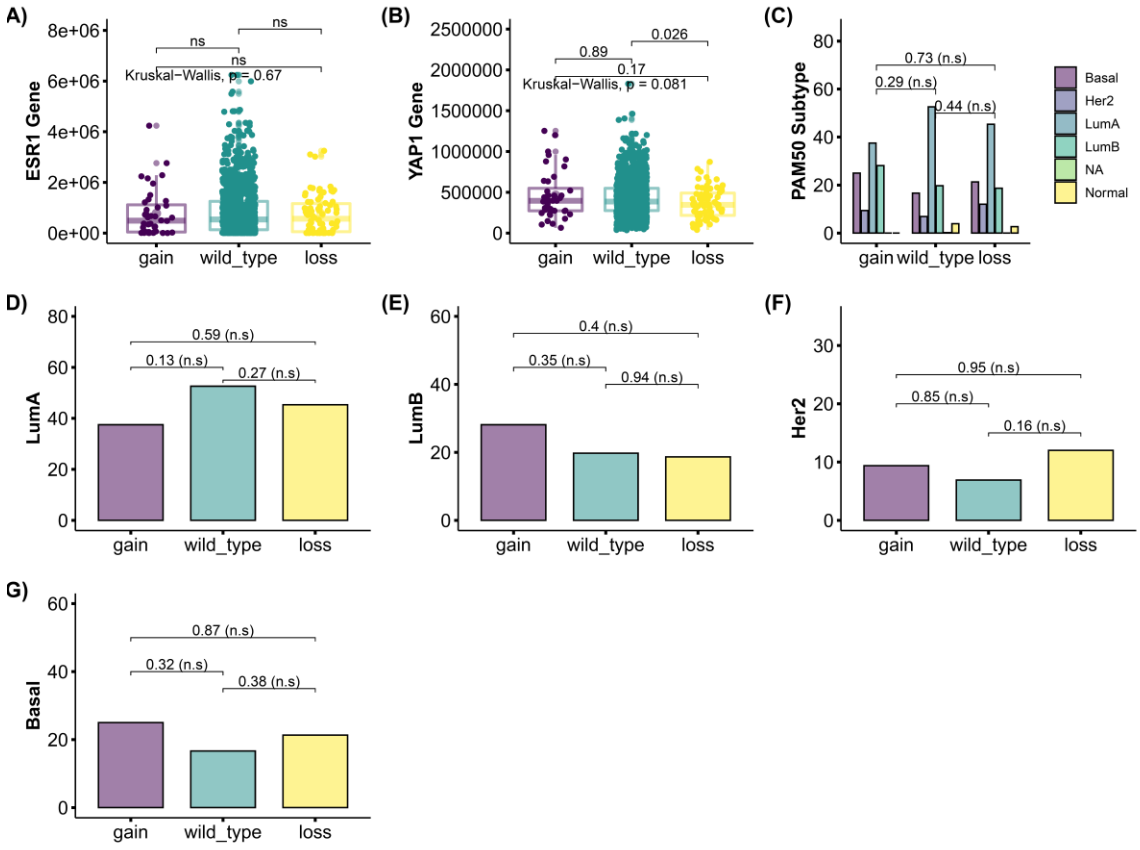

Figure 3.3.2A.2: (A) shows copy number variations of *PTPN11*/SHP2 does not associate with ESR1 expression. (B) shows *PTPN11*/SHP2 copy number loss associate with lower YAP1

expression. (C) shows copy number variations of *PTPN11*/SHP2 does not associate with any other PAM50 subtype. There was no significant association to subtype as seen in (D) correlation of Luminal A, (E) correlation of Luminal B, (F) correlation of HER2 subtype, and (G) correlation of basal subtype to copy number changes of *PTPN11*/SHP2.

3.3.2B: Clinical Correlation of *PTPN11*/SHP2 copy number changes in Luminal A Subtype:

We did not observe any associations of *PTPN11*/SHP2 copy number variations to clinical phenotype. To identify if *PTPN11*/SHP2 has any subtype-specific role, *PTPN11*/SHP2 copy number variations were correlated to clinical parameters within the Luminal A subtype. We do not observe a significant association of *PTPN11*/SHP2 copy number variations and age (A), tumor size (B), node status (C), metastasis (D), and stage (E) in the Luminal A subtype of BRCA TCGA cohort. Details of analysis provided in table 3.3.2B.

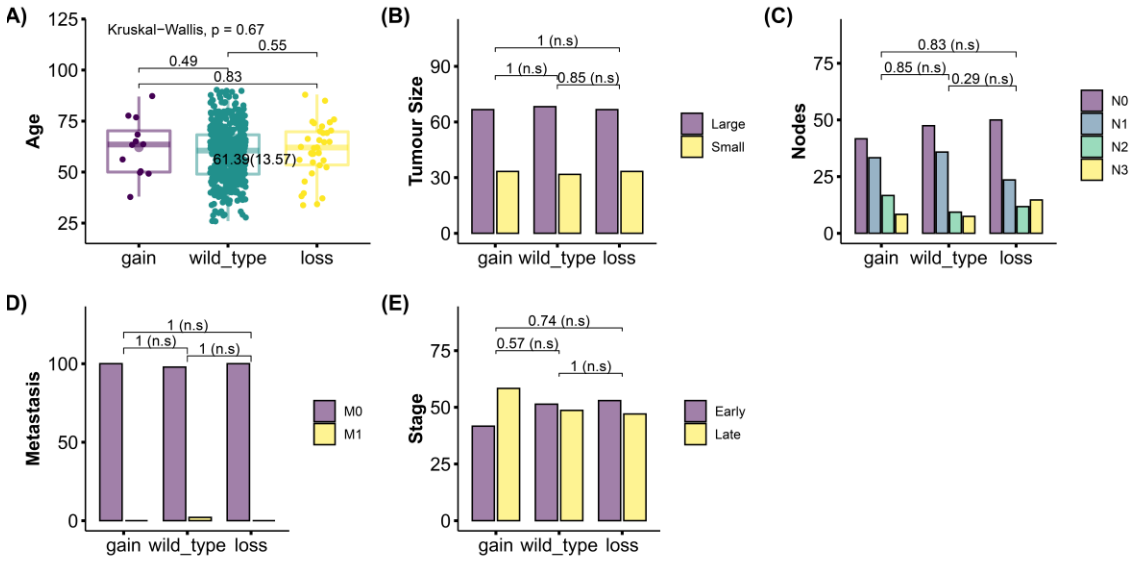

Figure 3.3.2B: Within Luminal A subtype of TCGA cohort, copy number changes of *PTPN11*/SHP2 do not associate with any clinicopathological phenotype including (A) age, (B) tumor size, (C) nodes positivity, (D) metastasis, and (E) stage.

3.3.2C: Clinical Correlation of *PTPN11*/SHP2 copy number changes in Luminal B Subtype:

PTPN11/SHP2 copy number variations were also correlated to clinical parameters within the Luminal B subtype to identify any subtype-specific role of *PTPN11*/SHP2. We do not observe any significant correlation of *PTPN11*/SHP2 copy number variations and clinical parameters including age (A), tumor size (B), node status (C), metastasis (D), and stage (E) in the Luminal B subtype of BRCA TCGA cohort. Details of analysis provided in table 3.3.2C.

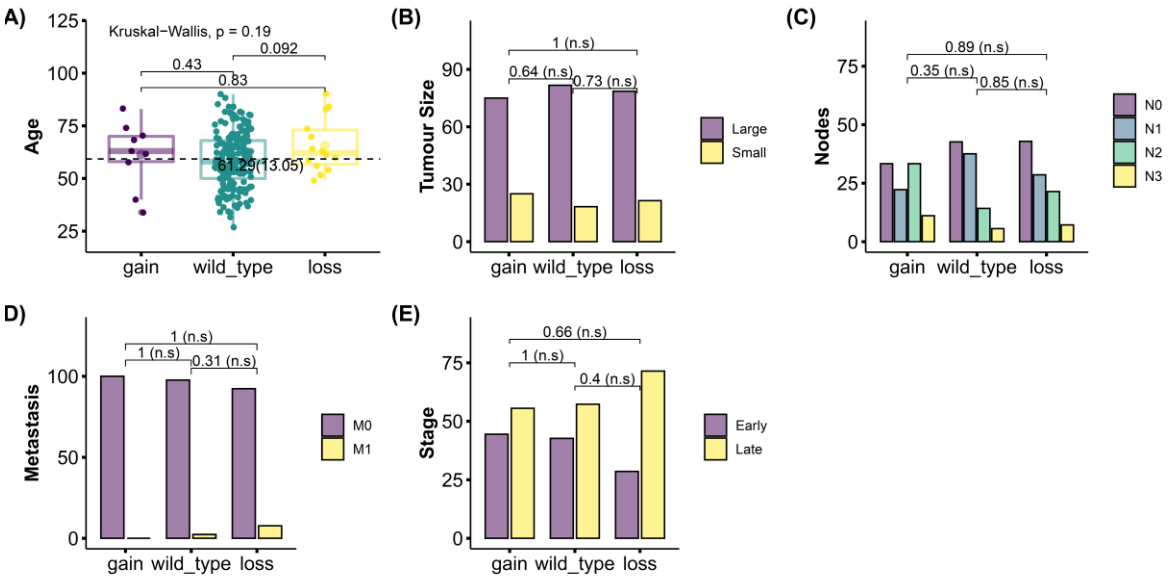

Figure 3.3.2C: In the Luminal B subtype, *PTPN11*/SHP2 copy number changes do not associate with any clinicopathological phenotype including (A) age, (B) tumor size, (C) node status, (D) metastasis, and (E) stage.

3.3.2D: Clinical Correlation of *PTPN11*/SHP2 copy number changes in HER2 Subtype:

PTPN11/SHP2 copy number variations were correlated to clinical parameters within the HER2 subtype to examine its role in EGFR driven neoplasia. We do not observe a significant correlation of *PTPN11*/SHP2 copy number variations and clinical parameters like age (A), tumor size (B), node status (C), metastasis (D), and stage (E) of the HER2 subtype of BRCA TCGA cohort. Details of analysis provided in table 3.3.2D.

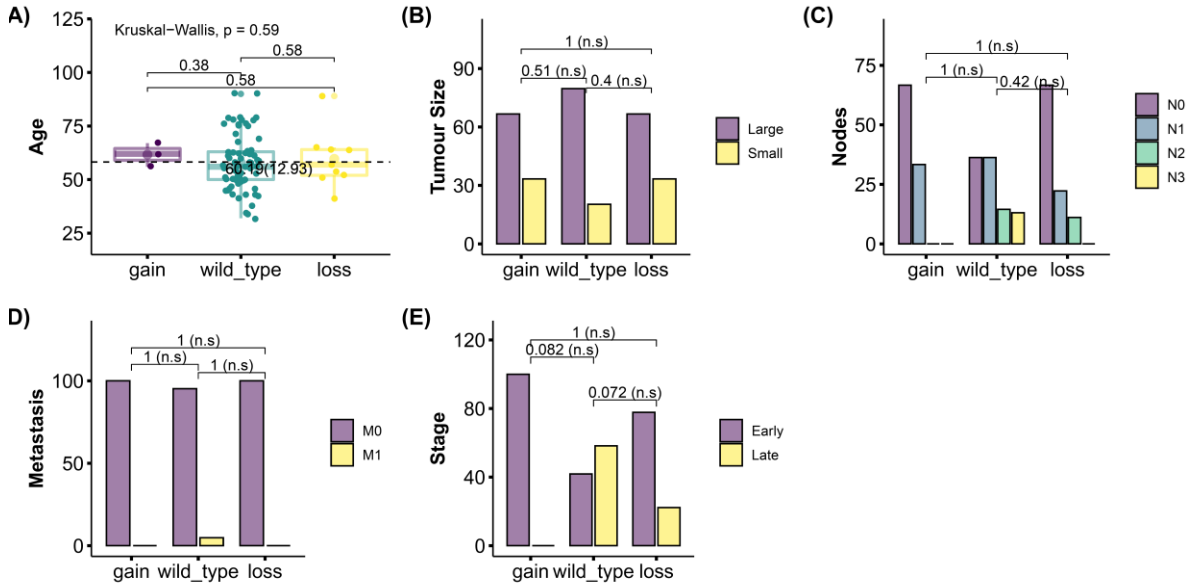

Figure 3.3.2D: In HER2 subtype, copy number changes of *PTPN11*/SHP2 do not associate with any clinicopathological phenotype including (A) age, (B) tumor size, (C) lymph node status, (D) metastasis, and (E) stage.

3.3.2E: Clinical Correlation of *PTPN11*/SHP2 copy number changes in Basal Subtype:

PTPN11/SHP2 copy number variations were correlated to clinical parameters within the basal subtype. We do not observe a significant correlation between *PTPN11*/SHP2 copy number changes and clinical parameters including age (A), tumor size (B), node status (C), metastasis (D), and stage (E) in the Basal subtype of BRCA TCGA cohort. Details of analysis provided in table 3.3.2E.

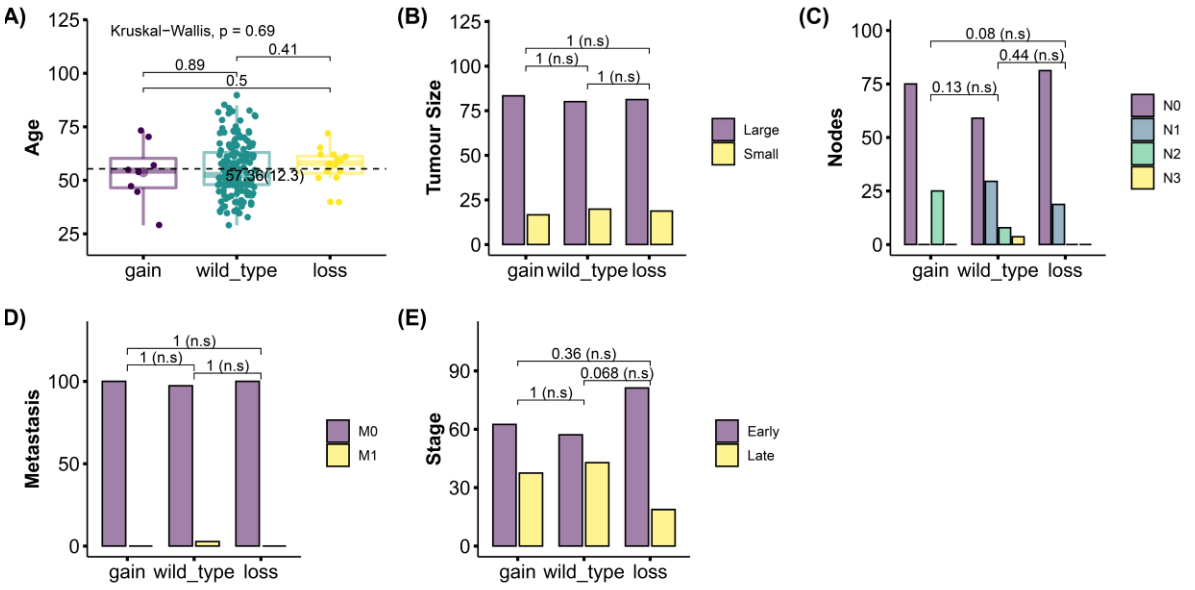

Figure 3.3.2E: In the Basal subtype, copy number changes of *PTPN11*/SHP2 do not associate with any clinicopathological phenotype including (A) age, (B) tumor size, (C) node status, (D) metastasis, and (E) stage.

3.3.2F: Clinical Correlation of *PTPN11*/SHP2 copy number changes in *YAP1* high expression group of patients:

We have observed in section 3.3.2A.2, *PTPN11*/SHP2 copy number loss in TCGA correlates to low *YAP1* expression. To understand the clinical role of *PTPN11*/SHP2 copy number changes in the *YAP1* high subgroup of TCGA BRCA patients we looked into the association of copy number changes and clinical parameters within the *YAP1* high subset of patients (*YAP1* gene expression above the third quartile). We do not observe a significant correlation between *PTPN11*/SHP2 copy number variations and age (A), tumor size (B), node status (C), metastasis (D), and stage (E) in the *YAP1* high subset of the BRCA TCGA cohort unlike observed in METABRIC cohort. Details of analysis provided in table 3.3.2F.

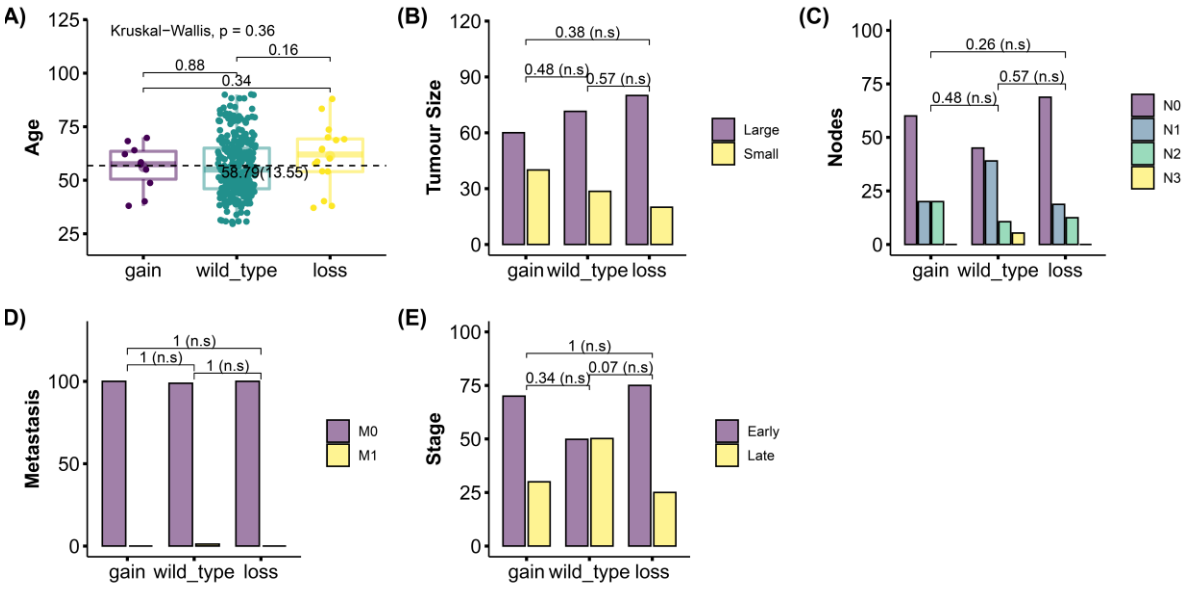

Figure 3.3.2F: In *YAP1* high subtype, copy number changes of *PTPN11*/SHP2 do not associate with any clinicopathological phenotype including (A) age, (B) tumor size, (C) node status, (D) metastasis, and (E) stage.

3.3.2G: Clinical Correlation of Phospho (tyrosine 542) *PTPN11*/SHP2 protein expression to the clinical phenotype of patients at diagnosis:

PTPN11/SHP2 is a phosphatase and TCGA provides RPPA data of around 225 protein and phosphoproteins. Phospho SHP2-Y542 is the active form of the phosphatase. In our study, we report for the first time, the association of active *PTPN11*/SHP2 to clinicopathological parameters and understand the effect of *PTPN11*/SHP2 phosphatase in tumorigenesis. Phospho SHP2 Y542 protein expression was correlated to clinical parameters in total BRCA patients using level 4 RPPA data from TCGA 2015. We do not observe a significant correlation between phospho SHP2 Y542 protein expression and age (A). However, low expression of phospho SHP2-Y542 correlates to larger tumor size (B), more N2 positivity (C), late-stage cancer (E), and luminal subtype of breast cancer (F). There was no significant correlation between metastasis and active protein (D).

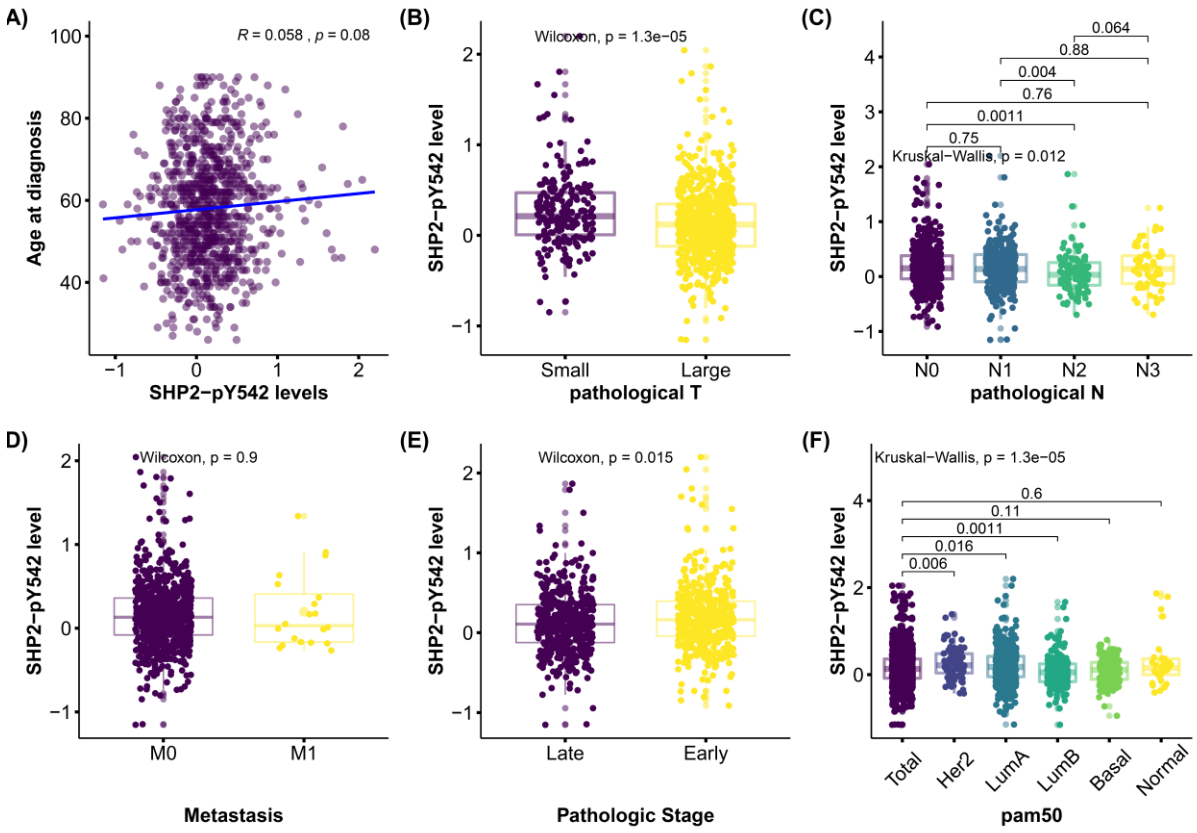

Figure 3.3.2G: (A) shows phosphorylated SHP2 Y542 does not associate with the age of onset of breast cancer disease or (D) to metastasis. However, (B) low expression levels of Phospho SHP2 Y542 significantly associates with larger tumor size, (C) LN2 positivity, (E) late-stage cancer, and (F) specificity to a Luminal subtype of breast cancer at diagnosis.

3.3.2H: Clinical Correlation of Phospho (tyrosine 542) *PTPN11*/SHP2 protein expression to the clinical phenotype of Luminal A patients at diagnosis:

To re-confirm our observation in section 3.3.1B, if *PTPN11*/SHP2 positively correlates to the aggressive nature of Luminal A cancer, phospho SHP2 Y542 protein expression was correlated to the luminal subtype of patients. We grouped patients into two groups, expressing high (above 3rd quartile) and low (below 1st quartile) levels of phospho SHP2 Y542. We correlated clinical parameters within the Luminal A subtype of BRCA patients to phospho SHP2 Y542 subsets. We do not observe a significant correlation between phospho SHP2 Y542 protein expression and age

(A), metastasis (E), and stage (F). However, low expression of phospho SHP2-Y542 protein correlates to low *YAP1* gene expression (B), larger tumor size (C), more N2/N3 positivity (D) in the luminal A subtype of breast cancer. Details of analysis in table 3.3.2H. In summary, our RPPA data analysis suggests a similar trend as observed in the METABRIC cohort, low expression of phospho SHP2 Y542 associates with aggressive tumors at diagnosis, and might behave as a putative tumor suppressor in Luminal A subtype of patients.

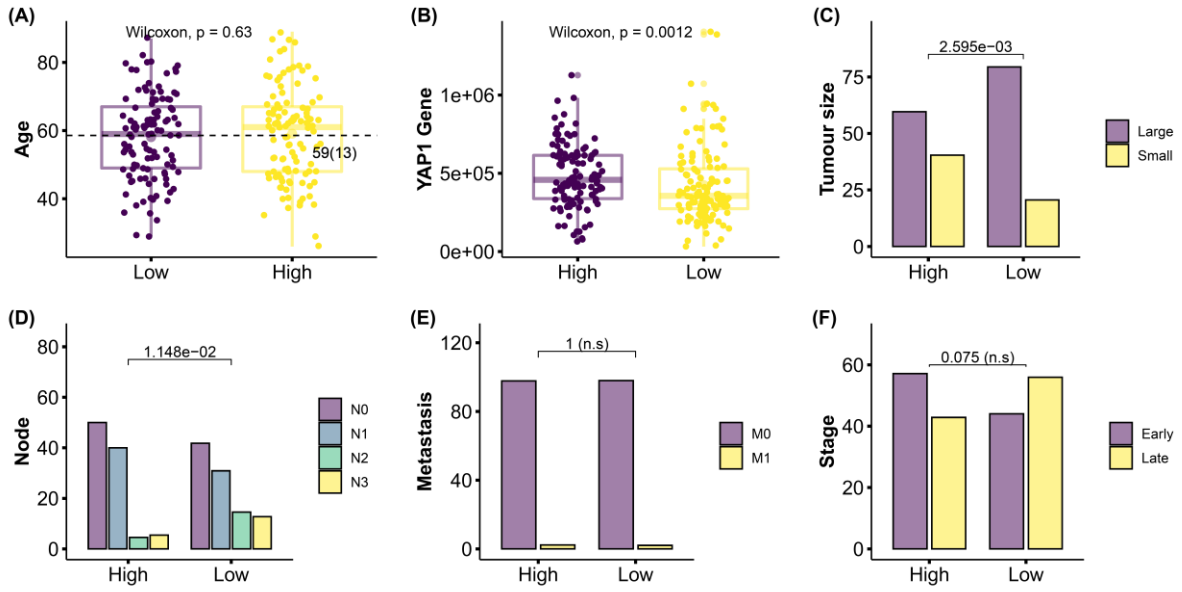

Figure 3.3.2H: In Luminal A subtype, (A) phospho SHP2 Y542 does not associate with the age of patients at diagnosis, (E) the number of metastasized sites, and (F) stage of cancer. However, (B) phospho Y542 *PTPN11*/SHP2 expression shows a negative association with *YAP1* expression, (C) larger tumor size, (D) LN2 and LN3 positivity as compared to high phospho SHP2 Y542 expression.

3.3.2I: Clinical Correlation of Phospho (tyrosine 542) *PTPN11*/SHP2 protein expression to the clinical phenotype of Luminal B patients at diagnosis:

Likewise, phospho SHP2 Y542 protein expression was also correlated to clinical parameters in the Luminal B subtype of BRCA patients using level 4 RPPA data from TCGA 2015. We do not observe a significant correlation of phospho SHP2 Y542 protein expression with age (A), larger

tumor size (C), metastasis (E), and stage (F). However, Phospho (tyrosine 542) *PTPN11*/SHP2 protein expression positively correlates to *YAP1* gene expression (B) and N3 positivity (D) in the luminal B subtype. Details of analysis in table 3.3.2I. In Summary, copy number analysis from the METABRIC cohort (section 3.3.1C) together with the phosphoprotein study in TCGA, *PTPN11*/SHP2 might function pro-tumorigenic in the Luminal B subtype of breast cancer patients.

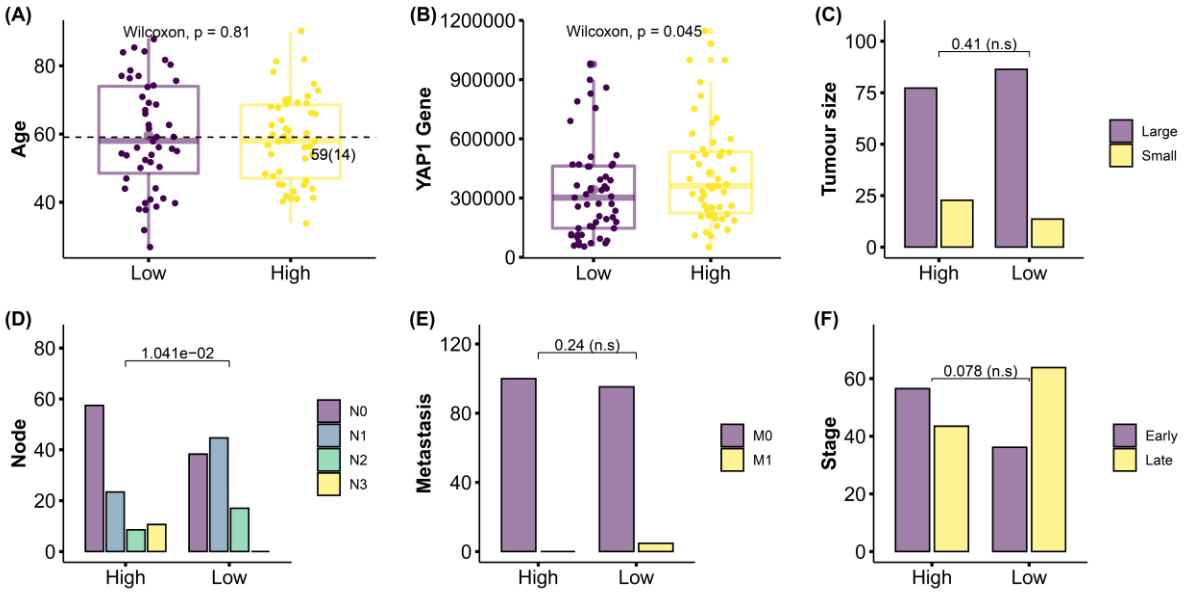

Figure 3.3.2I: In the Luminal B subtype, (A) phospho SHP2 Y542 does not associate with the age of patients at diagnosis. (B) Expression of *YAP1* and phospho SHP2 Y542 show a positive correlation. However, (C) phospho SHP2 Y542 expression levels do not associate with any clinical parameter including tumor size, (E) the number of metastasized sites, and (F) stage of cancer at diagnosis. (D) shows Phospho SHP2 Y542 shows a positive correlation to lymph node positivity.

3.3.2J: Clinical Correlation of Phospho (tyrosine 542) *PTPN11*/SHP2 protein expression to the clinical phenotype of HER2 patients at diagnosis:

PTPN11/SHP2 is a positive regulator of EGFR/HER2 signaling, we assessed the same using TCGA phosphoprotein data of *PTPN11*/SHP2 in the HER2 subtype of BRCA patients. We do not

observe any significant correlation between phospho SHP2 Y542 and age (A), *YAP1* gene expression (B), larger tumor size (C), node positivity (D), metastasis (E), and stage (F). In summary, we re-confirmed our observation from METABRIC in TCGA, *PTPN11*/SHP2 does not associate significantly with HER2 to co-operate in tumorigenesis.

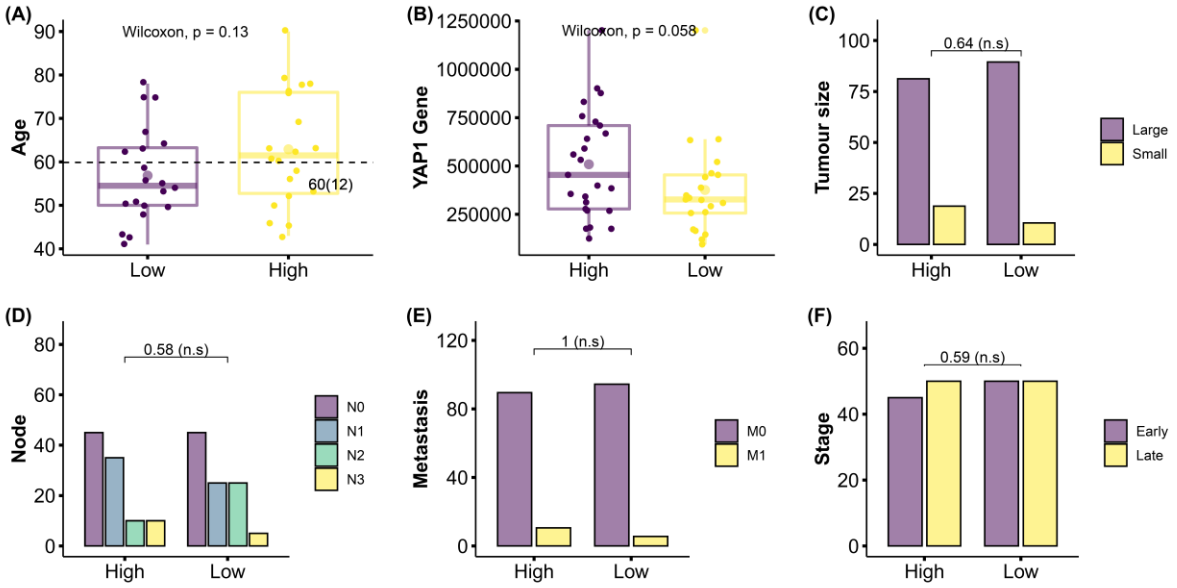

Figure 3.3.2J: In HER2 subtype, phospho SHP2 Y542 expression does not associate with any clinical parameter including (A) age, (B) *YAP1* gene expression, (C) larger tumor size, (D) node positivity, (E) metastasis, and (F) stage.

3.3.2K: Clinical Correlation of Phospho (tyrosine 542) *PTPN11*/SHP2 protein expression to the clinical phenotype of Basal patients at diagnosis:

Phospho SHP2 Y542 expression was correlated to clinical parameters in the Basal subtype of BRCA patients using level 4 RPPA data from TCGA 2015 to identify its prognostic effect in the Basal subtype of breast cancer. We do not observe a significant correlation between Phospho SHP2 Y542 expression and age (A), larger tumor size (C), node positivity (D), metastasis (E), and stage (F). However, Phospho SHP2 Y542 expression shows a positive correlation to *YAP1* gene expression (B).

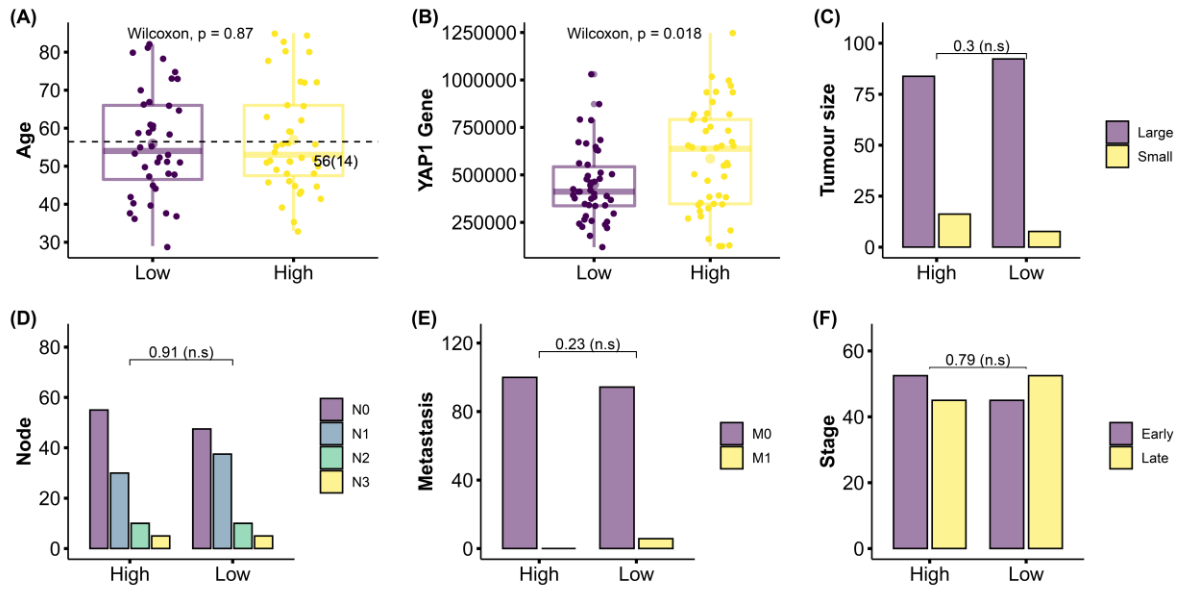

Figure 3.3.2K: In Basal subtype, (B) *YAP1* and phospho Y542 *PTPN11*/SHP2 are positively correlated. Phospho Y542 *PTPN11*/SHP2 expression does not associate with any clinical parameter including (A) age, (B) tumor size, (C) node positivity, (E) metastasis, and (F) stage.

3.4: Discussion

The results of our analysis of the METABRIC dataset show loss of *PTPN11*/SHP2 correlate to the early onset of breast cancer disease at least in the UK/Canadian cohort. We observe patients with *PTPN11*/SHP2 copy number loss are diagnosed with grade 3 and late-stage cancer at diagnosis with poor 4 years OS and DSS in the METABRIC cohort. Furthermore, we find *PTPN11*/SHP2 copy number loss correlates to low ER expression and low frequency of ER subtype. Within the Luminal A subtype, *PTPN11*/SHP2 copy number loss correlates to late-stage cancer and poor 4 years of disease-specific survival. Interestingly, copy number loss of *PTPN11*/SHP2 correlates to lesser lymph node positivity. In our study, we report *PTPN11*/SHP2 functions like a putative tumor suppressor precisely in the Luminal A subtype and as protumorigenic in the Luminal B subtype of breast cancer patients in the METABRIC cohort.

Analysis of the TCGA dataset independently suggested *PTPN11*/SHP2 copy number variations do not correlate to any clinical parameters in the total breast cancer dataset. However, analysis of phosphoprotein expression suggested a similar trend observed in our METABRIC study.

PTPN11/SHP2 being a phosphatase, we report for the first time, correlation of its active phosphorylated protein expression to clinical parameters using TCGA RPPA 2015 data in breast cancer. We observe active *PTPN11*/SHP2 indeed functions as a tumor suppressor, wherein low activity of *PTPN11*/SHP2 associates to more aggressive tumors at diagnosis with larger tumor size and LN2 positivity and lower expression in the Luminal subtype in the total TCGA dataset. Moreover, when we analyse specific subtype and correlate active *PTPN11*/SHP2 expression groups to clinical parameters, we observed low expression of phospho SHP2 Y542 associates with larger tumor size and greater lymph node positivity suggesting its plausible tumor suppressor role in the Luminal A subtype. Contrarily, phospho SHP2 Y542 expression positively correlates to lymph node positivity and suggestive of its pro-tumorigenic role in the Luminal B subtype. This is in agreement with our observation in the METABRIC cohort.

The oncogenic function of *PTPN11*/SHP2 has been reported in the backgrounds of HER2, EGFR, and PI3K-AKT in breast cancer (Aceto et al. 2012; K. Zhang et al. 2016). We report from our analysis using two independent cohorts, *PTPN11*/SHP2 does not show any strong associations in co-operating with HER2 driven breast cancer.

PTPN11/SHP2 was also reported to promote TNBC by mediating crosstalk between EGFR and wnt signaling (Aceto et al. 2012), while inhibition of *PTPN11*/SHP2 has been reported to promote basal to luminal A transition (H. Zhao and Agazie 2015). Our analysis suggests *PTPN11*/SHP2 does not associate with the Basal subtype.

In the context of *YAP1* driven cancer, *PTPN11* ortholog Csw functions as a tumor suppressor in Yki overexpressing epithelial discs. Clinical data suggest a strong association between *YAP1* and *PTPN11*/SHP2 expression at least in the METABRIC cohort. We looked into *YAP1* overexpressing subtype, a known oncogene in breast cancer. We report *PTPN11*/SHP2 loss is inversely correlated to YAP1 expression in the METABRIC cohort. Furthermore, in the *YAP1* high expressing a subset of METABRIC patients, we observe a loss of *PTPN11*/SHP2 associate with grade 3 tumors and poor 4 years DSS. However, we do not observe any association with any clinical parameter in the *YAP1* high expressing subtype of patients in the TCGA cohort. However, *YAP1* functions as a putative tumor suppressor in the luminal subgroup of breast cancer patients (Cao, Sun, and Yao 2017; Lehn et al. 2014). Hence it will be interesting to investigate the role of *PTPN11*/SHP2 in *YAP1* driven breast tumorigenesis.

The functional duality of molecules like kinases and phosphatases in cancer is a challenging area for cancer treatment and targeted therapeutic courses. We report in our study patients with loss or low activity of *PTPN11*/SHP2 is diagnosed with an aggressive tumor, however, *PTPN11*/SHP2 does not seem to behave like an ideal tumor suppressor candidate from our analysis. Since it is a phosphatase it can function in a dose-dependent manner. Suboptimal levels above wildtype such as gain of copy number could allow it to behave differently, depending on upstream molecular cues/context. Loss of function genetics could be a valuable tool to understand its intrinsic behaviour. Its role in the context of the YAP1 background also needs further elucidation.

3.5: Supplementary data

Table 3.3.1A.1

(A)

Feature	group	mean	sd	n
age	gain	62.9	13.0	101
age	loss	59.1	13.8	281
age	wild_type	61.3	12.8	1495

(B)

group1	group2	p	p.adj	p.format	p.signif	method
wild_type	loss	0.006732	0.02	0.0067	**	Wilcoxon
wild_type	gain	0.281471	0.28	0.2815	ns	Wilcoxon
loss	gain	0.015198	0.03	0.0152	*	Wilcoxon

(C)

Feature	group	mean	sd	n
tumour size (mm)	gain	28.7	14.6	100
tumour size (mm)	loss	28.2	19.2	281
tumour size (mm)	wild_type	25.6	14.3	1478

(D)

group1	group2	p	p.adj	p.format	p.signif	method
wild_type	loss	0.037987	0.076	0.038	*	Wilcoxon
wild_type	gain	0.008023	0.024	0.008	**	Wilcoxon
loss	gain	0.263789	0.260	0.264	ns	Wilcoxon

(E)

ln_status	gain	loss	wild_type
N0	43	137	806
N1	37	91	467
N2	11	31	158
N3	10	23	69

(F)

group1	group2	p_value	p_format	method	alt_hyp
gain	loss	0.71976305	n.s	Fisher	two.sided
gain	wild_type	0.04135894	4.1e−02	Fisher	two.sided
wild_type	loss	0.07744135	n.s	Fisher	two.sided

(G)

GRADE	gain	loss	wild_type
I	4	11	148
II	38	73	624
III	55	191	662

(H)

group1	group2	p_value	p_format	method	alt_hyp
gain	loss	6.211931e−02	n.s	Fisher	two.sided
gain	wild_type	4.651370e−02	4.7e−02	Fisher	two.sided
wild_type	loss	3.864305e−12	3.9e−12	Fisher	two.sided

(I)

stage_type	gain	loss	wild_type
Early	67	173	1018
Late	8	26	87

(J)

group1	group2	p_value	p_format	method	alt_hyp
gain	loss	0.68435692	n.s	Fisher	two.sided
gain	wild_type	0.37900269	n.s	Fisher	two.sided
wild_type	loss	0.02009187	2e−02	Fisher	two.sided

Table 3.3.1A.2

(A)

subtype	gain	loss	wild_type
ER/PR	89	147	1219
HER2	9	33	113
TNBC	5	104	184

(B)

CLAUDIN_SUBTYPE	gain	loss	wild_type
Basal	6	86	104
claudin−low	5	30	162
Her2	13	52	151
LumA	28	50	594
LumB	43	48	362
NC	0	1	5
Normal	6	14	117

(C)

subtype	group1	group2	n	percent	method	p
ER/PR	gain	loss	89	6.1%	Fisher exact count	1.4e−09
ER/PR	loss	wild_type	147	10.1%	Fisher exact count	8.5e−25
ER/PR	wild_type	gain	1219	83.8%	Fisher exact count	n.s

(D)

subtype	group1	group2	n	percent	method	p
LumA	gain	loss	28	4.2%	Fisher exact count	1.7e−02
LumA	loss	wild_type	50	7.4%	Fisher exact count	1.3e−113
LumA	wild_type	gain	594	88.4%	Fisher exact count	1.4e−101

(E)

subtype	group1	group2	n	percent	method	p
TNBC	gain	loss	5	1.7%	Fisher exact count	1.8e−09
TNBC	loss	wild_type	104	35.5%	Fisher exact count	3.9e−02
TNBC	wild_type	gain	184	62.8%	Fisher exact count	1.3e−24

(F)

subtype	group1	group2	n	percent	method	p
Basal	gain	loss	6	3.1%	Fisher exact count	1.8e−16
Basal	loss	wild_type	86	43.9%	Fisher exact count	n.s
Basal	wild_type	gain	104	53.1%	Fisher exact count	2.3e−20

Table 3.3.1.B

(A)

Feature	group	mean	sd	n
age	gain	65.1	12.0	28
age	loss	63.5	12.0	50
age	wild_type	62.5	12.6	594

(B)

group1	group2	p	p.adj	p.format	p.signif	method
wild_type	gain	0.3802	1	0.38	ns	Wilcoxon
wild_type	loss	0.6206	1	0.62	ns	Wilcoxon
gain	loss	0.6580	1	0.66	ns	Wilcoxon

(C)

Feature	group	mean	sd	n
tumour size (mm)	gain	26.4	12.5	28
tumour size (mm)	loss	25.1	12.4	50
tumour size (mm)	wild_type	23.6	11.9	593

(D)

group1	group2	p	p.adj	p.format	p.signif	method
wild_type	gain	0.1093	0.33	0.11	ns	Wilcoxon
wild_type	loss	0.4952	0.82	0.50	ns	Wilcoxon
gain	loss	0.4118	0.82	0.41	ns	Wilcoxon

(G)

GRADE	gain	loss	wild_type
I	2	8	105
II	17	25	319
III	7	16	143

(H)

group1	group2	p_value	p_format	method	alt_hyp
gain	loss	0.4598227	n.s	Fisher	two.sided
gain	wild_type	0.3874894	n.s	Fisher	two.sided
wild_type	loss	0.5247375	n.s	Fisher	two.sided

(I)

stage_type	gain	loss	wild_type
Early	22	36	428
Late	0	6	22

(J)

group1	group2	p_value	p_format	method	alt_hyp
gain	loss	0.08571499	n.s	Fisher	two.sided
gain	wild_type	0.61486480	n.s	Fisher	two.sided
wild_type	loss	0.02436096	2.4e−02	Fisher	two.sided

(E)

ln_status	gain	loss	wild_type
N0	11	31	346
N1	15	9	173
N2	1	8	58
N3	1	2	17

(F)

group1	group2	p_value	p_format	method	alt_hyp
gain	loss	0.006450094	6.5e−03	Fisher	two.sided
gain	wild_type	0.043497355	4.3e−02	Fisher	two.sided
wild_type	loss	0.191151292	n.s	Fisher	two.sided

Table 3.3.1.C

(A)

Feature	group	mean	sd	n
age	gain	60.9	16.3	13
age	loss	60.6	13.7	52
age	wild_type	57.9	12.9	151

(B)

group1	group2	p	p.adj	p.format	p.signif	method
wild_type	loss	0.2436	0.73	0.24	ns	Wilcoxon
wild_type	gain	0.5590	1.00	0.56	ns	Wilcoxon
loss	gain	0.9935	1.00	0.99	ns	Wilcoxon

(C)

Feature	group	mean	sd	n
tumour size (mm)	gain	31.3	13.8	13
tumour size (mm)	loss	29.0	24.3	52
tumour size (mm)	wild_type	29.1	15.5	148

(D)

group1	group2	p	p.adj	p.format	p.signif	method
wild_type	loss	0.1655	0.5	0.17	ns	Wilcoxon
wild_type	gain	0.3367	0.5	0.34	ns	Wilcoxon
loss	gain	0.1861	0.5	0.19	ns	Wilcoxon

(G)

GRADE	gain	loss	wild_type
I	1	0	3
II	3	12	35
III	9	38	104

(H)

group1	group2	p_value	p_format	method	alt_hyp
gain	loss	0.2574895	n.s	Fisher	two.sided
gain	wild_type	0.4287418	n.s	Fisher	two.sided
wild_type	loss	0.8728453	n.s	Fisher	two.sided

(I)

stage_type	gain	loss	wild_type
Early	8	29	84
Late	1	4	14

(J)

group1	group2	p_value	p_format	method	alt_hyp
gain	loss	1	n.s	Fisher	two.sided
gain	wild_type	1	n.s	Fisher	two.sided
wild_type	loss	1	n.s	Fisher	two.sided

(E)

ln_status	gain	loss	wild_type
N0	6	24	63
N1	6	19	50
N2	1	4	24
N3	0	5	14

(F)

group1	group2	p_value	p_format	method	alt_hyp
gain	loss	0.8084736	n.s	Fisher	two.sided
gain	wild_type	0.6141621	n.s	Fisher	two.sided
wild_type	loss	0.5424265	n.s	Fisher	two.sided

Table 3.3.1.D

(A)

Feature	group	mean	sd	n
age	gain	60.9	16.3	13
age	loss	60.6	13.7	52
age	wild_type	57.9	12.9	151

(B)

group1	group2	p	p.adj	p.format	p.signif	method
wild_type	loss	0.2436	0.73	0.24	ns	Wilcoxon
wild_type	gain	0.5590	1.00	0.56	ns	Wilcoxon
loss	gain	0.9935	1.00	0.99	ns	Wilcoxon

(C)

Feature	group	mean	sd	n
tumour size (mm)	gain	31.3	13.8	13
tumour size (mm)	loss	29.0	24.3	52
tumour size (mm)	wild_type	29.1	15.5	148

(D)

group1	group2	p	p.adj	p.format	p.signif	method
wild_type	loss	0.1655	0.5	0.17	ns	Wilcoxon
wild_type	gain	0.3367	0.5	0.34	ns	Wilcoxon
loss	gain	0.1861	0.5	0.19	ns	Wilcoxon

(G)

GRADE	gain	loss	wild_type
I	1	0	3
II	3	12	35
III	9	38	104

(H)

group1	group2	p_value	p_format	method	alt_hyp
gain	loss	0.2574895	n.s	Fisher	two.sided
gain	wild_type	0.4287418	n.s	Fisher	two.sided
wild_type	loss	0.8728453	n.s	Fisher	two.sided

(I)

stage_type	gain	loss	wild_type
Early	8	29	84
Late	1	4	14

(J)

group1	group2	p_value	p_format	method	alt_hyp
gain	loss	1	n.s	Fisher	two.sided
gain	wild_type	1	n.s	Fisher	two.sided
wild_type	loss	1	n.s	Fisher	two.sided

(E)

ln_status	gain	loss	wild_type
N0	6	24	63
N1	6	19	50
N2	1	4	24
N3	0	5	14

(F)

group1	group2	p_value	p_format	method	alt_hyp
gain	loss	0.8084736	n.s	Fisher	two.sided
gain	wild_type	0.6141621	n.s	Fisher	two.sided
wild_type	loss	0.5424265	n.s	Fisher	two.sided

Table 3.3.1.E

(A)

Feature	group	mean	sd	n
age	gain	54.5	21.9	6
age	loss	54.5	14.1	86
age	wild_type	55.0	13.5	104

(B)

group1	group2	p	p.adj	p.format	p.signif	method
loss	wild_type	0.7126	1	0.71	ns	Wilcoxon
loss	gain	0.9056	1	0.91	ns	Wilcoxon
wild_type	gain	0.9109	1	0.91	ns	Wilcoxon

(C)

Feature	group	mean	sd	n
tumour size (mm)	gain	26.8	13.2	6
tumour size (mm)	loss	30.5	21.7	86
tumour size (mm)	wild_type	28.3	15.5	101

(D)

group1	group2	p	p.adj	p.format	p.signif	method
loss	wild_type	0.4798	1	0.48	ns	Wilcoxon
loss	gain	0.8803	1	0.88	ns	Wilcoxon
wild_type	gain	0.9892	1	0.99	ns	Wilcoxon

(G)

GRADE	gain	loss	wild_type
I	0	0	2
II	0	4	13
III	6	82	89

(H)

group1	group2	p_value	p_format	method	alt_hyp
gain	loss	1.00000000	n.s	Fisher	two.sided
gain	wild_type	1.00000000	n.s	Fisher	two.sided
wild_type	loss	0.06650298	n.s	Fisher	two.sided

(I)

stage_type	gain	loss	wild_type
Early	3	45	71
Late	0	6	7

(J)

group1	group2	p_value	p_format	method	alt_hyp
gain	loss	1.0000000	n.s	Fisher	two.sided
gain	wild_type	1.0000000	n.s	Fisher	two.sided
wild_type	loss	0.7660584	n.s	Fisher	two.sided

(E)

ln_status	gain	loss	wild_type
N0	2	34	55
N1	2	35	39
N2	0	10	5
N3	2	7	5

(F)

group1	group2	p_value	p_format	method	alt_hyp
gain	loss	0.2601762	n.s	Fisher	two.sided
gain	wild_type	0.1031511	n.s	Fisher	two.sided
wild_type	loss	0.1337815	n.s	Fisher	two.sided

Table 3.3.1.F:

(A)

Feature	group	mean	sd	n
age	gain	61.2	11.6	11
age	loss	56.5	14.6	77
age	wild_type	58.2	12.6	382

(B)

group1	group2	p	p.adj	p.format	p.signif	method
loss	wild_type	0.1056	0.32	0.11	ns	Wilcoxon
loss	gain	0.1938	0.39	0.19	ns	Wilcoxon
wild_type	gain	0.4714	0.47	0.47	ns	Wilcoxon

(C)

Feature	group	mean	sd	n
tumour size (mm)	gain	37.1	26.9	11
tumour size (mm)	loss	26.0	14.0	77
tumour size (mm)	wild_type	25.0	14.5	378

(D)

group1	group2	p	p.adj	p.format	p.signif	method
loss	wild_type	0.32464	0.42	0.325	ns	Wilcoxon
loss	gain	0.21108	0.42	0.211	ns	Wilcoxon
wild_type	gain	0.09251	0.28	0.093	ns	Wilcoxon

(G)

GRADE	gain	loss	wild_type
I	0	5	64
II	4	21	163
III	6	50	143

(H)

group1	group2	p_value	p_format	method	alt_hyp
gain	loss	7.290068e−01	n.s	Fisher	two.sided
gain	wild_type	2.663759e−01	n.s	Fisher	two.sided
wild_type	loss	6.339375e−05	6.3e−05	Fisher	two.sided

(I)

stage_type	gain	loss	wild_type
Early	8	51	271
Late	1	9	25

(J)

group1	group2	p_value	p_format	method	alt_hyp
gain	loss	1.0000000	n.s	Fisher	two.sided
gain	wild_type	0.5565269	n.s	Fisher	two.sided
wild_type	loss	0.1449919	n.s	Fisher	two.sided

(E)

ln_status	gain	loss	wild_type
N0	5	34	206
N1	5	24	116
N2	1	14	48
N3	0	5	12

(F)

group1	group2	p_value	p_format	method	alt_hyp
gain	loss	0.8452014	n.s	Fisher	two.sided
gain	wild_type	0.7784404	n.s	Fisher	two.sided
wild_type	loss	0.1736633	n.s	Fisher	two.sided

Table 3.3.2.A.1

(A)

Feature	group1	group2	p	p.adj	p.format	p.signif	method
age	wild_type	loss	0.1760597	0.53	0.18	ns	Wilcoxon
age	wild_type	gain	0.4105191	0.82	0.41	ns	Wilcoxon
age	loss	gain	0.9918518	0.99	0.99	ns	Wilcoxon

(B)

Tumour Size	gain	wild_type	loss
Large	21	708	53
Small	8	251	21

(C)

Node Status	gain	wild_type	loss
N0	16	477	43
N1	7	346	18
N2	7	104	8
N3	2	71	6

(D)

Stage	gain	wild_type	loss
Early	17	481	43
Late	15	488	32

Table 3.3.2.A.2

A)

Gene	group1	group2	p	p.adj	p.format	p.signif	method
ESR1	wild_type	loss	0.5642636	1	0.56	ns	Wilcoxon
ESR1	wild_type	gain	0.4802821	1	0.48	ns	Wilcoxon
ESR1	loss	gain	0.8311771	1	0.83	ns	Wilcoxon

(C)

pam50	gain	loss	wild_type
Basal	8	16	166
Her2	3	9	69
LumA	12	34	525
LumB	9	14	197
Normal	0	2	39

B)

Gene	group1	group2	p	p.adj	p.format	p.signif	method
YAP1	wild_type	loss	0.02567026	0.077	0.026	*	Wilcoxon
YAP1	wild_type	gain	0.88872856	0.890	0.889	ns	Wilcoxon
YAP1	loss	gain	0.16625823	0.330	0.166	ns	Wilcoxon

D)

pam50	group1	group2	n	percent	pvalue	p.format
LumA	gain	loss	12	2.1%	0.5918733	0.59 (n.s)
LumA	loss	wild_type	34	6.0%	0.2731034	0.27 (n.s)
LumA	wild_type	gain	525	91.9%	0.1325846	0.13 (n.s)

(E)

pam50	group1	group2	n	percent	pvalue	p.format
LumB	gain	loss	9	4.1%	0.4045881	0.4 (n.s)
LumB	loss	wild_type	14	6.4%	0.9403595	0.94 (n.s)
LumB	wild_type	gain	197	89.5%	0.3457631	0.35 (n.s)

F)

pam50	group1	group2	n	percent	pvalue	p.format
Her2	gain	loss	3	3.7%	0.9526258	0.95 (n.s)
Her2	loss	wild_type	9	11.1%	0.1598453	0.16 (n.s)
Her2	wild_type	gain	69	85.2%	0.8529860	0.85 (n.s)

(G)

pam50	group1	group2	n	percent	pvalue	p.format
Basal	gain	loss	8	4.2%	0.8703490	0.87 (n.s)
Basal	loss	wild_type	16	8.4%	0.3753641	0.38 (n.s)
Basal	wild_type	gain	166	87.4%	0.3155087	0.32 (n.s)

Table 3.3.2.B:

(A)

Feature	group1	group2	p	p.adj	p.format	p.signif	method
age	wild_type	loss	0.5477217	1	0.55	ns	Wilcoxon
age	wild_type	gain	0.4865193	1	0.49	ns	Wilcoxon
age	loss	gain	0.8314596	1	0.83	ns	Wilcoxon

(B)

Tumour Size	gain	wild_type	loss
Large	8	346	22
Small	4	161	11

(C)

Node Status	gain	wild_type	loss
N0	5	249	17
N1	4	188	8
N2	2	49	4
N3	1	39	5

(D)

Stage	gain	wild_type	loss
Early	5	261	18
Late	7	247	16

(E)

Metastasis	gain	wild_type	loss
M0	11	418	27
M1	0	9	0

Table 3.3.2.C:

(A)

Feature	group1	group2	p	p.adj	p.format	p.signif	method
age	wild_type	loss	0.09181527	0.28	0.092	ns	Wilcoxon
age	wild_type	gain	0.42986918	0.86	0.430	ns	Wilcoxon
age	loss	gain	0.82532801	0.86	0.825	ns	Wilcoxon

(B)

Tumour Size	gain	wild_type	loss
Large	6	152	11
Small	2	34	3

(C)

Node Status	gain	wild_type	loss
N0	3	84	6
N1	2	74	4
N2	3	28	3
N3	1	11	1

(D)

Stage	gain	wild_type	loss
Early	4	82	4
Late	5	110	10

(E)

Metastasis	gain	wild_type	loss
M0	9	168	12
M1	0	4	1

Table 3.3.2.D:

(A)

Feature	group1	group2	p	p.adj	p.format	p.signif	method
age	wild_type	gain	0.3819723	1	0.38	ns	Wilcoxon
age	wild_type	loss	0.5838684	1	0.58	ns	Wilcoxon
age	gain	loss	0.5784348	1	0.58	ns	Wilcoxon

(B)

Tumour Size	gain	wild_type	loss
Large	2	51	6
Small	1	13	3

(C)

Node Status	gain	wild_type	loss
N0	2	25	6
N1	1	25	2
N2	0	10	1
N3	0	9	0

(D)

Stage	gain	wild_type	loss
Early	3	28	7
Late	0	39	2

(E)

Metastasis	gain	wild_type	loss
M0	3	60	7
M1	0	3	0

Table 3.3.2.E:

(A)

Feature	group1	group2	p	p.adj	p.format	p.signif	method
age	wild_type	gain	0.8941817	1	0.89	ns	Wilcoxon
age	wild_type	loss	0.4063554	1	0.41	ns	Wilcoxon
age	gain	loss	0.4997193	1	0.50	ns	Wilcoxon

(B)

Tumour Size	gain	wild_type	loss
Large	5	129	13
Small	1	32	3

(C)

Node Status	gain	wild_type	loss
N0	6	98	13
N1	0	49	3
N2	2	13	0
N3	0	6	0

(D)

Stage	gain	wild_type	loss
Early	5	92	13
Late	3	69	3

(E)

Metastasis	gain	wild_type	loss
M0	7	145	12
M1	0	4	0

Table 3.3.2.F:

(A)

Feature	group1	group2	p	p.adj	p.format	p.signif	method
age	wild_type	gain	0.8803023	0.88	0.88	ns	Wilcoxon
age	wild_type	loss	0.1586327	0.48	0.16	ns	Wilcoxon
age	gain	loss	0.3422035	0.68	0.34	ns	Wilcoxon

(B)

Tumour Size	gain	wild_type	loss
Large	6	193	12
Small	4	77	3

(C)

Node Status	gain	wild_type	loss
N0	6	127	11
N1	2	110	3
N2	2	30	2
N3	0	15	0

(D)

Stage	gain	wild_type	loss
Early	7	136	12
Late	3	137	4

(E)

Metastasis	gain	wild_type	loss
M0	10	250	15
M1	0	3	0

Table 3.3.2.G:

(A)

Feature	group1	group2	p	p.adj	p.format	p.signif	method
age	Low	High	0.8087083	0.81	0.81	ns	Wilcoxon

(B)

Tumour Size	High	Low
Large	34	38
Small	10	6

(C)

Node Status	High	Low
N0	27	18
N1	11	21
N2	4	8
N3	5	0

(D)

Stage	High	Low
Early	26	17
Late	20	30

(E)

Metastasis	High	Low
M0	43	40
M1	0	2

Table 3.3.2.H:

(A)

Feature	group1	group2	p	p.adj	p.format	p.signif	method
age	Low	High	0.6342309	0.63	0.63	ns	Wilcoxon

(B)

Tumour Size	High	Low
Large	62	85
Small	42	22

(C)

Node Status	High	Low
N0	55	46
N1	44	34
N2	5	16
N3	6	14

(D)

Stage	High	Low
Early	60	48
Late	45	61

(E)

Metastasis	High	Low
M0	87	96
M1	2	2

Chapter 4: Function of *PTPN11*/SHP2 in tumorigenesis of breast epithelial cells

4.1.1: Introduction

Src homology phosphatase 2 (SHP2) encoded by the *PTPN11* gene is one of the few phosphatases to function as an oncogene (S. Zhao, Sedwick, and Wang 2015). *PTPN11*/SHP2 has two N terminal SH2 domains, N-SH2 and C-SH2, a middle phosphatase domain, and a C terminal proline-rich tail with tyrosine 542 and 580 phosphorylated by Src Kinases (Neel, Gu, and Pao 2003; S. Zhao, Sedwick, and Wang 2015). Characterization of phosphorylation profile regulated by *PTPN11*/SHP2 activity and its localization has identified 53 different proteins including ERK, P38, and many adhesion kinases (Corallino et al. 2016). Among other bonafide targets, *PTPN11*/SHP2 is known to facilitate dephosphorylation of B catenin and enable VE-Cadherin recovery at adheren junctions of endothelial cells (Timmerman et al. 2012). Furthermore, *PTPN11*/SHP2 targets Tyr117 of Vimentin and prevent lamellipodia formation and cell migration in MEFs and NIH3T3 cells (Yang et al. 2019). Besides, *PTPN11*/SHP2 also promotes Tks5 dephosphorylation in Src transformed Mouse Embryonic Fibroblast (MEFs) and NIH3T3 to reduces podosome rosette formation and cell migration (Y. R. Pan et al. 2013).

In the context of cell cycle regulation, depletion of *PTPN11*/SHP2 interferes with checkpoint kinase 1 (CHK1) activation and delay in both Cyclin E accumulation and G1-S arrest (Tsang et al. 2012). Moreover, catalytically active *PTPN11*/SHP2 modulates Polo-like Kinase 1 (PLK1) and Aurora B activity to regulate chromosomal alignment, restoring checkpoint function at metaphase (Liu, Zheng, and Qu 2012). Alternatively, kinase-inactive *PTPN11*/SHP2 is involved in regulating the nuclear Cell Division Cycle (CDC) 25C translocation to the cytoplasm through 14-3-3β and inducing G2-M arrest (L. Yuan et al. 2005).

In response to DNA damage, the phosphatase activity of nuclear *PTPN11*/SHP2 is shown to be enhanced in embryonic fibroblast cells to activate c-Abl kinase via its SH3 domain which stabilizes P73 and allow transcription of target genes including $P21^{Cip1}$ and initiate apoptosis (L.

Yuan et al. 2003). Besides, *PTPN11*/SHP2 along with Protein Tyrosine Phosphatase 1B (PTP-1B) and Phosphatase and Tensin homolog (PTEN) has been reported to mediate Rb/E2F associated apoptosis possibly by caspase8 and caspase3 activation (Morales et al. 2014).

The tumor suppressor role of *PTPN11*/SHP2, if any, has been recently reported in hepatocellular cancer (Bard-Chapeau et al., 2011) and oesophageal squamous cell cancer (Qi et al., 2017) by dephosphorylation of the phosphorylated Signal Transducer and Activator of Transcription factor 3 (pSTAT3). In the context of breast cancer, *PTPN11*/SHP2 functions as an oncogene by repressing let-7 miRNAs in HER2 overexpressing breast epithelial cells (Aceto et al. 2012).

4.1.2: Literature survey of the role of *PTPN11*/SHP2 upon DNA damage

We also looked into the publicly available literature on the role of *PTPN11*/SHP2 in DNA Damage in various cell systems. In our understanding, cell cycle checkpoint activation and cell cycle arrest are tightly regulated processes and involves a myriad of kinases: Ataxia telangiectasia (ATM) /ATM and Rad3 related (ATR), c-Abl, CHK1/CHK2, and P38 and phosphatases like Cdc25A, Cdc25B, Cdc25C, and Wee1-Myelin Transcription Factor 1 (MYT1) (Bulavin, Amundson, and Fornace 2002). Cdc25A functions mostly during early to late G1 along with Cdc25B and Cdc25C and allows S-phase entry by promoting dephosphorylation and activation of CDK2-CyclinE and Cyclin-Dependent Kinase (CDK) 2-Cyclin A complexes; Cdc25A, Cdc25B, and Cdc25C co-operate to promote mitotic entry by dephosphorylating and activating CDK1-CyclinB during G2-M transition (Boutros, Dozier, and Ducommun 2006). Upon DNA damage in the G1-S phase in HeLa cells, Phospho SHP2-Y542 induces CHK-1 Ser 317 phosphorylation by an unknown mechanism and helps in G1-S arrest and DNA repair (Tsang et al. 2012). Alternatively, SHP2 also helps in cell cycle arrest at the G2-M phase of the cell cycle in a catalytically independent manner as inactive SHP2 C459S was able to prevent nuclear translocation of Cdc25C and inhibit mitotic entry (L. Yuan et al. 2005).

Exposure to genotoxic stress later in the cell cycle, ATM activates P38 and CHK1 / CHK2; besides P38 phosphorylates Cdc25B and Cdc25C at Ser309 and Ser216 respectively (Han and Sun 2007). In an independent study, CHK1 is reported to phosphorylate Ser216 residue of Cdc25C and create a docking site of 14-3-3β that allows Cdc25C and 14-3-3β interaction and translocation to the cytoplasm, preventing entry into mitosis (Peng et al. 1997). *PTPN11*/SHP2 constitutively associates with 14-3-3β and helps in this G2-M arrest upon DNA damage by stabilizing the

interaction between Cdc25c and 14-3-3β in embryonic fibroblast immortalized by SV-40 T antigen (L. Yuan, Yu, and Qu 2003).

Extracellular signal Regulated Kinase (ERK) 1/2 activity is known to induce apoptosis in P53 independent manner but ATM-dependent manner by upregulating $p21^{cip}$ genes (Tang et al. 2002). Yuan, Yu, & Qu, 2003 also showed pP38 activity did not affect G2-M arrest in wild type but alters G2-M arrest in $SHP2^{\Delta/\Delta}$ cells. The role of P38 in DNA damage has been independently studied, pP38 allows AKT mediated phosphorylation of E1 associated Protein 300 (EP300) at Ser 1834 as observed in normal human fibroblast to enable acetylation of DNA lesions which relaxes the DNA around these lesions and let DNA repair genes recognize the damage followed by subsequent degradation of EP300 and recruitment of nucleotide excision repair machinery at the site of damage (Wang et al. 2013). We hypothesize *PTPN11*/SHP2 controls p38 activation and EP300 stabilization, knockdown of *PTPN11*/SHP2 allows degradation of EP300 and hence its target P73 and inhibits cell death.

Alternately, during DNA damage, *PTPN11*/SHP2 suggested to promote c-Abl activation, such that the deletion of 46-110 amino acid of the N-terminal region of SHP2 was sufficient to induce resistance to cell death upon cisplatin treatment and decrease P73 and $p21^{cip}$ levels needed to induce apoptosis; *PTPN11*/SHP2 via its SH2 domain is constitutively and physically associated with c-Abl SH3 domain and regulates DNA damage-induced apoptosis via P73 stabilization (L. Yuan et al. 2005). c-Abl associates with 14-3-3 and remain sequestered in the cytoplasm, however, is translocated to the nucleus by JNK phosphorylation of 14-3-3 and P73 phosphorylation together with acetylation by EP300 to form P73-EP300-Pin1 complex. This prevents ubiquitin-mediated proteasomal degradation by ITCH, an E3 ubiquitin ligase, and transcription of P73 responsive genes, including pro-apoptotic and P21 mediated cell cycle arrest genes (Costanzo et al. 2014b). Besides c-Abl further mediates YAP phosphorylation at Tyr 357 upon DNA damage and this allows YAP to change its binding partner from Runt related transcription factor 1 (RUNX1) to P73 via its WW domain preventing the binding of ITCH and recruitment of P73 to pro-apoptotic gene promoters like BAX (Levy et al. 2008).

PTPN11/SHP2 also activates PLK1 to phosphorylate BUBR1 and activate Aurora B kinase to localize it on the kinetochore for proper formation of kinetochore to spindle mitotic tubules and

formation of metaphase plate as observed in HeLa cells (Liu, Zheng, and Qu 2012). A summary of our literature survey is presented in the flowchart below:

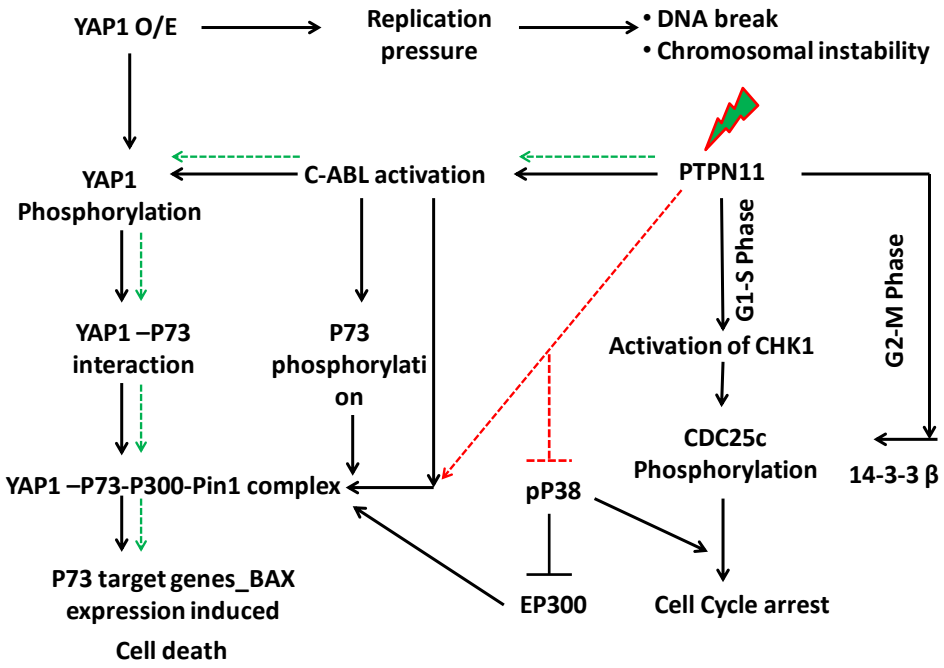

To assess any putative tumor suppressor role of loss of *PTPN11*/SHP2 in breast cancer as observed in our breast cancer clinical metadata analysis (in Chapter 3), we knocked down *PTPN11*/SHP2 in MCF10A, a non-transformed breast epithelial cell line. We sought to verify the possible tumor suppressor role of *PTPN11*/SHP2 by studying the effects of its loss in the transformation of, otherwise, normal breast epithelial cells. Using normal cells was important to examine the molecular context of its tumor suppressor role unperturbed by hormonal receptor signaling. We report *PTPN11*/SHP2 knockdown in MCF10A promotes hallmarks of cancer like an increase in migration and a decrease in chemosensitivity to epirubicin without affecting proliferation. The knockdown of *PTPN11*/SHP2 functions as a negative regulator of tumorigenesis at least in MCF10A, as observed in our study.

4.2: Methods

Cell culture

MCF10A cells were harvested in DMEM media from thermofisher scientific (#10566-016) with 100units/ml of Penstrep (#15140122). Growth media was supplemented with 5% horse serum (#26050088, GIBCO) and 20ng/ml of EGF (#E9644, Sigma), 0.5ug/ml of hydrocortisone (#H0888-5G, Sigma), 100ng/ml of cholera toxin (#C8052-1MG, Sigma) and 10ug/ml of insulin (# I1882-100MG, Sigma).

Mycoplasma Testing

Cells were routinely checked for mycoplasma contamination and cleared (if any) using LookOutO mycoplasma elimination Kit (#MP0030).

Cell Passaging

Monolayer MCF10A cells from passage 23 to passage 32 were used for all experiments. Media from monolayer cells was aspirated, rinsed with DPBS (3D8537-500ML), and trypsinised for 10-15 mins using 0.05% Trypsin EDTA (# 25300054, Thermofisher Scientific). The cells were incubated at 37 degrees C, 5% CO2; dissociated cells were resuspended in DMEM with 10% horse serum and centrifuged at 2000 RPM, 6mins. Cells were seeded in a 1:4 ratio and they reach confluency of 80-90% by 3-4 days. The cells were cultured for 6 passages at any time and discarded.

siRNA transfection

Cells were seeded at 0.16 million per 6 well and scaled down according to the plate used. 24 hours post-seeding, cells were rinsed in DPBS and grown in serum-free media (growth media without horse serum and pen strep) 24 hours before transfection. Cells were transfected using lipofectamine RNAi max (#13778150, Thermofisher Scientific) and two independent Accell *PTPN11* siRNA, Targeted Region: 3'UTR (A-003947-18-0005, denoted as **#18** and A-003947-19-0010, denoted as **#19**) at 500nM and 1uM concentrations, respectively, in serum-free media. The equimolar concentration of *LACZ* siRNA was used as a control for each. 24 hours post-transfection, the transfection media was aspirated out and cells were replenished with growth

media. Following 48 hours of transfection, growth media was aspirated out and cells were rinsed in serum-free media 1 hour before the second shot of transfection. Cells were again transfected and 48 hours post-second transfection all experiments were carried out. All experiments were carried out using both the siRNA, data for si18 is shown. Knockdown efficiency was 60-70% estimated at the protein level. The sequences of *LACZ* siRNA used is below:

LACZ: 5'-CGUACGCGGAAUACUUCGA-3'

3'-GCAUGCGCCUUAUGAAGCU-5'

(dTdT overhang)

RNA isolation and qPCR

Total RNA was isolated using TRIzol reagent (Sigma) and estimated using nanodrop. 500ng RNA was converted to cDNA with superscript III first-strand synthesis for RT-PCR (#1191-7010). Synthesized RNA was diluted in DNAse free water and mixed with SYBR fast qPCR master mix from Kappa biosystems (KK4601) and processed using the BioRad CFX96 real-time qPCR system. All mRNA quantification of the target gene was optimized to housekeeping control, GAPDH, or an average of housekeeping controls (ACTB, RPLPO, or PUM1) and quantitated using the ΔΔCT method or average RNU. Primer sequences used are as follows:

Gene	Sequence
PTPN11	F: CGGAAAGTGTGAAGTCTCCAG
	R: GCGGGAGGAACATGACATC
YAP1	F: ACGTTCATCTGGGACAGCAT
	R: GTTGGGAGATGGCAAAGACA
GAPDH	F: AATGAAGGGGTCATTGATGG
	R: AAGGTGAAGGTCGGAGTCAA
B-Actin	F: TTCCTGGGCATGGAGTC
	R: CAGGTCTTTGCGGATGTC
RPLPO	F: GGCTGTGGTGCTGATGGGCAAGAA
	R: TTCCCCCGGATATGAGGCAGCAGT
PUM1	F: CCGGAGATTGCTGGACATATAA
	R: TGGCACGCTCCAGTTTC

Cell lysis and western blotting

Cells were washed thrice in ice-cold DPBS, followed by the addition of cell lysis buffer (RIPA: 20mM Tris (pH=8), 420mM NaCl, 10% glycerol, 0.5% NP40, 0.1mM EDTA, water to add up the volume) and incubated in ice for 40 mins to allow complete lysis. The lysates were collected using a cell scraper and centrifuged at 13,000 RPM, 15mins. The supernatant was collected in labelled tubes and mixed with 1X lamelli buffer and heated at 95 degrees, 5mins. SDS PAGE was run at 70V in stacking gel and at 100V in resolving gel and then transferred to the PVDF membrane for 90mins at 90V and 4-degree C. The transferred membrane was blocked in 5% BSA or 5% Milk for 1 hour followed by the addition of primary antibody in 2% BSA or 2% Milk and then incubated overnight at 4-degree C. The following day, the primary antibody was removed and the membrane was washed thrice with (0.1%) TBST. A secondary antibody conjugated to HRP was added in 1:10,000 dilutions in 2% BSA or 2% milk and incubated for 1hour at room temperature. Secondary antibody incubation was followed by 0.1% TBST wash and developed using an ECL kit (Merck). Densitometry analysis was used for quantitation of protein expression levels using Image J. The expression levels were normalized to housekeeping genes, GAPDH, or β Actin.

Cell Number

PTPN11/SHP2 knocked down cells were trypsinised and centrifuged at 2000 RPM, 6mins. The cell pellets were dissolved in 1ml growth media and counted using a haemocytometer.

Cell Size

Immunofluorescence images were captured at 63x oil objective in Leica SP8 confocal microscope. ROI of each cell was calculated for the area using Image J. A total of 100 cells across 3 biological replicates were analysed.

Cell morphology

Immunofluorescence images were captured at 63x oil objective in Leica SP8 confocal microscope. At least 60% of the cell population were imaged and analysed for change in morphology.

MTT assay

10ul of 5mg/ml of MTT (#M5655-100MG) was added to 100ul of cells in growth media. Growth media alone is used as a blank. We incubated the cells after MTT addition for 3.5 hours at 37-degree C and aspirated the media with MTT. Post 3.5 hours, 100ul of DMSO (#D2438-50ml, Sigma) added, kept in a shaker for 5mins and measured absorbance at 570nM and 650nM.

Immunofluorescence microscopy

Growth media was aspirated and cells were rinsed in DPBS. Cells were fixed with 4% PFA (Sigma) for 10mins. PFA was aspirated and cells were rinsed again in PBS, for 10mins each, repeated thrice. Cells were permeabilised and blocked with 2% FBS in 0.03% PBST (30ul Triton X (Sigma) in 10ml DPBS) for 30mins. Following permeabilization, the primary antibody was diluted in DPBS before adding and incubated overnight at 4-degree C. Following primary incubation, cells were rinsed in 0.05% PBST (5ul Tween20 (Sigma) in 10ml DPBS) for 10mins each, repeated thrice. Cells were mounted in prolong gold Antifade DAPI or incubated in DAPI (1:1000) for 1 min and washed with DPBS before mounting (#P36931 and D9542).

Wound healing assay

Monolayer cells were treated with 10ug/ml of mitomycin C (Sigma M4287) for 2 hours before initial scratch. Cells were wounded using a 10ul sterile micropipette tip. Scratch was rinsed with DPBS, following which growth media were added to wells. Cells were acclimatized at 37-degree C for 10mins before recording a 0-hour wound distance. 3 areas per sample were recorded. 24 hours post initial wound, images of the same area recorded at 0-hour were re-measured with EVOS FL Auto. Wound distance was calculated using ImageJ, grid lines 1, 3, 5, and 7 were used for all analyses, and an average of a total of 12 data points per sample was used for all analyses. For analysis, 24-hour wound distance was subtracted from 0-hour wound distance and normalized to 0-hour wound distance (as the initial scratch was not the same across samples) and multiplied by 100 (percentage wound closure). We performed a double normalization by subtracting the percentage wound closure of every sample from its control siLACZ. Data points were plotted in GraphPad prism.

Transwell invasion assay

K913-24 transwell assay kit was used to compare the invasion capacity of *PTPN11*/SHP2 knockdown cells. For invasion assay, we serum-starved *PTPN11*/SHP2 knockdown cells at 72 hours of knockdown (18-24 hours before invasion assay). Post which cells were then trypsinised and seeded at a concentration of 0.5-1 million cells/collagen-coated wells. The standard curve was plotted using MCF10A and growth media was used as blank. 24 hours later, cells that migrated to the lower chamber were processed using the manufacturer's protocol.

Flow cytometry and cell cycle analysis

Cells were trypsinised and centrifuged at 2000 RPM, 6mins. The cell pellet was washed with DPBS by gentle vortexing and centrifuged at 2000 RPM, 6mins. The step was repeated twice. Following DPBS wash, cells were fixed in ice-cold 70% ethanol for 30 mins. Post fixation samples were centrifuged at 2000 RPM, 6mins. The cell pellet was washed with DPBS and centrifuged again at 2000 RPM, 6mins. Cells were treated with RNAse (DS0003) (to remove any RNA contamination) for 5mins in ice. Following incubation, 5ul of Propidium Iodide (PI) in a 1million cells/sample was added 5mins before the acquisition. The samples were acquired in BD FACS Calibur and BD FACS Celesta. An analysis was performed in BD software.

Apoptosis

Following epirubicin treatment for 24 hours, cells in media supernatant were collected in labelled tubes. Attached cells were trypsinised and collected in the respective tube and centrifuged at 2000 RPM, 6mins, 4-degree C. Cells were washed with ice-cold DPBS and centrifuged at 2000 RPM, 6mins. The cell pellet was dissolved in ice-cold 90ul 1X Annexin binding buffer and added 5ul of Annexin V and 5ul Propidium iodide. The samples were incubated for 5mins with 0.25mM CaCl2 in dark and imaged and analysed in Operetta, Perkin Elmer.

Antibodies

The following antibodies were used:

Antibody Name	Catalog number	Working Conc.	Dilution in
SHP-2 (D50F2) Rabbit mAb	3397	1:1000	2% BSA
Phospho-SHP-2 (Tyr542) Antibody rabbit mAb	3351	1:1000	2% BSA
Anti-YAP1 antibody [EP1674Y]	ab52771	1:1000	2% Milk
Anti-YAP1 (phospho Y357) antibody	ab62751	1:2000	2% BSA
cABL	2862	1:1000	2% BSA
Anti-p73 antibody [EP436Y]	ab40658	1:5000	2% Milk
Anti-Bax antibody [E63]	ab32503	1:10,000	2% Milk
Anti-gamma H2A.X (phospho S139) antibody [9F3]	ab26350	1:10,000	2% Milk
Anti-Ki67 antibody [EPR3610]	ab92742	1:100	DPBS
Anti-MMP9 antibody [EP1254]	ab76003	1:10,000	2% BSA
Purified Mouse Anti-E-Cadherin Clone 36/E-Cadherin (RUO)	610181	1:1000	2% BSA
Purified Mouse Anti-N-Cadherin Clone 32/N-Cadherin (RUO)	610920	1:1000	2% BSA
Purified Mouse Anti-Fibronectin Clone 10/Fibronectin (RUO)	610077	1:1000	2% BSA
B catenin	#9562S	1:1000/1:500	2% BSA or DPBS
Propidium Iodide - 1.0 mg/mL Solution in Water	P3566	1ul/million cells	DPBS
Annexin V, Alexa Fluor® 488 Conjugate	A13201	5ul/million cells	DPBS
Vimentin	V9 clone, Santacruz	1:1000	2% BSA
B actin	Santacruz	1:1000	2% BSA
Lamin B1	16048	1:1000	2% Milk
B Tubulin	Rg000140	1:2000	2% Milk
GAPDH	RG000110	1:2500	2% Milk
Secondary Anti-Rabbit Alexa 568	Invitrogen, Molecular probes	1:10,000	DPBS
Secondary Anti-Rabbit Alexa 488	Invitrogen, Molecular probes	1:10,000	DPBS
Secondary Anti-Rabbit HRP	Invitrogen, Molecular probes	1:10,000	2% Milk/BSA
Secondary Anti-Mouse HRP	Invitrogen, Molecular probes	1:10,000	2% Milk/BSA
Secondary Anti-Rat HRP	Invitrogen, Molecular probes	1:10,000	2% Milk/BSA

Statistical Analysis

Column statistics (GraphPad Prism) was used for statistical analysis, $p<0.05$ was considered significant. Unpaired T-Test was used for survival assay. P values are flagged as * ($p<0.05$), ** ($p<0.01$) and *** ($p<0.001$).

4.3: Results

4.3.1: siRNA mediated silencing of *PTPN11*/SHP2 in MCF10A

We successfully knocked down *PTPN11*/SHP2 in the monolayer culture of MCF10A with two independent siRNAs. We achieved 50-70% depletion of SHP2 protein (A, B) and 80-90% depletion of *PTPN11* mRNA expression (C) in si18/19 transfected MCF10A cells.

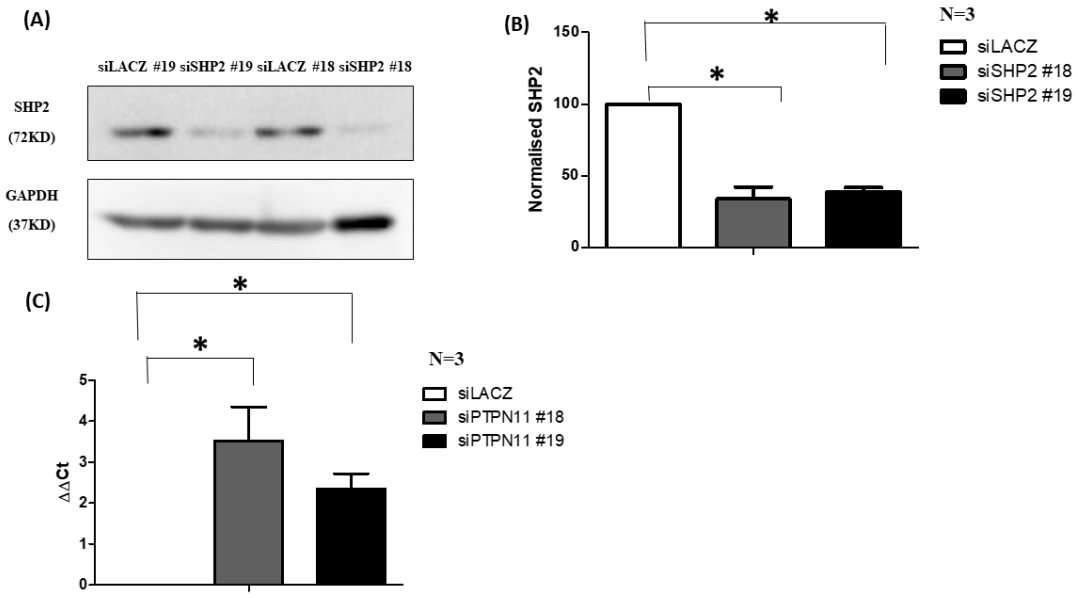

Figure 4.3.1: (A) Western blot (WB) showing expression of *PTPN11*/SHP2 in MCF10A transfected with individual *PTPN11*/SHP2 siRNA #18 and #19, GAPDH was used as a loading control. (B) Densitometric analysis of the protein expression level shows a 60% knockdown. (C) qPCR of *PTPN11* mRNA in MCF10A transfected with individual siRNA #18 and #19 shows 2.5-3.5 CT difference from LACZ control, data normalized to the average of housekeeping gene controls, β-Actin, Pum1, and RPLPO.

4.3.2: Effect of PTPN11/SHP2 knockdown on the transformation of MCF10A

4.3.2A: Effect of PTPN11/SHP2 knockdown on proliferation and survival

We report from our clinical data analysis of TCGA RPPA in chapter 3, low expression of Phospho-SHP2Y542 correlates to significantly larger tumor size in breast adenocarcinoma. To understand the role of *PTPN11*/SHP2 expression alone in proliferation and survival of breast epithelial cells we looked at a widely used proliferation marker, Ki67, upon *PTPN11*/SHP2 knockdown (A, B). We do not observe any significant change in the proliferation index of MCF10A cells upon *PTPN11*/SHP2 knockdown. We also examined cell survival upon *PTPN11*/SHP2 knockdown by MTT assay for 4 days. We measured cell survival at 72 hours (Day 0), 96 hours (Day 1), 120 hours (Day 2), 144 hours (Day 3) of the first transfection (C, D).

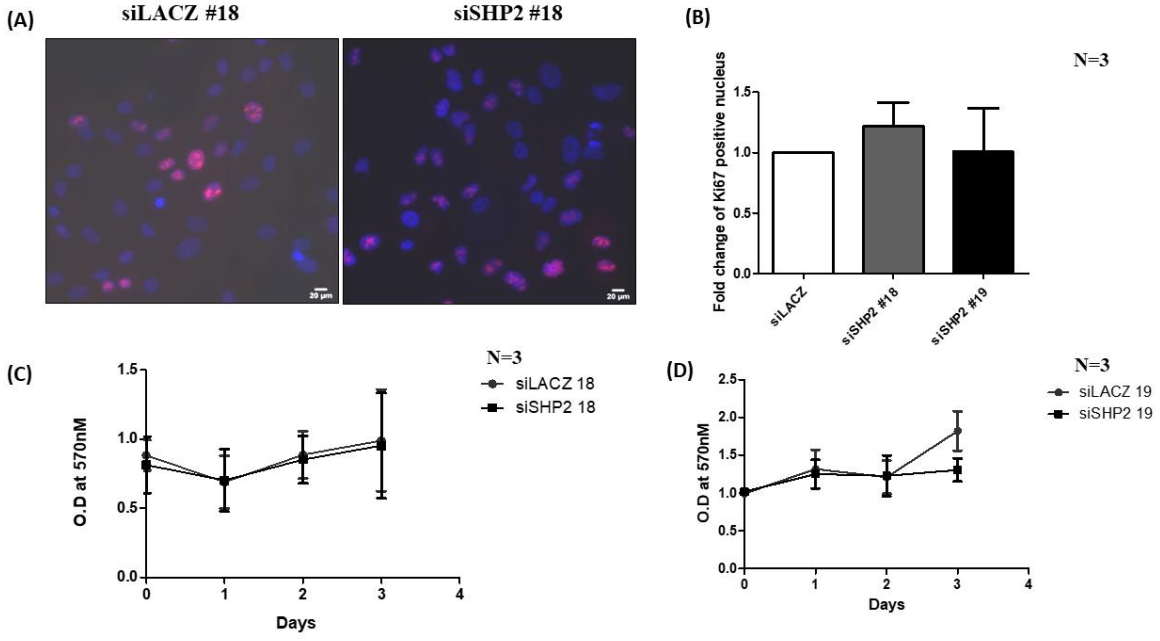

Figure 4.3.2A: (A) Immunofluorescence (IF) images showing proliferation index Ki67, a bonafide proliferation marker in control, and *PTPN11*/SHP2 knockdown cells. Ki67 was probed with a secondary antibody, Alexa 568 (Red), and DAPI stained the nucleus (Blue). We imaged at 20x lens and analysed in Perkin Elmer's Operetta system. We counted the ki67 positive nucleus and normalized to the total number of nucleus per field (n=100 cells). The cells were also imaged at

40x using a DM8 Epifluorescence microscope for the image provided. The image for si18 is shown, however, data was reconfirmed with si19. The scale bar in A is 20uM. (B) shows the quantitation of Ki67 change between SHP2 knockdown cells and control. (C) and (D) shows there was no change observed in cell survival in all 4 days of our assays using siRNA 18 and 19 respectively. Cell survival O.D values were normalized to day 0 and plotted in graph pad prism. For each biological replicate, we had 4 technical replicates.

4.3.2B: Effect of *PTPN11*/SHP2 knockdown on cell cycle

PTPN11/SHP2 has been reported to regulate cell cycle checkpoints including the G1-S transition (Tsang et al. 2012), G2-M phase (L. Yuan et al. 2005), and transition from metaphase to anaphase (Liu, Zheng, and Qu 2012) upon DNA damage. We reconfirmed the effects of *PTPN11*/SHP2 knockdown on the cell cycle pattern in MCF10A and observed no significant change either with si18 or si19. We also assessed the effects of *PTPN11*/SHP2 knockdown upon DNA damage on cell cycle pattern post epirubicin (a DNA damaging drug) treatment for 24 hours. We did not observe changes in cell cycle patterns upon epirubicin treatment in *PTPN11*/SHP2 knockdown MCF10A (Supplementary figure 1A, 1B, 1C).

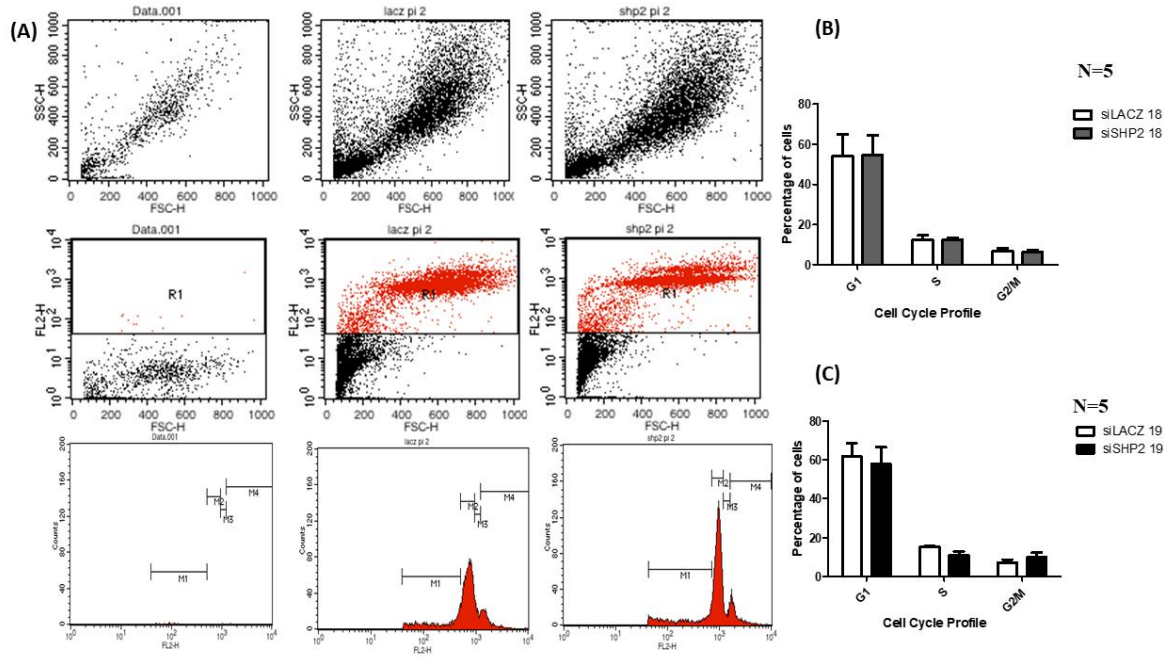

Figure 4.3.2B: (A) Flow analysis showing cell cycle pattern of control and *PTPN11*/SHP2 knockdown cells, with scatter plots showing selected population for analysis and histogram

showing cell cycle phases denoted with gate, M. Flow analysis for si18 is shown, however, data was reconfirmed with si19. M1 which is the sub G1 population was not quantitated in our analysis. For the cell cycle pattern, 10,000 cells were recorded by Flow cytometry after PI staining. (B) and (C) shows quantitation of cell count in G1 (M2), S (M3), and G2/M (M4) phases of the cell cycle, no significant change observed in *PTPN11*/SHP2 knockdown cells with si18 and si19 respectively.

4.3.2C: Effect of *PTPN11*/SHP2 knockdown on cell number and cell size

To re-confirm our observation on the effect of *PTPN11*/SHP2 knockdown on proliferation, we examined changes in cell size (A) and cell number (B) of MCF10A cells. We did not observe any significant change in any growth parameters of MCF10A upon *PTPN11*/SHP2 knockdown in our system.

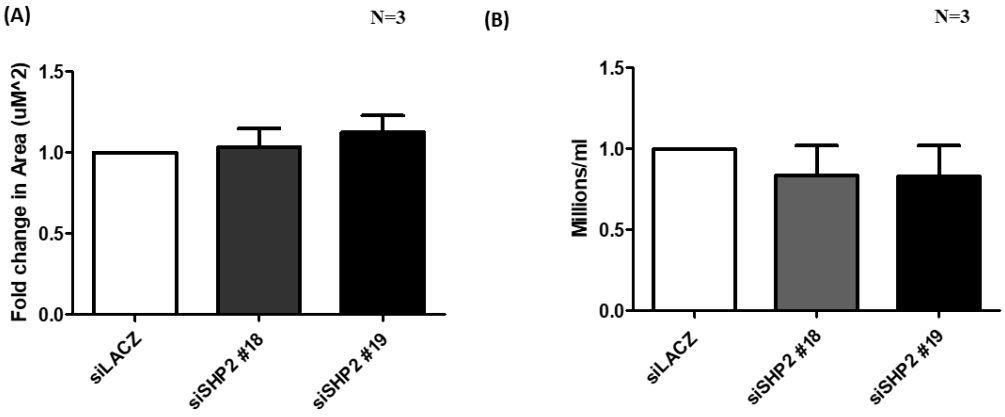

Figure 4.3.2C: (A) Cell size was measured by immunostaining of β-Catenin, an adheren junction protein to mark the borders of the cell. The cell size was quantitated by measuring the ROI of cells (area in um^2). At least 100 cells across 5 fields and 3 biological replicates were recorded for quantitation. There was no change observed in cell size. (B) Quantitation of cell number (Hemocytometer count) did not show any difference in *PTPN11*/SHP2 knockdown cells.

4.3.2D: Effect of *PTPN11*/SHP2 knockdown on migration and invasion

We assessed the effect of *PTPN11*/SHP2 knockdown on other hallmarks of cancer like migration and invasion. We observed *PTPN11*/SHP2 knockdown cells migrate 25% more in 24 hours of initial scratch (A, B). Interestingly, we also observed a change in cell morphology. A confluent

monolayer of MCF10A cells appeared cobblestone-like whereas *PTPN11*/SHP2 knockdown cells acquired mesenchymal or elongated morphology (C). However, we do not observe any change in invasion capacity (measured by fluorescence (D)) of *PTPN11*/SHP2 knockdown cells in both serum-free and media supplemented with 5% horse serum using both si18 (E) and si19 (F).

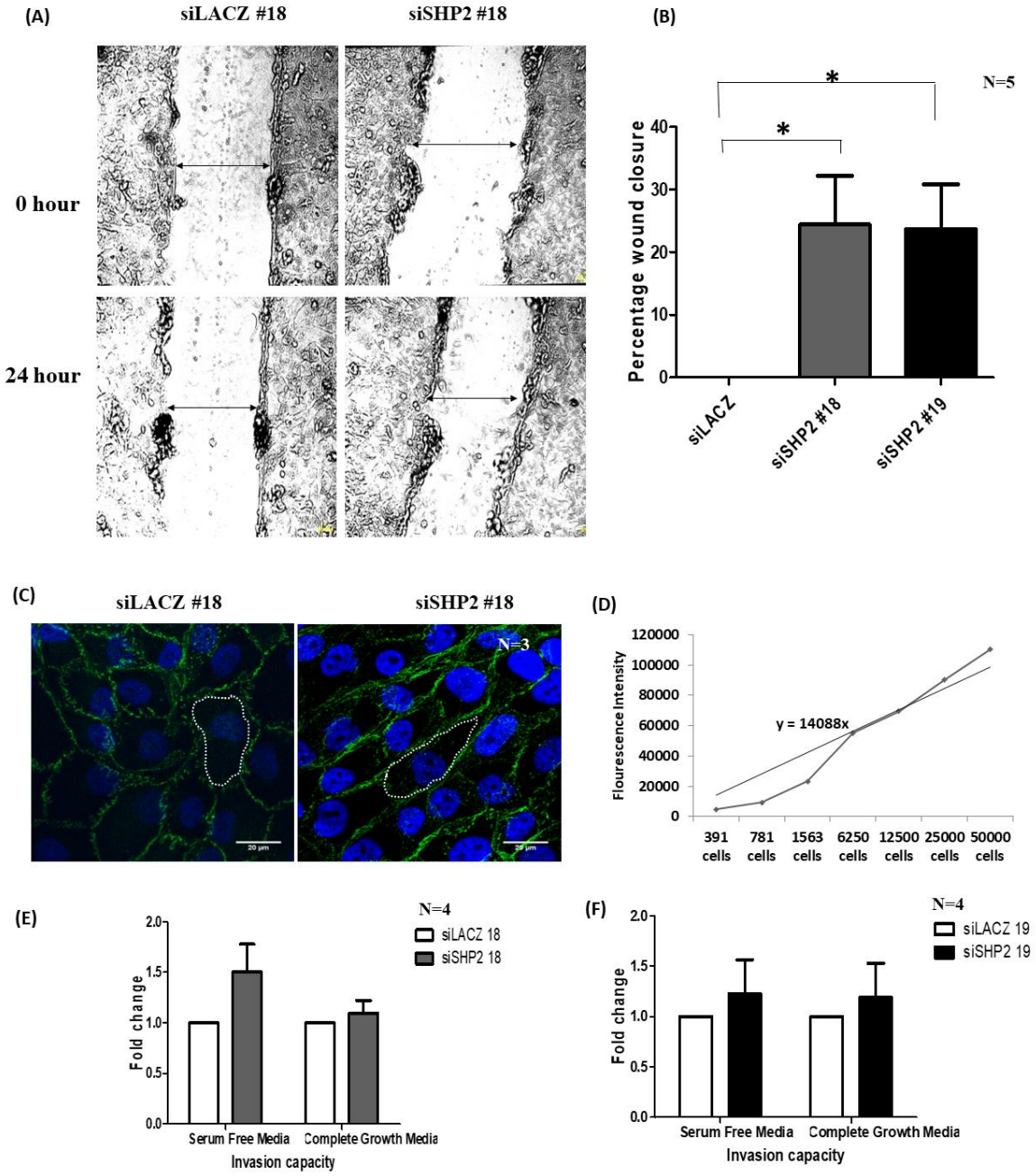

Figure 4.3.2D: (A) Scratch assay showing the initial wound at 0 hours and gap closure post 24 hours of scratch (shown by arrow). (B) Quantitation of the percentage wound closure normalized

to control. (C) shows IF images of MCF10A cells stained with β-catenin, adheren junction protein stained with Alexa 488 (Green), and DAPI (Blue) staining the nucleus. The white inlet is used to show the change in morphology from cobblestone to mesenchymal shape. (D) A standard curve showing fluorescence intensity versus cell number for transwell invasion assay Biovison kit. (E) and (F) shows *PTPN11*/SHP2 knockdown cells do not show any significant changes in the invasion capacity through a matrigel coated transwell when knockdown with si18 and si19 respectively.

4.3.2E: Effect of *PTPN11*/SHP2 knockdown on epithelial to mesenchymal transition status

PTPN11/SHP2 targets Vimentin and inhibits migration (Yang et al. 2019). We examined if *PTPN11*/SHP2 knockdown increases migration and transformation of MCF10A cells to mesenchymal morphology by epithelial to mesenchymal transition (EMT) and activation of mesenchymal markers. We assessed whether *PTPN11*/SHP2 knockdown targets expression of its bonafide target Vimentin, a mesenchymal marker. We also examined other bonafide EMT markers like E-cadherin, N-cadherin, Fibronectin, and Matrix Metalloprotease (MMP) 9. We observed approximately 2-fold increases in MMP9 (B), fibronectin (C), and Vimentin (D) expression but it was not significant across siRNAs. We did not observe any change in E-cadherin levels (E) and could not detect N-cadherin at the desired molecular size (data not shown). Our data suggest *PTPN11*/SHP2 knockdown increases migration due to an increase in other EMT markers as the sub-optimal increases in expression of Vimentin, fibronectin, and MMP9 are not sufficient to drive complete transformation or induce invasion. We also checked for β-catenin levels in the nucleus and cytoplasm by IF, but could not detect any changes in β-catenin levels upon *PTPN11*/SHP2 knockdown (data not shown).

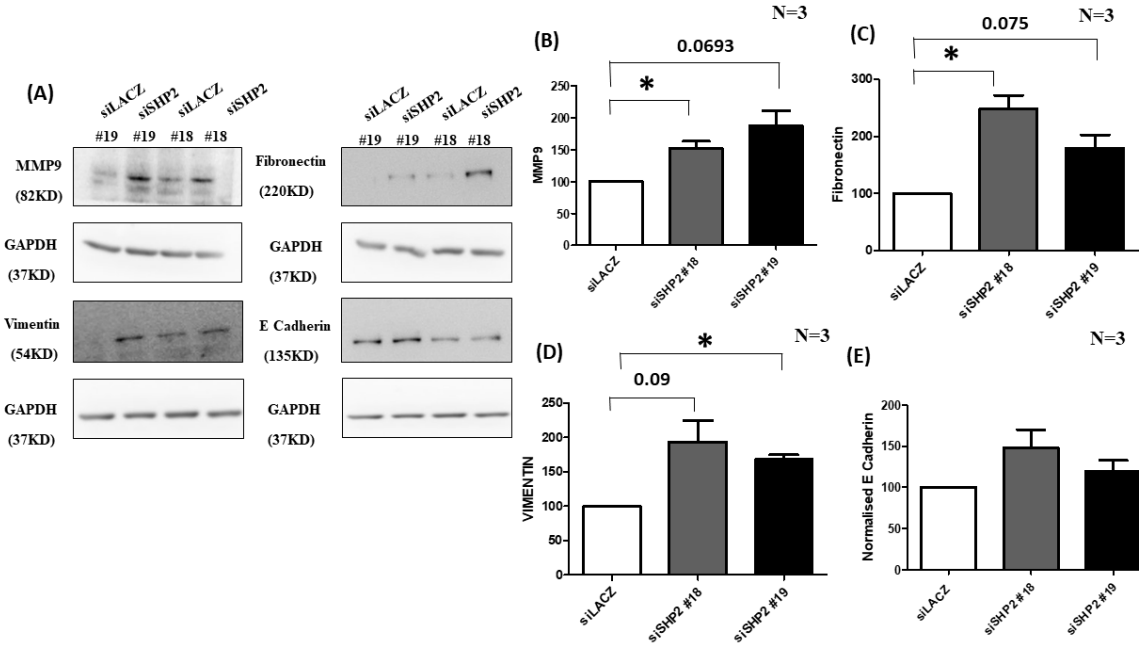

Figure 4.3.2E: (A) shows western blot for total MMP9, Vimentin, Fibronectin, and E cadherin. GAPDH was used as a loading control. Quantitation of representative blots shows a near significant increase in expression of (B) MMP9, (C) fibronectin, and (D) Vimentin but no (E) change in epithelial marker like E-cadherin. There were no detectable N-Cadherin levels in both control and *PTPN11*/SHP2 knockdown cells (data not shown).

4.3.2F: Effect of PTPN11/SHP2 knockdown on sensitivity to chemotherapeutic drugs

As discussed earlier, *PTPN11*/SHP2 plays a major role in cell cycle and DNA damage (Tsang et al. 2012). We, therefore, assessed the effect of *PTPN11*/SHP2 knockdown on chemosensitivity. We treated cells with chemotherapeutic drugs like carboplatin, epirubicin, and paclitaxel (Konecny et al., 2001). Carboplatin inhibits replication and transcription and induces DNA breaks and cell death (Jiang et al. 2015). Epirubicin intercalates between DNA and inhibits DNA and RNA synthesis, it induces double-stranded DNA breaks and cell death (Konecny et al. 2001). Paclitaxel interferes with mitotic spindle assembly and chromosomal segregation and cell death (Jordan and Wilson 2004). We determined the Inhibitory Concentration (IC) 50 of these cell cycle and DNA synthesis interfering drugs. We used concentration in the range of 100uM to 1000uM for carboplatin, 100nM-100uM for epirubicin, and 10nM-100uM for paclitaxel to optimize the

IC50. We observed MCF10A had high IC50 for carboplatin while paclitaxel was not effective in bringing about 50% cell death (Supplementary figure 2A, 2C). Epirubicin with IC50 of 1uM was the drug of choice for further treatments (Supplementary figure 2B). The effectivity of epirubicin (EPR) to introduce double-stranded DNA breaks in cells was measured by phosphorylation of Serine 139 gamma H2AX upregulation in MCF10A cells upon epirubicin treatment for 24hours (Supplementary figure 2D, 2E). We observed *PTPN11*/SHP2 knockdown cells show better survival upon epirubicin treatment for 24 hours at 1uM concentration of the drug (A, B). We examined if *PTPN11*/SHP2 knockdown cells show changes in apoptosis upon EPR treatment. *PTPN11*/SHP2 knocked down cells do not affect ploidy or cell cycle pattern upon EPR treatment (Supplementary figure 1). We observed *PTPN11*/SHP2 knocked cells had a 2-fold decrease in early apoptotic cells (Annexin positive), late apoptotic cells (Annexin+ PI double positive) and dead cells (PI positive) (C, D). We hypothesis from our data, *PTPN11*/SHP2 knockdown interferes with apoptotic marker synthesis and provides survival advantage to MCF10A cells. Our literature survey to understand the role *PTPN11*/SHP2 in DNA damage suggested a putative role of BAX in providing survival advantage to cells upon DNA damage in PTPN11/SHP2 knockdown cells.

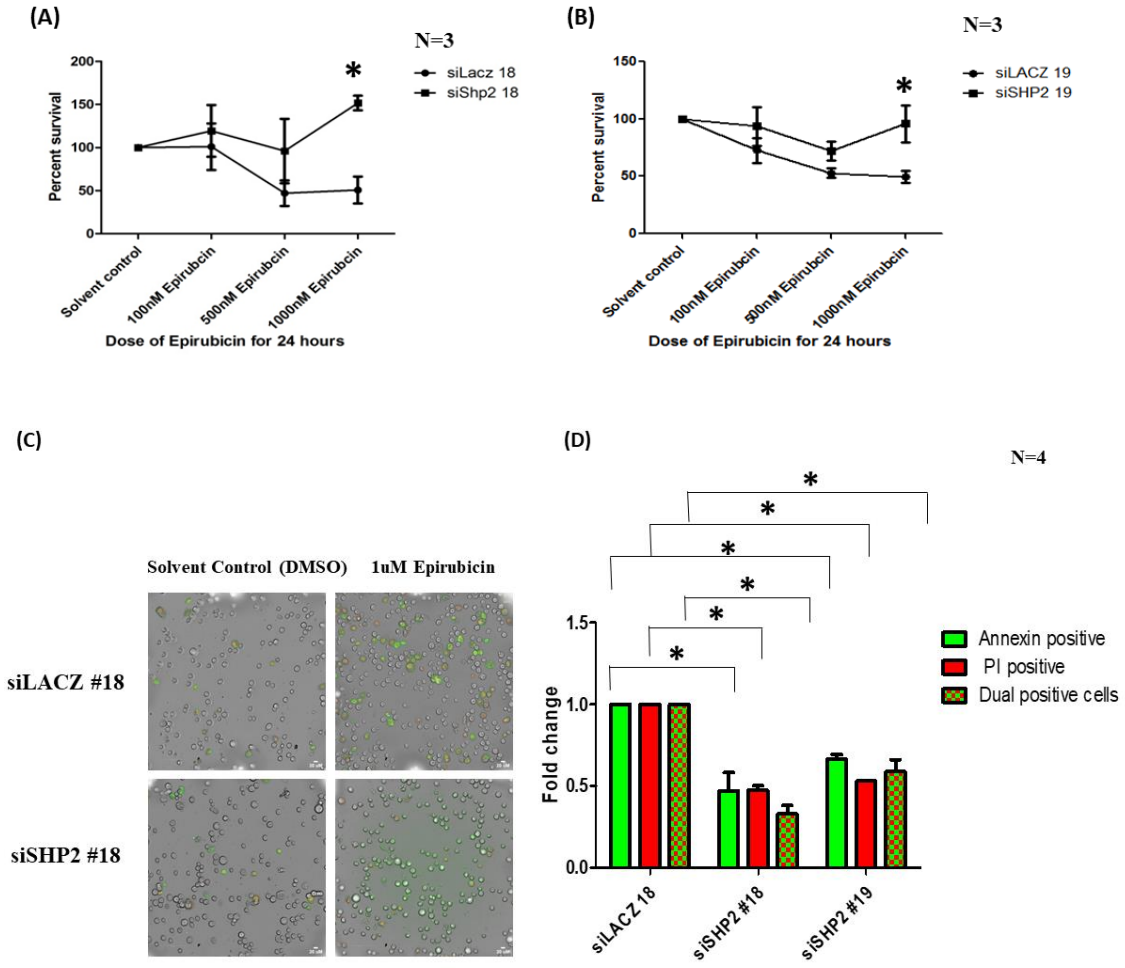

Figure 4.3.2F: (A) and (B) shows the results of MTT assay showing the dose-response curve upon EPR treatment in *PTPN11*/SHP2 knockdown and control cells. We observed an increased survival advantage in *PTPN11*/SHP2 knockdown cells at 1uM concentration of EPR with si18 and si19 respectively. (C) IF images showing the effect on apoptosis upon EPR treatment in *PTPN11*/SHP2 knockdown. The Scale bar is 20uM. (D) Quantitation shows a 2-fold decrease in Annexin positive, Annexin+ PI double-positive, and dead PI-positive cells. IF staining was performed with Annexin V (Alexa 488, green) and propidium iodide (red), imaged with 20X lens, and analyzed in Perkin Elmer operetta.

4.3.2G: Effect of *PTPN11*/SHP2 knockdown on BAX expression upon epirubicin treatment

We have previously shown the role of *PTPN11* upon DNA damage. One of the several aspects of *PTPN11* upon DNA damage is to induce c-Abl and mediate P73 stabilization and induction of apoptosis via BAX as hypothesized from our literature survey (4.1.2). We experimentally confirmed the effect of *PTPN11*/SHP2 knockdown on BAX expression (A). We also checked the expression of Phospho YAP1-Y357, c-Abl, and P73 (data not shown) but we did not observe any significant change in the expression of BAX and other predicted molecules (Data not shown) of our hypothesis (B). We report *PTPN11*/SHP2 employs other apoptotic pathways such that its knockdown decreases apoptosis and increases cellular survival.

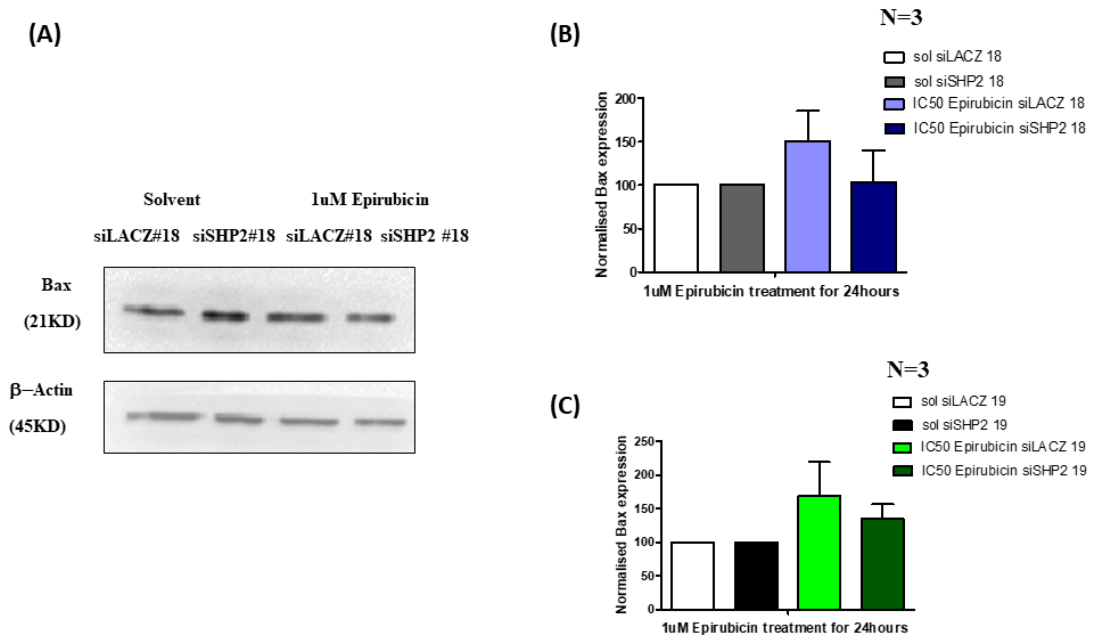

Figure 4.3.2G: (A) Western blot analysis showing the expression of BAX in 24-hour epirubicin (1uM) treated cells. β actin was used as a loading control. (B) and (C) shows densitometry analysis shows *PTPN11*/SHP2 knockdown does not affect BAX expression levels when knocked down with either si18 and si19.

4.4: Discussion

Constitutively active *PTPN11*/SHP2 is reported to function in positive feedback signaling of EGFR and other growth factor receptors (Agazie and Hayman 2003; Neel, Gu, and Pao 2003). Loss of *PTPN11*/SHP2 in HER2 overexpressing MCF10A inhibits breast cancer progression by interfering with tumor-initiating cell maintenance (Aceto et al. 2012). Alternatively, it is reported to inhibit migration and podosome formation by regulating the polymerization of Vimentin (Y. R. Pan et al. 2013; Yang et al. 2019). The overexpression or loss of *PTPN11*/SHP2 in the non-tumorigenic background like MCF10A has not been reported earlier. Our approach was to understand the intrinsic tumorigenic role of *PTPN11*/SHP2 in the non-transformed background using a loss of function genetics. The results of our study show knockdown of *PTPN11*/SHP2 at least in MCF10A functions in priming cells to more migratory behaviour.

The role of *PTPN11*/SHP2 as a putative tumor suppressor from our clinical study in chapter 3 was re-confirmed experimentally. The knockdown of *PTPN11*/SHP2 in MCF10A did not affect any growth parameters but increased migration and chemoresistance. We propose, *PTPN11*/SHP2 being a phosphatase, functions like a key which helps to auto-tune signaling pathways and change cellular fate. We also report *PTPN11*/SHP2 suppression increases vimentin, fibronectin, and MMP9 mesenchymal markers which is not significant enough to increases migration in *PTPN11*/SHP2 knocked down breast epithelial cells. The turnover of these mesenchymal markers is tightly controlled in a non-transformed cell line like MCF10A and *PTPN11*/SHP2 knockdown alone is not sufficient for complete transformation and invasiveness and other players seem to be involved.

In the context of DNA damage, *PTPN11*/SHP2 is reported to regulate death due to DNA damage and cell cycle by regulating Cdc25c, c-Abl, and BAX (Tsang et al. 2012; L. Yuan, Yu, and Qu 2003). Our findings suggest a loss of *PTPN11*/SHP2 provides a survival advantage to the cells by decreasing apoptosis upon DNA damage. However, it is not via BAX as predicted from literature mining studies. BAX being a global apoptotic molecule might be under the control of several signaling pathways and *PTPN11*/SHP2 loss does not alter BAX levels. *PTPN11*/SHP2 could be interacting with other apoptotic markers that need to be further investigated.

Whether or not *PTPN11*/SHP2 is a tumor suppressor is a question that needs detailed context-specific analysis. Inhibition of *PTPN11*/SHP2 is reported to induce a transition to the Basal

subtype from the luminal subtype of breast cancer (H. Zhao and Agazie 2015). The scope of the study allows investigation of the loss of *PTPN11*/SHP2 in 2D monolayer MCF10A cells. MCF10A in monolayer culture expresses both luminal and basal markers (Qu et al. 2015). This study limits the analysis of whether *PTPN11*/SHP2 functions as a tumor suppressor is limited to any subgroup of breast cancer. Since breast cancer is a heterogeneous disease, each requiring a specific therapeutic course, elucidation of *PTPN11*/SHP2 behaviour in specific subtype and individual context becomes more relevant for cancer therapy and diagnosis.

In Summary, our study shows loss of *PTPN11*/SHP2 promotes migratory behaviour and provides survival advantage upon anthracycline treatment in breast epithelial cells, which are evident hallmarks of epithelial cancer. Cell culture validation together with clinical observations in METABRIC 2012 and TCGA RPPA data 2015 (Chapter 3), *PTPN11*/SHP2 is a negative regulator in breast tumorigenesis. Whether like EGFR, prominent oncogene such as YAP1, provides a context to tumorigenic behaviour of a phosphatase like *PTPN11*/SHP2 in breast cancer needs investigation and is discussed in Chapter 5.

4.4: Supplementary data

Figure 1:

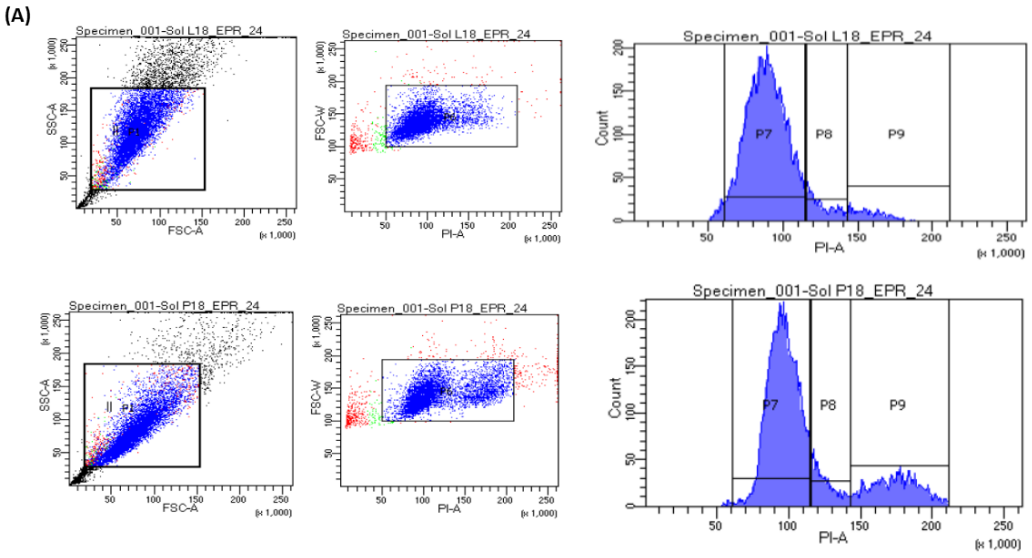

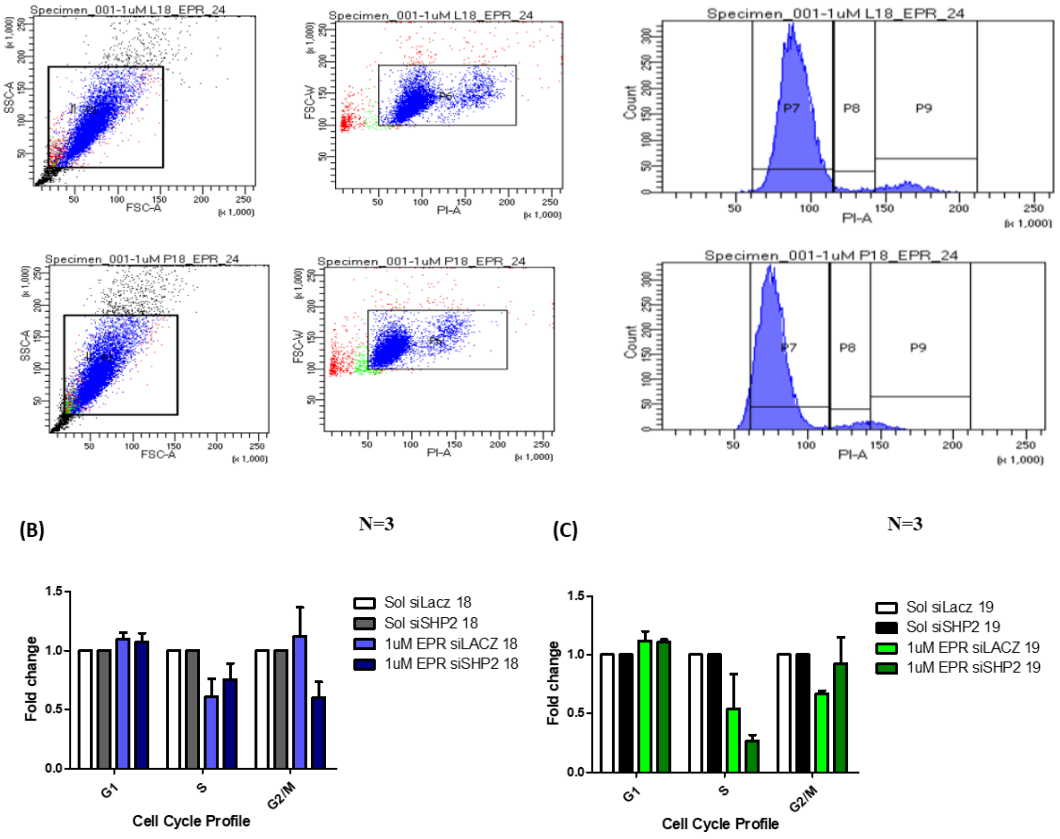

Figure 1: (A) Flow analysis showing cell cycle pattern upon epirubicin treatment for 24 hours, represented are the scatter plots showing selected population for analysis and histogram showing cell cycle phases denoted with gate, P. Flow analysis for si18 is shown, however, data was reconfirmed with si19. For the cell cycle pattern, 10,000 cells were recorded by Flow cytometry after PI staining. (B) Quantitation of cell count in G1 (P7), S (P8), and G2/M (P9) phase show no significant change in *PTPN11*/SHP2 knockdown cells with si18 and si19 respectively.

Figure 2:

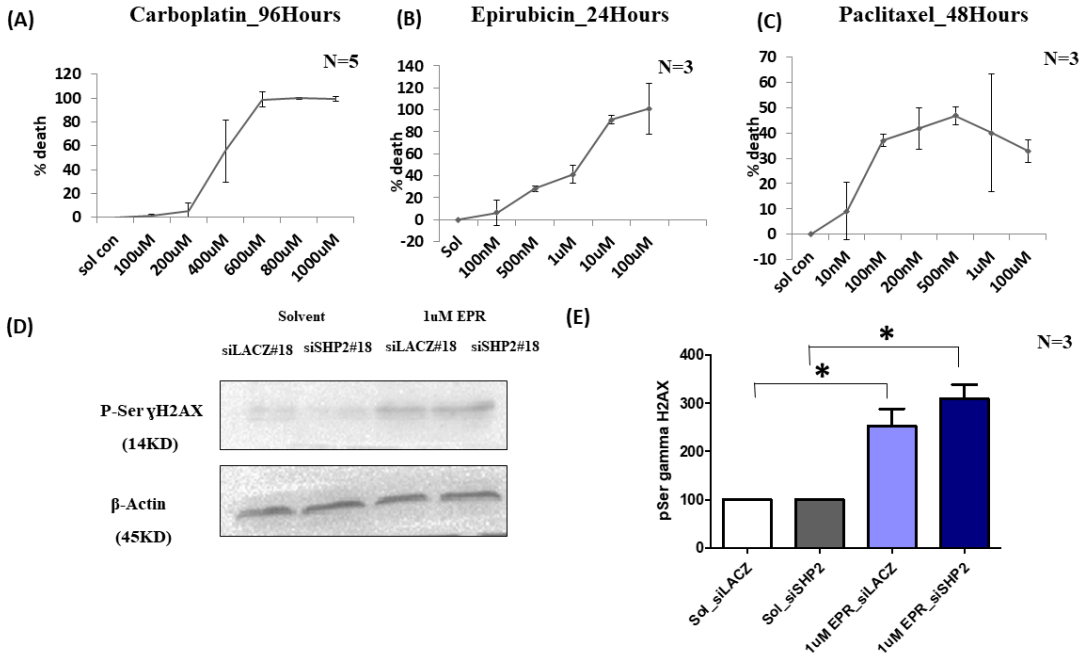

Figure 2: (A) MTT assay shows the dose-response curve of 3 chemotherapeutic drugs in MCF10A, IC50 for carboplatin was 400uM. (B) Epirubicin showed an IC50 of 1uM at 24 hours (C) while for Paclitaxel the IC50 could not be determined as cell death plateaued at 45-50 percent. (D) Effectivity of epirubicin (EPR), an anthracycline which induces double-stranded DNA breaks in cells, western blot showing phosphorylation of Serine 139 gamma H2AX upregulation in MCF10A cells upon epirubicin treatment for 24hours, (E) shows quantitation by densitometry analysis and a 3-fold increase in Serine 139 gamma H2AX phosphorylation.

Chapter 5: Function of *PTPN11*/SHP2 in tumorigenesis in the background of YAP1 overexpression

5.1: Introduction

The hippo pathway effector YAP1 is a prominent oncogene in breast cancer (D. Pan 2010). *PTPN11*/SHP2 association with YAP1 is recently reported in HCC, AGS gastric epithelial cells, and non-small cell lung cancer (NSCLC) (Chen et al., 2019; Kim et al., 2018; Tsutsumi et al., 2013). At low cell density of gastric epithelial cells, *PTPN11*/SHP2 is reported to physically interact with YAP1/TAZ and is translocated to the nucleus to dephosphorylate parafibromin and activate the wnt signaling pathway (Tsutsumi et al. 2013). Moreover, the nuclear association of YAP1 and *PTPN11*/SHP2 correlates to poor prognosis of NSCLC patients possibly due to activation of wnt signaling and higher c-myc and cyclin D1 expression (Chen et al. 2019). Furthermore, in SK-Hep1 cells, *PTPN11*/SHP2 -YAP1 nuclear association was pro-tumorigenic, while in HCC patient samples, higher nuclear YAP1 correlated to low cytoplasmic *PTPN11*/SHP2 and poor prognosis (Kim et al., 2018).In breast cancer, both YAP1 and *PTPN11*/SHP2 are pro-tumorigenic (Overholtzer et al., 2006; Aceto et al., 2012). Studies on gastric epithelial cells, NSCLC, and HCC patients suggest, YAP1 may influence *PTPN11*/SHP2 localization and hence its tumorigenic function. To assess the influence on *PTPN11*/SHP2 localization and its tumorigenic function in the presence of a prominent oncogene like YAP1 in breast cancer, we investigated the effect of over-expression of YAP1 in MCF10A breast epithelial cells with and without *PTPN11*/SHP2 activity (the latter was achieved by its knock-down).

5.2: Methods

Stable over-expression of YAP1 in MCF10A

MCF10A cells were cultured to 60% confluency and transduced with a cocktail solution of 2ml, 48hours retroviral particles, pQCXIH, and 8 ug/ml Polybrene (Sigma). pQCXIH carrying wild type YAP1 (YAP1-WT) and constitutively active YAP1 (YAP1-5SA) inserts were used as genetic backgrounds to check the role of *PTPN11*/SHP2 in YAP1 driven tumors and pQCXIH was used as empty vector control. Post 4 hours of transduction, a top-up of growth media of 12 ml was

added to plates. The following day, a growth medium change was given to cells. 48hours of viral transduction, selection with 100ug/ml of Hygromycin (Sigma) was given and cells were selected until 50% cells died in control MCF10A plates. Following selection, plates were rinsed in DPBS and added fresh growth media to allow them to grow till 80-90% confluency. As cells grew completely, stocks were prepared and used for all experiments. Retroviral vector, pQCXIH cloned with YAP1, and YAP-5SA was a generous donation from Dr. Madhura Kulkarni, Center for Translational Cancer Research, Prashanti Cancer Care Mission, and IISER Pune.

Details of all other methods used in this chapter are described in Chapter 4. All experiments were repeated with #18 and #19 siRNA, data of #18 is shown here. Column statistics (GraphPad Prism) was used for statistical analysis, $p<0.05$ was considered significant.

5.3: Results

5.3.1: Overexpression of YAP1 in MCF10A

We successfully transduced MCF10A cells to stably overexpress YAP1-WT and YAP1-5SA using the pQCXIH vector (A). In YAP1-WT overexpressing MCF10A, once the cells reach confluency, the hippo pathway is turned on and YAP1- WT is phosphorylated by upstream LATS kinase at Ser 127 and relocated to the cytoplasm by 14-3-3β (Meng, Moroishi, and Guan 2016). In the case of overexpression of YAP1-5SA, in which all five serine (S) residues including S127 were mutated to alanine (A) that prevents phosphorylation of YAP1 at S127 and hence results in constitutive translocation of YAP1 into the nucleus even at high confluency and continued transcription of YAP1 driven genes (Pavel et al. 2018). These two genetic systems are expected to confirm our observation from the *Drosophila* screen viz Csw (the ortholog of *PTPN11*/SHP2) functioning as a tumor suppressor in the context of over-expressed Yorkie. Figure A gives the vector map of pQCXIH used for stably overexpressing YAP1-WT and YAP1-5SA. We observed a fold change of 1.5x and a 3x increase in YAP1 expression in YAP1-WT and YAP1-5SA transduced MCF10A cells, respectively as compared to MCF10A cells with the empty vector control (B and C).

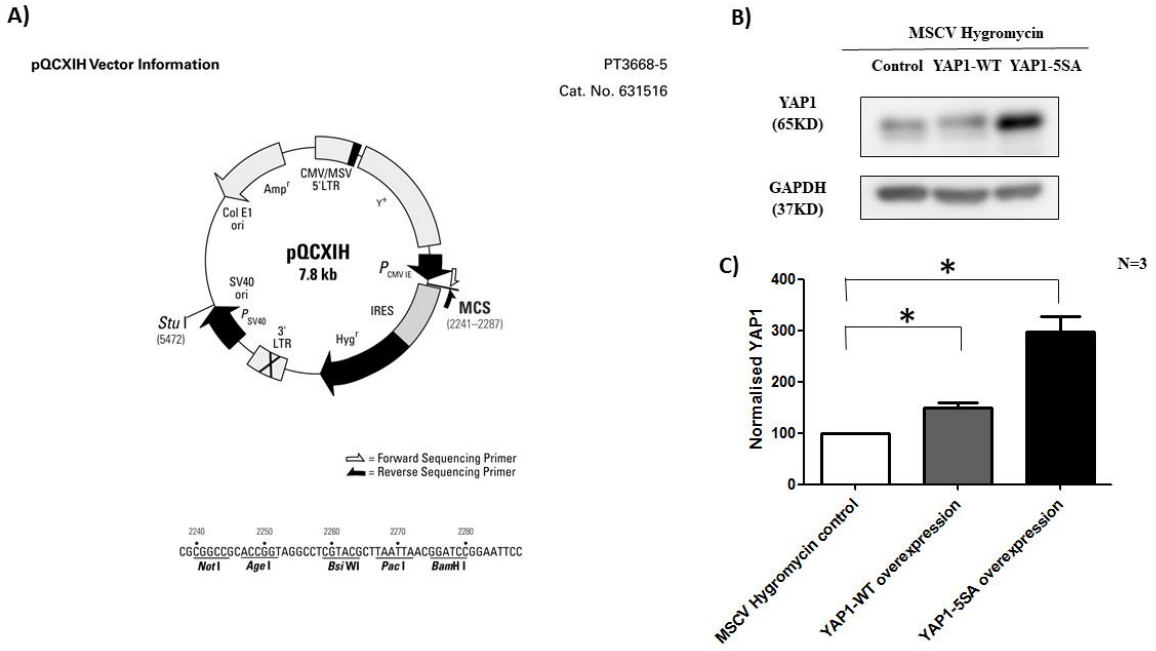

Figure 5.3.1: (A) YAP1 was overexpressed under a hygromycin selection vector of 7.8kb in MCF10A by transduction of 48 hours. Vector map shown in, image reproduced from clontech. (B) Western blots showing expression of YAP1. MSCV vector control, YAP1-WT cloned MSCV and YAP1-5SA cloned MSCV. GAPDH was used as a loading control. (C) Densitometry analysis of blot shows a 1.5-fold increase in YAP1-WT protein expression and a 3-fold increase in constitutive YAP1-5SA expression.

5.3.2: Effect of YAP1 overexpression on *PTPN11*/SHP2 expression and activity

Phospho-SHP2Y542 is a marker for *PTPN11*/SHP2 activity. Overexpression of YAP1, both WT and constitutive 5SA, decreases *PTPN11*/SHP2 phosphorylation at Y542 with no change in *PTPN11*/SHP2 total protein levels (A, B) or RNA levels (C). This may reflect decreased *PTPN11*/SHP2 activity with increased YAP1 expression.

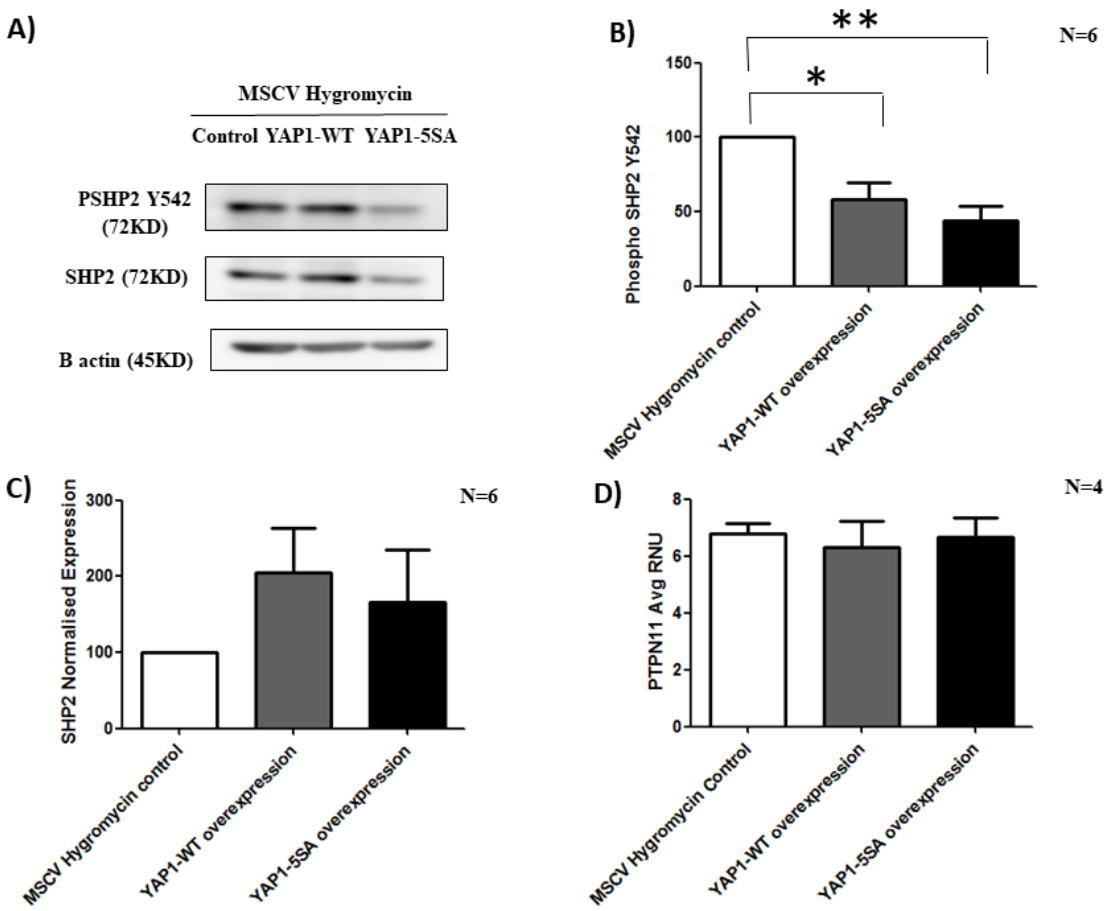

Figure 5.3.2: (A) Overexpression of YAP1, both wild type and constitutively active, results in the decrease in the levels of phospho-SHP2 without affecting total *PTPN11*/SHP2 expression. Western blot for total *PTPN11*/SHP2, phospho-SHP2, and B actin. (B) Densitometric analysis of the Western blot of phospho-SHP2. (C) Densitometric analysis of the Western blot of total *PTPN11*/SHP2. (D) Transcript levels of *PTPN11* by qRT-PCR normalized to GAPDH.

5.3.3: Effect of YAP1 overexpression on Phospho-SHP2Y542 subcellular localization

As reported in the literature, YAP1 regulates *PTPN11*/SHP2 localization however our preliminary data suggested a plausible association between YAP1 and *PTPN11*/SHP2 activity (Figure 5.3.2). We investigated changes in the subcellular localization of Phospho-SHP2Y542 and not SHP2 total protein as we did not observe any change from our densitometric analysis (Figure 5.3.2). We selected the confluent monolayer of YAP1-overexpressing MCF10A cells for all localization studies. YAP1 localization itself is influenced by cellular confluency and mechanical cues (Meng,

Moroishi, and Guan 2016). To understand the role of YAP1 expression alone on *PTPN11*/SHP2 activity, devoid of any external contributions from mechanical cues and YAP1 localization itself. Although overexpression of YAP1 leads to decreased Phospho-SHP2Y542 levels, we did not observe any considerable change in the subcellular localization of Phospho-SHP2Y542. However, in MCF10A cells overexpressing YAP1-5SA, Phospho-SHP2Y542 shows more punctate distribution on the membrane unlike the uniform distribution observed in the case of empty vector control or MCF10A cells overexpressing YAP1-WT (A, B). We speculate this punctate appearance of Phospho SHP2 could result from a change in membrane localization of receptors. However, the observation needs further experimental validation with high-resolution microscopy. We re-confirmed the localization of SHP2 and Phospho-SHP2Y542 by fractionation assay (REAP protocol, (Suzuki et al. 2010)). We did not see any considerable change in the levels of *PTPN11*/SHP2 or Phospho-SHP2Y542 in the nuclei or cytoplasm of cells over-expressing YAP1-WT or YAP1-5SA (C, D).

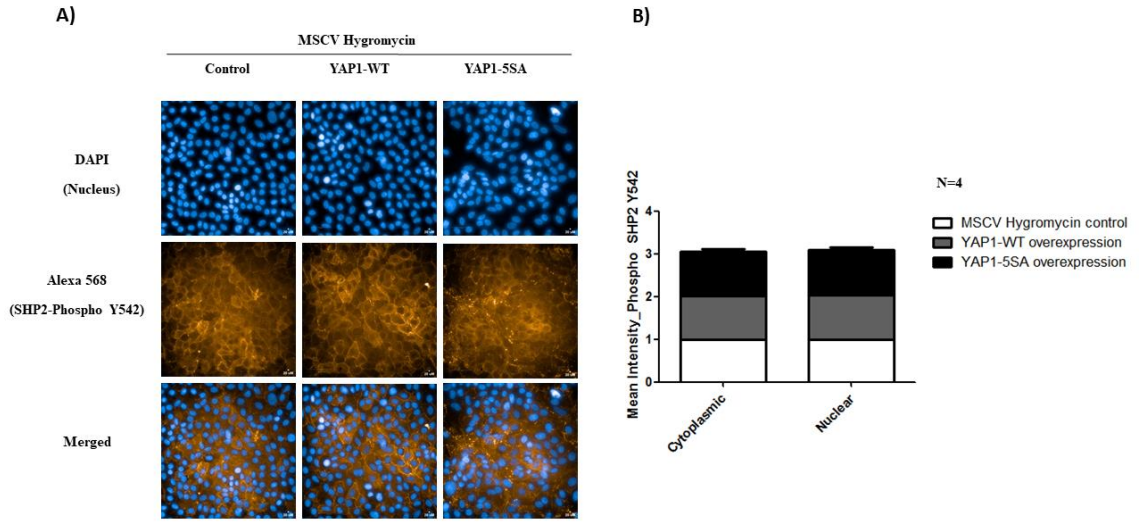

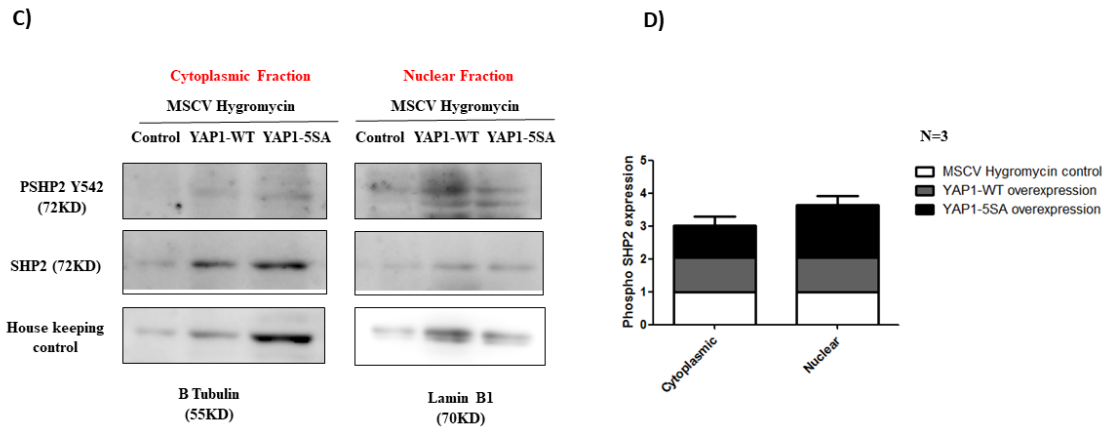

Figure 5.3.3: (A) Overexpression of YAP1-WT or YAP1-5SA does not affect the subcellular localization of Phospho-SHP2Y542 as observed either by immunofluorescence imaging and (B) Quantitation in operetta, 40X air, Scale bar in A is 20uM. (C) Subcellular localization was also re-confirmed by cellular fractionation assays followed by Western blot analysis. β-tubulin was used as a control for cytoplasmic fraction, while Lamin B1 was used as a control for the nucleus for Western blot analysis. (D) Densitometry analysis of the above Western blot shows no significant change in the expression of *PTPN11*/SHP2 or Phospho-SHP2Y542.

5.3.4: Effect of knockdown of *PTPN11*/SHP2 in the background of overexpressed YAP1 on the morphology of MCF10A cells

As described in chapter 4, knockdown of *PTPN11*/SHP2 induces changes in the morphology of MCF10A: from cobblestone to mesenchymal shape. We investigated changes in morphology upon overexpression of YAP1-WT and YAP1-5SA in the presence or the absence of *PTPN11*/SHP2. We did not observe any morphological changes in MCF10A cells over-expressing YAP1-WT along or in the background of the knockdown of *PTPN11*/SHP2. However, overexpression of YAP1-5SA alone causes mesenchymal morphology of MCF10A cells and the degree of change was higher compared to the change caused by the knockdown of *PTPN11*/SHP2. The combined effect, i.e. caused by the over-expression of YAP1-5SA and the knockdown of *PTPN11*/SHP2 was similar to YAP1-5SA alone.

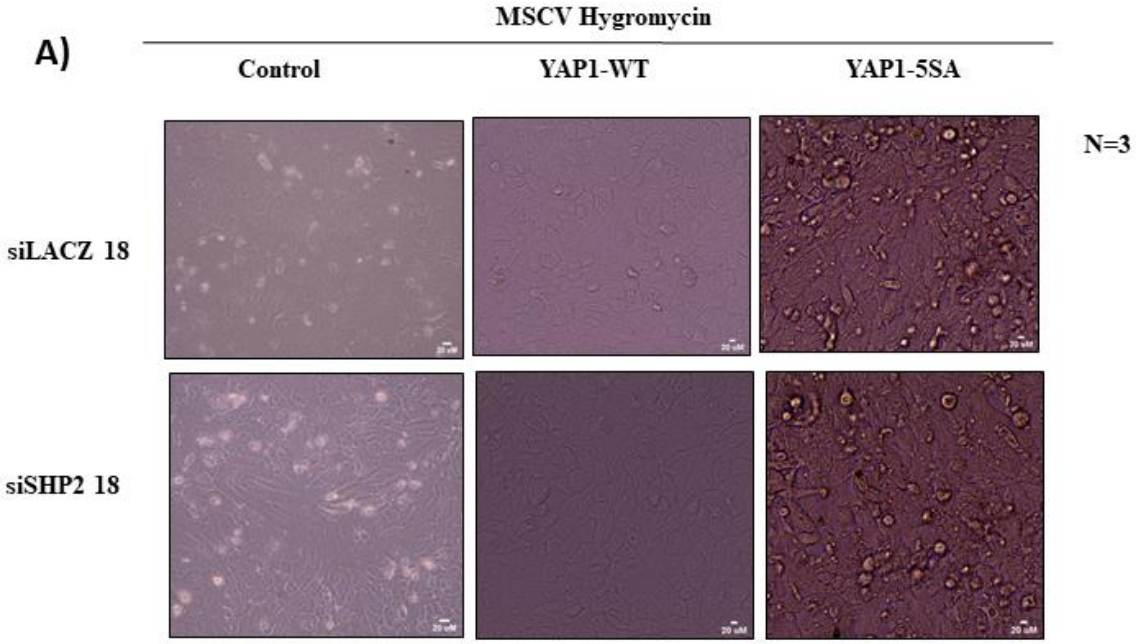

Figure 5.3.4: (A) Morphological changes in MCF10A cells caused by the knockdown of *PTPN11*/SHP2 in the normal background or the background of the over-expression of YAP1-WT or YAP1-5SA. Scale bar 20uM. Images recorded in Evos FL Auto. YAP1-WT appears to suppress the effect of knockdown of *PTPN11*/SHP2. The severity of the morphological change is higher in cells over-expressing YAP1-5SA, which appears to be saturated as knockdown of *PTPN11*/SHP2 in this background did not alter the degree of morphological changes.

5.3.5: Effect of knock-down of *PTPN11*/SHP2 in the background of overexpressed YAP1 on the proliferation of MCF10A cells

YAP1 has been reported to increase cell proliferation (Varelas 2014). Although we did not observe any effect of the knockdown of *PTPN11*/SHP2 on cell proliferation, we examined the phenotypic effects of over-expression of YAP1 in the background with and without *PTPN11*/SHP2. While we did observe increased cell proliferation due to the over-expression of YAP-WT, we did not see such changes when we over-expressed constitutively active YAP1-5SA. There was no impact of *PTPN11*/SHP2 knockdown on the phenotypic effect of the over-expressing YAP1-WT or YAP1-5SA.

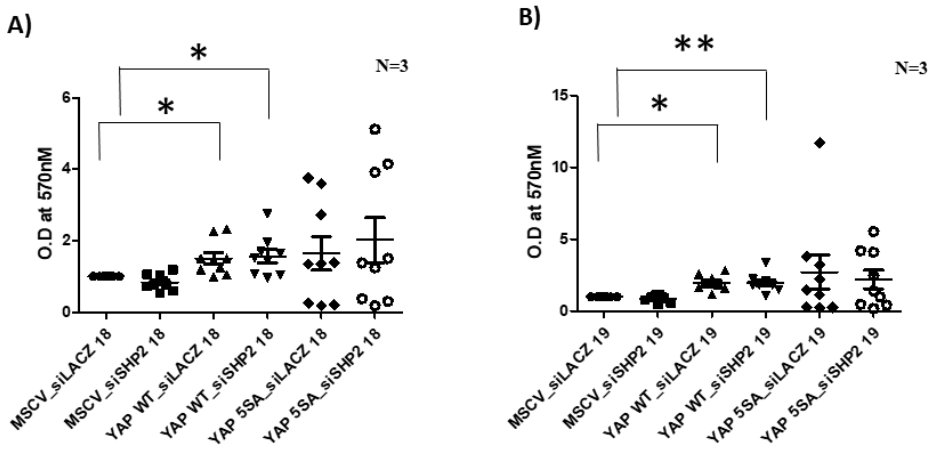

Figure 5.3.5: (A) MTT assay showing the effect of over-expression of YAP and/or knockdown of *PTPN11*/SHP2 with siSHP18 and (B) with siSHP19 on cell proliferation, while over-expression of YAP1-WT had a marginal increase in the cell proliferation by 2-fold, there was no effect in any other combinations.

5.3.6: Effect of overexpression YAP1 and knockdown of *PTPN11*/SHP2 on cell migration

Wound healing scratch assay was performed to investigate if YAP1 and *PTPN11*/SHP2 have any combined effect on cell migration. As described in chapter 4, we observed accelerated cell migration in the background of the knockdown of *PTPN11*/SHP2. Over-expression of YAP1-WT or YAP1-5SA does not significantly affect migration post 24 hours of initial scratch in our system. Over-expression of YAP1-WT appears to suppress the accelerated rate of migration caused by the knockdown of *PTPN11*/SHP2 by 5%-15%. Over-expression of YAP1-5SA, however, did not affect the increased migration caused by the knockdown of *PTPN11*/SHP2.

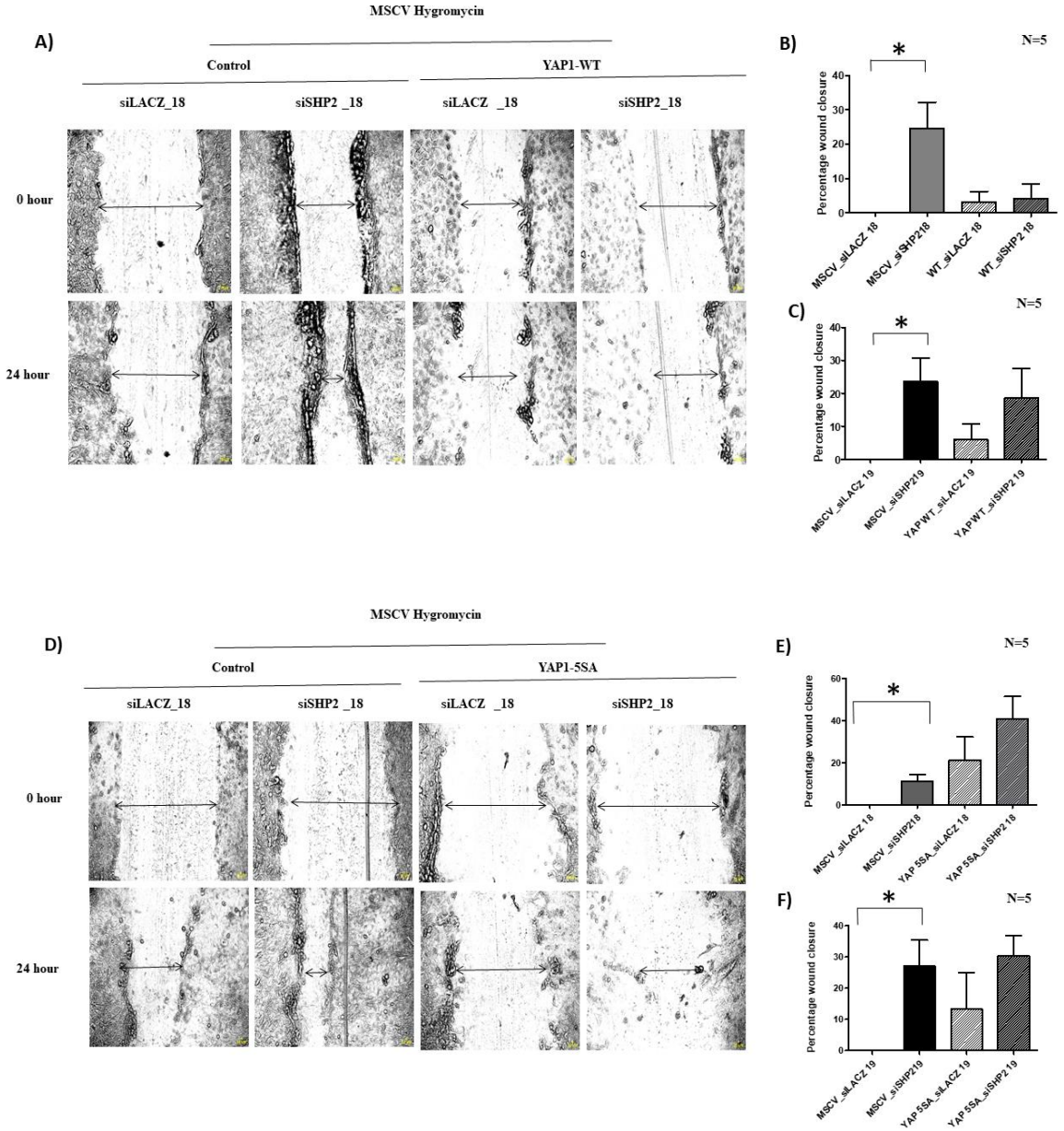

Figure 5.3.6: Wound healing scratch assay to measure the migration capacity of MCF10A cells. (A) and (C) show the level of gap-filling after 24h of the scratch, (B), and (D) show the quantitation of these experiments. The migration capacity of cells in which *PTPN11*/SHP2 is knocked down is increased by nearly 25% as compared to empty vector control, which is also reported in the previous chapter. There was no effect of the over-expression of YAP1-WT and YAP1-5SA. While over-expression of YAP1-WT appears to suppress the effect of the knockdown of *PTPN11*/SHP2 to some extent, over-expression of YAP1-5SA did not affect the increased migration caused by the knockdown of *PTPN11*/SHP2.

5.3.7: Effect of overexpression YAP1 and knockdown of *PTPN11*/SHP2 on cell death

YAP1 is reported to decrease cell death in cells (Varelas 2014). In our experiments, overexpression of YAP1-WT resulted in decreased cell death. However, over-expression of YAP1-5SA, which did not affect cell proliferation did not have any impact on cell death either. Neither of them showed any change in their phenotypic effect when over-expressed in the background with knockdown of *PTPN11*/SHP2 (A, B).

We reported in our study in chapter 4, *PTPN11*/SHP2 knockdown provides a survival advantage to cells, which are treated with cytotoxic chemical epirubicin at 1uM concentration. Overexpression of YAP1-WT and YAP1-5SA did not affect the survival of cells upon treatment with 1uM epirubicin. Overexpression of YAP1-WT without *PTPN11*/SHP2 shows increased survival upon 1uM epirubicin treatment for 24hours. However, overexpression of YAP1-5SA with and without *PTPN11*/SHP2 nullifies the effect of *PTPN11*/SHP2 knockdown on chemosensitivity.

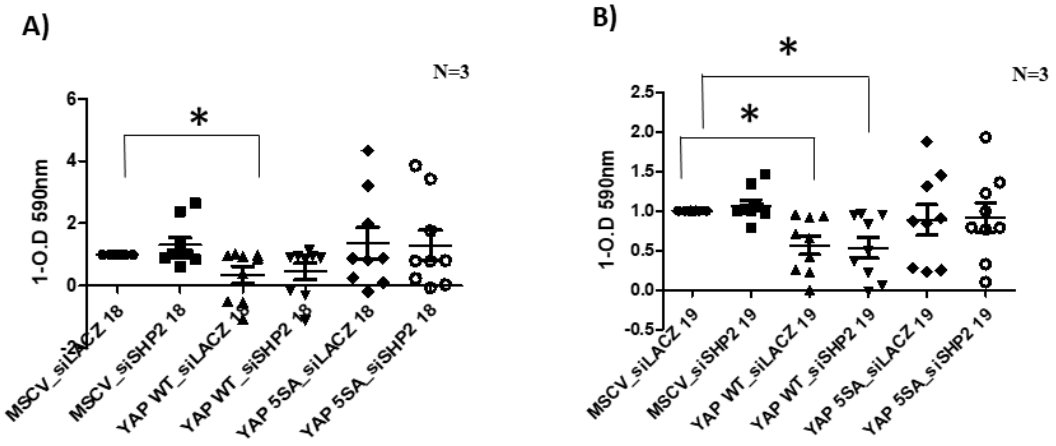

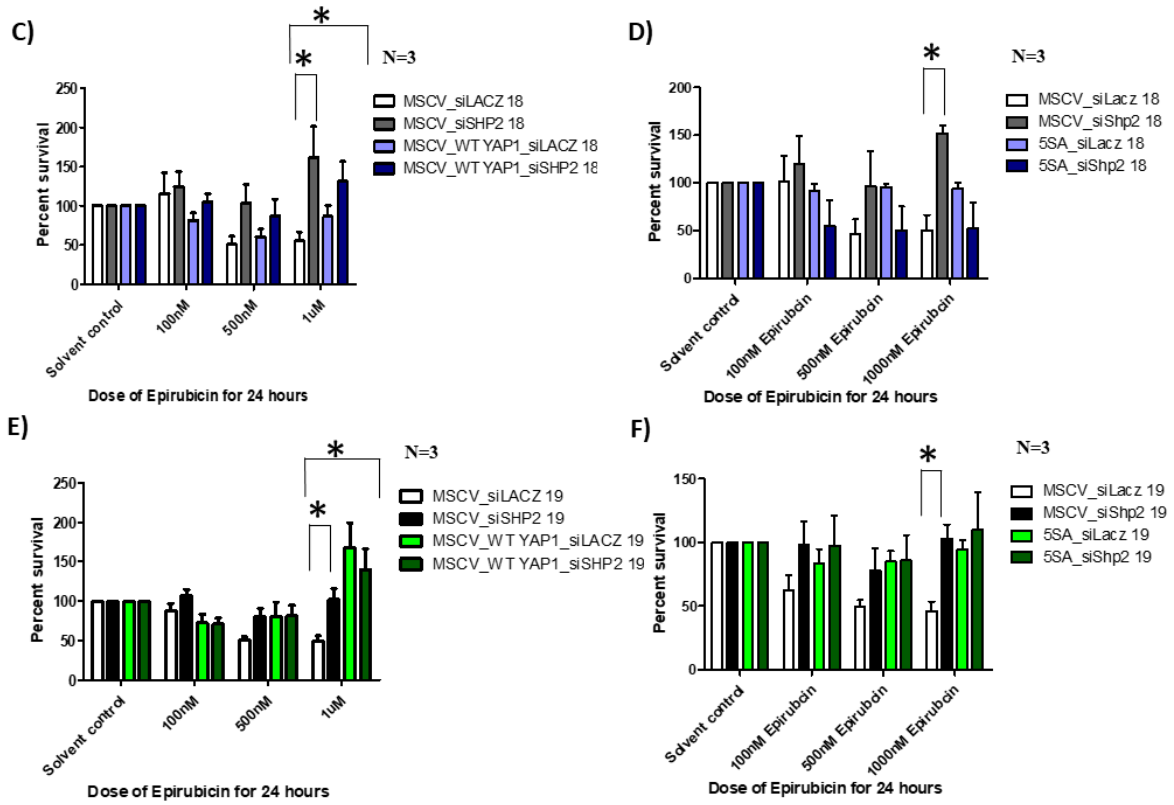

Figure 5.3.7: (A) and (B) shows MTT assay (1-O. D value) showing cell death in YAP1 overexpressing MCF10A with and without *PTPN11*/SHP2 knockdown using si18 and si19 respectively. (C) shows the increased survival of *PTPN11*/SHP2 knockdown (si18) cells alone and together in the background of YAP1-WT overexpressing MCF10A at 1uM conc. of epirubicin. (D) shows the increased survival of *PTPN11*/SHP2 knockdown (si18) cells alone and the effect is lost in the background of YAP1-5SA overexpressing MCF10A at 1uM conc. of epirubicin. (E) shows increased survival of *PTPN11*/SHP2 knockdown (si19) cells and together in the background of YAP1-WT overexpressing MCF10A at 1uM conc. of epirubicin. (F) shows an increase in survival of *PTPN11*/SHP2 knockdown (si19) cells however in the background of YAP1-5SA overexpressing MCF10A the chemoresistance is lost at 1uM conc. for 24 hours. MTT assay results were normalized to solvent control.

5.4: Discussion

The oncogenic role of YAP1 has been reported in several studies, wherein copy number amplification of YAP1 in MCF10A is shown to promote anchorage-independent growth, EMT,

growth factor independent proliferation, and decreased apoptosis (Overholtzer et al. 2006). Overexpression of constitutively active YAP1-5SA is also reported to promote proliferation even in highly confluent cultures by inducing autophagy in 2D and 3D cultures of MCF10A (Pavel et al. 2018; B. Zhao et al. 2009). In recent studies, the oncogenic role of YAP1 in breast cancer stands controversial as new data suggests, loss of heterozygosity of YAP1 amplicon, or its knockdown in MDA-MB231 and MCF7 leads to increased migration and tumor growth (M. Yuan et al. 2008). Furthermore, YAP1 expression negatively correlates to relapse-free survival in the luminal subgroup of breast cancer patients (Cao, Sun, and Yao 2017; Lehn et al. 2014). In a sample of 137 Indian breast cancer patients, the YAP1 promoter was reported to be methylated in 67.15% of cases with decreased YAP1 mRNA expression suggestive of its putative tumor suppressor role (Real et al. 2018).

From experimental evidence in our work, overexpression of either YAP1-WT or constitutively active YAP1-5SA resulted only in a marginal increase in cell proliferation, migration, and cell survival (in the context of DNA damage). As they were not significant, we infer that overexpression of YAP1 alone is not sufficient to drive tumorigenesis.

We also observed that overexpression of YAP1 decreases the levels of phospho-SHP2 indicating possible interaction and regulation of *PTPN11*/SHP2 by the hippo pathway effector. However, this interaction was not evident in any of the phenotypic assays suggesting more complex interactions during tumorigenesis. This may reflect a possible dual role (oncogenic vs tumor suppression) of both YAP1 and *PTPN11*/SHP2 in breast cancer progression. Therefore, a detailed investigation of the phenotypic effect of YAP- *PTPN11*/SHP2 interaction is required to unravel complex pathways associated with breast carcinogenesis.

Overexpression in MCF10A of YAP1-5SA alone or the context of knockdown of LATS is shown to induce expression of Connective Tissue Growth Factor (CTGF) and Cysteine-rich angiogenic inducer 61 (CYR61) and transforms MCF10A to mesenchymal morphology, with no effect in proliferation (J. Zhang, Smolen, and Haber 2008). Overexpression of YAP1-5SA in MCF10A activates LATS to induce Neurofibromatosis 2 (NF2) expression in MCF10A cells, preventing stress fiber formation and cell migration (Moroishi et al. 2015). These observations further support the complexity of the YAP1 function as an oncogene. Thus, studying the role of *PTPN11*/SHP2 in tumorigenesis in YAP1 overexpression background is challenging and an alternative approach

to answering the same could be employed. It would be interesting to check the effects of knockdown of LATS kinase in the presence and absence of *PTPN11*/SHP2 (caused by its knockdown) and record changes in migration and proliferation.

Summary and Future Perspective of study

Organ growth is a tightly coordinated process, any dysregulation either due to loss of function of negative growth regulators or overactivation of growth promoters often leads to cancer. Typically, solid tumors involve at least two driver gene mutations, one in an oncogene and the other in a tumor suppressor gene or both in an oncogene that alters at least twelve different signaling pathways (Vogelstein et al. 2013). Our laboratory identified a large number of tumor suppressor genes co-operating with oncogenes like Yki and EGFR to drive tumorigenesis in an RNAi mediated screen of the *Drosophila* genome. Bioinformatic analyses reported in this study of the positives identified in the independent screens suggested hippo signaling pathway and autophagy pathways play a relevant role in both Yki and EGFR driven tumors in flies. The sensitivity of Yki as a key growth regulator is evident in our STRING analysis as we observe a larger biological hub among the positives identified in the Yki screen which is enriched in major growth regulatory pathways. Many of the negative growth regulators identified in the screen and their corresponding human orthologs (obtained using DIOPT) included hippo pathway components, P53, and many other known tumor suppressors thereby reflecting the specificity of this RNAi mediated *Drosophila* screen. Many of the positives we identified from STRING analysis also identified to be conserved and were part of the large hub in flies and humans alike with the conservation of important biological processes in these interactomes controlling the event of tumorigenesis. Among many others, we report in this study, hippo signaling, and ubiquitin-related proteolysis are most conserved in Yki driven cancer from flies to humans. *csw* is one of the few candidates we analyzed, a conserved gene in Yki driven tumors. We hypothesized it to be an essential gene, both in flies and humans, as it was a major component of the hub that mediates interactions between many MAPK related pathway genes. This was interesting as Csw orthologs are reported to participate in positive feedback signaling of the Ras-MAPK pathway (Neel, Gu, and Pao 2003). However, *csw* was negative in EGFR driven tumorigenesis in our genetic screen (Groth et al. 2019), suggestive of its redundancy in EGFR signaling. However, its role in the context of YAP1 was intriguing.

Molecularly, Csw is a non-receptor protein tyrosine phosphatase, and its human ortholog *PTPN11*/SHP2 functions as an oncogene (Neel, Gu, and Pao 2003; Sondka et al. 2018). As reported from previous literature, *PTPN11*/SHP2 participates in positive feedback signaling of the

EGFR pathway and drive hematologic malignancies and solid tumors including breast adenocarcinoma, prostate adenocarcinoma, lung adenocarcinoma, and colorectal cancer (Aceto et al., 2012; Prahallad et al., 2015; Richine et al., 2016; Schneeberger et al., 2015; Zhang et al., 2016). *PTPN11*/SHP2, through suppression of the JAK/STAT pathway, seems to function in inhibiting oncogenesis in hepatocellular carcinoma and esophageal squamous cell cancer (Bard-Chapeau et al. 2011; Qi et al. 2017). These observations suggest that *PTPN11*/SHP2 may function either as an oncogene or a tumor suppressor, perhaps in different cellular and molecular contexts. To verify this, we carried out a retrospective investigation of publicly available clinical metadata followed by experimental validation of our hypothesis.

We report from clinical analysis using two independent breast cancer datasets, METABRIC 2012 and TCGA RPPA Level 4 2015 data, *PTPN11*/SHP2 shows putative tumor suppressor function in breast cancer. *PTPN11*/SHP2 copy number loss in Luminal A subtype of METABRIC cohort correlates to late-stage cancer and poor 4 years of disease-specific survival. Low expression of Phospho-*PTPN11*/SHP2 Y542 in luminal A correlates to larger tumor size and greater lymph node positivity. Alternatively, *PTPN11*/SHP2 functions as a putative oncogene in the luminal B subtype. A detailed pathway enrichment analysis of phosphoproteins in TCGA RPPA Level 4 2015 data as correlated to Phospho-*PTPN11*/SHP2 Y542 expression levels could give us insights into the context in which it may function as a tumor suppressor in the luminal A subgroup of patients in the TCGA cohort. Since *PTPN11*/SHP2 is a phosphatase, its phosphoprotein expression rather than gene expression and its implications on proteins and phospho-proteins of cancer patients are relevant in the identification of the upstream cues that is responsible for switching between its dual role in tumorigenesis. TCGA level 4 RPPA data provides the expression of a limited number of 225 protein and phosphoprotein data which could be used to understand the context of *PTPN11*/SHP2 function, however, the data can be biased due to analysis on limited data availability.

Experimental validation of our clinical results by transient silencing of *PTPN11*/SHP2 in non-transformed MCF10A showed that knockdown of *PTPN11*/SHP2 promotes migration, changes in cell shape to mesenchymal morphology, and decreased sensitivity to chemotherapeutic drugs like epirubicin. We examined like its *Drosophila* ortholog Csw if *PTPN11*/SHP2 functions as a tumor suppressor in YAP1 driven oncogenesis. However, we do not observe any additional increase in migration rate or changes in chemosensitivity upon knockdown of *PTPN11*/SHP2 in

YAP1-overexpressing MCF10A. Instead, YAP1-5SA suppresses the effect of *PTPN11*/SHP2 knockdown on chemoresistance. YAP1's role as an oncogene in breast cancer is itself controversial from the recently available literature (Cao, Sun, and Yao 2017; Lehn et al. 2014; Real et al. 2018; Strano and Blandino 2007; M. Yuan et al. 2008). *PTPN11*/SHP2 suppression together with LATS knockdown in MCF10A could provide an unambiguous understanding of the role of the Hippo pathway in tumor suppressor function of *PTPN11*/SHP2.

Our study limits mechanistic understanding of how *PTPN11*/SHP2 may function as a tumor suppressor in breast cancer cohorts of TCGA, METABRIC, and in *in-vitro* cell culture studies using MCF10A. An alternative approach to understanding *PTPN11*/SHP2 tumor suppressor function in the luminal A subtype of breast cancer could be by silencing of *PTPN11*/SHP2 in luminal A cell lines like T47D. As reported by others, the silencing of *PTPN11*/SHP2 in T47D decreased migration rate and EMT while inhibition of *PTPN11*/SHP2 in the luminal B cell line, MCF7 also is reported to decrease cell growth (Li et al. 2014; Sun et al. 2017). PTPN11/SHP2 oncogenic and tumor suppressor role might be dependent on *in-vitro* and *in-vivo* conditions that need to be clearly defined. The dual nature of *PTPN11*/SHP2 is also reported during mammary gland development, *in-vivo*, *PTPN11*/SHP2 promotes STAT5 and inhibits STAT3 at different stages of mammary gland development. Selective deletion of *PTPN11*/SHP2 in mouse mammary glands interferes with mammopoiesis and lactation possibly due to the disruption of epithelial architecture and lobulo-alveolar outgrowth while enhancing apoptosis and involution of mammary glands (Ke et al. 2006). This reiterates the complexity and how understanding the context specificity of *PTPN11*/SHP2's role in tumorigenesis is necessary depending on the tissue type, the upstream cues, subtype of cancer, stage of cancer, and dose dependence of its substrate. Our study suggests *PTPN11*/SHP2 functions as a negative regulator of tumorigenesis that does not seem to follow the definition of an ideal tumor suppressor rather a key that tunes signaling pathways during growth and tumorigenesis.

Appendix

Table 2.3.1						
FLY		606	41	30		
CG Number	**Trans-ID**	**YKI**	**EGFR**	**SOCS**	**Gene Symbol**	**All Orthologs with DIOPT score ≥ 2**
CG10497	107320	YKI	EGFR		Sdc	SDC2, SDC3, SDC4, SDC1
CG11228	104169	YKI	EGFR		hpo	STK3, STK4
CG12072	106174	YKI	EGFR		wts	LATS2, LATS1, STK38L, STK38
CG3352	108863	YKI	EGFR		ft	FAT4, CDH23, DCHS1, DCHS2, FAT1, FAT2, FAT3
CG4114	109281	YKI	EGFR		ex	FRMD1, FRMD6
CG4379	101524	YKI	EGFR		PKA-C1	PRKACA, PRKACB, PRKACG, PRKX
CG6053	108601	YKI	EGFR		Dnai2	DNAI2
CG6318	104627	YKI	EGFR		Xrcc2	XRCC2
CG6792	104176	YKI	EGFR		Plzf	MYNN, ZBTB17, ZBTB24
CG6964	107413	YKI	EGFR		Gug	RERE, ATN1
CG7706	103727	YKI	EGFR			SLC4A1AP
CG11241	110651		EGFR			AGXT2
CG11801	103506		EGFR		Elo68beta	ELOVL4, ELOVL2, ELOVL7, ELOVL1, ELOVL5
CG12756	101457		EGFR		Eaf6	MEAF6
CG12836	101907		EGFR			TCTE3, TCTEX1D2
CG13296	106770		EGFR			PRDM13
CG13852	108080		EGFR		mats	MOB1B, MOB1A, MOB3B, MOB3A, MOB3C
CG14005	105773		EGFR			MSANTD1
CG14480	106633		EGFR			FAM192A
CG31852	103622		EGFR		Tap4	IGBP1
CG31926	107437		EGFR			CTSD, CTSE, NAPSA, PGA3, PGA5, PGC, REN, PGA4, BACE1

CG32483	106263		EGFR			SCPEP1
CG4220	104620		EGFR		elB	ZNF703, ZNF503
CG42282	104204		EGFR		NimA	PEAR1, MEGF6
CG4429	100817		EGFR		eIF4H1	EIF4H, EIF4B
CG4623	106485		EGFR		Gdap1	GDAP1, GDAP1L1
CG4747	100783		EGFR			GLYR1, HIBADH
CG4842	102064		EGFR			HPGD
CG5640	105986		EGFR		Utx	UTY, KDM6A, KDM6B
CG5941	107297		EGFR		MCTS1	MCTS1
CG6345	107280		EGFR			CDK5RAP1
CG6844	101760		EGFR		nAChRalpha2	CHRNA2, CHRNA4, CHRNA6, CHRNA3, CHRNA5, CHRNA1, CHRNB1, CHRNB2, CHRNB3, CHRNB4, CHRND, CHRNE, CHRNG, CHRFAM7A, CHRNA7, CHRNA9, CHRNA10
CG7143	110289		EGFR		DNApol-eta	POLH, POL
CG7438	104089		EGFR		Myo31DF	MYO1D, MYO1G, MYO1E, MYO1A, MYO1B, MYO1C, MYO1F, MYO1H
CG7873/44128	100708		EGFR		Src42A	FRK, FYN, FGR, SRC, YES1, ABL1, ABL2, BLK, BMX, BTK, HCK, ITK, JAK1, JAK2, JAK3, LCK, LYN, PTK6, SRMS, TEC, TXK, TYK2
CG7966	105629		EGFR			SELENBP1
CG8582	107823		EGFR		sh3beta	SH3BGR, SH3BGRL2, SH3BGRL, SH3BGRL3
CG9293	102002		EGFR		Ing5	ING4, ING5, ING2, ING3, ING1
CG9657	107361		EGFR			SLC5A6, SLC5A8, SLC5A12, SLC5A5, SLC5A9
CG9807	109220		EGFR		Rab9Db	RAB43
CG10026	107452	YKI				TTPA
CG10038	100272	YKI				FAM172A

CG10051	105900	YKI				ERMP1
CG10055	104464	YKI				SHQ1
CG10076	107335	YKI			spir	SPIRE1, SPIRE2
CG10086	108163	YKI				ARRDC2, ARRDC3, ARRDC4, TXNIP, ARRDC1, ARRDC5
CG10098	103744	YKI				SCRN3, SCRN1, SCRN2
CG10103	100771	YKI				IST1
CG10128	100805	YKI			tra2	TRA2A, TRA2B
CG1014	104759	YKI			robl62A	DYNLRB2, DYNLRB1
CG10157	104414	YKI			GILT2	IFI30
CG10197	109914	YKI			kn	EBF3, EBF2, EBF1, EBF4
CG10262	109012	YKI			PCNA	PCNA
CG10277	109001	YKI			godzilla	RNF13, RNF167, ZNRF4
CG10306	105991	YKI			eIF3k	EIF3K
CG10371	104774	YKI			PTPMT1	PTPMT1
CG10431	107869	YKI				THAP3, THAP5
CG10467	103787	YKI				GALM
CG10481	101787	YKI				XPR1
CG10521	100840	YKI			NetB	NTN1, NTN3, NTN5, NTNG2, NTNG1, LAMC1, LAMC3
CG10545	100011	YKI			Gbeta13F	GNB1, GNB2, GNB4, GNB3
CG10584	106620	YKI				METTL22
CG10622	101554	YKI			Sucb	SUCLG2, SUCLA2
CG10637	109507	YKI			Nak	AAK1, BMP2K
CG10638	102914	YKI				AKR1B10, AKR1A1, AKR1D1, AKR1B15, AKR1E2, AKR1B1, AKR1C2, AKR1C1, AKR1C3, AKR1C4
CG1064	108599	YKI			Snr1	SMARCB1
CG10718	108138	YKI			neb	KIF14
CG1072	108409	YKI			Awh	LHX8, LHX6
CG10739	100959	YKI			pigeon	GSAP
CG10809	110271	YKI				ANKRD54

CG10843	102988	YKI			Cyp4p3	CYP4A11, CYP4A22, CYP4B1, CYP4X1, CYP4Z1, CYP4F11, CYP4F12, CYP4V2, CYP4F2, CYP4F3, CYP4F8, CYP4F22, CYP19A1
CG10887	108553	YKI				LEO1
CG10938	108380	YKI			Prosalpha5	PSMA5
CG10961	110266	YKI			Traf6	TRAF6
CG10996	104158	YKI				GALM
CG11035	108566	YKI				DNAJC30
CG11052	104639	YKI				ACYP1, ACYP1
CG11124	104059	YKI			sPLA2	PLA2G3, PROCA1
CG11164	103608	YKI				RNASEH2B
CG11180	104340	YKI				PINX1
CG11289	107242	YKI				UGT1A3, UGT2B10, UGT1A1, UGT2A2, UGT2A3, UGT2B4, UGT2B7, UGT2B11, UGT2B15, UGT2B17, UGT2B28, UGT3A1, UGT3A2, UGT8
CG1130	105201	YKI			scrt	SCRT1, SCRT2, SNAI1, SNAI2, SNAI3
CG11328	100742	YKI			Nhe3	SLC9A6, SLC9A7, SLC9A9, SLC9A8
CG11396	103546	YKI				TRAPPC12
CG1149	108034	YKI			MstProx	TLR7, CD180, TLR3, TLR4, TLR5, TLR8, TLR9
CG11490	109668	YKI			Tbc1d15-17	TBC1D15, TBC1D17
CG11502	100762	YKI			svp	NR2F1, NR2F2, NR2F6, RXRA, RXRG, RXRB
CG11516	103931	YKI			Ptp99A	PTPRG, PTPRZ1, PTPN18, PTPN22
CG11523	106810	YKI				GSKIP
CG11539	104497	YKI				NAT9
CG11588	110048	YKI				TMX1, TMX4

CG11622	105976	YKI			Rlip	RALBP1
CG11637	102359	YKI			NijB	NINJ2, NINJ1
CG11654	104500	YKI			Ahcy	AHCY, AHCYL1, AHCYL2
CG1167	110574	YKI			Ras64B	RRAS2, RRAS, KRAS, HRAS, MRAS, NRAS, RAP1A, RAP1B, RALB, RIT2, RIT1, RALA
CG11679	103479	YKI				RMND1
CG11699	101491	YKI				TMEM242
CG11739	109445	YKI				SFXN1, SFXN3, SFXN5
CG11759	103548	YKI			Kap3	KIFAP3
CG11804	108101	YKI			ced-6	GULP1
CG11840	110318	YKI			Spp	HM13, SPPL3
CG11847	103351	YKI			Clbn	NEMF
CG11874	101661	YKI			alpha-Man-Ib	MAN1B1, MAN1A2, MAN1A1, MAN1C1
CG11885	101147	YKI				PSMG3
CG11926	103378	YKI			Mon1	MON1A, MON1B
CG11942	109539	YKI			SkpE	SKP1
CG11988	108239	YKI			neur	NEURL1B. NEURL1, NEURL2
CG12038	107527	YKI				FAM69C
CG12056	100743	YKI				CYB5D2
CG12073	104804	YKI			5-HT7	HTR7, HTR1A, HTR1B, HTR1D, HTR1F
CG12079	103412	YKI			ND-30	NDUFS3
CG12110	106137	YKI			plD	PLD2, PLD1
CG12117	108243	YKI			Sptr	SPR
CG12130	103604	YKI			Pal1	PAM, NHLRC3
CG12153	106989	YKI			Hira	HIRA
CG12178	110205	YKI			Nhe1	SLC9A8
CG1218	103372	YKI				HPF1
CG12194	109287	YKI				MFSD1
CG12201	109013	YKI			GC2	SLC25A22, SLC25A18
CG12220	109807	YKI			mRpL-32	MRPL32
CG12272	107954	YKI			Strumpellin	WASHC5

CG12283	101166	YKI			kek1	ISLR, ISLR2, LRRC24
CG12334	101922	YKI			Atg8b	GABARAP, GABARAPL1, GABARAPL2, MAP1LC3A, MAP1LC3B2, MAP1LC3B, MAP1LC3C
CG12367	103400	YKI			Hen1	HENMT1
CG12369	107450	YKI			Lac	NEGR1
CG12370	109558	YKI			Dh44-R2	CRHR2, CRHR1, CRHR1-IT1-CRHR1, CALCRL, CALCR
CG12402	102835	YKI				FBXL17, LRRC29
CG12408	102031	YKI			TpnC4	CALM1, CALML3, CALML4, CABP4, CALM3, CABP5, CALM2, CALML5, CABP7, CABP1, CABP2, CALN1, CALML6
CG12423	109083	YKI			klhl10	KLHL10
CG12442	105801	YKI			wuc	LIN52
CG12559	109573	YKI			rl	MAPK1, MAPK3, MAPK7, MAPK15, MAPK14, MAPK13, MAPK12, MAPK11
CG12605	108807	YKI				SCRT1, SCRT2, SNAI1, SNAI2, SNAI3
CG1264	100311	YKI			lab	HOXA1, HOXB1, HOXD1
CG12673	104097	YKI			olf413	MOXD1
CG1275	105418	YKI				CYBRD1, CYB561, CYB561A3
CG12769	102244	YKI				IKZF2
CG12783	101110	YKI				SVOP, SV2C, SV2B
CG13160	106594	YKI				ERMP1
CG13190	100835	YKI			cuff	DXO
CG13252	102110	YKI				CRIM1
CG13287	109806	YKI				PRDM8, ZNF488
CG13316	101991	YKI			Mnt	MNT
CG13366	108092	YKI				SPECC1L, SPECC1, SMTN, ADORA2A, SMTNL1, SMTNL2

CG13374	108271	YKI			pcl	CTSE, PGC, REN, PGA5, NAPSA, CTSD, PGA3, PGA4
CG13375	102154	YKI				RASD1, RASD2
CG13397	110794	YKI				NAGLU
CG1345	105129	YKI			Gfat2	GFPT2, GFPT1
CG13645	107262	YKI			Nmnat	NMNAT1, NMNAT3, NMNAT2
CG13663	110541	YKI				SAYSD1
CG1372	109716	YKI			yl	LRP2
CG1391	110770	YKI			sol	CAPN15
CG13916	108267	YKI			SA-2	STAG1, STAG2, STAG3
CG13930	104545	YKI				WDR78
CG13969	101366	YKI			bwa	ACER2, ACER1, ACER3
CG14025	102527	YKI			Bsg25D	NIN, NINL
CG1416	103637	YKI				AHSA1, AHSA2
CG14177	102145	YKI			Tmc	TMC2, TMC1, TMC3
CG1427	105727	YKI				SEPSECS
CG14286	106881	YKI				C8orf33
CG14291	107384	YKI				SGSH
CG14309	103061	YKI				HPSE2
CG14411	109622	YKI				MTMR10, MTMR12, MTMR11
CG14447	103551	YKI			Grip	GRIP1, GRIP2
CG14521	104056	YKI			DIP-gamma	OPCML, IGLON5, NTM, NEGR1, LSAMP
CG14527	105531	YKI				KEL, ECEL1, ECE2, ECEL1
CG14535	108308	YKI				KIF26B, KIF26A
CG14575	105556	YKI			CapaR	NMUR2, NMUR1, GHSR
CG14620	110403	YKI			tilB	LRRC6, LRRC46, CEP97
CG14648	110736	YKI			lost	MTHFSD
CG14671	103531	YKI				CCDC115
CG14691	102107	YKI				SV2A, SV2B, SV2C, SVOP
CG14744	108697	YKI				SLC8B1
CG14757	100695	YKI				SDHAF2
CG14861	101009	YKI				EFHD2, EFHD1
CG14909	106115	YKI			VhaM9.7-d	ATP6V0E1, ATP6V0E2

CG14966	100821	YKI				C15orf40
CG14996	106455	YKI			Chd64	TAGLN2, TAGLN3, CNN3, CNN1, CNN2, TAGLN
CG15015	108625	YKI			Cip4	TRIP10, FNBP1, FNBP1L
CG15019	102427	YKI				LLPH
CG15078	103778	YKI			Mctp	MCTP1, MCTP2
CG15106	101183	YKI			Jheh3	EPHX1
CG15116	106717	YKI				GPX4, GPX1, GPX7, GPX8
CG15150	101202	YKI				RNF4
CG15211	104929	YKI				CMTM4, CMTM6, CMTM3, CMTM7, PLP2, CKLF, CMTM5, PLLP, CMTM1, CMTM2, CMTM8
CG15221	105910	YKI				SV2C, SV2A
CG15254	109728	YKI				BMP1, ASTL, CUBN, MEP1A, MEP1B, TLL1, TLL2
CG15309	101370	YKI				YPEL1, YPEL2, YPEL4, YPEL3, YPEL5
CG15329	104239	YKI			hdm	MEIOB
CG15376	103499	YKI				MYT1L, ST18, MYT1
CG15390	100029	YKI				MTERF4
CG15427	101900	YKI			tutl	IGSF9, IGSF9B
CG1550	106694	YKI				TTLL12
CG15527	102725	YKI			RpS28A	RPS28
CG15532	104322	YKI			hdc	HECA
CG15749	104423	YKI			dmrt11E	DMRT2, DMRT3, DMRTA1, DMRTA2, DMRTB1, DMRTC2
CG15797	109438	YKI			ric8a	RIC8A, RIC8B
CG15804	101226	YKI			Dhc62B	DNAH12, DNAH1, DNAH3, DNAH7, DNHD1, DNAH6
CG1659	107987	YKI			unc-119	UNC119, UNC119B
CG16725	100392	YKI			Smn	SMN2, SMN1

CG16732	107424	YKI				UGT1A3, UGT2B10, UGT1A1, UGT2A2, UGT2A3, UGT2B4, UGT2B7, UGT2B11, UGT2B15, UGT2B17, UGT2B28, UGT3A1, UGT3A2, UGT8, UGT1A4, UGT1A5, UGT1A6, UGT1A7, UGT1A8, UGT1A9, UGT1A10
CG1675	110351	YKI			Ntm	NTMT1, METTL11B
CG16784	109430	YKI			pr	PTS
CG16840	100228	YKI			Art8	PRMT6, PRMT2, PRMT3
CG16858	106812	YKI			vkg	COL4A1, COL3A1, COL4A3, COL4A4, COL4A5, COL5A1, COL11A1, COL16A1, COL24A1, COL27A1, COL1A1, COL1A2, COL2A1, COL4A2, COL4A6, COL5A2, COL5A3, COL7A1, COL11A2, COL19A1
CG16863	110221	YKI				ZBED1, DHRSX
CG16922	104604	YKI			Myo10A	MYO15A, MYO15B, MYO10, MYO7A, MYO7B
CG16944	104576	YKI			sesB	SLC25A4, SLC25A5, SLC25A6, SLC25A31
CG1697	100200	YKI			rho-4	RHBDL1, RHBDL2, RHBDL3
CG16985	107909	YKI				ACOT13
CG16987	105309	YKI			daw	TGFB1, INHBC, INHBE, TGFB2, INHBA, INHBB, TGFB3
CG17011	107218	YKI			lectin-30A	CLEC3B
CG17030	108804	YKI				UBE2L3, UBE2L6
CG1707	101560	YKI			Glo1	GLO1
CG17075	103741	YKI				ZDHHC1, ZDHHC11, ZDHHC11B, ZDHHC21, ZDHHC19
CG17100	106783	YKI			cwo	BHLHE40, BHLHE41, HELT, HES1, HES2, HES4, HES6

CG17149	106147	YKI			Su(var)3-3	KDM1A, KDM1B
CG17150	109562	YKI			Dnah3	DNAH3, DNAH7, DNAH1, DNAH5, DNAH6, DNAH8, DNAH9, DNAH10, DNAH11, DNAH12, DNAH17, DNHD1, DYNC2H1, DYNC1H1
CG1716	106459	YKI			Set2	SETD2, SETD1A
CG17174	104248	YKI			ACXB	ADCY2, ADCY4, ADCY7, ADCY1, ADCY3, ADCY8
CG17184	103951	YKI			Arfip	ARFIP2, ARFIP1
CG17192	102035	YKI				PLA1A
CG17212	107760	YKI			rho-6	RHBDL1, RHBDL2, RHBDL3
CG17224	101772	YKI				UPP1, UPP2
CG17266	110097	YKI				PPIH, PPIL6, PPID, PPIG, NKTR
CG17269	106210	YKI			Fancd2	FANCD2
CG17271	101754	YKI				MCFD2
CG17280	101523	YKI			levy	COX6A1, COX6A2
CG17286	101882	YKI			spd-2	CEP192
CG17302	100337	YKI			Prosbeta4 R2	PSMB2
CG17322	110057	YKI				UGT1A3, UGT2B10, UGT8, UGT1A1, UGT2A2, UGT2A3, UGT2B4, UGT2B7, UGT2B11, UGT2B15, UGT2B17, UGT2B28, UGT3A1, UGT3A2
CG17484	103063	YKI			p120ctn	CTNND2, PKP4, ARVCF, PKP3, PKP2, PKP1, CTNND1
CG17566	109921	YKI			gammaTub 37C	TUBG1, TUBG2, TUBD1
CG17746	100178	YKI				PPM1A, PPM1N, PPM1B
CG1795	105962	YKI			Ogg1	OGG1
CG17974	102724	YKI				PI15, R3HDML, CRISPLD2, CLEC18C, CRISPLD1, CLEC18B, CLEC18A, GLIPR1L1

CG17988	101665	YKI			Ance-3	ACE, ACE2, TMEM27
CG17996	109429	YKI				CMC1
CG1812	104656	YKI				KLHL22, KLHDC7A, KBTBD11, KLHDC7B, KLHL26, KLHL9, KBTBD13, KLHL13, KLHL14, KLHL34, KLHL32, KLHL15, KLHL36, KLHL42, KLHL31
CG18193	102812	YKI			COX7AL	COX7A1, COX7A2, COX7A2L
CG18374	110806	YKI			Gk1	GK, GK2, GK5, SHPK
CG1840	108492	YKI				SELENOK
CG18505	105745	YKI			Acyp2	ACYP1, ACYP2
CG1857	108366	YKI			nec	SERPINI1, SERPINI2, SERPINE1, SERPINE2, SERPINE3, SERPINA1, SERPINB7, SERPINC1, SERPIND1
CG18609	100172	YKI				ELOVL7, ELOVL1, ELOVL2, ELOVL4, ELOVL5
CG18617	109763	YKI			Vha100-2	ATP6V0A4, ATP6V0A1, ATP6V0A2, TCIRG1
CG1862	105139	YKI			ephrin	EFNB2, EFNB1, EFNB3, EFNA1, EFNA2, EFNA3, EFNA4, EFNA5,
CG18641	102771	YKI				LIPI
CG18642	101333	YKI			Bem46	ABHD13
CG18659	104988	YKI				DENND1B, DENND1C, DENND1A
CG18662	101973	YKI				PHPT1
CG1868	106709	YKI			Smyd4-1	SMYD4, SMYD5
CG18764	107494	YKI				ZNF274, ZNF8
CG18811	110272	YKI			Capr	CAPRIN1, CAPRIN2
CG18814	106349	YKI				HPGD
CG1942	107788	YKI				MOGAT2, DGAT2L6, DGAT2, MOGAT1, AWAT1, MOGAT3, AWAT2, DGAT2L7P
CG1969	103542	YKI				GNPNAT1

CG2006	109100	YKI				DTWD1
CG2075	104705	YKI			aly	LIN9
CG2092	104674	YKI			scra	ANLN
CG2110	108486	YKI			Cyp4ad1	CYP4V2, CYP4A11, CYP4A22, CYP4B1, CYP4F2, CYP4F3, CYP4F11, CYP4F12, CYP4F22, CYP4X1, CYP4Z1
CG2118	110398	YKI				MCCC1, PCCA
CG2121	109845	YKI				UNC93A, UNC93B1
CG2140	107821	YKI			Cyt-b5	CYB5A, CYB5B
CG2277	108903	YKI				NT5DC1
CG2302	101806	YKI			nAChRalpha3	CHRNA6, CHRNA2, CHRNA4, CHRNA3, CHRNA5, CHRNA1, CHRNB1, CHRNB2, CHRNB3, CHRNB4, CHRND, CHRNE, CHRNG, CHRFAM7A, CHRNA7, CHRNA9, CHRNA10
CG2330	109002	YKI				NCDN
CG2397	104735	YKI			Cyp6a13	TBXAS1, CYP3A4, CYP3A5, CYP3A7-CYP3A51P, CYPA43
CG2520	105767	YKI			lap	PICALM, SNAP91
CG2617	106224	YKI				RNF26, MGRN1, RNF157
CG2621	101538	YKI			sgg	GSK3B, GKS3A
CG2662	106361	YKI				SAMD13, SAMD1
CG2736	102672	YKI				SCARB2, SCARB1
CG2788	100545	YKI			dot	UGT1A3, UGT2B10, UGT1A1, UGT2A2, UGT2A3, UGT2B4, UGT2B7, UGT2B11, UGT2B15, UGT2B17, UGT2B28, UGT3A1, UGT3A2, UGT8, UGT1A4, UGT1A5, UGT1A6, UGT1A7, UGT1A8, UGT1A9, UGT1A10
CG2818	108972	YKI				GPCPD1
CG2819	110594	YKI			Pph13	ESX1
CG2852	102376	YKI				PPIB, PPIC

CG2862	110597	YKI				HINT1, HINT2
CG2932	110761	YKI			Klf15	KLF15
CG2984	105249	YKI			Pp2c1	PPM1D
CG2995	110662	YKI			G9a	EHMT1, EHMT2, SUV39H1, SUV39H2
CG30005	101955	YKI			gstt2	GSTT2B, GSTT2, GSTT1
CG30008	102817	YKI				ELOVL7, ELOVL4, ELOVL1
CG30011	107051	YKI			gem	TFCP2, TFCP2L1, UBP1, GRHL1, GRHL3
CG30047	100371	YKI				ERMP1
CG30268	101626	YKI				CFAP61
CG30410	100275	YKI			Rpi	RPIA
CG30417	107378	YKI			tbrd-3	BRD2, BRD3, BRD4, BRDT
CG30421	103553	YKI			Usp15-31	USP31, USP43, USP11
CG30423	106411	YKI				LEPROT, LEPROTL1
CG3071	107206	YKI				UTP15
CG3086	110317	YKI			MAPk-Ak2	MAPKAPK3, MAPKAPK2, MAPKAPK5
CG3091	109832	YKI				TTPAL, CLVS1, CLVS2, RLBP1, SEC14L4, TTPA
CG31006	109525	YKI			stops	ASB17
CG31094	106364	YKI			LpR1	VLDLR, LRP8, LDLR
CG31119	108098	YKI			HDAC11	HDAC11
CG31139	102665	YKI				POGLUT1, KDELC1, KDELC2
CG31146	104209	YKI			Nlg1	NLGN1, NLGN3, NLGN4X, NLGN4Y, NLGN2
CG31195	104743	YKI				GPR158, GPR179
CG31198	107738	YKI				ANPEP, ENPEP, LVRN, TRHDE, ERAP1, ERAP2, LNPEP, NPEPPS
CG31202	109700	YKI			alpha-Man-Ic	MAN1A2, MAN1C1, MAN1A1
CG3121	106848	YKI				RSPH4A, RSPH6A
CG31410	100445	YKI			Npc2e	NPC2
CG31426	100304	YKI			eIF2D	EIF2D

CG31427	100427	YKI				ANPEP, ENPEP, ERAP1, ERAP2, LNPEP, LVRN, TRHDE
CG31482	101730	YKI				GLIPR2, CRISPLD2, CRISPLD1
CG31528	109886	YKI				UBQLN4, UBQLN2, UBQLNL, UBQLN1
CG3153	101233	YKI			Npc2b	NPC2
CG3159	104371	YKI			Eaat2	SLC1A2, SLC1A1, SLC1A3, SLC1A4, SLC1A5, SLC1A6
CG31651	110647	YKI			pgant5	GALNT1, GALNT13, GALNT3, GALNT4, GALNT5, GALNTL6, GALNT7, GALNT10, GALNT11, GALNT12, GALNTL5, GALNT6, POC1B-GALNT4
CG31659	103022	YKI				APOD
CG31851	104306	YKI			Naa20B	NAA20
CG31860	103398	YKI			ZnT33D	SLC30A3, SLC30A2, SLC30A8
CG3187	110639	YKI			Sirt4	SIRT4
CG32022	100506	YKI				WRB
CG3204	107745	YKI			Rap2l	RAP2A, RAP2B, RAP2C, RAP1A
CG32063	105787	YKI			S-Lap3	LAP3, NPEPL1
CG32082	110374	YKI			IRSp53	BAIAP2, BAIAP2L1, BAIAP2L2
CG32110	107634	YKI				SENP1, SENP2, SENP3, SENP5
CG32180	105301	YKI			Eip74EF	ELF2, ELF1, ELF4
CG32190	100688	YKI			NUCB1	NUCB2, NUCB1
CG32196	101791	YKI				GGCT
CG32238	109628	YKI				TTLL1, TTLL9, TTLL5, TTL
CG32250	108323	YKI			PMP34	SLC25A17
CG32333	100303	YKI				FAM135A, FAM135B
CG32343	104385	YKI			Atac3	GABPB2, FLJ10038
CG32351	107316	YKI			S-Lap2	LAP3, NPEPL1
CG32376	101917	YKI				PRSS57

CG32441	102827	YKI				EMC10
CG32528	105356	YKI			parvin	PARVB, PARVA, PARVG
CG32568	103317	YKI				PPP2R5E, PPP2R5A, PPP2R5B, PPP2R5C, PPP2R5D
CG32578	107774	YKI			PIG-Q	PIGQ
CG32598	109386	YKI			betaNACtes6	BTF3, BTF3L4
CG32616	109155	YKI			Ste12DOR	CSNK2B
CG3262	110038	YKI				NUBPL
CG32632	105756	YKI			Tango13	TPST1, TPST2
CG32697	104427	YKI			Ptpmeg2	PTPN9
CG32717	100685	YKI			sdt	MPP5, CASK, MPP1, MPP2, MPP3, MPP4, MPP6, MPP7
CG32832	102996	YKI				MPC2
CG33056	101024	YKI				OARD1
CG33096	104875	YKI				ABHD17C, ABHD17B, ABHD17A
CG33145	104256	YKI			GalT1	B3GALT1, B3GALT2, B3GALT5, B3GALNT1, B3GNT4
CG33156	103902	YKI				NADK
CG33193	101323	YKI			sav	SAV1
CG33288	108718	YKI				RPGR, RCC1
CG33336	103001	YKI			p53	TP63, TP73, TP53
CG33346	100352	YKI				ENDOG
CG33349	101808	YKI			ppk25	ASIC4, ASIC2, ASIC5
CG3347	100453	YKI				CXXC1
CG33474	102875	YKI				PEX11G
CG33653	110055	YKI			Cadps	CADPS, CADPS2
CG33695	109095	YKI				C17orf49
CG33957	101645	YKI			Plp	PCNT, AKAP9
CG33960	108030	YKI			Sema-2b	SEMA4C, SEMA4A, SEMA4D, SEMA4G, SEMA3A, SEMA3C, SEMA3D, SEMA3E, SEMA3F, SEMA3G, SEMA4B, SEMA4F, SEMA6A, SEMA6B, SEMA6C, SEMA7A,

CG33980	104981	YKI			Vsx2	VSX2, VSX1
CG3403	110742	YKI			Mob4	MOB4, HSPE1-MOB4
CG34041	103005	YKI				P4HA1, P4HA3, P4HA2
CG34058	107741	YKI			ppk11	SCNN1B, SCNN1G, ASIC1, ASIC4, ASIC2, ASIC5
CG34120	100384	YKI				ABCA12, ABCA13, ABCA1, ABCA4, ABCA2, ABCA3, ABCA5, ABCA6, ABCA7, ABCA8, ABCA9, ABCA10
CG3424	100519	YKI			path	SLC36A3, SLC36A2, SLC36A1, SLC36A4
CG34242	103881	YKI				SMIM20
CG3428	104424	YKI			pall	FBXO28
CG3434	108324	YKI				QTRT2
CG34353	107519	YKI				LSAMP
CG34360	105014	YKI			Glut4E	ZNF704, ZNF395, SLC2A4RG
CG34375	102586	YKI				SIAH1, SIAH2, SIAH3
CG34377	103192	YKI				SAMD5, SAMSN1, SASH3
CG34387	103844	YKI			futsch	MAP1A, MAP1B, MAP1S
CG34392	110077	YKI			Epac	RAPGEF4, RAPGEF3, RAPGEF5, RAPGEFL1
CG34405	101695	YKI			NaCP60E	SCN8A, SCN3A, SCN5A, SCN9A, SCN10A, SCN11A, CACNA1A, CACNA1C, CACNA1D, CACNA1S, NALCN, SCN1A, SCN2A, SCN4A, SCN7A
CG34414	106127	YKI			spri	RIN2, RIN1, RIN3, RINL
CG34424	107787	YKI				ST20-MTHFS, MTHFS
CG3491	107845	YKI				SBNO2, SBNO1
CG3495	108926	YKI			Gmer	TSTA3
CG3499	105143	YKI			YME1L	YME1L1, SPG7
CG3508	100500	YKI			Hexim	HEXIM1, HEXIM2
CG3513	107668	YKI				EPPIN-WFDC6
CG3524	105855	YKI			FASN	FASN
CG3525	103784	YKI			eas	ETNK1, ETNK2

CG3530	110786	YKI				MTMR7, MTMR8, MTMR6, MTMR1, MTMR2
CG3566	102685	YKI				CYB5A, CYB5B
CG3578	100598	YKI			bi	TBX2, TBX3, TBX1, TBX4, TBX5, TBX15, TBX18
CG3587	108263	YKI				KTI12
CG3599	106976	YKI			Btnd	BTD, VNN2, VNN1, VNN3
CG3705	110661	YKI			aay	PSPH
CG3723	108658	YKI			Dhc93AB	DNAH9, DNAH17, DNAH11, DNAH1, DNAH2, DNAH3, DNAH5, DNAH6, DNAH7, DNAH8, DNAH10, DNAH12, DYNC2H1, DYNC1H1
CG3730	108850	YKI			csul	PRMT5
CG3798	108378	YKI			Nmda1	GRINA, TMBIM4, TMBIM1, FAIM2
CG3803	105443	YKI				COX15
CG3808	108653	YKI				TRMT2A, TRMT2B
CG3837	105549	YKI			Sdr	IGF1R, INSRR, INSR
CG3850	109584	YKI			sug	GLIS2
CG3858	101692	YKI			gcm	GCM1, GCM2
CG3891	106132	YKI			Nf-YA	NFYA
CG3942	106222	YKI				GPCPD1
CG3944	110797	YKI			ND-23	NDUFS8
CG3954	108352	YKI			csw	PTPN11, PTPN6
CG4008	110459	YKI			und	METAP2
CG40188	109995	YKI			Pzl	PIEZO1, PIEZO2
CG4019	107980	YKI			Eglp4	AQP4, AQP5, AQP6, AQP1, AQP2, AQP8, MIP
CG4109	107014	YKI			Syx8	STX8
CG4162	110181	YKI				SPTLC2, SPTLC3
CG4200	108593	YKI			sl	PLCG1, PLCG2
CG42235	107662/107975	YKI				SLC5A5, SLC5A6, SLC5A8, SLC5A12, SLC5A1, SLC5A2, SLC5A3, SLC5A4, SLC5A9, SLC5A10, SLC5A11
CG42249	101200	YKI				NT5E

CG42280	110361	YKI			ome	FAP, DPP4, DPP6, DPP10
CG42309	102757	YKI			Mlp60A	CSRP3, CSRP1, CSRP2
CG42314	109188	YKI			PMCA	ATP2B3, ATP2B1, ATP2B2, ATP2B4
CG42318	106488	YKI			app	ZDHHC14, ZDHHC18, ZDHHC9, ZDHHC8, ZDHHC5
CG42324	106215	YKI				TJAP1, BEGAIN
CG42343	107402/106021	YKI			DIP-beta	IGLON5, CXADR, NTM, OPCML, LSAMP, NEGR1
CG42345	101687	YKI			laccase2	CP, HEPHL1, HEPH
CG42366	108102	YKI				ICK, MAK, MOK
CG42368	103497	YKI			DIP-epsilon	LSAMP, NTM, OPCML, IGLON5, NEGR1
CG42396	106390	YKI				TRIM71
CG4244	103814	YKI			Su(dx)	ITCH, WWP2, WWP1, NEDD4L, NEDD4, SMURF2, SMURF1
CG42450	105315	YKI				RGS9, RGS11
CG42492	104973	YKI				OTOP2, OTOP1, OTOP3
CG42540	101372	YKI				STOM, STOML3, NPHS2
CG42551	107986	YKI			larp	LARP1B, LARP1
CG42588	100428	YKI				GTF3C2
CG42612	106969	YKI			plx	TBC1D1, TBC1D4, EVI5
CG42667	102909	YKI			rdgA	DGKZ, DGKI
CG42668	110074	YKI				OSBPL8, OSBPL5, OSBPL9, OSBPL11, OSBPL10
CG42672	105645	YKI				KIDINS220, NKPD1
CG42675	108939	YKI				ZC2HC1C, ZC2HC1A, ZC2HC1B
CG42679	100113	YKI			Lmpt	FHL2
CG42734	107238	YKI			Ank2	ANK2, ANK3, ANK1
CG42741	107324	YKI				KLF8, KLF12, KLF3, KLF14, KLF5
CG4278	103933	YKI				NIF3L1
CG42814	108204	YKI				NUDT14
CG4290	103739	YKI			Sik2	SIK2, SIK1, LOC102724428
CG43102	110150	YKI				ARHGEF17

CG43128	102218/108861	YKI			Shab	KCNB1, KCNB2, KCNF1, KCNS1, KCNS3, KCNV1, KCNV2, KCNS2, KCNG1, KCNG2, KCNG3, KCNG4
CG43224	103523	YKI			Gfrl	GFRAL, GFRA1, GFRA2, GFRA4, GFRA3
CG43226	108082	YKI			lute	BTBD3, BTBD6, BTBD2, BTBD1
CG43367	107981	YKI				NBEAL2, NBEAL1
CG43368	104168	YKI			cac	CACNA1B, CACNA1A, CACNA1E, CACNA1C, CACNA1D, , CACNA1S, CACNA1F
CG43374	105536	YKI			Cht6	CHIA, CHIT1, OVGP1, CHI3L2, CHI3L1
CG4356	101407	YKI			mAChR-A	CHRM1, CHRM3, CHRM5, CHRM4, CHRM2
CG43729	102798	YKI				STAC3, STAC2, STAC
CG43744	102442	YKI			bru-3	CELF5, CELF3, CELF4, CELF6, CELF1, CELF2
CG43749	110631	YKI			dysc	WHRN, PDZD7
CG4376	110719	YKI			Actn	ACTN2, ACTN1, ACTN4, ACTN3, SPTBN5 SPTBN5
CG43795	107979	YKI				GPR158, GPR179
CG43867	105096	YKI				PLEKHH1, PLEKHH2
CG44007	108981	YKI			Pde1c	PDE1A, PDE1B, PDE1C
CG44086	106358	YKI			RapGAP1	RAP1GTP2, RAP1GAP, SIPA1L3
CG44244	109071	YKI			Glycogenin	GYG1, GYG
CG4434	108274	YKI			bb8	GLUD1, GLUD2
CG44402	104181	YKI			yin	SLC15A2, SLC15A1, SLC15A4
CG44425	109933	YKI			Bx	LMO1, LMO3, LMO2
CG4495	110456	YKI			MICU1	MICU1
CG45049	102985	YKI				TMEM47, PERP

CG45477	104535/110310	YKI			mamo	SP1
CG45760	106410	YKI			JYalpha	ATP1A1, ATP4A, ATP12A, ATP1A2, ATP1A3, ATP1A4
CG4599	107813	YKI			Tpr2	DNAJC7
CG4610	106045	YKI				MTO1
CG4626	102339	YKI			fz4	FZD4, SFRP2, FZD10, FZD9, SFRP5, SFRP1
CG4681	103752	YKI				TEX9
CG4698	104671	YKI			Wnt4	WNT9B, WNT9A, WNT11, WNT1, WNT2B, WNT2, WNT3A, WNT3, WNT4, WNT5A, WNT5B, WNT6, WNT7A, WNT7B, WNT10A, WNT10B, WNT16
CG4721	100379	YKI				KEL, ECEL1
CG4767	101714	YKI			Tektin-A	TEKT4, TEKT1, TEKT5, TEKT3
CG4798	106934	YKI			l(2)k01209	UCKL1, UPRT, UCK1, UCK2
CG4802	108304	YKI			MTAP	MTAP
CG4900	105583	YKI			Irp-1A	ACO1, IREB2
CG4905	110602	YKI			Syn2	SNTG1, SNTG2
CG4952	106040	YKI			dac	DACH1, DACH2
CG5009	103761	YKI				ACOX1, ACOX2
CG5087	106663	YKI				UBE3B, UBE3C
CG5104	109822	YKI				SFT2D1, SFT2D2, SFT2D3
CG5110	104189	YKI				LAMTOR3
CG5125	110702	YKI			ninaC	MYO3A, MYO3B
CG5160	106081	YKI				RASL11B, RASL11A, RERGL
CG5165	105820	YKI			Pgm	PGM1, PGM5
CG5184	106653	YKI			mRpS11	MRPS11
CG5203	107447	YKI			STUB1	STUB1
CG5278	107919	YKI			sit	ELVOL7, ELOVL1, ELOVL4, ELOVL5, ELOVL2
CG5290	105655	YKI				TTC27

CG5345	103779	YKI			Eip55E	CTH
CG5417	101444	YKI			Srp14	SRP14
CG5445	100682	YKI				C6orf106
CG5565	100396	YKI				PUDP
CG5583	107292	YKI			Ets98B	SPDEF
CG5589	108642	YKI				DDX52
CG5634	104368	YKI			dsd	ATRN, ATRNL1
CG5671	101475	YKI	EGFR		Pten	PTEN, TPTE2
CG5701	100815	YKI			RhoBTB	RHOBTB1, RHOBTB2
CG5747	103726	YKI			mfr	FER1L6, OTOF, DYSF, MYOF, FER1L5
CG5748	108851	YKI			Hsf	HSF1, HSF2, HSF4
CG5784	100283	YKI			Mapmodulin	ANP32B, ANP32A, ANP32E, ANP32D, ANP32C
CG5846	107793	YKI				RFXANK, ANKRA2
CG5862	110238	YKI				DDRGK1
CG5874	106245	YKI			Nelf-A	NELFA
CG5886	106471	YKI				TXLNA, TXLNB, TXLNG
CG5887	104350	YKI			Desat1	SCD, SCD5
CG5948	104809	YKI				SOD3
CG5954	104563	YKI			l(3)mbt	L3MBTL3, L3MBTL4, L3MBTL1
CG6072	107573	YKI			sra	RCAN2, RCAN3, RCAN1
CG6091	109912	YKI			Duba	OTUD5, OTUD4
CG6103	101512	YKI			CrebB	CREB1, ATF1, CREM
CG6136	109421	YKI				CUTC
CG6145	104271	YKI				NADK
CG6147	110811	YKI			Tsc1	TSC1
CG6180	106923	YKI				PEBP1, PEBP4
CG6182	106667	YKI				TBC1D7, TBC1D7-LOC100130357
CG6186	106479	YKI			Tsf1	MELTF, LTF, TF
CG6214	105419	YKI			MRP	ABCC3, ABCC1, ABCC6, ABCC2, ABCC8, ABCC9, ABCC4, ABCC10, ABCC12, ABCC11, ABCC5

CG6235	104167	YKI			tws	PPP2R2D, PPP2R2A, PPP2R2B, PPP2R2C
CG6265	107430	YKI			Nep5	PHEX, MME
CG6287	100689	YKI				PHGDH
CG6363	110618	YKI			MRG15	MORF4L1, MORF4L2
CG6406	104577	YKI				FAM126A, FAM126B
CG6512	109629	YKI				AFG3L2, SPG7
CG6585	104162	YKI			Cyp308a1	TBXAS1, CYP3A4, CYP3A5, CYP3A43
CG6601	100774	YKI			Rab6	RAB6A, RAB6B, RAB6C, RAB41
CG4030	110346	YKI			Rbpn-5	RABEP1, EEA1, RABEP2
CG6613	108079	YKI				PLEKHM3, PLEKHM1, DEF8
CG6647	101336	YKI			porin	VDAC2, VDAC3, VDAC1
CG6660	101046	YKI				ELOVL7, ELOVL1, ELOVL2, ELOVL4, ELOVL5
CG6674	107226	YKI				TSSC4
CG6690	101104	YKI				QSOX2, QSOX1
CG6703	104793	YKI			CASK	CASK, MPP1, MPP2, MPP3, MPP4, MPP5, MPP6, MPP7
CG6707	110291	YKI				TMEM55B, TMEM55A
CG6721	105383	YKI			RasGAP1	RASA3, RASA2, RASA4B, RASA4, RASAL1
CG6725	107003	YKI			Sulf1	SULF1, SULF2
CG6726	108360	YKI				ACY1, ABHD14A, PM20D1, ABHD14A-ACY1
CG6734	106697	YKI				WDRS1
CG6751	107563	YKI			NCLB	PWP1
CG6754	110366	YKI			nbs	NBN
CG6835	110013	YKI			GSS	GSS
CG6863	110432	YKI			tok	BMP1, TLL1, TLL2, ASTL, CUBN, MEP1A, MEP1B
CG7053	106176	YKI			Atg101	ATG101
CG7112	103588	YKI			GAPcenA	RABGAP1, RABGAP1L
CG7113	110802	YKI			scu	HSD17B10
CG7128	108643	YKI			Taf8	TAF8

CG7134	103627	YKI			cdc14	CDC14B, CDC14A
CG7158	104135	YKI			Als2	ALS2, ALS2CL, MORN4
CG7176	100554	YKI			Idh	IDH1, IDH2
CG7183	109461	YKI				CCDC174
CG7192	105607	YKI			Mvb12	MVB12A, MVB12B
CG7210	105397	YKI			kel	KLHL3, KLHL2
CG7218	110269	YKI				TAPT1
CG7266	104465	YKI			Eip71CD	MSRA
CG7285	110739	YKI			AstC-R1	SSTR2, SSTR1, SSTR3, SSTR4, SSTR5, NPBWR1, MCHR1, MCHR2, NPBWR2, OPRD1, OPRK1, OPRL1, OPRM1
CG7365	106202	YKI				PLB1
CG7391	104507	YKI			Clk	CLOCK, NPAS2, PASD1
CG7404	108349	YKI			ERR	ESRRG, ESRRB, ESRRA, AR, ESR1, ESR2, NR3C1, NR3C2, PGR
CG7523	102694	YKI				TMEM192
CG7573	107984	YKI				ZMPSTE24
CG7586	100197	YKI			Mcr	C3, C4A, C4B, A2ML1, C5, CPAMD8, A2M
CG7670	100227	YKI			WRNexo	WRN
CG7694	108995	YKI				RNF181
CG7791	109658	YKI				MIPEP
CG7881	105576	YKI				SLC17A1, SLC17A3, SLC17A4, SLC17A5
CG7883	101537	YKI			eIF2Balpha	EIF2B1
CG7892	104885	YKI			nmo	NLK
CG7908	106335	YKI			Tace	ADAM17
CG7923	101190	YKI			Fad2	SCD, SCD5
CG7940	110235	YKI			Arp5	ACTR5
CG7946	100307	YKI				PSIP1, HDGF, HDGFRP2, HDGFRP3, HDGFL1
CG7952	105070	YKI			gt	DBP, TEF, HLF

CG8026	105681	YKI				SLC25A32
CG8027	109400	YKI				GNPTAB
CG8032	108652	YKI				PAOX, SMOX, KDM1A
CG8036	105633	YKI				TKT, TKTL2, TKTL1
CG8075	100819	YKI			Vang	VANGL1, VANGL2
CG8128	107574	YKI				NUDT6
CG8134	104940	YKI				F8A3, F8A1, F8A2
CG8141	101087	YKI				RNF5, RNF185
CG8156	100726	YKI			Arf51F	ARF6
CG8173	105661	YKI				PBK, MOS
CG8194	108790	YKI			RNaseX25	RNASET2
CG8196	101151	YKI			Ance-4	ACE, ACE2, TMEM27
CG8214	101132	YKI			Cep89	CEP89
CG8226	102728	YKI			Tom7	TOMM7
CG8228	110660	YKI			Vsp45	VPS45
CG8230	107019	YKI				DYM
CG8245	103562	YKI				TMEM53
CG8272	106686	YKI				LRRC29
CG8276	101090	YKI			Bin3	MEPCE
CG8286	109649	YKI			P58IPK	DNAJC3
CG8290	104095	YKI			ADD1	DNMT3B
CG8295	100719	YKI			Mlf	MLF2, MLF1
CG8321	104285	YKI				ARL6IP6
CG8357	100748	YKI			Drep1	CIDEA, CIDEB, CIDEC, DDFA
CG8372	100618	YKI				TMEM222
CG8428	105462	YKI				SPSN1, SPNS2, SPNS3
CG8451	104177	YKI			SLC5A11	SLC5A5, SLC5A6, SLC5A8, SLC5A12
CG8507	104321	YKI				LRPAP1
CG8519	102867	YKI				RASL11A, RASL11B, RERGL, RERG, RASL12
CG8596	109291	YKI			Cin7	MFSD8
CG8602	101575	YKI				MSFD1
CG8611	104379	YKI				DDX31
CG8612	106402	YKI			mRpL-50	MRPL50

CG8642	101888	YKI				FIBCD1, ANGPTL7, FCN2, FCN3, TNXB, ANGPTL4, FNC1, FGB, FGL1, TNC, TNN, TNR, ANGPT1, ANGPT2, ANGPT4, ANGPTL1, ANGPTL2,ANGPTL3, ANGPTL5, ANGPTL6, FGA, FGG, FGL2, MFAP4
CG8666	107776	YKI			Tsp39D	CD63
CG8709	107707	YKI			Lpin	LPIN3, LPIN2, LPIN1
CG8773	104260	YKI				ENPEP, ANPEP, ERAP1, ERAP2, TRHDE, LVRN, LNPEP, NPEPPS
CG8831	103724	YKI			Nup54	NUP54
CG8948	110812	YKI			Graf	ARHGAP26, ARHGAP10, ARHGAP42, OPHN1
CG8958	100547	YKI				CNBD2
CG8998	100629	YKI			Roc2	RNF7, RBX1
CG9089	110270	YKI			wus	DNAJC22
CG9117	107392	YKI				MBLAC1
CG9181	108888	YKI			Ptp61F	PTPN1, PTPN2
CG9241	103568	YKI			Mcm10	MCM10
CG9245	106842	YKI			Pis	CDIPT
CG9246	104868	YKI				NOC2L
CG9320	108211	YKI			Ns4	GNL1
CG9399	101455	YKI				MPC2
CG9413	108867	YKI				SLC7A9, SLC7A5, SLC7A6, SLC7A7, SLC7A8, SLC7A10
CG9449	102991	YKI				ACPP, ACP2, ACPT, ACP6
CG9474	108209	YKI			Snap24	SNAP25, SNAP23
CG9499	100643	YKI			ppk7	ASIC4, ASIC1, ASIC5, SCNN1B, SCNN1G
CG9501	110258	YKI			ppk14	ASIC1, ASIC2, ASIC3, ASIC4, ASIC5
CG9543	107588	YKI			epsilonCOP	COPE
CG9576	106196	YKI			Phf7	PHF7, G2E3, PHF6, PHF11

CG9588	100126	YKI				PSMD9
CG9610	106103	YKI			Poxm	PAX9, PAX1
CG9614	102352	YKI			pip	UST, HS2ST1
CG9646	103414	YKI				KIAA0930
CG9667	104484	YKI				ISY1, ISY1-RAB43
CG9701	105406	YKI				LCTL, KL, LCT, KLB GBA3
CG9749	100714	YKI			Abi	ABI2, ABI1, ABI3
CG9761	102584	YKI			Nep2	ECE1, MMEL1, MME, ECE2, PHEX, ECEL1
CG9765	101439	YKI			tcc	TACC1, TACC2, TACC3
CG9779	100295	YKI			Vps24	CHMP3, RNF103-CHMP3, RNF103
CG9865	101344	YKI				PIGM
CG9887	104324	YKI			VGlut	SLC17A6, SLC17A7, SLC17A8, SLC17A5
CG9934	110693	YKI				UBE4B
CG9945	105944	YKI				DCAF11
CG9947	105288	YKI				TMEM30A, TMEM30B
CG9952	100298	YKI			Ppa	FBXL14
CG9967	106352	YKI				MKRN2OS
CG9986	110352	YKI				C12orf4
CG10079	107130			SOCS	Egfr	EGFR
CG10130	107784			SOCS	Sec61beta	SEC61B
CG10374	106891			SOCS	Lsd1	PLIN3, PLIN1, PLIN5, PLIN2
CG10944	105279			SOCS	RpS6	RPS6
CG11027	101456			SOCS	Arf102F	ARF4, ARF5, ARF1, ARF3
CG12000	101990			SOCS	Prosbeta7	PSMB4
CG12192	100530			SOCS	Klp59D	KIF2B
CG12775	105819			SOCS	RpL21	RPL21
CG1796	101441			SOCS	Tango4	PLRG1
CG1877	108558			SOCS	Cul1	CUL1
CG2685	106918			SOCS		WBP11
CG2699	104179			SOCS	Pi3K21B	PIK3R3, PIK3R1

CG33871	109058			SOCS		HIST1H4C, HIST1H4B, HIST1H4I, HIST1H4F, HIST1H4K, HIST2H4A, HIST1H4G, HIST1H4E, HIST4H4, HIST1H4H, HIST1H4D, HIST1H4L, HIST1H4J, HIST1H4A, HIST2H4B
CG3997	108821			SOCS	RpL39	RPL39, RPL39L
CG4257	106980			SOCS	Stat92E	STAT5B, STAT5A, STAT6, STAT3, STAT4, STAT2, STAT1
CG5179	103561			SOCS	Cdk9	CDK9, CDK13, CDK12
CG5378	101467			SOCS	Rpn7	PSMD6
CG5525	106099			SOCS	Cct4	CCT4
CG5546	103926			SOCS	Med19	MED19
CG5859	100004			SOCS	ints8	INTS8
CG6033	105498			SOCS	drk	GRB2, GRAP, GRAP2, GRAPL
CG6090	109994			SOCS	RpL34	RPL34
CG7000	104210			SOCS	Snmp1	SCARB2, SCARB1, CD36
CG7283	109345			SOCS	RpL10Ab	RPL10A
CG8258	103905			SOCS		CCT8, CCT8L2
CG8385	103572			SOCS	Arf79F	ARF1, ARF3, ARL17B, ARF4, ARF5, ARL17A
CG8427	103560			SOCS	SmD3	SNRPD3
CG8977	106093			SOCS	CCT3	CCT3
CG9258	103702			SOCS	nrv1	ATP1B1, ATP1B2, ATP1B3, ATP1B4, ATP4B
CG9750	103483			SOCS	rpt	RUVBL2

Table 2.3.2.1				
#term ID	**term description**	**observed gene count**	**background gene count**	**false discovery rate**
GO:0009987	cellular process	166	6847	1.01E-09
GO:0046621	negative regulation of organ growth	7	19	0.00014
GO:0048638	regulation of developmental growth	17	218	0.00019
GO:0007154	cell communication	51	1505	0.00027
GO:0071840	cellular component organization or biogenesis	77	2753	0.00027
GO:0023052	signaling	49	1442	0.0003
GO:0048640	negative regulation of developmental growth	10	76	0.00036
GO:0016043	cellular component organization	72	2606	0.00075
GO:0044267	cellular protein metabolic process	52	1644	0.00075
GO:0040008	regulation of growth	18	300	0.00087
GO:0007010	cytoskeleton organization	25	540	0.00092
GO:0051128	regulation of cellular component organization	31	767	0.00092
GO:0046620	regulation of organ growth	8	54	0.0011
GO:0050794	regulation of cellular process	90	3635	0.0013
GO:0051716	cellular response to stimulus	52	1710	0.0013
GO:0006996	organelle organization	52	1727	0.0015
GO:0007165	signal transduction	41	1226	0.0015
GO:0009719	response to endogenous stimulus	13	177	0.0015

GO:0043412	macromolecule modification	41	1225	0.0015
GO:0071495	cellular response to endogenous stimulus	12	151	0.0015
GO:0007017	microtubule-based process	21	434	0.0016
GO:0044237	cellular metabolic process	95	3966	0.0016
GO:0050789	regulation of biological process	94	3908	0.0016
GO:0006464	cellular protein modification process	38	1127	0.0018
GO:0008285	negative regulation of cell population proliferation	9	86	0.0018
GO:0050896	response to stimulus	69	2621	0.0019
GO:0072089	stem cell proliferation	8	66	0.0019
GO:0051093	negative regulation of developmental process	13	192	0.002
GO:0003341	cilium movement	6	34	0.0027
GO:0051960	regulation of nervous system development	17	324	0.0027
GO:0010646	regulation of cell communication	31	869	0.0032
GO:0023051	regulation of signaling	31	872	0.0033
GO:0035556	intracellular signal transduction	18	366	0.0033
GO:0065007	biological regulation	100	4357	0.0033
GO:0008283	cell population proliferation	12	178	0.0035
GO:0000226	microtubule cytoskeleton organization	16	305	0.0037
GO:0016311	dephosphorylation	12	181	0.0039
GO:0043547	positive regulation of GTPase activity	9	102	0.0041
GO:2000026	regulation of multicellular organismal development	22	526	0.0041
GO:0033043	regulation of organelle organization	18	382	0.0043
GO:0070887	cellular response to chemical stimulus	17	346	0.0043
GO:0051241	negative regulation of multicellular organismal process	12	186	0.0044
GO:0009966	regulation of signal transduction	28	778	0.0049
GO:0051345	positive regulation of hydrolase activity	11	162	0.0054
GO:0007018	microtubule-based movement	11	164	0.0056

GO:0016192	vesicle-mediated transport	20	468	0.0056
GO:0022008	neurogenesis	30	875	0.0056
GO:0044260	cellular macromolecule metabolic process	60	2291	0.0056
GO:0050793	regulation of developmental process	26	703	0.0056
GO:0010648	negative regulation of cell communication	16	326	0.0057
GO:0023057	negative regulation of signaling	16	326	0.0057
GO:0042771	intrinsic apoptotic signaling pathway in response to DNA damage by p53 class mediator	3	4	0.0057
GO:1902531	regulation of intracellular signal transduction	16	326	0.0057
GO:0051239	regulation of multicellular organismal process	26	713	0.0058
GO:0006928	movement of cell or subcellular component	25	680	0.0067
GO:0009968	negative regulation of signal transduction	15	303	0.0075
GO:0009314	response to radiation	11	176	0.0079
GO:0009628	response to abiotic stimulus	18	414	0.0079
GO:0043065	positive regulation of apoptotic process	7	69	0.0079
GO:0007163	establishment or maintenance of cell polarity	12	208	0.0081
GO:0042981	regulation of apoptotic process	12	209	0.0083
GO:0016575	histone deacetylation	4	16	0.0086
GO:0016570	histone modification	11	181	0.0091
GO:0006793	phosphorus metabolic process	30	918	0.0092
GO:0007423	sensory organ development	19	463	0.0092
GO:0009725	response to hormone	9	124	0.0092
GO:0032870	cellular response to hormone stimulus	8	98	0.0092
GO:0048699	generation of neurons	28	832	0.0092
GO:0035329	hippo signaling	3	6	0.0094
GO:0051336	regulation of hydrolase activity	15	318	0.0094
GO:0051641	cellular localization	29	880	0.0094
GO:0050790	regulation of catalytic activity	20	510	0.0102

GO:0006644	phospholipid metabolic process	9	130	0.0113
GO:0001654	eye development	16	365	0.0123
GO:1901699	cellular response to nitrogen compound	7	79	0.0123
GO:0019538	protein metabolic process	55	2158	0.013
GO:0046626	regulation of insulin receptor signaling pathway	5	37	0.0137
GO:0007528	neuromuscular junction development	7	82	0.0141
GO:0035335	peptidyl-tyrosine dephosphorylation	5	38	0.0147
GO:0008152	metabolic process	105	4926	0.0148
GO:0045464	R8 cell fate specification	3	8	0.0148
GO:0051961	negative regulation of nervous system development	8	110	0.0148
GO:0071310	cellular response to organic substance	12	233	0.0148
GO:0001667	ameboidal-type cell migration	10	170	0.0154
GO:0008582	regulation of synaptic growth at neuromuscular junction	8	111	0.0154
GO:0046486	glycerolipid metabolic process	8	111	0.0154
GO:0048518	positive regulation of biological process	39	1393	0.0154
GO:0048522	positive regulation of cellular process	36	1247	0.0154
GO:0048523	negative regulation of cellular process	35	1198	0.0154
GO:0046627	negative regulation of insulin receptor signaling pathway	4	22	0.0156
GO:0044238	primary metabolic process	90	4093	0.0159
GO:0065009	regulation of molecular function	24	710	0.0159
GO:0051179	localization	54	2151	0.0166
GO:0050803	regulation of synapse structure or activity	10	175	0.0167
GO:0007399	nervous system development	31	1028	0.0169
GO:0009888	tissue development	31	1029	0.017
GO:0048583	regulation of response to stimulus	29	940	0.0175
GO:0006897	endocytosis	10	178	0.0178
GO:0010506	regulation of autophagy	7	90	0.018

GO:0006796	phosphate-containing compound metabolic process	28	901	0.0183
GO:0009653	anatomical structure morphogenesis	40	1465	0.0183
GO:0045595	regulation of cell differentiation	15	356	0.0184
GO:0006650	glycerophospholipid metabolic process	7	91	0.0185
GO:0007268	chemical synaptic transmission	11	214	0.0187
GO:0060429	epithelium development	29	949	0.0187
GO:0050807	regulation of synapse organization	9	150	0.0188
GO:0065008	regulation of biological quality	36	1285	0.02
GO:0001751	compound eye photoreceptor cell differentiation	9	152	0.0201
GO:0044093	positive regulation of molecular function	13	288	0.0201
GO:0046907	intracellular transport	21	607	0.0207
GO:0120031	plasma membrane bounded cell projection assembly	8	123	0.0208
GO:0032879	regulation of localization	16	404	0.021
GO:0046856	phosphatidylinositol dephosphorylation	3	11	0.0213
GO:0040007	growth	10	187	0.0216
GO:0042127	regulation of cell population proliferation	11	221	0.0217
GO:0044085	cellular component biogenesis	34	1201	0.0218
GO:0030154	cell differentiation	43	1644	0.0226
GO:0010631	epithelial cell migration	9	157	0.0229
GO:0046488	phosphatidylinositol metabolic process	6	71	0.0229
GO:0043553	negative regulation of phosphatidylinositol 3-kinase activity	2	2	0.0231
GO:0043085	positive regulation of catalytic activity	12	260	0.0232
GO:0010508	positive regulation of autophagy	4	28	0.024
GO:0042306	regulation of protein import into nucleus	3	12	0.024
GO:0044087	regulation of cellular component biogenesis	13	300	0.0248
GO:1901564	organonitrogen compound metabolic process	66	2860	0.0248
GO:0001745	compound eye morphogenesis	12	264	0.0249

GO:0022414	reproductive process	34	1220	0.0252
GO:0030182	neuron differentiation	22	671	0.0262
GO:0031146	SCF-dependent proteasomal ubiquitin-dependent protein catabolic process	5	50	0.0262
GO:0071704	organic substance metabolic process	94	4432	0.0262
GO:0051649	establishment of localization in cell	23	716	0.0263
GO:0001752	compound eye photoreceptor fate commitment	5	51	0.0272
GO:0048749	compound eye development	14	344	0.0272
GO:0019953	sexual reproduction	31	1089	0.0277
GO:0120036	plasma membrane bounded cell projection organization	20	592	0.0278
GO:0006470	protein dephosphorylation	7	105	0.0285
GO:0032501	multicellular organismal process	76	3441	0.0291
GO:0045570	regulation of imaginal disc growth	4	31	0.0291
GO:0070925	organelle assembly	14	349	0.0291
GO:0007276	gamete generation	27	916	0.0303
GO:0030238	male sex determination	2	3	0.0303
GO:0070884	regulation of calcineurin-NFAT signaling cascade	2	3	0.0303
GO:0042221	response to chemical	31	1107	0.0309
GO:0048468	cell development	35	1300	0.0309
GO:0009416	response to light stimulus	8	140	0.0314
GO:0016477	cell migration	12	280	0.0317
GO:0010212	response to ionizing radiation	4	33	0.0321
GO:0031338	regulation of vesicle fusion	4	33	0.0321
GO:1901701	cellular response to oxygen-containing compound	7	110	0.0321
GO:0000003	reproduction	35	1308	0.0327
GO:0045017	glycerolipid biosynthetic process	5	56	0.0328
GO:0002065	columnar/cuboidal epithelial cell differentiation	13	321	0.0332
GO:0048870	cell motility	13	322	0.0339

GO:0030522	intracellular receptor signaling pathway	4	34	0.0343
GO:0007405	neuroblast proliferation	5	57	0.0345
GO:0048589	developmental growth	9	177	0.0345
GO:0071417	cellular response to organonitrogen compound	5	57	0.0345
GO:0051049	regulation of transport	11	249	0.0353
GO:0099003	vesicle-mediated transport in synapse	7	115	0.038
GO:0006729	tetrahydrobiopterin biosynthetic process	2	4	0.0385
GO:0006898	receptor-mediated endocytosis	4	36	0.0385
GO:0007267	cell-cell signaling	13	329	0.0385
GO:0007270	neuron-neuron synaptic transmission	2	4	0.0385
GO:0009583	detection of light stimulus	5	59	0.0385
GO:0022607	cellular component assembly	29	1035	0.0385
GO:0031329	regulation of cellular catabolic process	9	182	0.0385
GO:0032956	regulation of actin cytoskeleton organization	6	87	0.0385
GO:0048519	negative regulation of biological process	36	1380	0.0385
GO:0048609	multicellular organismal reproductive process	30	1083	0.0385
GO:0099504	synaptic vesicle cycle	7	116	0.0385
GO:1901698	response to nitrogen compound	8	148	0.0385
GO:1903391	regulation of adherens junction organization	2	4	0.0385
GO:0008088	axo-dendritic transport	4	37	0.0402
GO:0009887	animal organ morphogenesis	22	720	0.0408
GO:0000096	sulfur amino acid metabolic process	3	18	0.0422
GO:0031099	regeneration	3	18	0.0422
GO:0060627	regulation of vesicle-mediated transport	7	121	0.0441
GO:0007275	multicellular organism development	53	2277	0.0445
GO:0032868	response to insulin	4	39	0.0463
GO:0048731	system development	41	1657	0.0469

GO:0035265	organ growth	3	19	0.047
GO:0006047	UDP-N-acetylglucosamine metabolic process	2	5	0.0473
GO:0048477	oogenesis	19	597	0.0473
GO:1901700	response to oxygen-containing compound	12	304	0.0478
GO:0006887	exocytosis	6	93	0.0479
GO:0008355	olfactory learning	4	40	0.0486
GO:0050768	negative regulation of neurogenesis	5	65	0.0486
GO:0051704	multi-organism process	35	1361	0.0487
GO:0030707	ovarian follicle cell development	12	306	0.0489
GO:0032502	developmental process	61	2729	0.05

Table 2.3.2.2

#term ID	term description	observed gene count	background gene count	false discovery rate
GO:0007552	metamorphosis	15	467	2.66E-05
GO:0009887	animal organ morphogenesis	18	720	2.66E-05
GO:0048707	instar larval or pupal morphogenesis	14	440	3.14E-05
GO:0046621	negative regulation of organ growth	5	19	3.33E-05
GO:0007472	wing disc morphogenesis	11	280	6.16E-05
GO:0060429	epithelium development	19	949	6.16E-05
GO:0008285	negative regulation of cell population proliferation	7	86	8.16E-05
GO:0035220	wing disc development	12	378	0.0001
GO:0007444	imaginal disc development	14	548	0.00011
GO:0007560	imaginal disc morphogenesis	12	389	0.00011
GO:0048737	imaginal disc-derived appendage development	11	335	0.00014
GO:0007476	imaginal disc-derived wing morphogenesis	10	272	0.00015
GO:0001654	eye development	11	365	0.00024
GO:0048640	negative regulation of developmental growth	6	76	0.00024
GO:0007423	sensory organ development	12	463	0.00029
GO:0043068	positive regulation of programmed cell death	6	89	0.00044
GO:0002009	morphogenesis of an epithelium	13	582	0.00045
GO:0035329	hippo signaling	3	6	0.00045
GO:0009653	anatomical structure morphogenesis	21	1465	0.00052
GO:0048749	compound eye development	10	344	0.00052
GO:0048638	regulation of developmental growth	8	218	0.00071
GO:0042127	regulation of cell population proliferation	8	221	0.00073

GO:0040008	regulation of growth	9	300	0.00091
GO:0009968	negative regulation of signal transduction	9	303	0.00096
GO:0043065	positive regulation of apoptotic process	5	69	0.0011
GO:0009966	regulation of signal transduction	14	778	0.0014
GO:0001745	compound eye morphogenesis	8	264	0.0021
GO:0001751	compound eye photoreceptor cell differentiation	6	152	0.0039
GO:0001752	compound eye photoreceptor fate commitment	4	51	0.0043
GO:0006915	apoptotic process	5	98	0.0043
GO:0030182	neuron differentiation	12	671	0.0043
GO:0035265	organ growth	3	19	0.0043
GO:0043067	regulation of programmed cell death	7	236	0.0053
GO:0048731	system development	20	1657	0.0053
GO:0012501	programmed cell death	6	170	0.006
GO:0000003	reproduction	17	1308	0.0067
GO:0008283	cell population proliferation	6	178	0.0069
GO:0042771	intrinsic apoptotic signaling pathway in response to DNA damage by p53 class mediator	2	4	0.007
GO:0051241	negative regulation of multicellular organismal process	6	186	0.0084
GO:0032501	multicellular organismal process	31	3441	0.0112
GO:0035556	intracellular signal transduction	8	366	0.0115
GO:0045570	regulation of imaginal disc growth	3	31	0.0116
GO:0060253	negative regulation of glial cell proliferation	2	6	0.0116
GO:0010212	response to ionizing radiation	3	33	0.0131
GO:0042981	regulation of apoptotic process	6	209	0.0133
GO:0007526	larval somatic muscle development	3	34	0.0138
GO:0031102	neuron projection regeneration	2	7	0.0138
GO:0032504	multicellular organism reproduction	15	1173	0.015
GO:0007389	pattern specification process	9	496	0.0168
GO:0030855	epithelial cell differentiation	8	396	0.0168
GO:0045464	R8 cell fate specification	2	8	0.0168
GO:0007525	somatic muscle development	4	87	0.0179
GO:0045571	negative regulation of imaginal disc growth	2	9	0.0194
GO:0002164	larval development	5	155	0.0198
GO:0009628	response to abiotic stimulus	8	414	0.0205
GO:0007165	signal transduction	15	1226	0.0211
GO:2000026	regulation of multicellular organismal development	9	526	0.023
GO:0031399	regulation of protein modification process	7	338	0.0259
GO:0032502	developmental process	25	2729	0.0294
GO:0007275	multicellular organism development	22	2277	0.0303
GO:0007399	nervous system development	13	1028	0.0303
GO:0009314	response to radiation	5	176	0.0303
GO:0018193	peptidyl-amino acid modification	7	349	0.0303

GO:0048732	gland development	5	176	0.0303
GO:0051716	cellular response to stimulus	18	1710	0.0312
GO:0051896	regulation of protein kinase B signaling	2	13	0.0312
GO:0051961	negative regulation of nervous system development	4	110	0.0326
GO:0003002	regionalization	8	461	0.0327
GO:0007166	cell surface receptor signaling pathway	8	467	0.035
GO:0035332	positive regulation of hippo signaling	2	15	0.0374
GO:0003006	developmental process involved in reproduction	11	816	0.0377
GO:0048523	negative regulation of cellular process	14	1198	0.0378
GO:0007446	imaginal disc growth	2	16	0.0409
GO:0120036	plasma membrane bounded cell projection organization	9	592	0.0409
GO:0048477	oogenesis	9	597	0.0426
GO:0022414	reproductive process	14	1220	0.043
GO:0035212	cell competition in a multicellular organism	2	17	0.0436
GO:0042067	establishment of ommatidial planar polarity	3	60	0.0436
GO:0030154	cell differentiation	17	1644	0.0444
GO:0048519	negative regulation of biological process	15	1380	0.0485
GO:0007431	salivary gland development	4	129	0.0496

Table 2.3.2.3

#term ID	term description	observed gene count	background gene count	false discovery rate
GO:0010467	gene expression	14	1160	9.38E-05
GO:0044237	cellular metabolic process	23	3966	0.00024
GO:0009987	cellular process	29	6847	0.00027
GO:0043170	macromolecule metabolic process	21	3350	0.00027
GO:0044238	primary metabolic process	23	4093	0.00027
GO:0016070	RNA metabolic process	11	931	0.00069
GO:0071704	organic substance metabolic process	23	4432	0.00069
GO:0002181	cytoplasmic translation	5	109	0.00072
GO:0044267	cellular protein metabolic process	14	1644	0.00072
GO:0006807	nitrogen compound metabolic process	21	3900	0.0011
GO:0044260	cellular macromolecule metabolic process	16	2291	0.0011
GO:0006458	'de novo' protein folding	3	20	0.0016
GO:0034641	cellular nitrogen compound metabolic process	14	1954	0.0031
GO:0006412	translation	6	304	0.0041
GO:0034645	cellular macromolecule biosynthetic process	9	863	0.006
GO:0044271	cellular nitrogen compound biosynthetic process	9	881	0.0064
GO:0006396	RNA processing	7	516	0.0065
GO:0042127	regulation of cell population proliferation	5	221	0.0065

GO:0061077	chaperone-mediated protein folding	3	42	0.0065
GO:0035282	segmentation	5	236	0.008
GO:0031325	positive regulation of cellular metabolic process	8	738	0.0082
GO:0002230	positive regulation of defense response to virus by host	2	12	0.0157
GO:0022613	ribonucleoprotein complex biogenesis	5	287	0.0157
GO:0048732	gland development	4	176	0.0209
GO:0035120	post-embryonic appendage morphogenesis	5	319	0.0219
GO:0048870	cell motility	5	322	0.0222
GO:0035114	imaginal disc-derived appendage morphogenesis	5	328	0.0235
GO:0007350	blastoderm segmentation	4	196	0.0245
GO:0048585	negative regulation of response to stimulus	5	342	0.0245
GO:0048749	compound eye development	5	344	0.0245
GO:0000398	mRNA splicing, via spliceosome	4	202	0.0252
GO:0010604	positive regulation of macromolecule metabolic process	7	735	0.0252
GO:0002165	instar larval or pupal development	6	542	0.0258
GO:0080134	regulation of response to stress	4	214	0.0267
GO:0048522	positive regulation of cellular process	9	1247	0.0269
GO:0010669	epithelial structure maintenance	2	25	0.0287
GO:0035218	leg disc development	3	102	0.0287
GO:0007560	imaginal disc morphogenesis	5	389	0.0302
GO:0007298	border follicle cell migration	3	120	0.0405
GO:0007351	tripartite regional subdivision	3	122	0.0412
GO:0008595	anterior/posterior axis specification, embryo	3	122	0.0412
GO:0090090	negative regulation of canonical Wnt signaling pathway	2	34	0.0426
GO:0007169	transmembrane receptor protein tyrosine kinase signaling pathway	3	128	0.044
GO:0007476	imaginal disc-derived wing morphogenesis	4	272	0.0446
GO:0007166	cell surface receptor signaling pathway	5	467	0.0457
GO:0008355	olfactory learning	2	40	0.0457
GO:0016477	cell migration	4	280	0.0457
GO:0018108	peptidyl-tyrosine phosphorylation	2	38	0.0457
GO:0030031	cell projection assembly	3	135	0.0457
GO:0120032	regulation of plasma membrane bounded cell projection assembly	2	40	0.0457
GO:0010033	response to organic substance	5	476	0.0458
GO:0007455	eye-antennal disc morphogenesis	2	42	0.0464
GO:0010628	positive regulation of gene expression	5	485	0.0485
GO:0019216	regulation of lipid metabolic process	2	44	0.0495
GO:0044085	cellular component biogenesis	8	1201	0.0495
GO:0009968	negative regulation of signal transduction	4	303	0.0499
GO:0001751	compound eye photoreceptor cell differentiation	3	152	0.05

GO:0007281	germ cell development	6	714	0.05
GO:0030707	ovarian follicle cell development	4	306	0.05
GO:0034660	ncRNA metabolic process	4	309	0.05
GO:0051173	positive regulation of nitrogen compound metabolic process	6	710	0.05
GO:0071840	cellular component organization or biogenesis	13	2753	0.05
GO:1901700	response to oxygen-containing compound	4	304	0.05

Table 2.3.2.4

#term ID	term description	observed gene count	background gene count	false discovery rate
dme04391	Hippo signaling pathway - fly	8	58	0.00076
dme04392	Hippo signaling pathway - multiple species	5	16	0.00076
dme01230	Biosynthesis of amino acids	6	65	0.0241
dme04120	Ubiquitin mediated proteolysis	7	99	0.0241
dme04140	Autophagy - animal	7	94	0.0241
dme04144	Endocytosis	8	119	0.0241
dme01100	Metabolic pathways	28	994	0.0421
dme04070	Phosphatidylinositol signaling system	5	63	0.0421
dme04214	Apoptosis - fly	5	62	0.0421

Table 2.3.2.5

#term ID	term description	observed gene count	background gene count	false discovery rate
dme04392	Hippo signaling pathway - multiple species	5	16	1.85E-06
dme04391	Hippo signaling pathway - fly	6	58	1.39E-05
dme04140	Autophagy - animal	5	94	0.0016

Table 2.3.2.6

#term ID	term description	observed gene count	background gene count	false discovery rate
dme03010	Ribosome	5	133	0.0003
dme03040	Spliceosome	4	117	0.0017
dme04068	FoxO signaling pathway	3	65	0.0035
dme04150	mTOR signaling pathway	3	96	0.0078
dme04320	Dorso-ventral axis formation	2	28	0.0089
dme04933	AGE-RAGE signaling pathway in diabetic complications	2	31	0.009
dme03050	Proteasome	2	51	0.0196

Table 2.3.3.1				
#term ID	**term description**	**observed gene count**	**background gene count**	**false discovery rate**
GO:0034220	ion transmembrane transport	161	995	3.17E-20
GO:0055085	transmembrane transport	178	1235	4.35E-18
GO:0006811	ion transport	181	1292	1.95E-17
GO:0006812	cation transport	133	866	5.39E-15
GO:0051179	localization	483	5233	5.39E-15
GO:0006810	transport	400	4130	1.46E-14
GO:0051234	establishment of localization	407	4248	3.06E-14
GO:0098655	cation transmembrane transport	113	720	2.96E-13
GO:0015672	monovalent inorganic cation transport	77	437	1.04E-10
GO:0042493	response to drug	123	900	1.04E-10
GO:0009987	cellular process	1053	14652	2.09E-10
GO:0008152	metabolic process	742	9569	2.13E-09
GO:0030001	metal ion transport	96	664	2.53E-09
GO:0052695	cellular glucuronidation	17	19	2.58E-09
GO:0006855	drug transmembrane transport	33	105	3.06E-09
GO:0015893	drug transport	40	155	3.30E-09
GO:0019585	glucuronate metabolic process	18	24	3.89E-09
GO:0044281	small molecule metabolic process	192	1779	3.95E-09
GO:0098656	anion transmembrane transport	63	353	5.20E-09
GO:0032787	monocarboxylic acid metabolic process	76	477	5.25E-09
GO:0098662	inorganic cation transmembrane transport	90	618	5.25E-09
GO:0007268	chemical synaptic transmission	68	402	5.77E-09
GO:0032870	cellular response to hormone stimulus	86	585	8.41E-09
GO:0007271	synaptic transmission, cholinergic	19	31	8.67E-09
GO:0019752	carboxylic acid metabolic process	111	854	8.92E-09
GO:1901564	organonitrogen compound metabolic process	450	5284	8.92E-09
GO:1902475	L-alpha-amino acid transmembrane transport	24	57	8.92E-09
GO:0044237	cellular metabolic process	681	8797	4.95E-08
GO:0065008	regulation of biological quality	322	3559	4.95E-08
GO:0009725	response to hormone	108	854	5.79E-08
GO:0071495	cellular response to endogenous stimulus	130	1106	6.03E-08
GO:0098660	inorganic ion transmembrane transport	94	707	8.48E-08
GO:0007267	cell-cell signaling	126	1073	1.16E-07
GO:1902600	proton transmembrane transport	34	137	1.20E-07
GO:0007399	nervous system development	216	2206	2.72E-07
GO:0009719	response to endogenous stimulus	148	1353	2.72E-07
GO:0006082	organic acid metabolic process	114	959	3.95E-07
GO:0043436	oxoacid metabolic process	112	943	5.63E-07

GO:0071704	organic substance metabolic process	694	9135	7.30E-07
GO:0042221	response to chemical	357	4153	8.01E-07
GO:0006629	lipid metabolic process	132	1192	1.03E-06
GO:0044255	cellular lipid metabolic process	110	946	1.99E-06
GO:0050896	response to stimulus	605	7824	2.00E-06
GO:0052697	xenobiotic glucuronidation	11	11	2.08E-06
GO:0048731	system development	353	4144	2.37E-06
GO:1901701	cellular response to oxygen-containing compound	105	896	2.79E-06
GO:1905039	carboxylic acid transmembrane transport	35	170	3.22E-06
GO:0006814	sodium ion transport	37	189	3.91E-06
GO:0006820	anion transport	71	524	4.16E-06
GO:0015711	organic anion transport	60	414	6.00E-06
GO:0044238	primary metabolic process	664	8811	9.15E-06
GO:0007274	neuromuscular synaptic transmission	14	28	1.06E-05
GO:0006865	amino acid transport	25	100	1.24E-05
GO:0010817	regulation of hormone levels	68	511	1.38E-05
GO:0070887	cellular response to chemical stimulus	240	2672	1.97E-05
GO:0009410	response to xenobiotic stimulus	43	262	2.29E-05
GO:0052696	flavonoid glucuronidation	9	9	3.50E-05
GO:0015813	L-glutamate transmembrane transport	11	18	5.21E-05
GO:0035725	sodium ion transmembrane transport	31	160	5.21E-05
GO:0046903	secretion	113	1070	8.32E-05
GO:0007275	multicellular organism development	382	4726	8.71E-05
GO:0051049	regulation of transport	165	1732	9.31E-05
GO:0071466	cellular response to xenobiotic stimulus	30	157	9.31E-05
GO:1901568	fatty acid derivative metabolic process	29	148	9.31E-05
GO:1901653	cellular response to peptide	44	289	9.31E-05
GO:0099133	ATP hydrolysis coupled anion transmembrane transport	9	11	9.49E-05
GO:0001539	cilium or flagellum-dependent cell motility	12	25	9.85E-05
GO:1901616	organic hydroxy compound catabolic process	18	62	9.85E-05
GO:1901700	response to oxygen-containing compound	141	1427	9.85E-05
GO:0046942	carboxylic acid transport	40	252	0.0001
GO:0007193	adenylate cyclase-inhibiting G protein-coupled receptor signaling pathway	21	85	0.00011
GO:1904224	negative regulation of glucuronosyltransferase activity	8	8	0.00013
GO:2001030	negative regulation of cellular glucuronidation	8	8	0.00013
GO:0006793	phosphorus metabolic process	190	2086	0.00016
GO:1901699	cellular response to nitrogen compound	69	568	0.00016
GO:0042391	regulation of membrane potential	54	408	0.00023
GO:0003341	cilium movement	17	61	0.00027
GO:0006796	phosphate-containing compound metabolic process	187	2065	0.00027

GO:0048856	anatomical structure development	402	5085	0.00027
GO:0060079	excitatory postsynaptic potential	19	76	0.00027
GO:1901565	organonitrogen compound catabolic process	101	958	0.00027
GO:0003091	renal water homeostasis	13	35	0.00028
GO:0060285	cilium-dependent cell motility	11	24	0.00032
GO:0006836	neurotransmitter transport	30	172	0.00036
GO:0019751	polyol metabolic process	22	102	0.00036
GO:0035094	response to nicotine	15	49	0.00036
GO:0022008	neurogenesis	144	1519	0.00045
GO:0032880	regulation of protein localization	95	901	0.00047
GO:0006631	fatty acid metabolic process	42	294	0.00048
GO:0005975	carbohydrate metabolic process	57	457	0.00051
GO:0009636	response to toxic substance	58	468	0.00051
GO:0032940	secretion by cell	99	959	0.00064
GO:0007610	behavior	64	541	0.00065
GO:0015991	ATP hydrolysis coupled proton transport	11	27	0.00068
GO:0071417	cellular response to organonitrogen compound	59	485	0.00068
GO:0006805	xenobiotic metabolic process	22	108	0.00071
GO:0010646	regulation of cell communication	275	3327	0.00077
GO:0032502	developmental process	418	5401	0.00096
GO:0001505	regulation of neurotransmitter levels	41	295	0.00098
GO:0001523	retinoid metabolic process	19	87	0.0011
GO:0043090	amino acid import	8	13	0.0011
GO:0048699	generation of neurons	134	1422	0.0011
GO:0051223	regulation of protein transport	70	622	0.0011
GO:0051960	regulation of nervous system development	86	817	0.0011
GO:0035690	cellular response to drug	42	310	0.0012
GO:0048468	cell development	139	1493	0.0012
GO:0071383	cellular response to steroid hormone stimulus	31	197	0.0012
GO:0071396	cellular response to lipid	58	486	0.0012
GO:0023051	regulation of signaling	275	3360	0.0014
GO:0032879	regulation of localization	215	2524	0.0014
GO:0003014	renal system process	21	107	0.0015
GO:0016192	vesicle-mediated transport	154	1699	0.0015
GO:0019538	protein metabolic process	333	4197	0.0015
GO:0033559	unsaturated fatty acid metabolic process	19	90	0.0015
GO:0006690	icosanoid metabolic process	20	99	0.0016
GO:0050796	regulation of insulin secretion	28	172	0.0016
GO:0016311	dephosphorylation	39	285	0.0018
GO:0032501	multicellular organismal process	489	6507	0.0019
GO:0034754	cellular hormone metabolic process	21	109	0.0019
GO:0070201	regulation of establishment of protein localization	72	662	0.0019

GO:0006887	exocytosis	81	774	0.0021
GO:0007187	G protein-coupled receptor signaling pathway, coupled to cyclic nucleotide second messenger	31	206	0.0022
GO:0010243	response to organonitrogen compound	89	876	0.0022
GO:0043269	regulation of ion transport	68	618	0.0022
GO:0051186	cofactor metabolic process	55	467	0.0022
GO:0071702	organic substance transport	178	2040	0.0022
GO:1901698	response to nitrogen compound	98	988	0.0022
GO:0065007	biological regulation	826	11740	0.0023
GO:0000413	protein peptidyl-prolyl isomerization	12	40	0.0024
GO:0006721	terpenoid metabolic process	20	103	0.0024
GO:0006813	potassium ion transport	28	178	0.0024
GO:0051716	cellular response to stimulus	468	6212	0.0024
GO:0048545	response to steroid hormone	42	324	0.0025
GO:0089718	amino acid import across plasma membrane	7	11	0.0025
GO:0007586	digestion	20	104	0.0026
GO:0046883	regulation of hormone secretion	36	261	0.0026
GO:0048878	chemical homeostasis	98	995	0.0026
GO:0051938	L-glutamate import	6	7	0.0026
GO:0071805	potassium ion transmembrane transport	27	169	0.0026
GO:0090407	organophosphate biosynthetic process	64	577	0.0026
GO:0019637	organophosphate metabolic process	99	1011	0.0028
GO:0095500	acetylcholine receptor signaling pathway	9	22	0.0029
GO:0006066	alcohol metabolic process	38	285	0.003
GO:0033993	response to lipid	84	825	0.003
GO:0045912	negative regulation of carbohydrate metabolic process	13	49	0.0031
GO:0006732	coenzyme metabolic process	39	297	0.0032
GO:0010975	regulation of neuron projection development	52	443	0.0032
GO:0030030	cell projection organization	103	1067	0.0032
GO:0043097	pyrimidine nucleoside salvage	7	12	0.0032
GO:0043174	nucleoside salvage	8	17	0.0032
GO:0051046	regulation of secretion	76	728	0.0032
GO:0098771	inorganic ion homeostasis	69	643	0.0032
GO:1901615	organic hydroxy compound metabolic process	50	420	0.0032
GO:1901652	response to peptide	51	431	0.0032
GO:0006807	nitrogen compound metabolic process	607	8352	0.0033
GO:1901575	organic substance catabolic process	144	1609	0.0034
GO:0071705	nitrogen compound transport	150	1690	0.0035
GO:0120036	plasma membrane bounded cell projection organization	100	1034	0.0035
GO:0060411	cardiac septum morphogenesis	16	74	0.0036
GO:0071384	cellular response to corticosteroid stimulus	14	58	0.0036

GO:1903530	regulation of secretion by cell	71	672	0.0036
GO:0035095	behavioral response to nicotine	6	8	0.0037
GO:0038003	opioid receptor signaling pathway	6	8	0.0037
GO:0042445	hormone metabolic process	28	186	0.0038
GO:0055072	iron ion homeostasis	17	83	0.0038
GO:0045922	negative regulation of fatty acid metabolic process	10	30	0.0039
GO:0030104	water homeostasis	15	67	0.004
GO:0055067	monovalent inorganic cation homeostasis	21	119	0.004
GO:0015804	neutral amino acid transport	11	37	0.0041
GO:0006464	cellular protein modification process	244	2999	0.0042
GO:0051239	regulation of multicellular organismal process	229	2788	0.0042
GO:0045055	regulated exocytosis	72	691	0.0044
GO:0006835	dicarboxylic acid transport	14	60	0.0045
GO:0000041	transition metal ion transport	21	121	0.0047
GO:0019432	triglyceride biosynthetic process	8	19	0.005
GO:0055076	transition metal ion homeostasis	21	122	0.0051
GO:0009056	catabolic process	161	1859	0.0052
GO:0050801	ion homeostasis	73	708	0.0052
GO:0009755	hormone-mediated signaling pathway	26	171	0.0054
GO:0010677	negative regulation of cellular carbohydrate metabolic process	12	46	0.0054
GO:0046164	alcohol catabolic process	12	46	0.0054
GO:0007197	adenylate cyclase-inhibiting G protein-coupled acetylcholine receptor signaling pathway	5	5	0.0055
GO:0034765	regulation of ion transmembrane transport	50	434	0.0055
GO:0038170	somatostatin signaling pathway	5	5	0.0055
GO:0044206	UMP salvage	5	5	0.0055
GO:0060294	cilium movement involved in cell motility	7	14	0.0055
GO:0120035	regulation of plasma membrane bounded cell projection organization	64	600	0.0055
GO:0050891	multicellular organismal water homeostasis	14	62	0.0056
GO:1901657	glycosyl compound metabolic process	23	143	0.0057
GO:0065009	regulation of molecular function	265	3322	0.0059
GO:1901654	response to ketone	27	183	0.0059
GO:0006826	iron ion transport	15	71	0.0061
GO:0019400	alditol metabolic process	8	20	0.0061
GO:0018208	peptidyl-proline modification	13	55	0.0062
GO:0055080	cation homeostasis	66	629	0.0062
GO:0071385	cellular response to glucocorticoid stimulus	13	55	0.0062
GO:0099131	ATP hydrolysis coupled ion transmembrane transport	14	63	0.0062
GO:0050767	regulation of neurogenesis	74	730	0.0066
GO:0032355	response to estradiol	21	126	0.0067
GO:2000026	regulation of multicellular organismal development	161	1876	0.0068

GO:0006766	vitamin metabolic process	20	117	0.0069
GO:0034762	regulation of transmembrane transport	57	524	0.007
GO:1905114	cell surface receptor signaling pathway involved in cell-cell signaling	45	383	0.007
GO:0006222	UMP biosynthetic process	6	10	0.0071
GO:0032328	alanine transport	6	10	0.0071
GO:0032486	Rap protein signal transduction	6	10	0.0071
GO:1901655	cellular response to ketone	17	90	0.0071
GO:0014070	response to organic cyclic compound	85	873	0.0072
GO:0030534	adult behavior	22	137	0.0072
GO:0008286	insulin receptor signaling pathway	16	82	0.0074
GO:0008610	lipid biosynthetic process	61	575	0.0074
GO:0003206	cardiac chamber morphogenesis	21	128	0.0075
GO:0007548	sex differentiation	33	252	0.0079
GO:0007207	phospholipase C-activating G protein-coupled acetylcholine receptor signaling pathway	5	6	0.008
GO:0035524	proline transmembrane transport	5	6	0.008
GO:0042940	D-amino acid transport	5	6	0.008
GO:0048869	cellular developmental process	278	3533	0.008
GO:0050708	regulation of protein secretion	48	422	0.008
GO:0051552	flavone metabolic process	5	6	0.008
GO:0071310	cellular response to organic substance	185	2219	0.008
GO:0071407	cellular response to organic cyclic compound	55	505	0.008
GO:0098712	L-glutamate import across plasma membrane	5	6	0.008
GO:1901135	carbohydrate derivative metabolic process	101	1083	0.008
GO:0006508	proteolysis	110	1203	0.0082
GO:0003181	atrioventricular valve morphogenesis	8	22	0.0087
GO:0046856	phosphatidylinositol dephosphorylation	8	22	0.0087
GO:0043412	macromolecule modification	254	3197	0.0088
GO:0062014	negative regulation of small molecule metabolic process	17	93	0.0089
GO:0030154	cell differentiation	272	3457	0.009
GO:0071375	cellular response to peptide hormone stimulus	32	245	0.0094
GO:0007417	central nervous system development	83	861	0.0104
GO:0017144	drug metabolic process	64	622	0.0104
GO:0001504	neurotransmitter uptake	7	17	0.0109
GO:0006071	glycerol metabolic process	7	17	0.0109
GO:0010648	negative regulation of cell communication	113	1255	0.011
GO:0044267	cellular protein metabolic process	281	3603	0.0115
GO:0015808	L-alanine transport	5	7	0.0118
GO:0019367	fatty acid elongation, saturated fatty acid	5	7	0.0118
GO:0023057	negative regulation of signaling	113	1258	0.0118
GO:0034625	fatty acid elongation, monounsaturated fatty acid	5	7	0.0118

GO:0034626	fatty acid elongation, polyunsaturated fatty acid	5	7	0.0118
GO:0009653	anatomical structure morphogenesis	167	1992	0.0119
GO:1904062	regulation of cation transmembrane transport	36	294	0.0119
GO:0030163	protein catabolic process	63	615	0.012
GO:0022607	cellular component assembly	192	2343	0.0125
GO:0048518	positive regulation of biological process	407	5459	0.0125
GO:0072337	modified amino acid transport	8	24	0.0127
GO:0043171	peptide catabolic process	9	31	0.0133
GO:0005996	monosaccharide metabolic process	27	198	0.0135
GO:0006833	water transport	7	18	0.0135
GO:0046174	polyol catabolic process	7	18	0.0135
GO:0045664	regulation of neuron differentiation	61	595	0.014
GO:0030182	neuron differentiation	88	940	0.0151
GO:0002274	myeloid leukocyte activation	59	574	0.016
GO:0099504	synaptic vesicle cycle	17	100	0.0164
GO:1902993	positive regulation of amyloid precursor protein catabolic process	6	13	0.0164
GO:2000009	negative regulation of protein localization to cell surface	6	13	0.0164
GO:0009416	response to light stimulus	35	290	0.0168
GO:0044597	daunorubicin metabolic process	5	8	0.0168
GO:0044598	doxorubicin metabolic process	5	8	0.0168
GO:1901379	regulation of potassium ion transmembrane transport	14	73	0.0168
GO:0098739	import across plasma membrane	15	82	0.0169
GO:0048638	regulation of developmental growth	36	302	0.0171
GO:0048523	negative regulation of cellular process	337	4454	0.018
GO:0015853	adenine transport	4	4	0.0182
GO:0019216	regulation of lipid metabolic process	42	373	0.0182
GO:0036101	leukotriene B4 catabolic process	4	4	0.0182
GO:0070779	D-aspartate import across plasma membrane	4	4	0.0182
GO:0097306	cellular response to alcohol	15	83	0.0182
GO:0045137	development of primary sexual characteristics	27	204	0.0186
GO:0060284	regulation of cell development	80	846	0.0187
GO:0007188	adenylate cyclase-modulating G protein-coupled receptor signaling pathway	25	183	0.019
GO:0010862	positive regulation of pathway-restricted SMAD protein phosphorylation	11	49	0.0192
GO:0031644	regulation of neurological system process	18	112	0.0192
GO:0051338	regulation of transferase activity	89	964	0.0192
GO:0042552	myelination	16	93	0.0193
GO:0000122	negative regulation of transcription by RNA polymerase II	77	809	0.0194
GO:0099132	ATP hydrolysis coupled cation transmembrane transport	13	66	0.0195

GO:0045833	negative regulation of lipid metabolic process	15	84	0.0197
GO:0007626	locomotory behavior	25	184	0.0198
GO:0010033	response to organic substance	223	2815	0.0205
GO:0016043	cellular component organization	384	5163	0.0205
GO:0045851	pH reduction	9	34	0.0205
GO:0050790	regulation of catalytic activity	183	2249	0.0205
GO:0007631	feeding behavior	16	94	0.0207
GO:0035329	hippo signaling	8	27	0.0209
GO:0006639	acylglycerol metabolic process	15	85	0.0213
GO:0007632	visual behavior	11	50	0.0213
GO:0001508	action potential	17	104	0.0214
GO:0001676	long-chain fatty acid metabolic process	17	104	0.0214
GO:0046520	sphingoid biosynthetic process	5	9	0.022
GO:0097105	presynaptic membrane assembly	5	9	0.022
GO:0035082	axoneme assembly	12	59	0.0226
GO:0043009	chordate embryonic development	56	550	0.0228
GO:0048814	regulation of dendrite morphogenesis	14	77	0.0232
GO:0007018	microtubule-based movement	33	276	0.0235
GO:0060341	regulation of cellular localization	73	766	0.0235
GO:1901016	regulation of potassium ion transmembrane transporter activity	11	51	0.0235
GO:0008217	regulation of blood pressure	24	177	0.0237
GO:0048608	reproductive structure development	44	405	0.0237
GO:0060412	ventricular septum morphogenesis	10	43	0.0237
GO:0015698	inorganic anion transport	23	167	0.0244
GO:0034312	diol biosynthetic process	6	15	0.0245
GO:0006641	triglyceride metabolic process	13	69	0.0251
GO:0009966	regulation of signal transduction	237	3033	0.0251
GO:0046717	acid secretion	13	69	0.0251
GO:0060627	regulation of vesicle-mediated transport	50	480	0.0253
GO:0019748	secondary metabolic process	11	52	0.0258
GO:0003279	cardiac septum development	17	107	0.026
GO:1902817	negative regulation of protein localization to microtubule	4	5	0.0263
GO:0042592	homeostatic process	127	1491	0.0265
GO:0008015	blood circulation	41	373	0.0266
GO:0030004	cellular monovalent inorganic cation homeostasis	16	98	0.0273
GO:0000038	very long-chain fatty acid metabolic process	8	29	0.0276
GO:0007035	vacuolar acidification	7	22	0.0276
GO:0032412	regulation of ion transmembrane transporter activity	28	224	0.0278
GO:0042758	long-chain fatty acid catabolic process	5	10	0.0283
GO:0098657	import into cell	60	609	0.0289
GO:0007588	excretion	10	45	0.0296

GO:0071214	cellular response to abiotic stimulus	33	282	0.0296
GO:0009628	response to abiotic stimulus	94	1052	0.0297
GO:0007213	G protein-coupled acetylcholine receptor signaling pathway	6	16	0.0298
GO:0008202	steroid metabolic process	30	248	0.0298
GO:0051128	regulation of cellular component organization	185	2306	0.03
GO:0009968	negative regulation of signal transduction	102	1160	0.0303
GO:0007154	cell communication	385	5219	0.0305
GO:0031324	negative regulation of cellular metabolic process	196	2463	0.0305
GO:0046486	glycerolipid metabolic process	43	401	0.0305
GO:0055086	nucleobase-containing small molecule metabolic process	64	662	0.0305
GO:0050807	regulation of synapse organization	22	161	0.0307
GO:0045017	glycerolipid biosynthetic process	29	238	0.0312
GO:0099173	postsynapse organization	11	54	0.0312
GO:0007218	neuropeptide signaling pathway	17	110	0.0314
GO:0055114	oxidation-reduction process	84	923	0.0314
GO:0006470	protein dephosphorylation	25	194	0.0317
GO:0000902	cell morphogenesis	61	626	0.0319
GO:0035295	tube development	74	793	0.0319
GO:0048511	rhythmic process	30	250	0.0319
GO:0006885	regulation of pH	15	91	0.0324
GO:0007264	small GTPase mediated signal transduction	29	239	0.0324
GO:0050773	regulation of dendrite development	19	131	0.0329
GO:1904063	negative regulation of cation transmembrane transport	14	82	0.0338
GO:0010332	response to gamma radiation	11	55	0.0343
GO:0030100	regulation of endocytosis	28	229	0.0344
GO:0001934	positive regulation of protein phosphorylation	85	941	0.0348
GO:0044057	regulation of system process	52	516	0.0348
GO:0001655	urogenital system development	34	299	0.0359
GO:0007288	sperm axoneme assembly	5	11	0.0359
GO:0032490	detection of molecule of bacterial origin	5	11	0.0359
GO:0055065	metal ion homeostasis	55	555	0.0359
GO:0060325	face morphogenesis	8	31	0.0359
GO:0071840	cellular component organization or biogenesis	392	5342	0.0359
GO:0097242	amyloid-beta clearance	5	11	0.0359
GO:0106070	regulation of adenylate cyclase-activating G protein-coupled receptor signaling pathway	5	11	0.0359
GO:1901679	nucleotide transmembrane transport	6	17	0.0359
GO:1902004	positive regulation of amyloid-beta formation	5	11	0.0359
GO:1903828	negative regulation of cellular protein localization	17	112	0.0359
GO:0002933	lipid hydroxylation	4	6	0.0362

GO:0030579	ubiquitin-dependent SMAD protein catabolic process	4	6	0.0362
GO:0060304	regulation of phosphatidylinositol dephosphorylation	4	6	0.0362
GO:0061002	negative regulation of dendritic spine morphogenesis	4	6	0.0362
GO:0071221	cellular response to bacterial lipopeptide	4	6	0.0362
GO:0051050	positive regulation of transport	81	892	0.0367
GO:0008406	gonad development	25	198	0.0373
GO:0010959	regulation of metal ion transport	39	360	0.0373
GO:0044262	cellular carbohydrate metabolic process	20	144	0.0373
GO:0048513	animal organ development	227	2926	0.0378
GO:0046661	male sex differentiation	21	155	0.038
GO:0003205	cardiac chamber development	22	166	0.0386
GO:0044085	cellular component biogenesis	201	2556	0.0391
GO:0008306	associative learning	13	75	0.0395
GO:0051452	intracellular pH reduction	8	32	0.0395
GO:0060271	cilium assembly	36	326	0.0395
GO:0043434	response to peptide hormone	39	362	0.0397
GO:0006879	cellular iron ion homeostasis	12	66	0.0399
GO:0009165	nucleotide biosynthetic process	33	291	0.0399
GO:0030317	flagellated sperm motility	12	66	0.0399
GO:0048519	negative regulation of biological process	365	4953	0.0399
GO:0048729	tissue morphogenesis	52	522	0.0399
GO:0043312	neutrophil degranulation	49	485	0.0401
GO:0002446	neutrophil mediated immunity	50	498	0.0407
GO:0044782	cilium organization	37	339	0.0407
GO:0048524	positive regulation of viral process	14	85	0.0407
GO:2000369	regulation of clathrin-dependent endocytosis	6	18	0.041
GO:1901137	carbohydrate derivative biosynthetic process	60	625	0.0413
GO:0003008	system process	149	1827	0.0418
GO:0023052	signaling	375	5108	0.0418
GO:0050804	modulation of chemical synaptic transmission	35	316	0.0418
GO:0009314	response to radiation	44	425	0.042
GO:0033157	regulation of intracellular protein transport	25	201	0.042
GO:0097164	ammonium ion metabolic process	23	179	0.0421
GO:0120031	plasma membrane bounded cell projection assembly	43	413	0.0422
GO:0099068	postsynapse assembly	5	12	0.0426
GO:0009117	nucleotide metabolic process	56	576	0.0428
GO:0060395	SMAD protein signal transduction	11	58	0.0428
GO:0009260	ribonucleotide biosynthetic process	25	202	0.0435
GO:0046173	polyol biosynthetic process	9	41	0.0435
GO:1903827	regulation of cellular protein localization	47	465	0.0458

GO:0032989	cellular component morphogenesis	67	720	0.046
GO:0001578	microtubule bundle formation	14	87	0.0466
GO:0022600	digestive system process	12	68	0.0466
GO:0097327	response to antineoplastic agent	14	87	0.0466
GO:0000185	activation of MAPKKK activity	6	19	0.0477
GO:0003190	atrioventricular valve formation	4	7	0.0477
GO:0006857	oligopeptide transport	4	7	0.0477
GO:0014047	glutamate secretion	6	19	0.0477
GO:0016926	protein desumoylation	4	7	0.0477
GO:0043654	recognition of apoptotic cell	4	7	0.0477
GO:0046621	negative regulation of organ growth	7	26	0.0477
GO:0048261	negative regulation of receptor-mediated endocytosis	6	19	0.0477
GO:0050793	regulation of developmental process	190	2416	0.0477
GO:1904646	cellular response to amyloid-beta	7	26	0.0477
GO:0045429	positive regulation of nitric oxide biosynthetic process	9	42	0.0479
GO:0019693	ribose phosphate metabolic process	46	455	0.0481
GO:0046620	regulation of organ growth	14	88	0.0488
GO:0050890	cognition	31	274	0.0489
GO:0002275	myeloid cell activation involved in immune response	51	519	0.0498
GO:0002444	myeloid leukocyte mediated immunity	51	519	0.0498
GO:0060562	epithelial tube morphogenesis	33	298	0.0498
GO:0006940	regulation of smooth muscle contraction	11	60	0.0499

Table 2.3.3.2 (YAP1 Hub)

#term ID	term description	observed gene count	background gene count	false discovery rate
GO:0009987	cellular process	687	14652	2.25E-37
GO:0050896	response to stimulus	446	7824	7.02E-26
GO:0042221	response to chemical	279	4153	3.14E-21
GO:0051716	cellular response to stimulus	366	6212	9.64E-21
GO:0070887	cellular response to chemical stimulus	204	2672	6.60E-20
GO:0051179	localization	317	5233	2.17E-18
GO:0065008	regulation of biological quality	242	3559	2.50E-18
GO:0071495	cellular response to endogenous stimulus	113	1106	6.48E-18
GO:0009719	response to endogenous stimulus	127	1353	1.17E-17
GO:0032870	cellular response to hormone stimulus	78	585	1.19E-17
GO:0009725	response to hormone	95	854	5.09E-17
GO:0006810	transport	263	4130	6.51E-17
GO:0051234	establishment of localization	267	4248	1.49E-16

GO:0065007	biological regulation	554	11740	3.06E-16
GO:0044237	cellular metabolic process	446	8797	3.89E-15
GO:0051049	regulation of transport	140	1732	1.07E-14
GO:0044281	small molecule metabolic process	142	1779	1.53E-14
GO:0007267	cell-cell signaling	102	1073	2.85E-14
GO:0007268	chemical synaptic transmission	58	402	2.85E-14
GO:0008152	metabolic process	470	9569	4.38E-14
GO:1901701	cellular response to oxygen-containing compound	90	896	8.45E-14
GO:0006812	cation transport	88	866	9.55E-14
GO:0010646	regulation of cell communication	214	3327	1.81E-13
GO:0007154	cell communication	297	5219	1.92E-13
GO:0050789	regulation of biological process	522	11116	2.05E-13
GO:0052695	cellular glucuronidation	17	19	2.49E-13
GO:0019585	glucuronate metabolic process	18	24	2.93E-13
GO:0007271	synaptic transmission, cholinergic	19	31	6.37E-13
GO:1901700	response to oxygen-containing compound	118	1427	6.37E-13
GO:0023051	regulation of signaling	213	3360	7.49E-13
GO:1901564	organonitrogen compound metabolic process	297	5284	7.73E-13
GO:0006811	ion transport	110	1292	9.44E-13
GO:0034220	ion transmembrane transport	93	995	9.92E-13
GO:0032787	monocarboxylic acid metabolic process	60	477	1.11E-12
GO:0042493	response to drug	87	900	1.34E-12
GO:0071704	organic substance metabolic process	447	9135	1.52E-12
GO:0023052	signaling	288	5108	1.71E-12
GO:0032879	regulation of localization	172	2524	2.01E-12
GO:0006796	phosphate-containing compound metabolic process	149	2065	2.75E-12
GO:0007399	nervous system development	156	2206	2.75E-12
GO:0044238	primary metabolic process	433	8811	4.07E-12
GO:0007165	signal transduction	270	4738	5.81E-12
GO:0010033	response to organic substance	183	2815	1.23E-11
GO:0010817	regulation of hormone levels	60	511	1.34E-11
GO:0006629	lipid metabolic process	101	1192	1.39E-11
GO:0071310	cellular response to organic substance	153	2219	3.18E-11
GO:0065009	regulation of molecular function	204	3322	5.16E-11
GO:0019752	carboxylic acid metabolic process	80	854	6.06E-11
GO:0048523	negative regulation of cellular process	253	4454	8.34E-11
GO:0055085	transmembrane transport	101	1235	9.46E-11
GO:0050794	regulation of cellular process	488	10484	9.55E-11
GO:0051239	regulation of multicellular organismal process	178	2788	1.19E-10
GO:0048731	system development	238	4144	1.95E-10
GO:0042391	regulation of membrane potential	50	408	3.38E-10
GO:0046903	secretion	90	1070	4.38E-10

GO:0048519	negative regulation of biological process	271	4953	4.38E-10
GO:0033993	response to lipid	76	825	4.41E-10
GO:0044255	cellular lipid metabolic process	83	946	4.41E-10
GO:0098655	cation transmembrane transport	69	720	8.96E-10
GO:0051223	regulation of protein transport	63	622	8.99E-10
GO:0045055	regulated exocytosis	67	691	1.11E-09
GO:0070201	regulation of establishment of protein localization	65	662	1.38E-09
GO:0009410	response to xenobiotic stimulus	38	262	1.61E-09
GO:1901699	cellular response to nitrogen compound	59	568	1.61E-09
GO:1901653	cellular response to peptide	40	289	1.66E-09
GO:0032940	secretion by cell	82	959	1.76E-09
GO:0051046	regulation of secretion	68	728	3.24E-09
GO:0071396	cellular response to lipid	53	486	3.33E-09
GO:0019637	organophosphate metabolic process	84	1011	3.57E-09
GO:0032501	multicellular organismal process	330	6507	3.57E-09
GO:0030001	metal ion transport	64	664	3.62E-09
GO:0052697	xenobiotic glucuronidation	11	11	5.11E-09
GO:1903530	regulation of secretion by cell	64	672	5.44E-09
GO:0006887	exocytosis	70	774	5.48E-09
GO:0050790	regulation of catalytic activity	146	2249	5.62E-09
GO:0009966	regulation of signal transduction	182	3033	6.68E-09
GO:0032880	regulation of protein localization	77	901	6.68E-09
GO:0009636	response to toxic substance	51	468	6.89E-09
GO:0048518	positive regulation of biological process	286	5459	6.89E-09
GO:0051128	regulation of cellular component organization	148	2306	8.15E-09
GO:0007274	neuromuscular synaptic transmission	14	28	8.42E-09
GO:0007193	adenylate cyclase-inhibiting G protein-coupled receptor signaling pathway	21	85	1.20E-08
GO:1901698	response to nitrogen compound	81	988	1.23E-08
GO:0007275	multicellular organism development	254	4726	1.40E-08
GO:0010648	negative regulation of cell communication	95	1255	1.53E-08
GO:0023057	negative regulation of signaling	95	1258	1.71E-08
GO:0014070	response to organic cyclic compound	74	873	1.99E-08
GO:0019220	regulation of phosphate metabolic process	115	1657	2.10E-08
GO:0016192	vesicle-mediated transport	117	1699	2.18E-08
GO:0016043	cellular component organization	271	5163	2.34E-08
GO:0043269	regulation of ion transport	59	618	2.34E-08
GO:0071840	cellular component organization or biogenesis	278	5342	2.76E-08
GO:0002274	myeloid leukocyte activation	56	574	3.14E-08
GO:0007187	G protein-coupled receptor signaling pathway, coupled to cyclic nucleotide second messenger	31	206	3.57E-08
GO:0048583	regulation of response to stimulus	216	3882	3.57E-08
GO:2000026	regulation of multicellular organismal development	124	1876	6.02E-08

GO:0005975	carbohydrate metabolic process	48	457	6.20E-08
GO:0060079	excitatory postsynaptic potential	19	76	6.33E-08
GO:1905114	cell surface receptor signaling pathway involved in cell-cell signaling	43	383	7.50E-08
GO:0048545	response to steroid hormone	39	324	7.55E-08
GO:0007610	behavior	53	541	7.58E-08
GO:0090407	organophosphate biosynthetic process	55	577	8.95E-08
GO:0010243	response to organonitrogen compound	72	876	1.03E-07
GO:0009056	catabolic process	122	1859	1.18E-07
GO:0048856	anatomical structure development	264	5085	1.24E-07
GO:0071417	cellular response to organonitrogen compound	49	485	1.24E-07
GO:0071466	cellular response to xenobiotic stimulus	26	157	1.33E-07
GO:0048878	chemical homeostasis	78	995	1.43E-07
GO:0071383	cellular response to steroid hormone stimulus	29	197	1.74E-07
GO:0051338	regulation of transferase activity	76	964	1.81E-07
GO:1901575	organic substance catabolic process	109	1609	1.87E-07
GO:0052696	flavonoid glucuronidation	9	9	1.91E-07
GO:0048522	positive regulation of cellular process	255	4898	2.06E-07
GO:1901652	response to peptide	45	431	2.12E-07
GO:0019216	regulation of lipid metabolic process	41	373	2.74E-07
GO:0032502	developmental process	275	5401	2.74E-07
GO:0009628	response to abiotic stimulus	80	1052	2.88E-07
GO:0035094	response to nicotine	15	49	3.06E-07
GO:0050708	regulation of protein secretion	44	422	3.13E-07
GO:0051960	regulation of nervous system development	67	817	3.64E-07
GO:0050793	regulation of developmental process	146	2416	3.68E-07
GO:0051050	positive regulation of transport	71	892	3.89E-07
GO:0046883	regulation of hormone secretion	33	261	3.95E-07
GO:0009968	negative regulation of signal transduction	85	1160	4.35E-07
GO:1902531	regulation of intracellular signal transduction	115	1764	4.45E-07
GO:0031399	regulation of protein modification process	114	1747	4.94E-07
GO:0009755	hormone-mediated signaling pathway	26	171	5.42E-07
GO:0002446	neutrophil mediated immunity	48	498	5.93E-07
GO:0035690	cellular response to drug	36	310	5.94E-07
GO:0050796	regulation of insulin secretion	26	172	5.94E-07
GO:0019751	polyol metabolic process	20	102	6.49E-07
GO:0043312	neutrophil degranulation	47	485	7.04E-07
GO:0002444	myeloid leukocyte mediated immunity	49	519	7.31E-07
GO:0015672	monovalent inorganic cation transport	44	437	7.31E-07
GO:0003008	system process	117	1827	7.72E-07
GO:0043299	leukocyte degranulation	48	507	9.31E-07
GO:0010647	positive regulation of cell communication	107	1631	1.08E-06

GO:1901565	organonitrogen compound catabolic process	73	958	1.12E-06
GO:1904224	negative regulation of glucuronosyltransferase activity	8	8	1.19E-06
GO:2001030	negative regulation of cellular glucuronidation	8	8	1.19E-06
GO:0003014	renal system process	20	107	1.21E-06
GO:0006805	xenobiotic metabolic process	20	108	1.37E-06
GO:0098662	inorganic cation transmembrane transport	54	618	1.39E-06
GO:0022008	neurogenesis	101	1519	1.43E-06
GO:0031325	positive regulation of cellular metabolic process	172	3060	1.44E-06
GO:0001505	regulation of neurotransmitter levels	34	295	1.57E-06
GO:0002275	myeloid cell activation involved in immune response	48	519	1.62E-06
GO:0045321	leukocyte activation	69	894	1.62E-06
GO:0048585	negative regulation of response to stimulus	99	1483	1.62E-06
GO:0048699	generation of neurons	96	1422	1.62E-06
GO:1901615	organic hydroxy compound metabolic process	42	420	1.62E-06
GO:0051246	regulation of protein metabolic process	154	2668	1.83E-06
GO:0071407	cellular response to organic cyclic compound	47	505	1.85E-06
GO:0098771	inorganic ion homeostasis	55	643	1.85E-06
GO:0034762	regulation of transmembrane transport	48	524	2.04E-06
GO:0006066	alcohol metabolic process	33	285	2.08E-06
GO:0023056	positive regulation of signaling	106	1638	2.09E-06
GO:0006807	nitrogen compound metabolic process	385	8352	2.39E-06
GO:1902600	proton transmembrane transport	22	137	2.41E-06
GO:0031324	negative regulation of cellular metabolic process	144	2463	2.59E-06
GO:0003091	renal water homeostasis	12	35	2.65E-06
GO:0002263	cell activation involved in immune response	53	620	3.13E-06
GO:1901616	organic hydroxy compound catabolic process	15	62	3.13E-06
GO:0034765	regulation of ion transmembrane transport	42	434	3.39E-06
GO:0001932	regulation of protein phosphorylation	92	1370	3.60E-06
GO:0008610	lipid biosynthetic process	50	575	4.46E-06
GO:0007188	adenylate cyclase-modulating G protein-coupled receptor signaling pathway	25	183	4.97E-06
GO:0042325	regulation of phosphorylation	96	1465	5.30E-06
GO:0002443	leukocyte mediated immunity	53	632	5.33E-06
GO:0045595	regulation of cell differentiation	107	1695	5.39E-06
GO:0010975	regulation of neuron projection development	42	443	5.46E-06
GO:0005996	monosaccharide metabolic process	26	198	5.51E-06
GO:0002366	leukocyte activation involved in immune response	52	616	5.67E-06
GO:0016311	dephosphorylation	32	285	5.67E-06
GO:0034754	cellular hormone metabolic process	19	109	5.67E-06
GO:0042592	homeostatic process	97	1491	5.96E-06
GO:0050801	ion homeostasis	57	708	6.08E-06

GO:0048468	cell development	97	1493	6.25E-06
GO:0050767	regulation of neurogenesis	58	730	7.04E-06
GO:1901568	fatty acid derivative metabolic process	22	148	7.13E-06
GO:0071375	cellular response to peptide hormone stimulus	29	245	7.61E-06
GO:0051186	cofactor metabolic process	43	467	7.70E-06
GO:0045912	negative regulation of carbohydrate metabolic process	13	49	8.27E-06
GO:0035556	intracellular signal transduction	98	1528	9.10E-06
GO:0001775	cell activation	73	1024	9.58E-06
GO:0055080	cation homeostasis	52	629	9.62E-06
GO:0006631	fatty acid metabolic process	32	294	9.88E-06
GO:0009893	positive regulation of metabolic process	177	3280	9.88E-06
GO:0098660	inorganic ion transmembrane transport	56	707	1.19E-05
GO:0006826	iron ion transport	15	71	1.23E-05
GO:0071214	cellular response to abiotic stimulus	31	282	1.23E-05
GO:0062014	negative regulation of small molecule metabolic process	17	93	1.26E-05
GO:0120035	regulation of plasma membrane bounded cell projection organization	50	600	1.26E-05
GO:0045017	glycerolipid biosynthetic process	28	238	1.28E-05
GO:0060341	regulation of cellular localization	59	766	1.33E-05
GO:0044267	cellular protein metabolic process	190	3603	1.38E-05
GO:0060627	regulation of vesicle-mediated transport	43	480	1.41E-05
GO:0001934	positive regulation of protein phosphorylation	68	941	1.49E-05
GO:0015991	ATP hydrolysis coupled proton transport	10	27	1.50E-05
GO:0060284	regulation of cell development	63	846	1.54E-05
GO:0032268	regulation of cellular protein metabolic process	141	2486	1.60E-05
GO:0000902	cell morphogenesis	51	626	1.74E-05
GO:0002252	immune effector process	67	927	1.76E-05
GO:0009967	positive regulation of signal transduction	95	1493	1.79E-05
GO:0030100	regulation of endocytosis	27	229	1.87E-05
GO:0032989	cellular component morphogenesis	56	720	1.88E-05
GO:0019538	protein metabolic process	214	4197	2.00E-05
GO:0045664	regulation of neuron differentiation	49	595	2.12E-05
GO:0009653	anatomical structure morphogenesis	118	1992	2.13E-05
GO:0044093	positive regulation of molecular function	105	1713	2.19E-05
GO:0045937	positive regulation of phosphate metabolic process	73	1052	2.19E-05
GO:0001523	retinoid metabolic process	16	87	2.33E-05
GO:0010677	negative regulation of cellular carbohydrate metabolic process	12	46	2.39E-05
GO:0008202	steroid metabolic process	28	248	2.44E-05
GO:1904062	regulation of cation transmembrane transport	31	294	2.44E-05
GO:0051240	positive regulation of multicellular organismal process	97	1551	2.61E-05

GO:0009892	negative regulation of metabolic process	152	2762	2.62E-05
GO:0030534	adult behavior	20	137	2.63E-05
GO:0051173	positive regulation of nitrogen compound metabolic process	160	2946	2.63E-05
GO:0095500	acetylcholine receptor signaling pathway	9	22	2.63E-05
GO:0030104	water homeostasis	14	67	2.85E-05
GO:0045922	negative regulation of fatty acid metabolic process	10	30	2.93E-05
GO:0042327	positive regulation of phosphorylation	69	984	2.95E-05
GO:0009605	response to external stimulus	111	1857	2.97E-05
GO:0032355	response to estradiol	19	126	3.09E-05
GO:0044248	cellular catabolic process	101	1646	3.24E-05
GO:0030030	cell projection organization	73	1067	3.27E-05
GO:0055065	metal ion homeostasis	46	555	3.56E-05
GO:0006721	terpenoid metabolic process	17	103	3.69E-05
GO:0046486	glycerolipid metabolic process	37	401	4.01E-05
GO:0009117	nucleotide metabolic process	47	576	4.02E-05
GO:0120036	plasma membrane bounded cell projection organization	71	1034	4.02E-05
GO:0007586	digestion	17	104	4.09E-05
GO:0006464	cellular protein modification process	161	2999	4.41E-05
GO:0007417	central nervous system development	62	861	4.52E-05
GO:0044092	negative regulation of molecular function	75	1119	4.54E-05
GO:0031323	regulation of cellular metabolic process	288	6082	4.55E-05
GO:0048584	positive regulation of response to stimulus	119	2054	4.70E-05
GO:0042445	hormone metabolic process	23	186	5.10E-05
GO:0017144	drug metabolic process	49	622	5.80E-05
GO:0051130	positive regulation of cellular component organization	75	1128	5.85E-05
GO:0051247	positive regulation of protein metabolic process	97	1587	5.91E-05
GO:0048869	cellular developmental process	183	3533	6.05E-05
GO:0050891	multicellular organismal water homeostasis	13	62	6.05E-05
GO:0048513	animal organ development	157	2926	6.06E-05
GO:0080090	regulation of primary metabolic process	283	5982	6.37E-05
GO:0019222	regulation of metabolic process	304	6516	6.54E-05
GO:0043434	response to peptide hormone	34	362	6.86E-05
GO:0010941	regulation of cell death	99	1638	7.08E-05
GO:0055082	cellular chemical homeostasis	51	665	7.08E-05
GO:0060411	cardiac septum morphogenesis	14	74	7.08E-05
GO:0022607	cellular component assembly	131	2343	7.16E-05
GO:0019432	triglyceride biosynthetic process	8	19	7.72E-05
GO:0051051	negative regulation of transport	39	450	7.73E-05
GO:0051094	positive regulation of developmental process	82	1286	8.39E-05
GO:0006690	icosanoid metabolic process	16	99	8.54E-05

GO:0030163	protein catabolic process	48	615	8.76E-05
GO:0007166	cell surface receptor signaling pathway	124	2198	9.01E-05
GO:0048638	regulation of developmental growth	30	302	9.13E-05
GO:0032412	regulation of ion transmembrane transporter activity	25	224	9.20E-05
GO:0045859	regulation of protein kinase activity	57	788	9.55E-05
GO:0019693	ribose phosphate metabolic process	39	455	9.59E-05
GO:0031401	positive regulation of protein modification process	75	1149	0.0001
GO:0043549	regulation of kinase activity	60	849	0.0001
GO:0006873	cellular ion homeostasis	46	584	0.00011
GO:0006979	response to oxidative stress	34	373	0.00011
GO:0009416	response to light stimulus	29	290	0.00011
GO:0010604	positive regulation of macromolecule metabolic process	162	3081	0.00011
GO:0030154	cell differentiation	178	3457	0.00011
GO:0035095	behavioral response to nicotine	6	8	0.00011
GO:0035295	tube development	57	793	0.00011
GO:0038003	opioid receptor signaling pathway	6	8	0.00011
GO:0046164	alcohol catabolic process	11	46	0.00011
GO:0003206	cardiac chamber morphogenesis	18	128	0.00012
GO:0009314	response to radiation	37	425	0.00012
GO:0033559	unsaturated fatty acid metabolic process	15	90	0.00012
GO:0044085	cellular component biogenesis	139	2556	0.00012
GO:0060429	epithelium development	70	1055	0.00012
GO:0001508	action potential	16	104	0.00014
GO:0010959	regulation of metal ion transport	33	360	0.00014
GO:0071384	cellular response to corticosteroid stimulus	12	58	0.00014
GO:0019725	cellular homeostasis	57	806	0.00016
GO:0043412	macromolecule modification	166	3197	0.00016
GO:0046856	phosphatidylinositol dephosphorylation	8	22	0.00016
GO:0048729	tissue morphogenesis	42	522	0.00016
GO:1904951	positive regulation of establishment of protein localization	35	397	0.00016
GO:0007631	feeding behavior	15	94	0.00017
GO:0043085	positive regulation of catalytic activity	85	1381	0.00017
GO:0051222	positive regulation of protein transport	33	365	0.00017
GO:0060562	epithelial tube morphogenesis	29	298	0.00017
GO:0000122	negative regulation of transcription by RNA polymerase II	57	809	0.00018
GO:0010675	regulation of cellular carbohydrate metabolic process	18	133	0.00018
GO:0055072	iron ion homeostasis	14	83	0.0002
GO:0032270	positive regulation of cellular protein metabolic process	90	1496	0.00021
GO:0032386	regulation of intracellular transport	31	335	0.00021

GO:0009259	ribonucleotide metabolic process	37	440	0.00022
GO:0045833	negative regulation of lipid metabolic process	14	84	0.00022
GO:0048608	reproductive structure development	35	405	0.00022
GO:0055086	nucleobase-containing small molecule metabolic process	49	662	0.00023
GO:0006470	protein dephosphorylation	22	194	0.00024
GO:0007218	neuropeptide signaling pathway	16	110	0.00024
GO:0000904	cell morphogenesis involved in differentiation	40	498	0.00025
GO:0002376	immune system process	129	2370	0.00025
GO:0006222	UMP biosynthetic process	6	10	0.00025
GO:0007197	adenylate cyclase-inhibiting G protein-coupled acetylcholine receptor signaling pathway	5	5	0.00025
GO:0019058	viral life cycle	20	166	0.00025
GO:0032486	Rap protein signal transduction	6	10	0.00025
GO:0038170	somatostatin signaling pathway	5	5	0.00025
GO:0044206	UMP salvage	5	5	0.00025
GO:0099131	ATP hydrolysis coupled ion transmembrane transport	12	63	0.00027
GO:0031644	regulation of neurological system process	16	112	0.00028
GO:0044403	symbiont process	48	650	0.00028
GO:0002758	innate immune response-activating signal transduction	20	168	0.00029
GO:0051348	negative regulation of transferase activity	29	310	0.0003
GO:1901654	response to ketone	21	183	0.0003
GO:0060322	head development	50	692	0.00031
GO:0060412	ventricular septum morphogenesis	10	43	0.00031
GO:0043408	regulation of MAPK cascade	51	712	0.00032
GO:0002218	activation of innate immune response	21	186	0.00036
GO:0006732	coenzyme metabolic process	28	297	0.00036
GO:0009890	negative regulation of biosynthetic process	89	1501	0.00036
GO:0031327	negative regulation of cellular biosynthetic process	88	1479	0.00036
GO:0033157	regulation of intracellular protein transport	22	201	0.00036
GO:0006836	neurotransmitter transport	20	172	0.00038
GO:0015813	L-glutamate transmembrane transport	7	18	0.00038
GO:0099132	ATP hydrolysis coupled cation transmembrane transport	12	66	0.00038
GO:1901657	glycosyl compound metabolic process	18	143	0.00038
GO:0062012	regulation of small molecule metabolic process	30	332	0.00039
GO:0071385	cellular response to glucocorticoid stimulus	11	55	0.00039
GO:0006109	regulation of carbohydrate metabolic process	19	158	0.0004
GO:0007207	phospholipase C-activating G protein-coupled acetylcholine receptor signaling pathway	5	6	0.00041
GO:0030182	neuron differentiation	62	940	0.00041
GO:0044262	cellular carbohydrate metabolic process	18	144	0.00041
GO:0051552	flavone metabolic process	5	6	0.00041

GO:0006950	response to stress	166	3267	0.00043
GO:0032388	positive regulation of intracellular transport	20	174	0.00043
GO:0006650	glycerophospholipid metabolic process	30	335	0.00044
GO:0007548	sex differentiation	25	252	0.00044
GO:0030003	cellular cation homeostasis	43	570	0.00045
GO:0007611	learning or memory	24	237	0.00047
GO:0043097	pyrimidine nucleoside salvage	6	12	0.00047
GO:0044057	regulation of system process	40	516	0.00048
GO:0051347	positive regulation of transferase activity	46	630	0.0005
GO:0055067	monovalent inorganic cation homeostasis	16	119	0.0005
GO:0007169	transmembrane receptor protein tyrosine kinase signaling pathway	39	499	0.00051
GO:0007264	small GTPase mediated signal transduction	24	239	0.00052
GO:0051129	negative regulation of cellular component organization	46	632	0.00053
GO:0071496	cellular response to external stimulus	28	305	0.00053
GO:0003279	cardiac septum development	15	107	0.00056
GO:0035239	tube morphogenesis	45	615	0.00057
GO:0000041	transition metal ion transport	16	121	0.00058
GO:0046474	glycerophospholipid biosynthetic process	23	225	0.00058
GO:0008286	insulin receptor signaling pathway	13	82	0.00059
GO:0050890	cognition	26	274	0.00059
GO:1904063	negative regulation of cation transmembrane transport	13	82	0.00059
GO:0009165	nucleotide biosynthetic process	27	291	0.0006
GO:0019400	alditol metabolic process	7	20	0.0006
GO:0031347	regulation of defense response	48	676	0.00062
GO:0002009	morphogenesis of an epithelium	34	414	0.00064
GO:1902993	positive regulation of amyloid precursor protein catabolic process	6	13	0.00064
GO:0097306	cellular response to alcohol	13	83	0.00065
GO:0007200	phospholipase C-activating G protein-coupled receptor signaling pathway	15	109	0.00066
GO:0003205	cardiac chamber development	19	166	0.00067
GO:0065003	protein-containing complex assembly	88	1514	0.00072
GO:0016310	phosphorylation	75	1236	0.00075
GO:0035303	regulation of dephosphorylation	21	198	0.00075
GO:0040008	regulation of growth	47	663	0.00075
GO:0043067	regulation of programmed cell death	88	1516	0.00075
GO:0006644	phospholipid metabolic process	33	402	0.00081
GO:0007626	locomotory behavior	20	184	0.00081
GO:0043410	positive regulation of MAPK cascade	39	512	0.00081
GO:0051172	negative regulation of nitrogen compound metabolic process	123	2307	0.00083
GO:0090316	positive regulation of intracellular protein transport	16	126	0.00086

GO:0098657	import into cell	44	609	0.00086
GO:1902532	negative regulation of intracellular signal transduction	39	514	0.00086
GO:0050804	modulation of chemical synaptic transmission	28	316	0.00087
GO:1902679	negative regulation of RNA biosynthetic process	74	1222	0.00088
GO:0016331	morphogenesis of embryonic epithelium	17	141	0.0009
GO:0007035	vacuolar acidification	7	22	0.00092
GO:0043933	protein-containing complex subunit organization	99	1770	0.00092
GO:0051091	positive regulation of DNA-binding transcription factor activity	24	250	0.00092
GO:0051701	interaction with host	18	156	0.00092
GO:0061024	membrane organization	50	729	0.00092
GO:0009260	ribonucleotide biosynthetic process	21	202	0.00093
GO:0044282	small molecule catabolic process	32	388	0.00093
GO:0044597	daunorubicin metabolic process	5	8	0.00093
GO:0044598	doxorubicin metabolic process	5	8	0.00093
GO:0045860	positive regulation of protein kinase activity	39	517	0.00093
GO:0099504	synaptic vesicle cycle	14	100	0.00093
GO:0003007	heart morphogenesis	23	235	0.00097
GO:0072175	epithelial tube formation	16	128	0.00097
GO:1903725	regulation of phospholipid metabolic process	12	75	0.00098
GO:0001841	neural tube formation	14	101	0.001
GO:0002576	platelet degranulation	16	129	0.001
GO:0008015	blood circulation	31	373	0.001
GO:0010558	negative regulation of macromolecule biosynthetic process	83	1425	0.001
GO:0019748	secondary metabolic process	10	52	0.001
GO:0030522	intracellular receptor signaling pathway	19	173	0.001
GO:0045137	development of primary sexual characteristics	21	204	0.001
GO:0045934	negative regulation of nucleobase-containing compound metabolic process	83	1424	0.001
GO:0007167	enzyme linked receptor protein signaling pathway	48	698	0.0011
GO:0009888	tissue development	92	1626	0.0011
GO:0045429	positive regulation of nitric oxide biosynthetic process	9	42	0.0011
GO:0048666	neuron development	51	758	0.0011
GO:0048812	neuron projection morphogenesis	35	448	0.0011
GO:0051899	membrane depolarization	11	64	0.0011
GO:1902533	positive regulation of intracellular signal transduction	61	959	0.0011
GO:0006996	organelle organization	157	3131	0.0012
GO:0006879	cellular iron ion homeostasis	11	66	0.0013
GO:0045088	regulation of innate immune response	30	361	0.0013
GO:0097105	presynaptic membrane assembly	5	9	0.0013
GO:0099173	postsynapse organization	10	54	0.0013

GO:1903507	negative regulation of nucleic acid-templated transcription	73	1220	0.0013
GO:0002064	epithelial cell development	19	179	0.0014
GO:0006855	drug transmembrane transport	14	105	0.0014
GO:0007213	G protein-coupled acetylcholine receptor signaling pathway	6	16	0.0014
GO:0010332	response to gamma radiation	10	55	0.0014
GO:0032410	negative regulation of transporter activity	12	79	0.0014
GO:0044283	small molecule biosynthetic process	41	569	0.0014
GO:0001838	embryonic epithelial tube formation	15	120	0.0015
GO:0007420	brain development	45	650	0.0015
GO:0008654	phospholipid biosynthetic process	24	261	0.0015
GO:0015853	adenine transport	4	4	0.0015
GO:0016032	viral process	41	571	0.0015
GO:0030855	epithelial cell differentiation	45	649	0.0015
GO:0032147	activation of protein kinase activity	29	347	0.0015
GO:0036101	leukotriene B4 catabolic process	4	4	0.0015
GO:0040011	locomotion	69	1144	0.0015
GO:0043086	negative regulation of catalytic activity	53	809	0.0015
GO:0045851	pH reduction	8	34	0.0015
GO:0048646	anatomical structure formation involved in morphogenesis	54	831	0.0015
GO:0001539	cilium or flagellum-dependent cell motility	7	25	0.0016
GO:0032868	response to insulin	21	213	0.0016
GO:0033674	positive regulation of kinase activity	40	553	0.0016
GO:1901135	carbohydrate derivative metabolic process	66	1083	0.0016
GO:0006071	glycerol metabolic process	6	17	0.0017
GO:0006875	cellular metal ion homeostasis	37	499	0.0017
GO:0007612	learning	16	137	0.0017
GO:0048259	regulation of receptor-mediated endocytosis	12	81	0.0017
GO:0051726	regulation of cell cycle	68	1129	0.0017
GO:0055076	transition metal ion homeostasis	15	122	0.0017
GO:0080134	regulation of response to stress	76	1299	0.0017
GO:0001655	urogenital system development	26	299	0.0018
GO:0006641	triglyceride metabolic process	11	69	0.0018
GO:0016042	lipid catabolic process	24	265	0.0018
GO:0042981	regulation of apoptotic process	85	1501	0.0018
GO:0051253	negative regulation of RNA metabolic process	76	1303	0.0018
GO:0051336	regulation of hydrolase activity	73	1238	0.0018
GO:0051704	multi-organism process	117	2222	0.0018
GO:0051952	regulation of amine transport	12	82	0.0018
GO:2001257	regulation of cation channel activity	17	152	0.0018
GO:0003281	ventricular septum development	11	70	0.0019

GO:0032869	cellular response to insulin stimulus	17	153	0.0019
GO:0048511	rhythmic process	23	250	0.0019
GO:1903827	regulation of cellular protein localization	35	465	0.0019
GO:1904646	cellular response to amyloid-beta	7	26	0.0019
GO:0007507	heart development	36	485	0.002
GO:0031960	response to corticosteroid	17	154	0.002
GO:0033572	transferrin transport	8	36	0.002
GO:0071392	cellular response to estradiol stimulus	8	36	0.002
GO:0006508	proteolysis	71	1203	0.0021
GO:0007265	Ras protein signal transduction	17	155	0.0021
GO:0015893	drug transport	17	155	0.0021
GO:0016055	Wnt signaling pathway	26	303	0.0021
GO:0046174	polyol catabolic process	6	18	0.0021
GO:0051047	positive regulation of secretion	31	393	0.0021
GO:0070482	response to oxygen levels	27	321	0.0021
GO:0001101	response to acid chemical	27	323	0.0022
GO:0010564	regulation of cell cycle process	46	684	0.0022
GO:0033762	response to glucagon	8	37	0.0022
GO:0035329	hippo signaling	7	27	0.0022
GO:0046677	response to antibiotic	26	305	0.0022
GO:0071236	cellular response to antibiotic	14	112	0.0022
GO:1901214	regulation of neuron death	25	288	0.0022
GO:0032490	detection of molecule of bacterial origin	5	11	0.0023
GO:0097242	amyloid-beta clearance	5	11	0.0023
GO:1902004	positive regulation of amyloid-beta formation	5	11	0.0023
GO:0006940	regulation of smooth muscle contraction	10	60	0.0024
GO:0007346	regulation of mitotic cell cycle	42	608	0.0024
GO:0050808	synapse organization	19	189	0.0024
GO:0071242	cellular response to ammonium ion	10	60	0.0024
GO:0001843	neural tube closure	12	86	0.0025
GO:0019217	regulation of fatty acid metabolic process	12	86	0.0025
GO:0043009	chordate embryonic development	39	550	0.0025
GO:0045892	negative regulation of transcription, DNA-templated	69	1169	0.0025
GO:0006914	autophagy	22	240	0.0026
GO:0008209	androgen metabolic process	7	28	0.0026
GO:0035335	peptidyl-tyrosine dephosphorylation	13	100	0.0026
GO:0060317	cardiac epithelial to mesenchymal transition	7	28	0.0026
GO:2000113	negative regulation of cellular macromolecule biosynthetic process	77	1348	0.0027
GO:0009161	ribonucleoside monophosphate metabolic process	22	242	0.0028
GO:0010605	negative regulation of macromolecule metabolic process	130	2558	0.0028

GO:0042127	regulation of cell population proliferation	88	1594	0.0028
GO:0045089	positive regulation of innate immune response	23	259	0.0028
GO:0007632	visual behavior	9	50	0.0029
GO:0034763	negative regulation of transmembrane transport	14	116	0.0029
GO:0072512	trivalent inorganic cation transport	8	39	0.0029
GO:0008217	regulation of blood pressure	18	177	0.003
GO:0008306	associative learning	11	75	0.003
GO:0019233	sensory perception of pain	11	75	0.003
GO:0031175	neuron projection development	42	616	0.003
GO:0043401	steroid hormone mediated signaling pathway	15	131	0.003
GO:0099068	postsynapse assembly	5	12	0.003
GO:0006936	muscle contraction	22	244	0.0031
GO:0080135	regulation of cellular response to stress	42	618	0.0032
GO:0009057	macromolecule catabolic process	59	970	0.0033
GO:0002933	lipid hydroxylation	4	6	0.0034
GO:0030162	regulation of proteolysis	48	742	0.0034
GO:0030579	ubiquitin-dependent SMAD protein catabolic process	4	6	0.0034
GO:0044087	regulation of cellular component biogenesis	54	867	0.0034
GO:0044257	cellular protein catabolic process	39	562	0.0034
GO:0060304	regulation of phosphatidylinositol dephosphorylation	4	6	0.0034
GO:0061002	negative regulation of dendritic spine morphogenesis	4	6	0.0034
GO:0071221	cellular response to bacterial lipopeptide	4	6	0.0034
GO:0071229	cellular response to acid chemical	19	196	0.0034
GO:1901655	cellular response to ketone	12	90	0.0034
GO:0003006	developmental process involved in reproduction	42	622	0.0035
GO:0034121	regulation of toll-like receptor signaling pathway	10	64	0.0035
GO:0048814	regulation of dendrite morphogenesis	11	77	0.0035
GO:0051641	cellular localization	113	2180	0.0035
GO:0009991	response to extracellular stimulus	35	486	0.0036
GO:1903508	positive regulation of nucleic acid-templated transcription	84	1520	0.0036
GO:0008406	gonad development	19	198	0.0037
GO:0019941	modification-dependent protein catabolic process	34	467	0.0037
GO:0046132	pyrimidine ribonucleoside biosynthetic process	6	21	0.0037
GO:0046173	polyol biosynthetic process	8	41	0.0037
GO:0046825	regulation of protein export from nucleus	8	41	0.0037
GO:0046827	positive regulation of protein export from nucleus	6	21	0.0037
GO:0010248	establishment or maintenance of transmembrane electrochemical gradient	5	13	0.0038
GO:0018027	peptidyl-lysine dimethylation	5	13	0.0038
GO:0034644	cellular response to UV	11	78	0.0038

GO:0051962	positive regulation of nervous system development	35	488	0.0038
GO:0006661	phosphatidylinositol biosynthetic process	15	136	0.004
GO:0010038	response to metal ion	27	339	0.004
GO:0010921	regulation of phosphatase activity	17	167	0.004
GO:0051588	regulation of neurotransmitter transport	12	92	0.004
GO:0048013	ephrin receptor signaling pathway	11	79	0.0041
GO:0048732	gland development	30	395	0.0041
GO:0031328	positive regulation of cellular biosynthetic process	98	1846	0.0042
GO:0010565	regulation of cellular ketone metabolic process	14	122	0.0043
GO:0042552	myelination	12	93	0.0043
GO:0060359	response to ammonium ion	14	122	0.0043
GO:0003181	atrioventricular valve morphogenesis	6	22	0.0044
GO:0071478	cellular response to radiation	16	153	0.0044
GO:0051384	response to glucocorticoid	15	138	0.0045
GO:0006468	protein phosphorylation	56	923	0.0046
GO:0009891	positive regulation of biosynthetic process	99	1876	0.0046
GO:0021915	neural tube development	16	154	0.0046
GO:0055114	oxidation-reduction process	56	923	0.0046
GO:2000379	positive regulation of reactive oxygen species metabolic process	12	94	0.0046
GO:0043654	recognition of apoptotic cell	4	7	0.0047
GO:0051938	L-glutamate import	4	7	0.0047
GO:0006646	phosphatidylethanolamine biosynthetic process	5	14	0.0048
GO:0016999	antibiotic metabolic process	14	124	0.0048
GO:0043666	regulation of phosphoprotein phosphatase activity	13	109	0.0048
GO:0048667	cell morphogenesis involved in neuron differentiation	30	400	0.0048
GO:0061061	muscle structure development	33	457	0.0048
GO:0001837	epithelial to mesenchymal transition	10	68	0.0049
GO:0022600	digestive system process	10	68	0.0049
GO:0046661	male sex differentiation	16	155	0.0049
GO:0050795	regulation of behavior	10	68	0.0049
GO:0072521	purine-containing compound metabolic process	34	478	0.005
GO:1901576	organic substance biosynthetic process	214	4656	0.005
GO:1903532	positive regulation of secretion by cell	28	364	0.005
GO:0002755	MyD88-dependent toll-like receptor signaling pathway	7	33	0.0051
GO:0003231	cardiac ventricle development	14	125	0.0051
GO:0006937	regulation of muscle contraction	16	156	0.0051
GO:0031349	positive regulation of defense response	28	365	0.0051
GO:0055078	sodium ion homeostasis	6	23	0.0051
GO:0021549	cerebellum development	12	96	0.0052
GO:0051090	regulation of DNA-binding transcription factor activity	30	403	0.0052

GO:0006511	ubiquitin-dependent protein catabolic process	33	461	0.0053
GO:0006814	sodium ion transport	18	189	0.0053
GO:0030900	forebrain development	28	366	0.0053
GO:0044260	cellular macromolecule metabolic process	283	6413	0.0053
GO:0051093	negative regulation of developmental process	55	910	0.0053
GO:0060548	negative regulation of cell death	57	953	0.0054
GO:0046890	regulation of lipid biosynthetic process	17	174	0.0056
GO:0071482	cellular response to light stimulus	12	97	0.0056
GO:0007588	excretion	8	45	0.0057
GO:0019218	regulation of steroid metabolic process	13	112	0.0057
GO:0050769	positive regulation of neurogenesis	31	425	0.0057
GO:0006816	calcium ion transport	21	242	0.0058
GO:0034312	diol biosynthetic process	5	15	0.0058
GO:0051254	positive regulation of RNA metabolic process	86	1596	0.0058
GO:0071361	cellular response to ethanol	5	15	0.0058
GO:0001941	postsynaptic membrane organization	6	24	0.0059
GO:0042594	response to starvation	17	175	0.0059
GO:0043271	negative regulation of ion transport	15	143	0.0059
GO:0060285	cilium-dependent cell motility	6	24	0.0059
GO:0051961	negative regulation of nervous system development	23	279	0.0062
GO:0071216	cellular response to biotic stimulus	17	176	0.0062
GO:0003151	outflow tract morphogenesis	10	71	0.0063
GO:0006928	movement of cell or subcellular component	75	1355	0.0063
GO:0022603	regulation of anatomical structure morphogenesis	57	961	0.0063
GO:0032413	negative regulation of ion transmembrane transporter activity	10	71	0.0063
GO:0046902	regulation of mitochondrial membrane permeability	10	71	0.0063
GO:0046916	cellular transition metal ion homeostasis	12	99	0.0063
GO:0097106	postsynaptic density organization	4	8	0.0063
GO:0036293	response to decreased oxygen levels	24	298	0.0064
GO:0002221	pattern recognition receptor signaling pathway	13	114	0.0065
GO:0008285	negative regulation of cell population proliferation	43	669	0.0065
GO:0048839	inner ear development	17	177	0.0065
GO:0071900	regulation of protein serine/threonine kinase activity	34	488	0.0065
GO:0046488	phosphatidylinositol metabolic process	19	211	0.0066
GO:0002253	activation of immune response	29	393	0.0068
GO:0006813	potassium ion transport	17	178	0.0068
GO:0030260	entry into host cell	12	100	0.0068
GO:0035304	regulation of protein dephosphorylation	14	130	0.0068
GO:1905330	regulation of morphogenesis of an epithelium	14	130	0.0068
GO:0006897	endocytosis	35	510	0.0069
GO:0010035	response to inorganic substance	34	491	0.007

GO:0050773	regulation of dendrite development	14	131	0.0071
GO:0051241	negative regulation of multicellular organismal process	63	1098	0.0071
GO:0097164	ammonium ion metabolic process	17	179	0.0071
GO:0006835	dicarboxylic acid transport	9	60	0.0073
GO:0019932	second-messenger-mediated signaling	22	266	0.0073
GO:0051603	proteolysis involved in cellular protein catabolic process	36	532	0.0073
GO:0055024	regulation of cardiac muscle tissue development	10	73	0.0073
GO:1901379	regulation of potassium ion transmembrane transport	10	73	0.0073
GO:0008584	male gonad development	14	132	0.0076
GO:0071902	positive regulation of protein serine/threonine kinase activity	26	340	0.0076
GO:0072001	renal system development	22	267	0.0076
GO:0031667	response to nutrient levels	32	455	0.0077
GO:0048806	genitalia development	8	48	0.0077
GO:0003095	pressure natriuresis	3	3	0.0078
GO:0006789	bilirubin conjugation	3	3	0.0078
GO:0019355	nicotinamide nucleotide biosynthetic process from aspartate	3	3	0.0078
GO:0034627	'de novo' NAD biosynthetic process	3	3	0.0078
GO:0034628	'de novo' NAD biosynthetic process from aspartate	3	3	0.0078
GO:0044211	CTP salvage	3	3	0.0078
GO:0045597	positive regulation of cell differentiation	54	908	0.0078
GO:0046620	regulation of organ growth	11	88	0.0078
GO:0046621	negative regulation of organ growth	6	26	0.0078
GO:0060084	synaptic transmission involved in micturition	3	3	0.0078
GO:0060415	muscle tissue morphogenesis	10	74	0.0078
GO:0070340	detection of bacterial lipopeptide	3	3	0.0078
GO:0071377	cellular response to glucagon stimulus	6	26	0.0078
GO:0071709	membrane assembly	6	26	0.0078
GO:0097352	autophagosome maturation	6	26	0.0078
GO:0003341	cilium movement	9	61	0.0079
GO:0048639	positive regulation of developmental growth	16	165	0.0079
GO:0010976	positive regulation of neuron projection development	21	251	0.008
GO:0001701	in utero embryonic development	24	306	0.0082
GO:0022414	reproductive process	74	1350	0.0082
GO:0031346	positive regulation of cell projection organization	26	343	0.0082
GO:0033554	cellular response to stress	83	1553	0.0082
GO:0046520	sphingoid biosynthetic process	4	9	0.0082
GO:0090394	negative regulation of excitatory postsynaptic potential	4	9	0.0082
GO:0097104	postsynaptic membrane assembly	4	9	0.0082

GO:0098815	modulation of excitatory postsynaptic potential	7	37	0.0082
GO:1990314	cellular response to insulin-like growth factor stimulus	4	9	0.0082
GO:2000807	regulation of synaptic vesicle clustering	4	9	0.0082
GO:0001504	neurotransmitter uptake	5	17	0.0083
GO:0001666	response to hypoxia	23	288	0.0083
GO:0006910	phagocytosis, recognition	5	17	0.0083
GO:0010866	regulation of triglyceride biosynthetic process	5	17	0.0083
GO:0031329	regulation of cellular catabolic process	46	743	0.0083
GO:0050433	regulation of catecholamine secretion	8	49	0.0083
GO:0001676	long-chain fatty acid metabolic process	12	104	0.0085
GO:0042698	ovulation cycle	9	62	0.0085
GO:0044242	cellular lipid catabolic process	16	167	0.0085
GO:0051924	regulation of calcium ion transport	20	236	0.0088
GO:0006163	purine nucleotide metabolic process	31	442	0.009
GO:0034622	cellular protein-containing complex assembly	50	832	0.0091
GO:0045806	negative regulation of endocytosis	8	50	0.0091
GO:0051930	regulation of sensory perception of pain	7	38	0.0091
GO:0003012	muscle system process	23	291	0.0092
GO:0001763	morphogenesis of a branching structure	16	169	0.0095
GO:0071805	potassium ion transmembrane transport	16	169	0.0095
GO:0009150	purine ribonucleotide metabolic process	30	425	0.0097
GO:0072329	monocarboxylic acid catabolic process	12	106	0.0097
GO:0030540	female genitalia development	5	18	0.01
GO:2000369	regulation of clathrin-dependent endocytosis	5	18	0.01
GO:0006939	smooth muscle contraction	8	51	0.0101
GO:0043161	proteasome-mediated ubiquitin-dependent protein catabolic process	21	257	0.0101
GO:0051171	regulation of nitrogen compound metabolic process	257	5827	0.0101
GO:0060071	Wnt signaling pathway, planar cell polarity pathway	8	51	0.0101
GO:1901016	regulation of potassium ion transmembrane transporter activity	8	51	0.0101
GO:0003073	regulation of systemic arterial blood pressure	11	92	0.0102
GO:0006091	generation of precursor metabolites and energy	28	388	0.0102
GO:0046718	viral entry into host cell	11	92	0.0102
GO:0033036	macromolecule localization	113	2268	0.0104
GO:0071260	cellular response to mechanical stimulus	10	78	0.0104
GO:0045893	positive regulation of transcription, DNA-templated	77	1435	0.0105
GO:0051567	histone H3-K9 methylation	4	10	0.0105
GO:0070072	vacuolar proton-transporting V-type ATPase complex assembly	4	10	0.0105
GO:1901990	regulation of mitotic cell cycle phase transition	26	351	0.0105
GO:0030879	mammary gland development	13	123	0.0106

GO:0044249	cellular biosynthetic process	207	4567	0.0106
GO:0009411	response to UV	14	139	0.0107
GO:0008104	protein localization	100	1966	0.0108
GO:0060070	canonical Wnt signaling pathway	11	93	0.0108
GO:0002220	innate immune response activating cell surface receptor signaling pathway	9	65	0.0109
GO:0042455	ribonucleoside biosynthetic process	7	40	0.0112
GO:0046849	bone remodeling	7	40	0.0112
GO:0072350	tricarboxylic acid metabolic process	7	40	0.0112
GO:0006691	leukotriene metabolic process	6	29	0.0116
GO:0007210	serotonin receptor signaling pathway	6	29	0.0116
GO:0050892	intestinal absorption	6	29	0.0116
GO:0060603	mammary gland duct morphogenesis	6	29	0.0116
GO:0072527	pyrimidine-containing compound metabolic process	11	94	0.0116
GO:2000171	negative regulation of dendrite development	6	29	0.0116
GO:0010721	negative regulation of cell development	23	298	0.0117
GO:0016241	regulation of macroautophagy	15	157	0.0117
GO:0032872	regulation of stress-activated MAPK cascade	18	208	0.0117
GO:0048261	negative regulation of receptor-mediated endocytosis	5	19	0.0117
GO:0007198	adenylate cyclase-inhibiting serotonin receptor signaling pathway	3	4	0.0118
GO:0008283	cell population proliferation	42	676	0.0118
GO:0033214	siderophore-dependent iron import into cell	3	4	0.0118
GO:0038124	toll-like receptor TLR6:TLR2 signaling pathway	3	4	0.0118
GO:0070779	D-aspartate import across plasma membrane	3	4	0.0118
GO:0071395	cellular response to jasmonic acid stimulus	3	4	0.0118
GO:0071726	cellular response to diacyl bacterial lipopeptide	3	4	0.0118
GO:0120031	plasma membrane bounded cell projection assembly	29	413	0.0118
GO:0009156	ribonucleoside monophosphate biosynthetic process	12	110	0.012
GO:0045666	positive regulation of neuron differentiation	25	337	0.0121
GO:0010769	regulation of cell morphogenesis involved in differentiation	21	263	0.0122
GO:0008277	regulation of G protein-coupled receptor signaling pathway	14	142	0.0123
GO:0043406	positive regulation of MAP kinase activity	21	264	0.0127
GO:0010935	regulation of macrophage cytokine production	4	11	0.013
GO:0033212	iron import into cell	4	11	0.013
GO:0045736	negative regulation of cyclin-dependent protein serine/threonine kinase activity	6	30	0.013
GO:0048871	multicellular organismal homeostasis	22	283	0.013
GO:0060736	prostate gland growth	4	11	0.013
GO:0071545	inositol phosphate catabolic process	4	11	0.013

GO:0106070	regulation of adenylate cyclase-activating G protein-coupled receptor signaling pathway	4	11	0.013
GO:1901661	quinone metabolic process	6	30	0.013
GO:0043069	negative regulation of programmed cell death	51	873	0.0132
GO:0050877	nervous system process	69	1271	0.0134
GO:0030902	hindbrain development	14	144	0.0136
GO:0045596	negative regulation of cell differentiation	42	683	0.0136
GO:0086010	membrane depolarization during action potential	7	42	0.0136
GO:2000310	regulation of NMDA receptor activity	5	20	0.0136
GO:0097237	cellular response to toxic substance	17	195	0.0139
GO:1901617	organic hydroxy compound biosynthetic process	15	161	0.014
GO:0010812	negative regulation of cell-substrate adhesion	8	55	0.0142
GO:0051649	establishment of localization in cell	84	1616	0.0142
GO:0061180	mammary gland epithelium development	8	55	0.0142
GO:0040013	negative regulation of locomotion	22	286	0.0144
GO:0045807	positive regulation of endocytosis	13	129	0.0145
GO:1902882	regulation of response to oxidative stress	10	83	0.0145
GO:0006367	transcription initiation from RNA polymerase II promoter	15	162	0.0146
GO:0030004	cellular monovalent inorganic cation homeostasis	11	98	0.0147
GO:0042752	regulation of circadian rhythm	11	98	0.0147
GO:0060325	face morphogenesis	6	31	0.0147
GO:1903170	negative regulation of calcium ion transmembrane transport	7	43	0.0151
GO:0001822	kidney development	20	251	0.0154
GO:0007565	female pregnancy	16	180	0.0154
GO:0009062	fatty acid catabolic process	10	84	0.0155
GO:0097305	response to alcohol	19	233	0.0155
GO:1903533	regulation of protein targeting	8	56	0.0155
GO:0050878	regulation of body fluid levels	32	483	0.0156
GO:0034394	protein localization to cell surface	5	21	0.0159
GO:0042573	retinoic acid metabolic process	5	21	0.0159
GO:0060444	branching involved in mammary gland duct morphogenesis	5	21	0.0159
GO:0097006	regulation of plasma lipoprotein particle levels	9	70	0.0159
GO:0007409	axonogenesis	25	346	0.016
GO:0071453	cellular response to oxygen levels	15	164	0.016
GO:0060992	response to fungicide	4	12	0.0161
GO:0070262	peptidyl-serine dephosphorylation	4	12	0.0161
GO:0045944	positive regulation of transcription by RNA polymerase II	61	1104	0.0162
GO:0030097	hemopoiesis	34	526	0.0165
GO:0042755	eating behavior	6	32	0.0165
GO:0045745	positive regulation of G protein-coupled receptor signaling pathway	6	32	0.0165

GO:0048524	positive regulation of viral process	10	85	0.0165
GO:0070286	axonemal dynein complex assembly	6	32	0.0165
GO:0031646	positive regulation of neurological system process	8	57	0.0167
GO:0060255	regulation of macromolecule metabolic process	264	6072	0.0168
GO:0006537	glutamate biosynthetic process	3	5	0.0169
GO:0010936	negative regulation of macrophage cytokine production	3	5	0.0169
GO:0015939	pantothenate metabolic process	3	5	0.0169
GO:0045446	endothelial cell differentiation	9	71	0.0169
GO:0050778	positive regulation of immune response	37	589	0.0169
GO:0050915	sensory perception of sour taste	3	5	0.0169
GO:0072511	divalent inorganic cation transport	22	291	0.0169
GO:0099560	synaptic membrane adhesion	3	5	0.0169
GO:0140052	cellular response to oxidised low-density lipoprotein particle stimulus	3	5	0.0169
GO:1903223	positive regulation of oxidative stress-induced neuron death	3	5	0.0169
GO:1903972	regulation of cellular response to macrophage colony-stimulating factor stimulus	3	5	0.0169
GO:2000809	positive regulation of synaptic vesicle clustering	3	5	0.0169
GO:0045935	positive regulation of nucleobase-containing compound metabolic process	90	1770	0.017
GO:0051188	cofactor biosynthetic process	18	218	0.017
GO:0023014	signal transduction by protein phosphorylation	25	349	0.0173
GO:0003158	endothelium development	10	86	0.0174
GO:0009790	embryo development	51	890	0.0179
GO:0003208	cardiac ventricle morphogenesis	9	72	0.0181
GO:0008542	visual learning	7	45	0.0181
GO:0098664	G protein-coupled serotonin receptor signaling pathway	5	22	0.0181
GO:1905809	negative regulation of synapse organization	5	22	0.0181
GO:0032228	regulation of synaptic transmission, GABAergic	6	33	0.0183
GO:0002224	toll-like receptor signaling pathway	10	87	0.0187
GO:0016571	histone methylation	10	87	0.0187
GO:0035567	non-canonical Wnt signaling pathway	10	87	0.0187
GO:0010720	positive regulation of cell development	32	491	0.0188
GO:0030099	myeloid cell differentiation	17	203	0.0191
GO:0051259	protein complex oligomerization	33	512	0.0191
GO:0072359	circulatory system development	47	807	0.0191
GO:0097190	apoptotic signaling pathway	22	295	0.0192
GO:0002087	regulation of respiratory gaseous exchange by neurological system process	4	13	0.0195
GO:0003188	heart valve formation	4	13	0.0195
GO:0006171	cAMP biosynthetic process	4	13	0.0195
GO:0030238	male sex determination	4	13	0.0195

GO:0035082	axoneme assembly	8	59	0.0195
GO:2000009	negative regulation of protein localization to cell surface	4	13	0.0195
GO:0003179	heart valve morphogenesis	7	46	0.0197
GO:0046434	organophosphate catabolic process	14	152	0.0197
GO:0098693	regulation of synaptic vesicle cycle	7	46	0.0197
GO:0090207	regulation of triglyceride metabolic process	6	34	0.0204
GO:0043576	regulation of respiratory gaseous exchange	5	23	0.0208
GO:1900407	regulation of cellular response to oxidative stress	9	74	0.0209
GO:0006220	pyrimidine nucleotide metabolic process	8	60	0.0211
GO:0060135	maternal process involved in female pregnancy	8	60	0.0211
GO:0010942	positive regulation of cell death	40	663	0.0214
GO:0090257	regulation of muscle system process	18	224	0.0214
GO:0071363	cellular response to growth factor stimulus	31	477	0.022
GO:0016358	dendrite development	10	90	0.0226
GO:0036465	synaptic vesicle recycling	6	35	0.0229
GO:0046676	negative regulation of insulin secretion	6	35	0.0229
GO:0019076	viral release from host cell	3	6	0.0232
GO:0060215	primitive hemopoiesis	3	6	0.0232
GO:0060696	regulation of phospholipid catabolic process	3	6	0.0232
GO:0060745	mammary gland branching involved in pregnancy	3	6	0.0232
GO:0070508	cholesterol import	3	6	0.0232
GO:0097119	postsynaptic density protein 95 clustering	3	6	0.0232
GO:0098712	L-glutamate import across plasma membrane	3	6	0.0232
GO:1900223	positive regulation of amyloid-beta clearance	3	6	0.0232
GO:1900227	positive regulation of NLRP3 inflammasome complex assembly	3	6	0.0232
GO:1902961	positive regulation of aspartic-type endopeptidase activity involved in amyloid precursor protein catabolic process	3	6	0.0232
GO:1904823	purine nucleobase transmembrane transport	3	6	0.0232
GO:0007158	neuron cell-cell adhesion	4	14	0.0233
GO:0030258	lipid modification	19	245	0.0233
GO:0044849	estrous cycle	4	14	0.0233
GO:0048589	developmental growth	24	340	0.0233
GO:1905564	positive regulation of vascular endothelial cell proliferation	4	14	0.0233
GO:0006213	pyrimidine nucleoside metabolic process	7	48	0.0234
GO:0006885	regulation of pH	10	91	0.0235
GO:0008593	regulation of Notch signaling pathway	10	91	0.0235
GO:0034383	low-density lipoprotein particle clearance	5	24	0.0235
GO:0071402	cellular response to lipoprotein particle stimulus	5	24	0.0235
GO:1903203	regulation of oxidative stress-induced neuron death	5	24	0.0235
GO:0007006	mitochondrial membrane organization	12	123	0.0239

GO:0099003	vesicle-mediated transport in synapse	11	107	0.0241
GO:0002223	stimulatory C-type lectin receptor signaling pathway	8	62	0.0242
GO:0050805	negative regulation of synaptic transmission	8	62	0.0242
GO:0000165	MAPK cascade	23	323	0.0249
GO:0007528	neuromuscular junction development	6	36	0.0249
GO:0106027	neuron projection organization	6	36	0.0249
GO:1903362	regulation of cellular protein catabolic process	19	248	0.0257
GO:0010557	positive regulation of macromolecule biosynthetic process	88	1758	0.0261
GO:0055008	cardiac muscle tissue morphogenesis	8	63	0.0261
GO:2001259	positive regulation of cation channel activity	8	63	0.0261
GO:0034764	positive regulation of transmembrane transport	16	194	0.0265
GO:0045995	regulation of embryonic development	12	125	0.0265
GO:0006706	steroid catabolic process	5	25	0.0267
GO:0008210	estrogen metabolic process	5	25	0.0267
GO:0043902	positive regulation of multi-organism process	14	159	0.0267
GO:1903829	positive regulation of cellular protein localization	21	287	0.0267
GO:0043687	post-translational protein modification	25	365	0.0268
GO:0071705	nitrogen compound transport	85	1690	0.0268
GO:0070848	response to growth factor	32	507	0.027
GO:0035337	fatty-acyl-CoA metabolic process	6	37	0.0274
GO:0034616	response to laminar fluid shear stress	4	15	0.0275
GO:0045408	regulation of interleukin-6 biosynthetic process	4	15	0.0275
GO:0060977	coronary vasculature morphogenesis	4	15	0.0275
GO:0050806	positive regulation of synaptic transmission	12	126	0.0276
GO:0035725	sodium ion transmembrane transport	14	160	0.0277
GO:0061138	morphogenesis of a branching epithelium	14	160	0.0277
GO:0051345	positive regulation of hydrolase activity	43	742	0.028
GO:0031647	regulation of protein stability	19	251	0.0282
GO:0031100	animal organ regeneration	9	79	0.0284
GO:1901566	organonitrogen compound biosynthetic process	71	1370	0.0284
GO:0050807	regulation of synapse organization	14	161	0.0289
GO:0006479	protein methylation	12	127	0.029
GO:0016202	regulation of striated muscle tissue development	12	127	0.029
GO:0048534	hematopoietic or lymphoid organ development	35	573	0.029
GO:2001233	regulation of apoptotic signaling pathway	26	388	0.029
GO:0045927	positive regulation of growth	19	252	0.0291
GO:0051302	regulation of cell division	15	179	0.0293
GO:0003190	atrioventricular valve formation	3	7	0.0296
GO:0043170	macromolecule metabolic process	314	7453	0.0296
GO:0045410	positive regulation of interleukin-6 biosynthetic process	3	7	0.0296

GO:0046824	positive regulation of nucleocytoplasmic transport	8	65	0.0298
GO:0060338	regulation of type I interferon-mediated signaling pathway	5	26	0.0298
GO:1903201	regulation of oxidative stress-induced cell death	8	65	0.0298
GO:2000463	positive regulation of excitatory postsynaptic potential	5	26	0.0298
GO:0007212	dopamine receptor signaling pathway	6	38	0.03
GO:0009112	nucleobase metabolic process	6	38	0.03
GO:0071248	cellular response to metal ion	14	162	0.03
GO:0006955	immune response	79	1560	0.0301
GO:1903050	regulation of proteolysis involved in cellular protein catabolic process	17	216	0.0301
GO:0031668	cellular response to extracellular stimulus	18	235	0.0307
GO:0050954	sensory perception of mechanical stimulus	14	163	0.0313
GO:1905475	regulation of protein localization to membrane	14	163	0.0313
GO:0007049	cell cycle	66	1263	0.0315
GO:1903169	regulation of calcium ion transmembrane transport	13	146	0.0318
GO:0002757	immune response-activating signal transduction	23	332	0.0319
GO:0007569	cell aging	8	66	0.0319
GO:0017158	regulation of calcium ion-dependent exocytosis	8	66	0.0319
GO:0040012	regulation of locomotion	49	881	0.0319
GO:0003184	pulmonary valve morphogenesis	4	16	0.032
GO:0007568	aging	19	255	0.032
GO:0036159	inner dynein arm assembly	4	16	0.032
GO:0043066	negative regulation of apoptotic process	48	859	0.032
GO:0098543	detection of other organism	4	16	0.032
GO:0046822	regulation of nucleocytoplasmic transport	11	113	0.0325
GO:0051282	regulation of sequestering of calcium ion	11	113	0.0325
GO:0043648	dicarboxylic acid metabolic process	10	97	0.0327
GO:0060043	regulation of cardiac muscle cell proliferation	6	39	0.0328
GO:0010628	positive regulation of gene expression	90	1826	0.033
GO:0048762	mesenchymal cell differentiation	12	130	0.0331
GO:0002520	immune system development	36	601	0.0332
GO:0003148	outflow tract septum morphogenesis	5	27	0.0333
GO:0045786	negative regulation of cell cycle	32	517	0.0333
GO:0071480	cellular response to gamma radiation	5	27	0.0333
GO:0009894	regulation of catabolic process	47	840	0.0335
GO:0002028	regulation of sodium ion transport	9	82	0.0338
GO:0007018	microtubule-based movement	20	276	0.0338
GO:0010821	regulation of mitochondrion organization	13	148	0.0344
GO:0032874	positive regulation of stress-activated MAPK cascade	13	148	0.0344
GO:0009119	ribonucleoside metabolic process	10	98	0.0345

GO:0044089	positive regulation of cellular component biogenesis	31	498	0.0347
GO:0000413	protein peptidyl-prolyl isomerization	6	40	0.036
GO:0002090	regulation of receptor internalization	6	40	0.036
GO:0002237	response to molecule of bacterial origin	22	317	0.036
GO:0010389	regulation of G2/M transition of mitotic cell cycle	13	149	0.036
GO:0010771	negative regulation of cell morphogenesis involved in differentiation	9	83	0.036
GO:0034381	plasma lipoprotein particle clearance	6	40	0.036
GO:0043255	regulation of carbohydrate biosynthetic process	9	83	0.036
GO:2001023	regulation of response to drug	9	83	0.036
GO:0016236	macroautophagy	12	132	0.0361
GO:0019722	calcium-mediated signaling	12	132	0.0361
GO:0034968	histone lysine methylation	8	68	0.0361
GO:0043405	regulation of MAP kinase activity	23	337	0.0361
GO:0009108	coenzyme biosynthetic process	14	167	0.0363
GO:0010629	negative regulation of gene expression	83	1670	0.0363
GO:0071241	cellular response to inorganic substance	15	185	0.0363
GO:1902749	regulation of cell cycle G2/M phase transition	14	167	0.0363
GO:0034599	cellular response to oxidative stress	17	222	0.0367
GO:0000278	mitotic cell cycle	37	628	0.0368
GO:0002682	regulation of immune system process	71	1391	0.0368
GO:0003056	regulation of vascular smooth muscle contraction	3	8	0.0368
GO:0003229	ventricular cardiac muscle tissue development	7	54	0.0368
GO:0008631	intrinsic apoptotic signaling pathway in response to oxidative stress	4	17	0.0368
GO:0009698	phenylpropanoid metabolic process	3	8	0.0368
GO:0009804	coumarin metabolic process	3	8	0.0368
GO:0014059	regulation of dopamine secretion	5	28	0.0368
GO:0031954	positive regulation of protein autophosphorylation	5	28	0.0368
GO:0042167	heme catabolic process	3	8	0.0368
GO:0046512	sphingosine biosynthetic process	3	8	0.0368
GO:0048384	retinoic acid receptor signaling pathway	4	17	0.0368
GO:0048488	synaptic vesicle endocytosis	5	28	0.0368
GO:0048813	dendrite morphogenesis	7	54	0.0368
GO:0050702	interleukin-1 beta secretion	3	8	0.0368
GO:0050768	negative regulation of neurogenesis	19	260	0.0368
GO:0055021	regulation of cardiac muscle tissue growth	7	54	0.0368
GO:0061028	establishment of endothelial barrier	5	28	0.0368
GO:0090181	regulation of cholesterol metabolic process	7	54	0.0368
GO:0106072	negative regulation of adenylate cyclase-activating G protein-coupled receptor signaling pathway	3	8	0.0368
GO:1901017	negative regulation of potassium ion transmembrane transporter activity	4	17	0.0368

GO:1902043	positive regulation of extrinsic apoptotic signaling pathway via death domain receptors	4	17	0.0368
GO:0040014	regulation of multicellular organism growth	8	69	0.0377
GO:0042180	cellular ketone metabolic process	8	69	0.0377
GO:0045844	positive regulation of striated muscle tissue development	8	69	0.0377
GO:0050764	regulation of phagocytosis	8	69	0.0377
GO:0045665	negative regulation of neuron differentiation	16	205	0.0379
GO:0033628	regulation of cell adhesion mediated by integrin	6	41	0.0381
GO:0042116	macrophage activation	6	41	0.0381
GO:1900449	regulation of glutamate receptor signaling pathway	6	41	0.0381
GO:0006766	vitamin metabolic process	11	117	0.0383
GO:0022900	electron transport chain	14	169	0.0383
GO:0046328	regulation of JNK cascade	14	169	0.0383
GO:0015850	organic hydroxy compound transport	12	134	0.0384
GO:0048754	branching morphogenesis of an epithelial tube	12	134	0.0384
GO:0022604	regulation of cell morphogenesis	28	442	0.0387
GO:0009066	aspartate family amino acid metabolic process	7	55	0.0389
GO:0046928	regulation of neurotransmitter secretion	7	55	0.0389
GO:0050776	regulation of immune response	48	873	0.0389
GO:1901216	positive regulation of neuron death	9	85	0.039
GO:0072522	purine-containing compound biosynthetic process	16	206	0.0391
GO:0030512	negative regulation of transforming growth factor beta receptor signaling pathway	8	70	0.04
GO:0000038	very long-chain fatty acid metabolic process	5	29	0.0402
GO:0006692	prostanoid metabolic process	5	29	0.0402
GO:0006693	prostaglandin metabolic process	5	29	0.0402
GO:0043277	apoptotic cell clearance	5	29	0.0402
GO:0046949	fatty-acyl-CoA biosynthetic process	5	29	0.0402
GO:1905314	semi-lunar valve development	5	29	0.0402
GO:2000027	regulation of animal organ morphogenesis	16	207	0.0404
GO:0001818	negative regulation of cytokine production	18	245	0.041
GO:0007162	negative regulation of cell adhesion	18	245	0.041
GO:0009152	purine ribonucleotide biosynthetic process	15	189	0.041
GO:0070588	calcium ion transmembrane transport	15	189	0.041
GO:0002573	myeloid leukocyte differentiation	10	102	0.0411
GO:0006790	sulfur compound metabolic process	23	343	0.0411
GO:0001892	embryonic placenta development	9	86	0.0412
GO:0006206	pyrimidine nucleobase metabolic process	4	18	0.0412
GO:0032288	myelin assembly	4	18	0.0412
GO:0051963	regulation of synapse assembly	9	86	0.0412
GO:0055025	positive regulation of cardiac muscle tissue development	6	42	0.0412
GO:0060537	muscle tissue development	20	284	0.0412

GO:0071702	organic substance transport	98	2040	0.0412
GO:0010977	negative regulation of neuron projection development	12	136	0.0415
GO:0043647	inositol phosphate metabolic process	7	56	0.0415
GO:0003195	tricuspid valve formation	2	2	0.0417
GO:0006097	glyoxylate cycle	2	2	0.0417
GO:0009060	aerobic respiration	8	71	0.0417
GO:0009199	ribonucleoside triphosphate metabolic process	17	227	0.0417
GO:0016488	farnesol catabolic process	2	2	0.0417
GO:0019075	virus maturation	2	2	0.0417
GO:0019747	regulation of isoprenoid metabolic process	2	2	0.0417
GO:0031635	adenylate cyclase-inhibiting opioid receptor signaling pathway	2	2	0.0417
GO:0033277	abortive mitotic cell cycle	2	2	0.0417
GO:0036304	umbilical cord morphogenesis	2	2	0.0417
GO:0042495	detection of triacyl bacterial lipopeptide	2	2	0.0417
GO:0042496	detection of diacyl bacterial lipopeptide	2	2	0.0417
GO:0042704	uterine wall breakdown	2	2	0.0417
GO:0044027	hypermethylation of CpG island	2	2	0.0417
GO:0046108	uridine metabolic process	2	2	0.0417
GO:0048738	cardiac muscle tissue development	13	154	0.0417
GO:0070980	biphenyl catabolic process	2	2	0.0417
GO:0090222	centrosome-templated microtubule nucleation	2	2	0.0417
GO:0090327	negative regulation of locomotion involved in locomotory behavior	2	2	0.0417
GO:1903966	monounsaturated fatty acid biosynthetic process	2	2	0.0417
GO:2000077	negative regulation of type B pancreatic cell development	2	2	0.0417
GO:0002764	immune response-regulating signaling pathway	24	365	0.0423
GO:0001578	microtubule bundle formation	9	87	0.0427
GO:0009267	cellular response to starvation	12	137	0.0427
GO:0090288	negative regulation of cellular response to growth factor stimulus	12	137	0.0427
GO:0097327	response to antineoplastic agent	9	87	0.0427
GO:0006739	NADP metabolic process	5	30	0.0436
GO:0010259	multicellular organism aging	5	30	0.0436
GO:0060271	cilium assembly	22	326	0.0436
GO:0009612	response to mechanical stimulus	16	210	0.0438
GO:0001885	endothelial cell development	6	43	0.0439
GO:0002091	negative regulation of receptor internalization	3	9	0.0439
GO:0015866	ADP transport	3	9	0.0439
GO:0030299	intestinal cholesterol absorption	3	9	0.0439
GO:0031532	actin cytoskeleton reorganization	7	57	0.0439
GO:0031943	regulation of glucocorticoid metabolic process	3	9	0.0439

GO:0031952	regulation of protein autophosphorylation	6	43	0.0439
GO:0034199	activation of protein kinase A activity	3	9	0.0439
GO:0035150	regulation of tube size	12	138	0.0439
GO:0043414	macromolecule methylation	17	229	0.0439
GO:0046660	female sex differentiation	10	104	0.0439
GO:0046855	inositol phosphate dephosphorylation	3	9	0.0439
GO:0060080	inhibitory postsynaptic potential	3	9	0.0439
GO:0060601	lateral sprouting from an epithelium	3	9	0.0439
GO:0061072	iris morphogenesis	3	9	0.0439
GO:0061303	cornea development in camera-type eye	3	9	0.0439
GO:1901028	regulation of mitochondrial outer membrane permeabilization involved in apoptotic signaling pathway	6	43	0.0439
GO:1902041	regulation of extrinsic apoptotic signaling pathway via death domain receptors	7	57	0.0439
GO:1904861	excitatory synapse assembly	3	9	0.0439
GO:0006637	acyl-CoA metabolic process	9	88	0.0445
GO:0050792	regulation of viral process	14	174	0.0446
GO:0071219	cellular response to molecule of bacterial origin	13	156	0.0446
GO:0010881	regulation of cardiac muscle contraction by regulation of the release of sequestered calcium ion	4	19	0.0459
GO:0030220	platelet formation	4	19	0.0459
GO:0042534	regulation of tumor necrosis factor biosynthetic process	4	19	0.0459
GO:0043951	negative regulation of cAMP-mediated signaling	4	19	0.0459
GO:0055022	negative regulation of cardiac muscle tissue growth	4	19	0.0459
GO:0030048	actin filament-based movement	10	105	0.046
GO:0009887	animal organ morphogenesis	47	865	0.047
GO:0070925	organelle assembly	38	666	0.047
GO:1901362	organic cyclic compound biosynthetic process	146	3230	0.047
GO:1903749	positive regulation of establishment of protein localization to mitochondrion	5	31	0.0474
GO:0006352	DNA-templated transcription, initiation	16	213	0.0477
GO:0014706	striated muscle tissue development	19	271	0.0484
GO:0043270	positive regulation of ion transport	18	252	0.0491
GO:0046394	carboxylic acid biosynthetic process	21	311	0.0491
GO:0017156	calcium ion regulated exocytosis	8	74	0.0492
GO:1901137	carbohydrate derivative biosynthetic process	36	625	0.0492
GO:0061097	regulation of protein tyrosine kinase activity	9	90	0.0496
GO:0051865	protein autoubiquitination	7	59	0.0497
GO:1901264	carbohydrate derivative transport	7	59	0.0497

Table 2.3.3.3

#term ID	term description	observed gene count	background gene count	false discovery rate
GO:0007274	neuromuscular synaptic transmission	13	28	8.70E-16
GO:0007271	synaptic transmission, cholinergic	13	31	1.26E-15
GO:0035094	response to nicotine	13	49	1.22E-13
GO:0060079	excitatory postsynaptic potential	13	76	1.33E-11
GO:0009636	response to toxic substance	22	468	3.69E-10
GO:0042493	response to drug	27	900	1.59E-08
GO:0035329	hippo signaling	8	27	1.61E-08
GO:1905114	cell surface receptor signaling pathway involved in cell-cell signaling	18	383	3.63E-08
GO:0035095	behavioral response to nicotine	6	8	4.82E-08
GO:0046777	protein autophosphorylation	13	198	2.92E-07
GO:0019367	fatty acid elongation, saturated fatty acid	5	7	1.72E-06
GO:0034625	fatty acid elongation, monounsaturated fatty acid	5	7	1.72E-06
GO:0034626	fatty acid elongation, polyunsaturated fatty acid	5	7	1.72E-06
GO:0042391	regulation of membrane potential	16	408	2.86E-06
GO:0038083	peptidyl-tyrosine autophosphorylation	7	48	9.44E-06
GO:0045859	regulation of protein kinase activity	21	788	9.44E-06
GO:0042761	very long-chain fatty acid biosynthetic process	5	13	1.11E-05
GO:0007268	chemical synaptic transmission	15	402	1.19E-05
GO:0006812	cation transport	21	866	2.97E-05
GO:0098655	cation transmembrane transport	19	720	3.25E-05
GO:0000185	activation of MAPKKK activity	5	19	3.88E-05
GO:0007165	signal transduction	57	4738	5.29E-05
GO:0032147	activation of protein kinase activity	13	347	6.05E-05
GO:1901564	organonitrogen compound metabolic process	61	5284	6.22E-05
GO:0006928	movement of cell or subcellular component	26	1355	6.60E-05
GO:0018193	peptidyl-amino acid modification	20	842	6.60E-05
GO:0003014	renal system process	8	107	6.71E-05
GO:0033674	positive regulation of kinase activity	16	553	7.27E-05
GO:0051347	positive regulation of transferase activity	17	630	8.03E-05
GO:0007166	cell surface receptor signaling pathway	34	2198	0.00012
GO:0045860	positive regulation of protein kinase activity	15	517	0.00014
GO:0042327	positive regulation of phosphorylation	21	984	0.00015
GO:0006468	protein phosphorylation	20	923	0.0002
GO:0001932	regulation of protein phosphorylation	25	1370	0.00021
GO:0030534	adult behavior	8	137	0.0003
GO:0060084	synaptic transmission involved in micturition	3	3	0.00031
GO:0060562	epithelial tube morphogenesis	11	298	0.00034
GO:0007154	cell communication	58	5219	0.00035
GO:0001841	neural tube formation	7	101	0.00036

GO:0035690	cellular response to drug	11	310	0.00043
GO:0006796	phosphate-containing compound metabolic process	31	2065	0.0005
GO:0021915	neural tube development	8	154	0.00054
GO:0035338	long-chain fatty-acyl-CoA biosynthetic process	4	18	0.00054
GO:0038096	Fc-gamma receptor signaling pathway involved in phagocytosis	6	73	0.00059
GO:0042542	response to hydrogen peroxide	7	112	0.00059
GO:0001934	positive regulation of protein phosphorylation	19	941	0.00066
GO:0051716	cellular response to stimulus	64	6212	0.0008
GO:0035295	tube development	17	793	0.00086
GO:0031401	positive regulation of protein modification process	21	1149	0.0009
GO:0031399	regulation of protein modification process	27	1747	0.001
GO:0002429	immune response-activating cell surface receptor signaling pathway	9	234	0.0011
GO:0007169	transmembrane receptor protein tyrosine kinase signaling pathway	13	499	0.0011
GO:0007267	cell-cell signaling	20	1073	0.0011
GO:0019220	regulation of phosphate metabolic process	26	1657	0.0011
GO:1901701	cellular response to oxygen-containing compound	18	896	0.0011
GO:0032870	cellular response to hormone stimulus	14	585	0.0013
GO:0046677	response to antibiotic	10	305	0.0014
GO:0034199	activation of protein kinase A activity	3	9	0.0018
GO:0016310	phosphorylation	21	1236	0.002
GO:0035239	tube morphogenesis	14	615	0.002
GO:0045736	negative regulation of cyclin-dependent protein serine/threonine kinase activity	4	30	0.0021
GO:0002223	stimulatory C-type lectin receptor signaling pathway	5	62	0.0023
GO:0002757	immune response-activating signal transduction	10	332	0.0025
GO:0006633	fatty acid biosynthetic process	6	104	0.0025
GO:0016477	cell migration	16	812	0.0029
GO:0007018	microtubule-based movement	9	276	0.003
GO:0071900	regulation of protein serine/threonine kinase activity	12	488	0.003
GO:0048870	cell motility	17	914	0.0032
GO:0032270	positive regulation of cellular protein metabolic process	23	1496	0.0033
GO:0034380	high-density lipoprotein particle assembly	3	13	0.0037
GO:0036109	alpha-linolenic acid metabolic process	3	13	0.0037
GO:0051726	regulation of cell cycle	19	1129	0.0043
GO:1901700	response to oxygen-containing compound	22	1427	0.0043
GO:0009725	response to hormone	16	854	0.0044
GO:0055085	transmembrane transport	20	1235	0.0045
GO:0001655	urogenital system development	9	299	0.0047
GO:0048729	tissue morphogenesis	12	522	0.0048

GO:0060429	epithelium development	18	1055	0.005
GO:0006914	autophagy	8	240	0.0053
GO:0007167	enzyme linked receptor protein signaling pathway	14	698	0.0053
GO:0097010	eukaryotic translation initiation factor 4F complex assembly	2	2	0.0055
GO:0046394	carboxylic acid biosynthetic process	9	311	0.0057
GO:1901570	fatty acid derivative biosynthetic process	5	82	0.0058
GO:0043651	linoleic acid metabolic process	3	17	0.006
GO:1901888	regulation of cell junction assembly	5	83	0.006
GO:1902043	positive regulation of extrinsic apoptotic signaling pathway via death domain receptors	3	17	0.006
GO:2001023	regulation of response to drug	5	83	0.006
GO:0001822	kidney development	8	251	0.0062
GO:0018205	peptidyl-lysine modification	8	250	0.0062
GO:0051179	localization	53	5233	0.0062
GO:0000079	regulation of cyclin-dependent protein serine/threonine kinase activity	5	86	0.0064
GO:0001843	neural tube closure	5	86	0.0064
GO:0019538	protein metabolic process	45	4197	0.0064
GO:0030148	sphingolipid biosynthetic process	5	86	0.0064
GO:0001523	retinoid metabolic process	5	87	0.0066
GO:0003008	system process	25	1827	0.0069
GO:0031098	stress-activated protein kinase signaling cascade	6	138	0.0069
GO:0046620	regulation of organ growth	5	88	0.0069
GO:0044267	cellular protein metabolic process	40	3603	0.0074
GO:0001823	mesonephros development	5	91	0.0076
GO:0048630	skeletal muscle tissue growth	2	3	0.0076
GO:0072137	condensed mesenchymal cell proliferation	2	3	0.0076
GO:0072330	monocarboxylic acid biosynthetic process	7	200	0.0076
GO:0010942	positive regulation of cell death	13	663	0.0085
GO:0036120	cellular response to platelet-derived growth factor stimulus	3	22	0.0096
GO:0048813	dendrite morphogenesis	4	54	0.0096
GO:0095500	acetylcholine receptor signaling pathway	3	22	0.0096
GO:0050778	positive regulation of immune response	12	589	0.0097
GO:0060800	regulation of cell differentiation involved in embryonic placenta development	2	4	0.0102
GO:0071557	histone H3-K27 demethylation	2	4	0.0102
GO:1903121	regulation of TRAIL-activated apoptotic signaling pathway	2	4	0.0102
GO:1903553	positive regulation of extracellular exosome assembly	2	4	0.0102
GO:1902041	regulation of extrinsic apoptotic signaling pathway via death domain receptors	4	57	0.0106
GO:0060828	regulation of canonical Wnt signaling pathway	7	218	0.0109

GO:0002376	immune system process	29	2370	0.0111
GO:0032268	regulation of cellular protein metabolic process	30	2486	0.0111
GO:0043065	positive regulation of apoptotic process	12	604	0.0111
GO:2001236	regulation of extrinsic apoptotic signaling pathway	6	158	0.0111
GO:0046621	negative regulation of organ growth	3	26	0.013
GO:0048584	positive regulation of response to stimulus	26	2054	0.013
GO:0050900	leukocyte migration	8	296	0.013
GO:0071377	cellular response to glucagon stimulus	3	26	0.013
GO:0006027	glycosaminoglycan catabolic process	4	62	0.0133
GO:0080134	regulation of response to stress	19	1299	0.0136
GO:0002758	innate immune response-activating signal transduction	6	168	0.0143
GO:0009888	tissue development	22	1626	0.0143
GO:0042221	response to chemical	43	4153	0.0143
GO:0044237	cellular metabolic process	76	8797	0.0144
GO:0051899	membrane depolarization	4	64	0.0144
GO:0071495	cellular response to endogenous stimulus	17	1106	0.0146
GO:0003009	skeletal muscle contraction	3	28	0.0148
GO:0014059	regulation of dopamine secretion	3	28	0.0148
GO:0045926	negative regulation of growth	7	235	0.0148
GO:0018105	peptidyl-serine phosphorylation	6	173	0.0157
GO:0060215	primitive hemopoiesis	2	6	0.0157
GO:1901621	negative regulation of smoothened signaling pathway involved in dorsal/ventral neural tube patterning	2	6	0.0157
GO:0009653	anatomical structure morphogenesis	25	1992	0.0168
GO:0006936	muscle contraction	7	244	0.0175
GO:0001731	formation of translation preinitiation complex	2	7	0.0193
GO:0009987	cellular process	111	14652	0.0193
GO:0035873	lactate transmembrane transport	2	7	0.0193
GO:0043983	histone H4-K12 acetylation	2	7	0.0193
GO:0044255	cellular lipid metabolic process	15	946	0.0196
GO:0090090	negative regulation of canonical Wnt signaling pathway	5	123	0.0196
GO:0007626	locomotory behavior	6	184	0.0198
GO:0006636	unsaturated fatty acid biosynthetic process	3	34	0.0221
GO:0048008	platelet-derived growth factor receptor signaling pathway	3	34	0.0221
GO:0072073	kidney epithelium development	5	128	0.0222
GO:0006807	nitrogen compound metabolic process	72	8352	0.0226
GO:0008152	metabolic process	80	9569	0.0229
GO:0043085	positive regulation of catalytic activity	19	1381	0.0229
GO:0003091	renal water homeostasis	3	35	0.0231
GO:0048814	regulation of dendrite morphogenesis	4	77	0.0232

GO:0042981	regulation of apoptotic process	20	1501	0.0245
GO:0071902	positive regulation of protein serine/threonine kinase activity	8	340	0.0245
GO:0048013	ephrin receptor signaling pathway	4	79	0.025
GO:0032501	multicellular organismal process	59	6507	0.0256
GO:0023014	signal transduction by protein phosphorylation	8	349	0.0278
GO:0051952	regulation of amine transport	4	82	0.0278
GO:0010941	regulation of cell death	21	1638	0.0287
GO:0035556	intracellular signal transduction	20	1528	0.0288
GO:0080135	regulation of cellular response to stress	11	618	0.0315
GO:0001657	ureteric bud development	4	86	0.0319
GO:0000902	cell morphogenesis	11	626	0.034
GO:0003157	endocardium development	2	11	0.034
GO:0031349	positive regulation of defense response	8	365	0.034
GO:0097284	hepatocyte apoptotic process	2	11	0.034
GO:0048583	regulation of response to stimulus	39	3882	0.0351
GO:0007610	behavior	10	541	0.0354
GO:0033559	unsaturated fatty acid metabolic process	4	90	0.0354
GO:0021700	developmental maturation	6	216	0.0355
GO:0006464	cellular protein modification process	32	2999	0.0361
GO:0048598	embryonic morphogenesis	10	545	0.0363
GO:0006979	response to oxidative stress	8	373	0.0364
GO:0009719	response to endogenous stimulus	18	1353	0.0364
GO:0043931	ossification involved in bone maturation	2	12	0.0364
GO:0043966	histone H3 acetylation	3	44	0.0364
GO:0051188	cofactor biosynthetic process	6	218	0.0364
GO:0043009	chordate embryonic development	10	550	0.0377
GO:0009893	positive regulation of metabolic process	34	3280	0.0397
GO:0050896	response to stimulus	67	7824	0.0397
GO:0042127	regulation of cell population proliferation	20	1594	0.04
GO:0051186	cofactor metabolic process	9	467	0.04
GO:0016573	histone acetylation	4	96	0.0405
GO:0007156	homophilic cell adhesion via plasma membrane adhesion molecules	5	158	0.0419
GO:1901565	organonitrogen compound catabolic process	14	958	0.0438
GO:0030030	cell projection organization	15	1067	0.0448
GO:0031325	positive regulation of cellular metabolic process	32	3060	0.0448
GO:0032787	monocarboxylic acid metabolic process	9	477	0.0448
GO:0040008	regulation of growth	11	663	0.0448
GO:0043967	histone H4 acetylation	3	49	0.0448
GO:0051348	negative regulation of transferase activity	7	310	0.0448
GO:1901699	cellular response to nitrogen compound	10	568	0.0448
GO:1903543	positive regulation of exosomal secretion	2	14	0.0448

GO:0006024	glycosaminoglycan biosynthetic process	4	101	0.0456
GO:0043412	macromolecule modification	33	3197	0.0456
GO:0008285	negative regulation of cell population proliferation	11	669	0.0461
GO:0050821	protein stabilization	5	166	0.048
GO:0043968	histone H2A acetylation	2	15	0.0481
GO:0043981	histone H4-K5 acetylation	2	15	0.0481
GO:0043982	histone H4-K8 acetylation	2	15	0.0481
GO:0051895	negative regulation of focal adhesion assembly	2	15	0.0481
GO:0009108	coenzyme biosynthetic process	5	167	0.0482
GO:0001508	action potential	4	104	0.0484
GO:0001676	long-chain fatty acid metabolic process	4	104	0.0484
GO:0006749	glutathione metabolic process	3	52	0.0484
GO:0007586	digestion	4	104	0.0484
GO:0031295	T cell costimulation	3	52	0.0484
GO:0030048	actin filament-based movement	4	105	0.049
GO:0001763	morphogenesis of a branching structure	5	169	0.0492
GO:0002684	positive regulation of immune system process	13	882	0.0498
GO:0048608	reproductive structure development	8	405	0.0498

Table 2.3.3.4

#term ID	term description	observed gene count	background gene count	false discovery rate
GO:0051179	localization	44	5233	3.68E-08
GO:0051234	establishment of localization	39	4248	6.83E-08
GO:0006810	transport	37	4130	4.81E-07
GO:0007169	transmembrane receptor protein tyrosine kinase signaling pathway	14	499	7.33E-07
GO:0051261	protein depolymerization	6	29	7.80E-07
GO:0038128	ERBB2 signaling pathway	6	31	9.26E-07
GO:0046488	phosphatidylinositol metabolic process	10	211	1.05E-06
GO:0046854	phosphatidylinositol phosphorylation	8	103	1.05E-06
GO:0048522	positive regulation of cellular process	39	4898	1.24E-06
GO:0038127	ERBB signaling pathway	7	72	1.81E-06
GO:0007259	receptor signaling pathway via JAK-STAT	6	41	2.08E-06
GO:0031328	positive regulation of cellular biosynthetic process	23	1846	2.80E-06
GO:0018108	peptidyl-tyrosine phosphorylation	9	195	3.72E-06
GO:0033036	macromolecule localization	25	2268	4.62E-06

GO:0035556	intracellular signal transduction	20	1528	1.04E-05
GO:0016310	phosphorylation	18	1236	1.09E-05
GO:0045935	positive regulation of nucleobase-containing compound metabolic process	21	1770	2.02E-05
GO:0019221	cytokine-mediated signaling pathway	13	655	2.36E-05
GO:0035723	interleukin-15-mediated signaling pathway	4	13	2.36E-05
GO:0044403	symbiont process	13	650	2.36E-05
GO:0002376	immune system process	24	2370	2.84E-05
GO:0006468	protein phosphorylation	15	923	2.84E-05
GO:0006928	movement of cell or subcellular component	18	1355	2.84E-05
GO:0007166	cell surface receptor signaling pathway	23	2198	2.85E-05
GO:0006890	retrograde vesicle-mediated transport, Golgi to endoplasmic reticulum	6	81	3.11E-05
GO:0016032	viral process	12	571	3.11E-05
GO:0016477	cell migration	14	812	3.11E-05
GO:0060396	growth hormone receptor signaling pathway	4	17	4.03E-05
GO:1901653	cellular response to peptide	9	289	4.03E-05
GO:1903288	positive regulation of potassium ion import across plasma membrane	3	3	4.19E-05
GO:0010557	positive regulation of macromolecule biosynthetic process	20	1758	4.72E-05
GO:0090150	establishment of protein localization to membrane	8	217	4.72E-05
GO:0006614	SRP-dependent cotranslational protein targeting to membrane	6	92	4.81E-05
GO:0038083	peptidyl-tyrosine autophosphorylation	5	48	4.81E-05
GO:0072594	establishment of protein localization to organelle	10	396	4.81E-05
GO:0045184	establishment of protein localization	18	1467	5.65E-05
GO:0030043	actin filament fragmentation	3	4	5.71E-05
GO:0051897	positive regulation of protein kinase B signaling	7	157	5.71E-05
GO:1903278	positive regulation of sodium ion export across plasma membrane	3	4	5.71E-05
GO:0044238	primary metabolic process	49	8811	5.85E-05
GO:0010628	positive regulation of gene expression	20	1826	6.13E-05
GO:0044267	cellular protein metabolic process	29	3603	6.54E-05
GO:0006629	lipid metabolic process	16	1192	6.63E-05
GO:0033365	protein localization to organelle	12	649	6.65E-05
GO:0050821	protein stabilization	7	166	6.72E-05
GO:0051704	multi-organism process	22	2222	7.06E-05
GO:0071375	cellular response to peptide hormone stimulus	8	245	7.06E-05
GO:0010033	response to organic substance	25	2815	7.50E-05
GO:0044249	cellular biosynthetic process	33	4567	7.52E-05
GO:0016071	mRNA metabolic process	12	667	7.55E-05
GO:0006796	phosphate-containing compound metabolic process	21	2065	7.99E-05
GO:0031325	positive regulation of cellular metabolic process	26	3060	9.21E-05

GO:0070816	phosphorylation of RNA polymerase II C-terminal domain	3	6	9.21E-05
GO:0071345	cellular response to cytokine stimulus	14	953	9.47E-05
GO:1901699	cellular response to nitrogen compound	11	568	9.71E-05
GO:0045944	positive regulation of transcription by RNA polymerase II	15	1104	9.93E-05
GO:0010467	gene expression	29	3733	0.0001
GO:1901576	organic substance biosynthetic process	33	4656	0.0001
GO:0006412	translation	9	362	0.00011
GO:0019915	lipid storage	4	28	0.00011
GO:0045893	positive regulation of transcription, DNA-templated	17	1435	0.00011
GO:0051254	positive regulation of RNA metabolic process	18	1596	0.00011
GO:0008104	protein localization	20	1966	0.00012
GO:0044237	cellular metabolic process	48	8797	0.00012
GO:1901698	response to nitrogen compound	14	988	0.00012
GO:0019216	regulation of lipid metabolic process	9	373	0.00013
GO:0040011	locomotion	15	1144	0.00013
GO:0071704	organic substance metabolic process	49	9135	0.00013
GO:0038114	interleukin-21-mediated signaling pathway	3	8	0.00014
GO:0046777	protein autophosphorylation	7	198	0.00014
GO:0071417	cellular response to organonitrogen compound	10	485	0.00014
GO:1903829	positive regulation of cellular protein localization	8	287	0.00014
GO:0010243	response to organonitrogen compound	13	876	0.00015
GO:0014065	phosphatidylinositol 3-kinase signaling	4	33	0.00015
GO:1903725	regulation of phospholipid metabolic process	5	75	0.00015
GO:0006661	phosphatidylinositol biosynthetic process	6	136	0.00016
GO:0016070	RNA metabolic process	27	3430	0.00016
GO:0030007	cellular potassium ion homeostasis	3	9	0.00016
GO:0036376	sodium ion export across plasma membrane	3	9	0.00016
GO:0071310	cellular response to organic substance	21	2219	0.00016
GO:1901701	cellular response to oxygen-containing compound	13	896	0.00017
GO:0072657	protein localization to membrane	9	405	0.00019
GO:1904851	positive regulation of establishment of protein localization to telomere	3	10	0.00019
GO:0015031	protein transport	16	1391	0.00023
GO:0019538	protein metabolic process	30	4197	0.00023
GO:0006458	'de novo' protein folding	4	39	0.00024
GO:0070757	interleukin-35-mediated signaling pathway	3	11	0.00024
GO:0071364	cellular response to epidermal growth factor stimulus	4	40	0.00026
GO:0044255	cellular lipid metabolic process	13	946	0.00027
GO:0008283	cell population proliferation	11	676	0.00029
GO:1901700	response to oxygen-containing compound	16	1427	0.00029
GO:0006883	cellular sodium ion homeostasis	3	13	0.00034

GO:0007019	microtubule depolymerization	3	13	0.00034
GO:0010248	establishment or maintenance of transmembrane electrochemical gradient	3	13	0.00034
GO:0030836	positive regulation of actin filament depolymerization	3	13	0.00034
GO:0060397	growth hormone receptor signaling pathway via JAK-STAT	3	13	0.00034
GO:0043551	regulation of phosphatidylinositol 3-kinase activity	4	46	0.00039
GO:0048878	chemical homeostasis	13	995	0.00041
GO:2000377	regulation of reactive oxygen species metabolic process	6	169	0.00042
GO:0032870	cellular response to hormone stimulus	10	585	0.00043
GO:0033043	regulation of organelle organization	14	1155	0.00043
GO:1903827	regulation of cellular protein localization	9	465	0.00044
GO:0044260	cellular macromolecule metabolic process	38	6413	0.00047
GO:0036092	phosphatidylinositol-3-phosphate biosynthetic process	4	51	0.00052
GO:0043603	cellular amide metabolic process	11	736	0.00053
GO:0007173	epidermal growth factor receptor signaling pathway	4	52	0.00055
GO:0016192	vesicle-mediated transport	17	1699	0.00055
GO:0034645	cellular macromolecule biosynthetic process	26	3518	0.00055
GO:0044271	cellular nitrogen compound biosynthetic process	26	3528	0.00058
GO:0034613	cellular protein localization	15	1367	0.0006
GO:0006909	phagocytosis	6	185	0.00062
GO:0019222	regulation of metabolic process	38	6516	0.00063
GO:0065008	regulation of biological quality	26	3559	0.00064
GO:0086009	membrane repolarization	3	19	0.00072
GO:0034764	positive regulation of transmembrane transport	6	194	0.00075
GO:0051173	positive regulation of nitrogen compound metabolic process	23	2946	0.00076
GO:0000184	nuclear-transcribed mRNA catabolic process, nonsense-mediated decay	5	118	0.00077
GO:0002252	immune effector process	12	927	0.00079
GO:2000737	negative regulation of stem cell differentiation	3	20	0.00079
GO:0006427	histidyl-tRNA aminoacylation	2	2	0.00086
GO:0043170	macromolecule metabolic process	41	7453	0.00087
GO:0050900	leukocyte migration	7	296	0.00089
GO:0002478	antigen processing and presentation of exogenous peptide antigen	5	123	0.0009
GO:0051641	cellular localization	19	2180	0.00095
GO:0061077	chaperone-mediated protein folding	4	63	0.00095
GO:0071495	cellular response to endogenous stimulus	13	1106	0.00095
GO:0099131	ATP hydrolysis coupled ion transmembrane transport	4	63	0.00095
GO:0010884	positive regulation of lipid storage	3	22	0.00097
GO:0038095	Fc-epsilon receptor signaling pathway	4	64	0.00097

GO:1901018	positive regulation of potassium ion transmembrane transporter activity	3	22	0.00097
GO:0099132	ATP hydrolysis coupled cation transmembrane transport	4	66	0.0011
GO:0006605	protein targeting	7	318	0.0012
GO:0010638	positive regulation of organelle organization	9	552	0.0012
GO:0071702	organic substance transport	18	2040	0.0012
GO:0008037	cell recognition	5	138	0.0013
GO:0010604	positive regulation of macromolecule metabolic process	23	3081	0.0013
GO:0042592	homeostatic process	15	1491	0.0013
GO:0050790	regulation of catalytic activity	19	2249	0.0013
GO:0065007	biological regulation	54	11740	0.0014
GO:0065009	regulation of molecular function	24	3322	0.0014
GO:0006413	translational initiation	5	142	0.0015
GO:0050789	regulation of biological process	52	11116	0.0017
GO:0110053	regulation of actin filament organization	6	235	0.0017
GO:1990573	potassium ion import across plasma membrane	3	28	0.0017
GO:0032879	regulation of localization	20	2524	0.0018
GO:0045648	positive regulation of erythrocyte differentiation	3	29	0.0018
GO:0046449	creatinine metabolic process	2	4	0.0018
GO:0038111	interleukin-7-mediated signaling pathway	3	30	0.0019
GO:0032869	cellular response to insulin stimulus	5	153	0.002
GO:0008286	insulin receptor signaling pathway	4	82	0.0021
GO:1900078	positive regulation of cellular response to insulin stimulus	3	31	0.0021
GO:0098657	import into cell	9	609	0.0022
GO:0000255	allantoin metabolic process	2	5	0.0023
GO:0006549	isoleucine metabolic process	2	5	0.0023
GO:0008064	regulation of actin polymerization or depolymerization	5	160	0.0023
GO:2001252	positive regulation of chromosome organization	5	160	0.0023
GO:0007339	binding of sperm to zona pellucida	3	34	0.0025
GO:0009987	cellular process	61	14652	0.0025
GO:0032212	positive regulation of telomere maintenance via telomerase	3	34	0.0025
GO:0006950	response to stress	23	3267	0.0027
GO:0070508	cholesterol import	2	6	0.0029
GO:0071805	potassium ion transmembrane transport	5	169	0.0029
GO:0097435	supramolecular fiber organization	7	383	0.0031
GO:1901998	toxin transport	3	37	0.0031
GO:0019220	regulation of phosphate metabolic process	15	1657	0.0033
GO:0019886	antigen processing and presentation of exogenous peptide antigen via MHC class II	4	96	0.0033
GO:0010886	positive regulation of cholesterol storage	2	7	0.0036

GO:0019530	taurine metabolic process	2	7	0.0036
GO:1904951	positive regulation of establishment of protein localization	7	397	0.0036
GO:0010468	regulation of gene expression	28	4533	0.0037
GO:0030260	entry into host cell	4	100	0.0037
GO:0060255	regulation of macromolecule metabolic process	34	6072	0.0037
GO:1901564	organonitrogen compound metabolic process	31	5284	0.0037
GO:0006139	nucleobase-containing compound metabolic process	28	4551	0.0039
GO:0006807	nitrogen compound metabolic process	42	8352	0.0042
GO:0006886	intracellular protein transport	10	836	0.0042
GO:0044093	positive regulation of molecular function	15	1713	0.0042
GO:0045596	negative regulation of cell differentiation	9	683	0.0042
GO:0046326	positive regulation of glucose import	3	43	0.0042
GO:0051128	regulation of cellular component organization	18	2306	0.0042
GO:0007595	lactation	3	44	0.0044
GO:0009611	response to wounding	8	547	0.0044
GO:0018193	peptidyl-amino acid modification	10	842	0.0044
GO:1901185	negative regulation of ERBB signaling pathway	3	44	0.0044
GO:0019637	organophosphate metabolic process	11	1011	0.0045
GO:0006573	valine metabolic process	2	9	0.0048
GO:0034641	cellular nitrogen compound metabolic process	30	5130	0.0048
GO:0038155	interleukin-23-mediated signaling pathway	2	9	0.0048
GO:0035722	interleukin-12-mediated signaling pathway	3	47	0.0051
GO:0043085	positive regulation of catalytic activity	13	1381	0.0051
GO:0050776	regulation of immune response	10	873	0.0054
GO:0002295	T-helper cell lineage commitment	2	10	0.0056
GO:0002684	positive regulation of immune system process	10	882	0.0057
GO:0051054	positive regulation of DNA metabolic process	5	209	0.0058
GO:0042127	regulation of cell population proliferation	14	1594	0.0059
GO:1901360	organic cyclic compound metabolic process	29	4963	0.0061
GO:0000165	MAPK cascade	6	323	0.0062
GO:0031295	T cell costimulation	3	52	0.0062
GO:0006105	succinate metabolic process	2	11	0.0063
GO:0006107	oxaloacetate metabolic process	2	11	0.0063
GO:0006357	regulation of transcription by RNA polymerase II	19	2633	0.0063
GO:0006457	protein folding	5	214	0.0063
GO:0006600	creatine metabolic process	2	11	0.0063
GO:0030879	mammary gland development	4	123	0.0063
GO:0032781	positive regulation of ATPase activity	3	53	0.0063
GO:0038110	interleukin-2-mediated signaling pathway	2	11	0.0063
GO:0050778	positive regulation of immune response	8	589	0.0063
GO:0051170	import into nucleus	4	122	0.0063

GO:0051345	positive regulation of hydrolase activity	9	742	0.0063
GO:0051649	establishment of localization in cell	14	1616	0.0063
GO:0070106	interleukin-27-mediated signaling pathway	2	11	0.0063
GO:2001223	negative regulation of neuron migration	2	11	0.0063
GO:0002757	immune response-activating signal transduction	6	332	0.0066
GO:0032355	response to estradiol	4	126	0.0067
GO:0042060	wound healing	7	461	0.0067
GO:0010867	positive regulation of triglyceride biosynthetic process	2	12	0.0068
GO:0030098	lymphocyte differentiation	5	226	0.0073
GO:0030217	T cell differentiation	4	131	0.0075
GO:0042325	regulation of phosphorylation	13	1465	0.0076
GO:0002286	T cell activation involved in immune response	3	61	0.0086
GO:0070102	interleukin-6-mediated signaling pathway	2	14	0.0086
GO:0086064	cell communication by electrical coupling involved in cardiac conduction	2	14	0.0086
GO:0050730	regulation of peptidyl-tyrosine phosphorylation	5	237	0.0087
GO:0051130	positive regulation of cellular component organization	11	1128	0.0088
GO:0034660	ncRNA metabolic process	7	497	0.0096
GO:0019725	cellular homeostasis	9	806	0.01
GO:0042306	regulation of protein import into nucleus	3	65	0.01
GO:2000145	regulation of cell motility	9	807	0.01
GO:0006464	cellular protein modification process	20	2999	0.0103
GO:0046931	pore complex assembly	2	16	0.0103
GO:0045785	positive regulation of cell adhesion	6	375	0.0109
GO:0060193	positive regulation of lipase activity	3	68	0.0109
GO:0070201	regulation of establishment of protein localization	8	662	0.0109
GO:0040008	regulation of growth	8	663	0.011
GO:0006396	RNA processing	9	825	0.0112
GO:0006910	phagocytosis, recognition	2	17	0.0112
GO:0040014	regulation of multicellular organism growth	3	69	0.0112
GO:0055082	cellular chemical homeostasis	8	665	0.0112
GO:0051240	positive regulation of multicellular organismal process	13	1551	0.0113
GO:0051052	regulation of DNA metabolic process	6	381	0.0114
GO:0006955	immune response	13	1560	0.0118
GO:0010001	glial cell differentiation	4	154	0.0118
GO:0051251	positive regulation of lymphocyte activation	5	260	0.0118
GO:0006103	2-oxoglutarate metabolic process	2	18	0.012
GO:0007265	Ras protein signal transduction	4	155	0.012
GO:0044265	cellular macromolecule catabolic process	9	842	0.0122
GO:0008380	RNA splicing	6	391	0.0125

GO:0038096	Fc-gamma receptor signaling pathway involved in phagocytosis	3	73	0.0125
GO:0001775	cell activation	10	1024	0.0129
GO:0002682	regulation of immune system process	12	1391	0.0129
GO:0031326	regulation of cellular biosynthetic process	25	4266	0.0129
GO:0046907	intracellular transport	12	1390	0.0129
GO:0060571	morphogenesis of an epithelial fold	2	19	0.0129
GO:0006368	transcription elongation from RNA polymerase II promoter	3	75	0.0131
GO:0050793	regulation of developmental process	17	2416	0.0131
GO:0043066	negative regulation of apoptotic process	9	859	0.0134
GO:0051249	regulation of lymphocyte activation	6	401	0.0136
GO:0034504	protein localization to nucleus	4	164	0.0137
GO:1903037	regulation of leukocyte cell-cell adhesion	5	278	0.0145
GO:0022613	ribonucleoprotein complex biogenesis	6	409	0.0147
GO:2000637	positive regulation of gene silencing by miRNA	2	21	0.0147
GO:0042593	glucose homeostasis	4	169	0.015
GO:0055065	metal ion homeostasis	7	555	0.015
GO:0051336	regulation of hydrolase activity	11	1238	0.0152
GO:0000398	mRNA splicing, via spliceosome	5	284	0.0154
GO:0051050	positive regulation of transport	9	892	0.0162
GO:0045321	leukocyte activation	9	894	0.0163
GO:0048584	positive regulation of response to stimulus	15	2054	0.0163
GO:0010876	lipid localization	5	293	0.017
GO:0019219	regulation of nucleobase-containing compound metabolic process	24	4133	0.017
GO:0050679	positive regulation of epithelial cell proliferation	4	178	0.017
GO:0008610	lipid biosynthetic process	7	575	0.0172
GO:0034383	low-density lipoprotein particle clearance	2	24	0.0176
GO:0050731	positive regulation of peptidyl-tyrosine phosphorylation	4	180	0.0176
GO:1902905	positive regulation of supramolecular fiber organization	4	180	0.0176
GO:0015672	monovalent inorganic cation transport	6	437	0.0187
GO:0050863	regulation of T cell activation	5	302	0.0188
GO:0080090	regulation of primary metabolic process	31	5982	0.0191
GO:0060485	mesenchyme development	4	187	0.0196
GO:0006814	sodium ion transport	4	189	0.02
GO:0045595	regulation of cell differentiation	13	1695	0.02
GO:0046718	viral entry into host cell	3	92	0.02
GO:0048519	negative regulation of biological process	27	4953	0.02
GO:0050852	T cell receptor signaling pathway	3	93	0.0204
GO:0050678	regulation of epithelial cell proliferation	5	311	0.0206
GO:2000379	positive regulation of reactive oxygen species metabolic process	3	94	0.0208

GO:0006351	transcription, DNA-templated	17	2569	0.0211
GO:0050870	positive regulation of T cell activation	4	193	0.0211
GO:0006397	mRNA processing	6	456	0.0218
GO:0007165	signal transduction	26	4738	0.0218
GO:0014066	regulation of phosphatidylinositol 3-kinase signaling	3	97	0.0222
GO:0002366	leukocyte activation involved in immune response	7	616	0.0229
GO:0043277	apoptotic cell clearance	2	29	0.023
GO:0050892	intestinal absorption	2	29	0.023
GO:0006366	transcription by RNA polymerase II	8	784	0.0231
GO:0090066	regulation of anatomical structure size	6	464	0.0231
GO:1902533	positive regulation of intracellular signal transduction	9	959	0.0231
GO:0031323	regulation of cellular metabolic process	31	6082	0.0234
GO:0033157	regulation of intracellular protein transport	4	201	0.0234
GO:0051338	regulation of transferase activity	9	964	0.0236
GO:0030155	regulation of cell adhesion	7	623	0.0237
GO:0006606	protein import into nucleus	3	101	0.0239
GO:0031399	regulation of protein modification process	13	1747	0.0239
GO:0043903	regulation of symbiosis, encompassing mutualism through parasitism	4	203	0.0239
GO:0051495	positive regulation of cytoskeleton organization	4	203	0.0239
GO:0033120	positive regulation of RNA splicing	2	31	0.0249
GO:0070670	response to interleukin-4	2	31	0.0249
GO:2000112	regulation of cellular macromolecule biosynthetic process	23	4050	0.0249
GO:0050794	regulation of cellular process	46	10484	0.0254
GO:0006898	receptor-mediated endocytosis	4	209	0.0256
GO:0043933	protein-containing complex subunit organization	13	1770	0.0259
GO:0071840	cellular component organization or biogenesis	28	5342	0.0259
GO:0001932	regulation of protein phosphorylation	11	1370	0.0265
GO:1901361	organic cyclic compound catabolic process	6	484	0.0266
GO:0043029	T cell homeostasis	2	33	0.0272
GO:0090322	regulation of superoxide metabolic process	2	33	0.0272
GO:0097009	energy homeostasis	2	33	0.0272
GO:0023052	signaling	27	5108	0.0274
GO:0001755	neural crest cell migration	2	35	0.0297
GO:0006875	cellular metal ion homeostasis	6	499	0.0299
GO:0048583	regulation of response to stimulus	22	3882	0.0303
GO:0051707	response to other organism	8	835	0.0305
GO:0006101	citrate metabolic process	2	36	0.0309
GO:0071392	cellular response to estradiol stimulus	2	36	0.0309
GO:0043484	regulation of RNA splicing	3	116	0.0318
GO:0006897	endocytosis	6	510	0.0323

GO:1905477	positive regulation of protein localization to membrane	3	117	0.0323
GO:0043549	regulation of kinase activity	8	849	0.0327
GO:0006952	defense response	10	1234	0.0345
GO:0042059	negative regulation of epidermal growth factor receptor signaling pathway	2	39	0.0348
GO:0002429	immune response-activating cell surface receptor signaling pathway	4	234	0.035
GO:0007154	cell communication	27	5219	0.0353
GO:0001936	regulation of endothelial cell proliferation	3	122	0.0356
GO:0043900	regulation of multi-organism process	5	372	0.0358
GO:0030097	hemopoiesis	6	526	0.0362
GO:0016999	antibiotic metabolic process	3	124	0.0366
GO:0090316	positive regulation of intracellular protein transport	3	126	0.0379
GO:0008284	positive regulation of cell population proliferation	8	878	0.0382
GO:0042307	positive regulation of protein import into nucleus	2	42	0.0387
GO:0055025	positive regulation of cardiac muscle tissue development	2	42	0.0387
GO:0051239	regulation of multicellular organismal process	17	2788	0.0396
GO:0048762	mesenchymal cell differentiation	3	130	0.0406
GO:0043408	regulation of MAPK cascade	7	712	0.0409
GO:0045637	regulation of myeloid cell differentiation	4	249	0.0413
GO:0033077	T cell differentiation in thymus	2	44	0.0415
GO:0001819	positive regulation of cytokine production	5	390	0.0416
GO:0045927	positive regulation of growth	4	252	0.0427
GO:0050999	regulation of nitric-oxide synthase activity	2	45	0.043
GO:0009967	positive regulation of signal transduction	11	1493	0.0434
GO:0048732	gland development	5	395	0.0434
GO:0045834	positive regulation of lipid metabolic process	3	135	0.044
GO:0048708	astrocyte differentiation	2	46	0.0443
GO:0050896	response to stimulus	36	7824	0.0461
GO:0009411	response to UV	3	139	0.0472
GO:0051049	regulation of transport	12	1732	0.0486

Table 2.3.3.5

#term ID	term description	observed gene count	background gene count	false discovery rate
hsa00040	Pentose and glucuronate interconversions	22	34	1.13E-10
hsa00140	Steroid hormone biosynthesis	26	58	2.80E-10
hsa00053	Ascorbate and aldarate metabolism	18	27	3.65E-09
hsa00983	Drug metabolism - other enzymes	27	76	3.97E-09
hsa01100	Metabolic pathways	142	1250	2.05E-08
hsa00830	Retinol metabolism	23	62	3.52E-08

hsa05204	Chemical carcinogenesis	25	76	4.34E-08
hsa00860	Porphyrin and chlorophyll metabolism	19	42	5.89E-08
hsa04725	Cholinergic synapse	29	111	1.41E-07
hsa00980	Metabolism of xenobiotics by cytochrome P450	22	70	5.98E-07
hsa00982	Drug metabolism - cytochrome P450	21	66	9.52E-07
hsa04014	Ras signaling pathway	39	228	7.07E-06
hsa04976	Bile secretion	20	71	8.79E-06
hsa05205	Proteoglycans in cancer	35	195	9.07E-06
hsa04080	Neuroactive ligand-receptor interaction	43	272	9.61E-06
hsa04024	cAMP signaling pathway	34	195	2.06E-05
hsa04726	Serotonergic synapse	23	112	0.0001
hsa04724	Glutamatergic synapse	22	112	0.00028
hsa04020	Calcium signaling pathway	29	179	0.00035
hsa04071	Sphingolipid signaling pathway	22	116	0.00037
hsa04916	Melanogenesis	20	98	0.00037
hsa04974	Protein digestion and absorption	19	90	0.00037
hsa05166	HTLV-I infection	36	250	0.00037
hsa05165	Human papillomavirus infection	42	317	0.0004
hsa04728	Dopaminergic synapse	23	128	0.00045
hsa04261	Adrenergic signaling in cardiomyocytes	24	139	0.00053
hsa04010	MAPK signaling pathway	39	293	0.00061
hsa04211	Longevity regulating pathway	18	88	0.00065
hsa04727	GABAergic synapse	18	88	0.00065
hsa05016	Huntington's disease	29	193	0.00075
hsa04218	Cellular senescence	25	156	0.0009
hsa04390	Hippo signaling pathway	24	152	0.0015
hsa04934	Cushing's syndrome	24	153	0.0015
hsa04137	Mitophagy - animal	14	63	0.0016
hsa04913	Ovarian steroidogenesis	12	49	0.002
hsa04918	Thyroid hormone synthesis	15	73	0.002
hsa04392	Hippo signaling pathway - multiple species	9	28	0.0022
hsa04911	Insulin secretion	16	84	0.0024
hsa00561	Glycerolipid metabolism	13	59	0.0026
hsa02010	ABC transporters	11	44	0.0028
hsa04371	Apelin signaling pathway	21	133	0.0028
hsa05224	Breast cancer	22	147	0.0039
hsa05110	Vibrio cholerae infection	11	48	0.0049
hsa04925	Aldosterone synthesis and secretion	16	93	0.0056
hsa00480	Glutathione metabolism	11	50	0.0063
hsa04926	Relaxin signaling pathway	19	130	0.0106
hsa04927	Cortisol synthesis and secretion	12	63	0.0107
hsa04971	Gastric acid secretion	13	72	0.0107

hsa05012	Parkinson's disease	20	142	0.0111
hsa05200	Pathways in cancer	52	515	0.0111
hsa05225	Hepatocellular carcinoma	22	163	0.0111
hsa04713	Circadian entrainment	15	93	0.012
hsa04120	Ubiquitin mediated proteolysis	19	134	0.0125
hsa04114	Oocyte meiosis	17	116	0.015
hsa04723	Retrograde endocannabinoid signaling	20	148	0.0154
hsa04550	Signaling pathways regulating pluripotency of stem cells	19	138	0.0158
hsa04912	GnRH signaling pathway	14	88	0.0169
hsa04360	Axon guidance	22	173	0.0182
hsa00590	Arachidonic acid metabolism	11	61	0.0189
hsa04213	Longevity regulating pathway - multiple species	11	61	0.0189
hsa04721	Synaptic vesicle cycle	11	61	0.0189
hsa04310	Wnt signaling pathway	19	143	0.0203
hsa05032	Morphine addiction	14	91	0.0203
hsa04142	Lysosome	17	123	0.0215
hsa04140	Autophagy - animal	17	125	0.0245
hsa04919	Thyroid hormone signaling pathway	16	115	0.0251
hsa01522	Endocrine resistance	14	95	0.026
hsa04150	mTOR signaling pathway	19	148	0.026
hsa04722	Neurotrophin signaling pathway	16	116	0.026
hsa04022	cGMP-PKG signaling pathway	20	160	0.0264
hsa04964	Proximal tubule bicarbonate reclamation	6	23	0.0281
hsa04979	Cholesterol metabolism	9	48	0.0281
hsa05033	Nicotine addiction	8	40	0.0304
hsa04152	AMPK signaling pathway	16	120	0.032
hsa04977	Vitamin digestion and absorption	6	24	0.032
hsa04915	Estrogen signaling pathway	17	133	0.0358
hsa04966	Collecting duct acid secretion	6	25	0.0366
hsa04072	Phospholipase D signaling pathway	18	145	0.0369
hsa04151	PI3K-Akt signaling pathway	35	348	0.0369
hsa04015	Rap1 signaling pathway	23	203	0.0373
hsa04750	Inflammatory mediator regulation of TRP channels	13	92	0.0386
hsa01230	Biosynthesis of amino acids	11	72	0.0398
hsa05167	Kaposi's sarcoma-associated herpesvirus infection	21	183	0.0427
hsa05217	Basal cell carcinoma	10	63	0.0427
hsa05146	Amoebiasis	13	94	0.0428
hsa05152	Tuberculosis	20	172	0.0428
hsa04720	Long-term potentiation	10	64	0.0447
hsa04970	Salivary secretion	12	86	0.05

Table 2.3.3.6				
#term ID	**term description**	**observed gene count**	**background gene count**	**false discovery rate**
hsa01100	Metabolic pathways	116	1250	6.11E-16
hsa00040	Pentose and glucuronate interconversions	22	34	1.20E-15
hsa00140	Steroid hormone biosynthesis	26	58	1.20E-15
hsa00983	Drug metabolism - other enzymes	27	76	1.66E-14
hsa00053	Ascorbate and aldarate metabolism	18	27	3.23E-13
hsa04725	Cholinergic synapse	29	111	7.26E-13
hsa04080	Neuroactive ligand-receptor interaction	43	272	2.17E-12
hsa05204	Chemical carcinogenesis	24	76	3.26E-12
hsa00830	Retinol metabolism	22	62	4.50E-12
hsa00860	Porphyrin and chlorophyll metabolism	19	42	5.91E-12
hsa04014	Ras signaling pathway	38	228	9.86E-12
hsa05205	Proteoglycans in cancer	35	195	1.19E-11
hsa00980	Metabolism of xenobiotics by cytochrome P450	22	70	2.34E-11
hsa00982	Drug metabolism - cytochrome P450	21	66	5.85E-11
hsa04024	cAMP signaling pathway	33	195	1.80E-10
hsa05165	Human papillomavirus infection	41	317	1.13E-09
hsa05166	HTLV-I infection	36	250	1.13E-09
hsa04020	Calcium signaling pathway	29	179	6.75E-09
hsa05200	Pathways in cancer	52	515	1.01E-08
hsa05016	Huntington's disease	29	193	2.86E-08
hsa04726	Serotonergic synapse	22	112	3.39E-08
hsa04261	Adrenergic signaling in cardiomyocytes	24	139	5.87E-08
hsa04728	Dopaminergic synapse	23	128	6.04E-08
hsa04916	Melanogenesis	20	98	8.90E-08
hsa04218	Cellular senescence	25	156	9.42E-08
hsa04010	MAPK signaling pathway	35	293	1.12E-07
hsa04071	Sphingolipid signaling pathway	21	116	2.13E-07
hsa04934	Cushing's syndrome	24	153	2.40E-07
hsa04211	Longevity regulating pathway	18	88	4.00E-07
hsa04727	GABAergic synapse	18	88	4.00E-07
hsa04724	Glutamatergic synapse	20	112	4.89E-07
hsa04976	Bile secretion	16	71	6.43E-07
hsa04390	Hippo signaling pathway	23	152	7.15E-07
hsa04371	Apelin signaling pathway	21	133	1.34E-06
hsa05224	Breast cancer	22	147	1.52E-06
hsa04151	PI3K-Akt signaling pathway	35	348	3.74E-06
hsa04137	Mitophagy - animal	14	63	4.09E-06
hsa04911	Insulin secretion	16	84	4.09E-06

hsa05225	Hepatocellular carcinoma	22	163	6.61E-06
hsa00561	Glycerolipid metabolism	13	59	1.04E-05
hsa04913	Ovarian steroidogenesis	12	49	1.04E-05
hsa05012	Parkinson's disease	20	142	1.06E-05
hsa04925	Aldosterone synthesis and secretion	16	93	1.15E-05
hsa04926	Relaxin signaling pathway	19	130	1.15E-05
hsa04918	Thyroid hormone synthesis	14	73	1.59E-05
hsa04120	Ubiquitin mediated proteolysis	19	134	1.60E-05
hsa04723	Retrograde endocannabinoid signaling	20	148	1.67E-05
hsa04114	Oocyte meiosis	17	116	3.45E-05
hsa05110	Vibrio cholerae infection	11	48	4.01E-05
hsa04360	Axon guidance	21	173	4.08E-05
hsa04713	Circadian entrainment	15	93	4.09E-05
hsa04015	Rap1 signaling pathway	23	203	4.12E-05
hsa04022	cGMP-PKG signaling pathway	20	160	4.27E-05
hsa00480	Glutathione metabolism	11	50	5.09E-05
hsa04971	Gastric acid secretion	13	72	5.25E-05
hsa04550	Signaling pathways regulating pluripotency of stem cells	18	138	6.74E-05
hsa04927	Cortisol synthesis and secretion	12	63	6.89E-05
hsa04140	Autophagy - animal	17	125	6.90E-05
hsa05167	Kaposi's sarcoma-associated herpesvirus infection	21	183	7.51E-05
hsa04912	GnRH signaling pathway	14	88	7.98E-05
hsa04919	Thyroid hormone signaling pathway	16	115	9.05E-05
hsa04310	Wnt signaling pathway	18	143	9.39E-05
hsa05152	Tuberculosis	20	172	9.39E-05
hsa04722	Neurotrophin signaling pathway	16	116	9.49E-05
hsa04072	Phospholipase D signaling pathway	18	145	0.0001
hsa05032	Morphine addiction	14	91	0.0001
hsa04915	Estrogen signaling pathway	17	133	0.00012
hsa04150	mTOR signaling pathway	18	148	0.00013
hsa04152	AMPK signaling pathway	16	120	0.00013
hsa01522	Endocrine resistance	14	95	0.00015
hsa04213	Longevity regulating pathway - multiple species	11	61	0.0002
hsa04721	Synaptic vesicle cycle	11	61	0.0002
hsa00190	Oxidative phosphorylation	16	131	0.00031
hsa04714	Thermogenesis	22	228	0.00042
hsa05146	Amoebiasis	13	94	0.00046
hsa04979	Cholesterol metabolism	9	48	0.00068
hsa04392	Hippo signaling pathway - multiple species	7	28	0.00077
hsa00590	Arachidonic acid metabolism	10	61	0.00078
hsa05142	Chagas disease (American trypanosomiasis)	13	101	0.00083

hsa05217	Basal cell carcinoma	10	63	0.00095
hsa05226	Gastric cancer	16	147	0.00095
hsa05033	Nicotine addiction	8	40	0.00097
hsa04720	Long-term potentiation	10	64	0.001
hsa04974	Protein digestion and absorption	12	90	0.001
hsa04062	Chemokine signaling pathway	18	181	0.0011
hsa04750	Inflammatory mediator regulation of TRP channels	12	92	0.0012
hsa05120	Epithelial cell signaling in Helicobacter pylori infection	10	66	0.0012
hsa04742	Taste transduction	11	81	0.0015
hsa05211	Renal cell carcinoma	10	68	0.0015
hsa04070	Phosphatidylinositol signaling system	12	97	0.0017
hsa05161	Hepatitis B	15	142	0.0017
hsa05323	Rheumatoid arthritis	11	84	0.0018
hsa01230	Biosynthesis of amino acids	10	72	0.0021
hsa04068	FoxO signaling pathway	14	130	0.0021
hsa04961	Endocrine and other factor-regulated calcium reabsorption	8	47	0.0021
hsa04966	Collecting duct acid secretion	6	25	0.0021
hsa04970	Salivary secretion	11	86	0.0021
hsa05144	Malaria	8	47	0.0021
hsa01200	Carbon metabolism	13	116	0.0022
hsa05414	Dilated cardiomyopathy (DCM)	11	88	0.0024
hsa04960	Aldosterone-regulated sodium reabsorption	7	37	0.0025
hsa04270	Vascular smooth muscle contraction	13	119	0.0026
hsa04260	Cardiac muscle contraction	10	76	0.0028
hsa04975	Fat digestion and absorption	7	39	0.0032
hsa04972	Pancreatic secretion	11	95	0.004
hsa00564	Glycerophospholipid metabolism	11	96	0.0043
hsa05214	Glioma	9	68	0.0045
hsa04350	TGF-beta signaling pathway	10	83	0.0048
hsa04933	AGE-RAGE signaling pathway in diabetic complications	11	98	0.0049
hsa04530	Tight junction	15	167	0.0063
hsa04910	Insulin signaling pathway	13	134	0.0064
hsa05010	Alzheimer's disease	15	168	0.0065
hsa00562	Inositol phosphate metabolism	9	73	0.0067
hsa04340	Hedgehog signaling pathway	7	46	0.0068
hsa01040	Biosynthesis of unsaturated fatty acids	5	23	0.0071
hsa04964	Proximal tubule bicarbonate reclamation	5	23	0.0071
hsa04217	Necroptosis	14	155	0.0078
hsa04514	Cell adhesion molecules (CAMs)	13	139	0.0081
hsa04924	Renin secretion	8	63	0.0091
hsa05034	Alcoholism	13	142	0.0094

hsa00790	Folate biosynthesis	5	26	0.0107
hsa04512	ECM-receptor interaction	9	81	0.0116
hsa05215	Prostate cancer	10	97	0.0118
hsa05203	Viral carcinogenesis	15	183	0.0123
hsa04923	Regulation of lipolysis in adipocytes	7	53	0.0125
hsa05160	Hepatitis C	12	131	0.0125
hsa04216	Ferroptosis	6	40	0.0128
hsa04921	Oxytocin signaling pathway	13	149	0.0128
hsa05140	Leishmaniasis	8	70	0.0149
hsa04520	Adherens junction	8	71	0.016
hsa04540	Gap junction	9	87	0.0164
hsa00020	Citrate cycle (TCA cycle)	5	30	0.0166
hsa00030	Pentose phosphate pathway	5	30	0.0166
hsa00760	Nicotinate and nicotinamide metabolism	5	30	0.0166
hsa04962	Vasopressin-regulated water reabsorption	6	44	0.0181
hsa00052	Galactose metabolism	5	31	0.0182
hsa04110	Cell cycle	11	123	0.0186
hsa04142	Lysosome	11	123	0.0186
hsa04370	VEGF signaling pathway	7	59	0.0188
hsa04930	Type II diabetes mellitus	6	46	0.0211
hsa05220	Chronic myeloid leukemia	8	76	0.0211
hsa04145	Phagosome	12	145	0.0224
hsa04914	Progesterone-mediated oocyte maturation	9	94	0.0233
hsa01521	EGFR tyrosine kinase inhibitor resistance	8	78	0.0236
hsa01212	Fatty acid metabolism	6	48	0.0243
hsa04670	Leukocyte transendothelial migration	10	112	0.0243
hsa04144	Endocytosis	17	242	0.0244
hsa04932	Non-alcoholic fatty liver disease (NAFLD)	12	149	0.0258
hsa05206	MicroRNAs in cancer	12	149	0.0258
hsa04614	Renin-angiotensin system	4	23	0.028
hsa05231	Choline metabolism in cancer	9	98	0.028
hsa05223	Non-small cell lung cancer	7	66	0.029
hsa04922	Glucagon signaling pathway	9	100	0.0307
hsa05210	Colorectal cancer	8	85	0.0341
hsa04510	Focal adhesion	14	197	0.0374
hsa04611	Platelet activation	10	123	0.0393
hsa03015	mRNA surveillance pathway	8	89	0.0417
hsa03320	PPAR signaling pathway	7	72	0.0417
hsa00471	D-Glutamine and D-glutamate metabolism	2	5	0.042
hsa04973	Carbohydrate digestion and absorption	5	42	0.0456
hsa05212	Pancreatic cancer	7	74	0.0459
hsa05213	Endometrial cancer	6	58	0.0468

hsa00310	Lysine degradation	6	59	0.0498

Table 2.3.3.7				
#term ID	**term description**	**observed gene count**	**background gene count**	**false discovery rate**
hsa04392	Hippo signaling pathway - multiple species	10	28	6.44E-12
hsa04080	Neuroactive ligand-receptor interaction	13	272	3.82E-06
hsa04725	Cholinergic synapse	9	111	4.94E-06
hsa00062	Fatty acid elongation	5	25	5.43E-05
hsa05205	Proteoglycans in cancer	8	195	0.0018
hsa04390	Hippo signaling pathway	7	152	0.0022
hsa05020	Prion diseases	4	33	0.0022
hsa04140	Autophagy - animal	6	125	0.0044
hsa04310	Wnt signaling pathway	6	143	0.0075
hsa05012	Parkinson's disease	6	142	0.0075
hsa04010	MAPK signaling pathway	8	293	0.0119
hsa04924	Renin secretion	4	63	0.0127
hsa04611	Platelet activation	5	123	0.0186
hsa04918	Thyroid hormone synthesis	4	73	0.0186
hsa04926	Relaxin signaling pathway	5	130	0.0204
hsa04915	Estrogen signaling pathway	5	133	0.021
hsa05033	Nicotine addiction	3	40	0.0257
hsa04540	Gap junction	4	87	0.0262
hsa04723	Retrograde endocannabinoid signaling	5	148	0.0262
hsa04727	GABAergic synapse	4	88	0.0262
hsa04750	Inflammatory mediator regulation of TRP channels	4	92	0.0262
hsa04912	GnRH signaling pathway	4	88	0.0262
hsa04962	Vasopressin-regulated water reabsorption	3	44	0.0262
hsa01522	Endocrine resistance	4	95	0.0264
hsa04340	Hedgehog signaling pathway	3	46	0.0264
hsa04961	Endocrine and other factor-regulated calcium reabsorption	3	47	0.0264
hsa05110	Vibrio cholerae infection	3	48	0.0264
hsa04913	Ovarian steroidogenesis	3	49	0.0267
hsa05030	Cocaine addiction	3	49	0.0267
hsa04923	Regulation of lipolysis in adipocytes	3	53	0.0307
hsa04062	Chemokine signaling pathway	5	181	0.0384
hsa04919	Thyroid hormone signaling pathway	4	115	0.0384
hsa04213	Longevity regulating pathway - multiple species	3	61	0.0404
hsa04927	Cortisol synthesis and secretion	3	63	0.0427
hsa04720	Long-term potentiation	3	64	0.0432

hsa05031	Amphetamine addiction	3	65	0.0437
hsa01040	Biosynthesis of unsaturated fatty acids	2	23	0.0488

Table 2.3.3.8				
#term ID	**term description**	**observed gene count**	**background gene count**	**false discovery rate**
hsa04012	ErbB signaling pathway	10	83	7.03E-11
hsa04630	Jak-STAT signaling pathway	12	160	7.03E-11
hsa05161	Hepatitis B	11	142	1.70E-10
hsa05223	Non-small cell lung cancer	9	66	1.70E-10
hsa01521	EGFR tyrosine kinase inhibitor resistance	9	78	4.03E-10
hsa04960	Aldosterone-regulated sodium reabsorption	7	37	3.14E-09
hsa04917	Prolactin signaling pathway	8	69	4.08E-09
hsa04973	Carbohydrate digestion and absorption	7	42	5.21E-09
hsa05160	Hepatitis C	9	131	1.66E-08
hsa05205	Proteoglycans in cancer	10	195	2.43E-08
hsa05200	Pathways in cancer	14	515	2.70E-08
hsa05221	Acute myeloid leukemia	7	66	6.18E-08
hsa04919	Thyroid hormone signaling pathway	8	115	9.53E-08
hsa05212	Pancreatic cancer	7	74	1.11E-07
hsa05162	Measles	8	133	2.42E-07
hsa04066	HIF-1 signaling pathway	7	98	5.95E-07
hsa04933	AGE-RAGE signaling pathway in diabetic complications	7	98	5.95E-07
hsa05213	Endometrial cancer	6	58	6.34E-07
hsa04062	Chemokine signaling pathway	8	181	1.85E-06
hsa05220	Chronic myeloid leukemia	6	76	2.54E-06
hsa01522	Endocrine resistance	6	95	8.34E-06
hsa04217	Necroptosis	7	155	8.34E-06
hsa05215	Prostate cancer	6	97	8.54E-06
hsa04964	Proximal tubule bicarbonate reclamation	4	23	1.25E-05
hsa04151	PI3K-Akt signaling pathway	9	348	1.81E-05
hsa05203	Viral carcinogenesis	7	183	2.04E-05
hsa05230	Central carbon metabolism in cancer	5	65	2.16E-05
hsa05214	Glioma	5	68	2.57E-05
hsa04380	Osteoclast differentiation	6	124	2.63E-05
hsa04024	cAMP signaling pathway	7	195	2.65E-05
hsa04976	Bile secretion	5	71	2.83E-05
hsa04971	Gastric acid secretion	5	72	2.92E-05
hsa04068	FoxO signaling pathway	6	130	3.00E-05
hsa04072	Phospholipase D signaling pathway	6	145	5.31E-05
hsa05206	MicroRNAs in cancer	6	149	5.56E-05
hsa05210	Colorectal cancer	5	85	5.56E-05

hsa05224	Breast cancer	6	147	5.56E-05
hsa05226	Gastric cancer	6	147	5.56E-05
hsa04658	Th1 and Th2 cell differentiation	5	88	6.05E-05
hsa04666	Fc gamma R-mediated phagocytosis	5	89	6.22E-05
hsa04925	Aldosterone synthesis and secretion	5	93	7.42E-05
hsa05231	Choline metabolism in cancer	5	98	9.22E-05
hsa04660	T cell receptor signaling pathway	5	99	9.32E-05
hsa04961	Endocrine and other factor-regulated calcium reabsorption	4	47	9.32E-05
hsa04659	Th17 cell differentiation	5	102	0.0001
hsa04931	Insulin resistance	5	107	0.00012
hsa04978	Mineral absorption	4	51	0.00012
hsa04923	Regulation of lipolysis in adipocytes	4	53	0.00013
hsa05167	Kaposi's sarcoma-associated herpesvirus infection	6	183	0.00013
hsa04510	Focal adhesion	6	197	0.00019
hsa05321	Inflammatory bowel disease (IBD)	4	62	0.00022
hsa04810	Regulation of actin cytoskeleton	6	205	0.00023
hsa03010	Ribosome	5	130	0.00027
hsa04664	Fc epsilon RI signaling pathway	4	67	0.00027
hsa04926	Relaxin signaling pathway	5	130	0.00027
hsa04910	Insulin signaling pathway	5	134	0.00028
hsa04915	Estrogen signaling pathway	5	133	0.00028
hsa05165	Human papillomavirus infection	7	317	0.00028
hsa05211	Renal cell carcinoma	4	68	0.00028
hsa01524	Platinum drug resistance	4	70	0.00029
hsa04550	Signaling pathways regulating pluripotency of stem cells	5	138	0.0003
hsa04662	B cell receptor signaling pathway	4	71	0.0003
hsa03320	PPAR signaling pathway	4	72	0.00031
hsa04918	Thyroid hormone synthesis	4	73	0.00031
hsa05218	Melanoma	4	72	0.00031
hsa04260	Cardiac muscle contraction	4	76	0.00036
hsa04150	mTOR signaling pathway	5	148	0.00038
hsa04911	Insulin secretion	4	84	0.0005
hsa04970	Salivary secretion	4	86	0.00054
hsa05225	Hepatocellular carcinoma	5	163	0.00056
hsa04974	Protein digestion and absorption	4	90	0.00062
hsa05164	Influenza A	5	168	0.00062
hsa04360	Axon guidance	5	173	0.0007
hsa04972	Pancreatic secretion	4	95	0.00072
hsa04620	Toll-like receptor signaling pathway	4	102	0.00092
hsa04930	Type II diabetes mellitus	3	46	0.0012
hsa04722	Neurotrophin signaling pathway	4	116	0.0014

hsa04152	AMPK signaling pathway	4	120	0.0016
hsa04650	Natural killer cell mediated cytotoxicity	4	124	0.0018
hsa03040	Spliceosome	4	130	0.0021
hsa04014	Ras signaling pathway	5	228	0.0021
hsa04370	VEGF signaling pathway	3	59	0.0023
hsa04213	Longevity regulating pathway - multiple species	3	61	0.0024
hsa04261	Adrenergic signaling in cardiomyocytes	4	139	0.0025
hsa05166	HTLV-I infection	5	250	0.003
hsa05100	Bacterial invasion of epithelial cells	3	72	0.0037
hsa04022	cGMP-PKG signaling pathway	4	160	0.004
hsa04010	MAPK signaling pathway	5	293	0.0058
hsa04020	Calcium signaling pathway	4	179	0.0058
hsa04211	Longevity regulating pathway	3	88	0.0061
hsa04750	Inflammatory mediator regulation of TRP channels	3	92	0.0069
hsa05222	Small cell lung cancer	3	92	0.0069
hsa04914	Progesterone-mediated oocyte maturation	3	94	0.0071
hsa05146	Amoebiasis	3	94	0.0071
hsa05169	Epstein-Barr virus infection	4	194	0.0072
hsa04070	Phosphatidylinositol signaling system	3	97	0.0075
hsa04015	Rap1 signaling pathway	4	203	0.0083
hsa05142	Chagas disease (American trypanosomiasis)	3	101	0.0083
hsa04668	TNF signaling pathway	3	108	0.0097
hsa04725	Cholinergic synapse	3	111	0.0104
hsa04670	Leukocyte transendothelial migration	3	112	0.0105
hsa04071	Sphingolipid signaling pathway	3	116	0.0114
hsa04975	Fat digestion and absorption	2	39	0.0126
hsa04611	Platelet activation	3	123	0.0131
hsa04140	Autophagy - animal	3	125	0.0136
hsa05219	Bladder cancer	2	41	0.0136
hsa04144	Endocytosis	4	242	0.0137
hsa00970	Aminoacyl-tRNA biosynthesis	2	44	0.015
hsa05418	Fluid shear stress and atherosclerosis	3	133	0.0154
hsa04210	Apoptosis	3	135	0.0159
hsa04979	Cholesterol metabolism	2	48	0.0172
hsa05110	Vibrio cholerae infection	2	48	0.0172
hsa04145	Phagosome	3	145	0.0186
hsa04932	Non-alcoholic fatty liver disease (NAFLD)	3	149	0.0198
hsa04218	Cellular senescence	3	156	0.0222
hsa04920	Adipocytokine signaling pathway	2	69	0.0318
hsa05168	Herpes simplex infection	3	181	0.0319
hsa04520	Adherens junction	2	71	0.033
hsa05133	Pertussis	2	74	0.0352

hsa04540	Gap junction	2	87	0.0467
hsa04912	GnRH signaling pathway	2	88	0.0473

References

Aceto, Nicola et al. 2012. “Tyrosine Phosphatase SHP2 Promotes Breast Cancer Progression and Maintains Tumor-Initiating Cells via Activation of Key Transcription Factors and a Positive Feedback Signaling Loop.” *Nature Medicine* 18(4): 529–37.

Agazie, Y. M., and M. J. Hayman. 2003. “Molecular Mechanism for a Role of SHP2 in Epidermal Growth Factor Receptor Signaling.” *Molecular and Cellular Biology* 23(21): 7875–86.

Bard-Chapeau, Emilie A. et al. 2011. “Ptpn11/Shp2 Acts as a Tumor Suppressor in Hepatocellular Carcinogenesis.” *Cancer Cell* 19(5): 629–39.

Bernard, Philip S. et al. 2009. “Supervised Risk Predictor of Breast Cancer Based on Intrinsic Subtypes.” *Journal of Clinical Oncology* 27(8): 1160–67.

Boutros, Rose, Christine Dozier, and Bernard Ducommun. 2006. “The When and Wheres of CDC25 Phosphatases.” *Current Opinion in Cell Biology* 18(2): 185–91.

Brohée, Sylvain, and Jacques van Helden. 2006. “Evaluation of Clustering Algorithms for Protein-Protein Interaction Networks.” *BMC Bioinformatics* 7.

Bulavin, Dmitry V., Sally A. Amundson, and Albert J. Fornace. 2002. “P38 and Chk1 Kinases: Different Conductors for the G2/M Checkpoint Symphony.” *Current Opinion in Genetics and Development* 12(1): 92–97.

Candi, Eleonora, Massimiliano Agostini, Gerry Melino, and Francesca Bernassola. 2014. “How the TP53 Family Proteins TP63 and TP73 Contribute to Tumorigenesis: Regulators and Effectors.” *Human Mutation* 35(6): 702–14.

Cao, Lanqing, Ping-li Sun, and Min Yao. 2017. “Expression of YES-Associated Protein (YAP) and Its Clinical Signi Fi Cance in Breast Cancer Tissues ☆ , ☆☆.” : 166–74.

Cerami, Ethan et al. 2012. “The CBio Cancer Genomics Portal: An Open Platform for Exploring Multidimensional Cancer Genomics Data.” *Cancer Discovery* 2(5): 401–4.

Chen, Ming Jenn et al. 2019. “Association of Nuclear Localization of SHP2 and YAP1 with Unfavorable Prognosis in Non-Small Cell Lung Cancer.” *Pathology Research and Practice*

215(4): 801–6. https://doi.org/10.1016/j.prp.2019.01.027.

Ciriello, Giovanni et al. 2015. “Comprehensive Molecular Portraits of Invasive Lobular Breast Cancer.” *Cell* 163(2): 506–19.

Corallino, Salvatore et al. 2016. “Alterations in the Phosphoproteomic Profile of Cells Expressing a Non-Functional Form of the SHP2 Phosphatase.” *New Biotechnology* 33(5): 524–36.

Costanzo, Antonio et al. 2014a. “TP63 and TP73 in Cancer, an Unresolved ‘Family’ Puzzle of Complexity, Redundancy and Hierarchy.” *FEBS Letters* 588(16): 2590–99. http://dx.doi.org/10.1016/j.febslet.2014.06.047.

———. 2014b. “TP63 and TP73 in Cancer, an Unresolved ‘Family’ Puzzle of Complexity, Redundancy and Hierarchy.” *FEBS Letters* 588(16): 2590–99.

Curtis, Christina et al. 2012. “The Genomic and Transcriptomic Architecture of 2,000 Breast Tumours Reveals Novel Subgroups.” *Nature* 486(7403): 346–52.

DAMAS, RAMADANY. 2019. “No Title سلطنة عمانペインクリニック学会治療指針２.” ペインクリニック学会治療指針２ 4(1): 75–84.

Feng, H. et al. 2012. “Dynamin 2 Mediates PDGFRα-SHP-2-Promoted Glioblastoma Growth and Invasion.” *Oncogene* 31(21): 2691–2702.

Groth, Casper et al. 2019. “Genome-Wide RNAi Screen for Context-Dependent Tumor Suppressors Identified Using in Vivo Models for Neoplasia in Drosophila.”

Han, Jiahuai, and Peiqing Sun. 2007. “The Pathways to Tumor Suppression via Route P38.” *Trends in Biochemical Sciences* 32(8): 364–71.

Hanahan, Douglas, and Robert A. Weinberg. 2011. “Hallmarks of Cancer: The next Generation.” *Cell* 144(5): 646–74. http://dx.doi.org/10.1016/j.cell.2011.02.013.

He, Xionglei, and Jianzhi Zhang. 2006. “Why Do Hubs Tend to Be Essential in Protein Networks?” *PLoS Genetics* 2(6): 0826–34.

Herranz, Héctor et al. 2012. “Oncogenic Cooperation between SOCS Family Proteins and EGFR Identified Using a Drosophila Epithelial Transformation Model.” *Genes and Development*

26(14): 1602–11.

Herranz, Héctor, Ruifen Weng, and Stephen M. Cohen. 2014. “Crosstalk between Epithelial and Mesenchymal Tissues in Tumorigenesis and Imaginal Disc Development.” *Current Biology* 24(13): 1476–84.

Jeong, H., S. P. Mason, A. L. Barabási, and Z. N. Oltvai. 2001. “Lethality and Centrality in Protein Networks.” *Nature* 411(6833): 41–42.

Jiang, Shuai et al. 2015. “Paclitaxel Enhances Carboplatin-DNA Adduct Formation and Cytotoxicity.” *Chemical Research in Toxicology* 28(12): 2250–52.

Jordan, Mary Ann, and Leslie Wilson. 2004. “Microtubules As a Target For.” 4(April).

Ke, Yuehai et al. 2006. “Conditional Deletion of Shp2 in the Mammary Gland Leads to Impaired Lobulo-Alveolar Outgrowth and Attenuated Stat5 Activation.” *Journal of Biological Chemistry* 281(45): 34374–80.

Keshet, R et al. 2014. “C-Abl Antagonizes the YAP Oncogenic Function.” *Cell death and differentiation* 22(6): 1–11. http://www.ncbi.nlm.nih.gov/pubmed/25361080.

Khuri, Sawsan, and Stefan Wuchty. 2015. “Essentiality and Centrality in Protein Interaction Networks Revisited.” *BMC Bioinformatics* 16(1): 1–8.

Kim, Jinho et al. 2012. “Network Rewiring Is an Important Mechanism of Gene Essentiality Change.” *Scientific Reports* 2: 1–7.

Konecny, Gottfried et al. 2001. “Drug Interactions and Cytotoxic Effects of Paclitaxel in Combination with Carboplatin, Epirubicin, Gemcitabine or Vinorelbine in Breast Cancer Cell Lines and Tumor Samples.” *Breast Cancer Research and Treatment* 67(3): 223–33.

Lambert, Arthur W., Diwakar R. Pattabiraman, and Robert A. Weinberg. 2017. “Emerging Biological Principles of Metastasis.” *Cell* 168(4): 670–91.

Lehn, Sophie et al. 2014. “Decreased Expression of Yes-Associated Protein Is Associated with Outcome in the Luminal A Breast Cancer Subgroup and with an Impaired Tamoxifen Response.” *BMC Cancer* 14(1): 1–16.

Levy, Dan, Yaarit Adamovich, Nina Reuven, and Yosef Shaul. 2008. “Yap1 Phosphorylation by

C-Abl Is a Critical Step in Selective Activation of Proapoptotic Genes in Response to DNA Damage." *Molecular Cell* 29(3): 350–61.

Li, Jun et al. 2014. "Tyrosine Phosphatase Shp2 Mediates the Estrogen Biological Action in Breast Cancer via Interaction with the Estrogen Extranuclear Receptor." *PLoS ONE* 9(7).

Liu, Xia, Hong Zheng, and Cheng Kui Qu. 2012. "Protein Tyrosine Phosphatase Shp2 (Ptpn11) Plays an Important Role in Maintenance of Chromosome Stability." *Cancer Research* 72(20): 5296–5306.

Lu, Chenqi et al. 2010. "Why Do Essential Proteins Tend to Be Clustered in the Yeast Interactome Network?" *Molecular BioSystems* 6(5): 871–77.

Matalkah, Fatimah, Elisha Martin, Hua Zhao, and Yehenew M. Agazie. 2016. "SHP2 Acts Both Upstream and Downstream of Multiple Receptor Tyrosine Kinases to Promote Basal-like and Triple-Negative Breast Cancer." *Breast Cancer Research* 18(1): 1–14.

McGranahan, Nicholas, and Charles Swanton. 2017. "Clonal Heterogeneity and Tumor Evolution: Past, Present, and the Future." *Cell* 168(4): 613–28.

Meng, Zhipeng, Toshiro Moroishi, and Kun-liang Guan. 2016. "Mechanisms of Hippo Pathway Regulation." : 1–17.

von Mering, Christian et al. 2003. "STRING: A Database of Predicted Functional Associations between Proteins." *Nucleic Acids Research* 31(1): 258–61.

———. 2005. "STRING: Known and Predicted Protein-Protein Associations, Integrated and Transferred across Organisms." *Nucleic Acids Research* 33(DATABASE ISS.): 433–37.

Miles, Wayne O., Nicholas J. Dyson, and James A. Walker. 2011. "Modeling Tumor Invasion and Metastasis in Drosophila." *DMM Disease Models and Mechanisms* 4(6): 753–61.

Morales, Liza D. et al. 2014. "Protein Tyrosine Phosphatases PTP-1B, SHP-2, and PTEN Facilitate Rb/E2F-Associated Apoptotic Signaling." *PLoS ONE* 9(5): 1–9.

Moroishi, Toshiro et al. 2015. "A YAP/TAZ-Induced Feedback Mechanism Regulates Hippo Pathway Homeostasis." *Genes and Development* 29(12): 1271–84.

Moroishi, Toshiro, Carsten Gram Hansen, and Kun Liang Guan. 2015. "The Emerging Roles of

YAP and TAZ in Cancer." *Nature Reviews Cancer* 15(2): 73–79. http://dx.doi.org/10.1038/nrc3876.

Muenst, Simone et al. 2013. "Src Homology Phosphotyrosyl Phosphatase-2 Expression Is an Independent Negative Prognostic Factor in Human Breast Cancer." *Histopathology* 63(1): 74–82.

Neel, Benjamin G., Haihua Gu, and Lily Pao. 2003. "The 'Shp'ing News: SH2 Domain-Containing Tyrosine Phosphatases in Cell Signaling." *Trends in Biochemical Sciences* 28(6): 284–93.

Nik-Zainal, Serena et al. 2016. "Landscape of Somatic Mutations in 560 Breast Cancer Whole-Genome Sequences." *Nature* 534(7605): 47–54.

Ning, Kang et al. 2010. "Examination of the Relationship between Essential Genes in PPI Network and Hub Proteins in Reverse Nearest Neighbor Topology." *BMC Bioinformatics* 11.

Overholtzer, Michael et al. 2006. "Transforming Properties of YAP, a Candidate Oncogene on the Chromosome 11q22 Amplicon." *Proceedings of the National Academy of Sciences of the United States of America* 103(33): 12405–10.

Pan, Duojia. 2010. "The Hippo Signaling Pathway in Development and Cancer." *Developmental Cell* 19(4): 491–505. http://dx.doi.org/10.1016/j.devcel.2010.09.011.

Pan, Yi Ru et al. 2013. "Protein Tyrosine Phosphatase SHP2 Suppresses Podosome Rosette Formation in Src-Transformed Fibroblasts." *Journal of Cell Science* 126(2): 657–66.

Pang, Kaifang, Huanye Sheng, and Xiaotu Ma. 2010. "Understanding Gene Essentiality by Finely Characterizing Hubs in the Yeast Protein Interaction Network." *Biochemical and Biophysical Research Communications* 401(1): 112–16.

Patel, Yogin et al. 2016. "A Novel Double-Negative Feedback Loop between MiR-489 and the HER2-SHP2-MAPK Signaling Axis Regulates Breast Cancer Cell Proliferation and Tumor Growth." *Oncotarget* 7(14): 18295–308.

Pavel, Mariana et al. 2018. "Contact Inhibition Controls Cell Survival and Proliferation via YAP/TAZ-Autophagy Axis." *Nature Communications* 9(1).

Peng, Cheng Yuan et al. 1997. “Mitotic and G2 Checkpoint Control: Regulation of 14-3-3 Protein Binding by Phosphorylation of Cdc25c on Serine-216.” *Science* 277(5331): 1501–5.

Perou, Charles M. et al. 2000. “Molecular Portraits of Human Breast Tumours.” *Nature* 406(6797): 747–52.

Polyak, Kornelia. 2011. “Review Series Introduction Heterogeneity in Breast Cancer.” *J.Clin.Invest.* 121(10): 2011–13.

Prahallad, Anirudh et al. 2015. “PTPN11 Is a Central Node in Intrinsic and Acquired Resistance to Targeted Cancer Drugs.” *Cell Reports* 12(12): 1978–85.

Qi, Chen et al. 2017. “Shp2 Inhibits Proliferation of Esophageal Squamous Cell Cancer via Dephosphorylation of Stat3.” *International Journal of Molecular Sciences* 18(1).

Qu, Ying et al. 2015. “Evaluation of MCF10A as a Reliable Model for Normal Human Mammary Epithelial Cells.” *PLoS ONE* 10(7): 1–16.

Real, Sumayya Abdul Sattar et al. 2018. “Aberrant Promoter Methylation of YAP Gene and Its Subsequent Downregulation in Indian Breast Cancer Patients.” *BMC Cancer* 18(1): 1–15.

Richine, B. M. et al. 2016. “Syk Kinase and Shp2 Phosphatase Inhibition Cooperate to Reduce FLT3-ITD-Induced STAT5 Activation and Proliferation of Acute Myeloid Leukemia.” *Leukemia* 30(10): 2094–97.

Ruffalo, Matthew, Mehmet Koyutürk, and Roded Sharan. 2015. “Network-Based Integration of Disparate Omic Data To Identify ‘Silent Players’ in Cancer.” *PLoS Computational Biology* 11(12): 1–12.

Salah, Z, and R I Aqeilan. 2011. “WW Domain Interactions Regulate the Hippo Tumor Suppressor Pathway.” : 1–6.

Schneeberger, Valentina E. et al. 2015. “Inhibition of Shp2 Suppresses Mutant EGFR-Induced Lung Tumors in Transgenic Mouse Model of Lung Adenocarcinoma.” *Oncotarget* 6(8): 6191–6202.

Sondka, Zbyslaw et al. 2018. “The COSMIC Cancer Gene Census: Describing Genetic Dysfunction across All Human Cancers.” *Nature Reviews Cancer* 18(11): 696–705.

http://dx.doi.org/10.1038/s41568-018-0060-1.

Strano, Sabrina, and Giovanni Blandino. 2007. “YAP1 Meets Tumor Suppression.” *Molecular Cell* 27(6): 863–64.

Sun, Xuan et al. 2017. “Shp2 Plays a Critical Role in IL-6-Induced EMT in Breast Cancer Cells.” *International Journal of Molecular Sciences* 18(2).

Suzuki, Keiko et al. 2010. “REAP : A Two Minute Cell Fractionation Method.”

Szklarczyk, Damian et al. 2015. “STRING V10: Protein-Protein Interaction Networks, Integrated over the Tree of Life.” *Nucleic Acids Research* 43(D1): D447–52.

———. 2017. “The STRING Database in 2017: Quality-Controlled Protein-Protein Association Networks, Made Broadly Accessible.” *Nucleic Acids Research* 45(D1): D362–68.

Tang, Damu et al. 2002. “ERK Activation Mediates Cell Cycle Arrest and Apoptosis after DNA Damage Independently of P53.” *Journal of Biological Chemistry* 277(15): 12710–17.

Timmerman, Ilse et al. 2012. “The Tyrosine Phosphatase SHP2 Regulates Recovery of Endothelial Adherens Junctions through Control of β-Catenin Phosphorylation.” *Molecular Biology of the Cell* 23(21): 4212–25.

Tsang, Yiu Huen et al. 2012. “Novel Functions of the Phosphatase SHP2 in the DNA Replication and Damage Checkpoints.” *PLoS ONE* 7(11).

Tsutsumi, Ryouhei et al. 2013. “YAP and TAZ, Hippo Signaling Targets, Act as a Rheostat for Nuclear SHP2 Function.” *Developmental Cell* 26(6): 658–65.

Tubbs, Anthony, and André Nussenzweig. 2017. “Endogenous DNA Damage as a Source of Genomic Instability in Cancer.” *Cell* 168(4): 644–56.

Varelas, Xaralabos. 2014. “The Hippo Pathway Effectors TAZ and YAP in Development, Homeostasis and Disease.” *Development (Cambridge)* 141(8): 1614–26.

Vissers, Joseph H.A., Samuel A. Manning, Aishwarya Kulkarni, and Kieran F. Harvey. 2016. “A Drosophila RNAi Library Modulates Hippo Pathway-Dependent Tissue Growth.” *Nature Communications* 7: 1–6.

Vogelstein, Bert et al. 2013. “Cancer Genome Landscapes.” *Science* 340(6127): 1546–58.

Wang, Qi En et al. 2013. “P38 MAPK- and Akt-Mediated P300 Phosphorylation Regulates Its Degradation to Facilitate Nucleotide Excision Repair.” *Nucleic Acids Research* 41(3): 1722–33.

Washburn, Alexandros, and Alexandros Washburn. 2013. “Why Should We Care About Cities?” *The Nature of Urban Design* 4(June): 15–50.

Wu, Ming, José Carlos Pastor-Pareja, and Tian Xu. 2010. “Interaction between RasV12 and Scribbled Clones Induces Tumour Growth and Invasion.” *Nature* 463(7280): 545–48.

Yang, Cheng Yi et al. 2019. “Correction: Src and SHP2 Coordinately Regulate the Dynamics and Organization of Vimentin Filaments during Cell Migration (Oncogene, (2019), 38, 21, (4075-4094), 10.1038/S41388-019-0705-X).” *Oncogene* 38(21): 4197–98.

Yuan, Liangping et al. 2003. “Role of SHP-2 Tyrosine Phosphatase in the DNA Damage-Induced Cell Death Response.” *Journal of Biological Chemistry* 278(17): 15208–16.

Yuan, Liangping, Wen Mei Yu, and Cheng Kui Qu. 2003. “DNA Damage-Induced G2/M Checkpoint in SV40 Large T Antigen-Immortalized Embryonic Fibroblast Cells Requires SHP-2 Tyrosine Phosphatase.” *Journal of Biological Chemistry* 278(44): 42812–20.

Yuan, Liangping, Wen Mei Yu, Min Xu, and Cheng Kui Qu. 2005. “SHP-2 Phosphatase Regulates DNA Damage-Induced Apoptosis and G 2/M Arrest in Catalytically Dependent and Independent Manners, Respectively.” *Journal of Biological Chemistry* 280(52): 42701–6.

Yuan, M. et al. 2008. “Yes-Associated Protein (YAP) Functions as a Tumor Suppressor in Breast.” *Cell Death and Differentiation* 15(11): 1752–59.

Zhang, Jianmin, Gromoslaw A. Smolen, and Daniel A. Haber. 2008. “Negative Regulation of YAP by LATS1 Underscores Evolutionary Conservation of the Drosophila Hippo Pathway.” *Cancer Research* 68(8): 2789–94.

Zhang, K. et al. 2016. “Shp2 Promotes Metastasis of Prostate Cancer by Attenuating the PAR3/PAR6/APKC Polarity Protein Complex and Enhancing Epithelial-to-Mesenchymal Transition.” *Oncogene* 35(10): 1271–82.

Zhao, Bin et al. 2009. “Both TEAD-Binding and WW Domains Are Required for the Growth Stimulation and Oncogenic Transformation Activity of Yes-Associated Protein.” *Cancer Research* 69(3): 1089–98.

Zhao, Hua, and Yehenew M. Agazie. 2015. “Inhibition of SHP2 in Basal-like and Triple-Negative Breast Cells Induces Basal-to-Luminal Transition, Hormone Dependency, and Sensitivity to Anti-Hormone Treatment.” *BMC Cancer* 15(1): 1–12.

Zhao, S., D. Sedwick, and Z. Wang. 2015. “Genetic Alterations of Protein Tyrosine Phosphatases in Human Cancers.” *Oncogene* 34(30): 3885–94.

Zheng, Jian et al. 2016. “Pancreatic Cancer Risk Variant in LINC00673 Creates a MiR-1231 Binding Site and Interferes with PTPN11 Degradation.” *Nature Genetics* 48(7): 747–57.

Preprint of Publication

Genome-wide RNAi screen for context-dependent tumor suppressors identified using *in vivo* models for neoplasia in *Drosophila*

Casper Groth[1,2], Pooja Vaid[1], Aditi Khatpe[1], Nelchi Prashali[1], Avantika Ahiya[1], Diana Andrejeva[2], Madhumita Chakladar[1], Sanket Nagarkar[1], Rachel Paul[1], Teresa Eichenlaub[2], Hector Herranz[2], TS Sridhar[3], Stephen M. Cohen[2]* and LS Shashidhara[14]*

Addresses

(1) Indian Institute of Science Education and Research (IISER) Dr. Homi Bhabha Road, Pashan, Pune 411 008, INDIA

(2) Department of Cellular and Molecular Medicine, University of Copenhagen, Blegdamsvej 3, Copenhagen 2200N Denmark

(3) Division of Molecular Medicine, St Johns Research Institute, Bangalore, India

(4) Ashoka University, Sonepat, India

- Authors for correspondence

Author contributions
HH, CG, TE, SMC and LSS designed the screen.
CG, PV, AK, NP, AA, SN and RP carried out the genetic screen and participated in data analysis.
DA and MC carried out computational analysis.
SMC, TLS and LSS conceived of, designed and coordinated the study.
SMC and LSS analyzed the data and drafted the manuscript.
All authors gave final approval for publication and agree to be held accountable for the work performed therein.

Keywords

Tumorigenesis, Neoplasia, *Drosophila*, EGFR, Hippo pathway

Total 22 pages including this cover page

Abstract

Genetic approaches in *Drosophila* have successfully identified many genes involved in regulation of growth control as well as genetic interactions relevant to the initiation and progression of cancer *in vivo*. Here, we report on large-scale RNAi-based screens to identify potential tumor suppressor genes that interact with known cancer-drivers: The Epidermal Growth Factor Receptor and the Hippo pathway transcriptional cofactor Yorkie. These screens were designed to identify genes whose depletion drove tissue expressing EGFR or Yki from a state of benign overgrowth into neoplastic transformation *in vivo*. We also report on an independent screen aimed to identify genes whose depletion suppressed formation of neoplastic tumors in an existing EGFR-dependent neoplasia model. Many of the positives identified here are known to be functional in growth control pathways. We also find a number of novel connections to Yki and EGFR driven tissue growth, mostly unique to one of the two. Thus, resources provided here would be useful to all researchers who study negative regulators of growth in the context of activated EGFR and/or Yki and positive regulators of growth in the context of activated EGFR.

Introduction

Studies in genetic models of tissue growth have identified networks of signalling pathways that cooperate to control growth during animal development (reviewed in [1, 2]). Normal tissue growth involves controlling the rates of cell proliferation and cell death, as well as cell size, cell shape, etc. Signalling pathways mediate hormonal and neuroendocrine regulation of growth, which depend on nutritional status. Cell interactions also contribute to coordinating growth of cells within a tissue.

Growth regulatory pathways include both positive and negative elements to allow for feedback regulation. These feedback systems confer robustness to deal with intrinsic biological noise, and with a fluctuating external environment [3]. They also provide the means for different

regulatory pathways to interact [4, 5] [6]. In the context of tumor formation, this robustness is reflected in the difficulty in generating significant mis-regulation of growth - a two-fold change in expression of many growth regulators seldom has a substantial effect on tissue size in *Drosophila* genetic models. More striking is the difficulty in transitioning from benign overgrowth to neoplasia: hyperplasia does not normally lead to neoplasia without additional genetic alterations (eg [7-9]).

Cancers typically show mis-regulation of multiple growth regulatory pathways. Mutational changes and changes in gene expression status contribute to driving cell proliferation, overcoming cell death and cellular senescence, as well as to allowing cells to evade the checkpoints that normally serve to eliminate aberrant cells. These changes alter the normal balance of cellular regulatory mechanisms, from initial cellular transformation through disease progression [10, 11]. For many tumor types, specific mutations have been identified as potent cancer drivers, with well-defined roles in disease [12, 13]. However, most human tumors carry hundreds of mutations, whose functional relevance is unknown. The spectrum of mutation varies from patient to patient, and also within different parts of the same tumor [14]. Evidence is emerging that some of these genetic variants can cooperate with known cancer drivers during cellular transformation or disease progression. The mutational landscape of an individual tumor is likely to contain conditional oncogenes or tumor suppressors that modulate important cellular regulatory networks.

Sequence-based approaches used to identify cancer genes favor those with large individual effects that stand out from the 'background noise' of the mutational landscape in individual cancers [10, 11]. *In vivo* experimental approaches are needed to assign function to candidate cancer genes identified by tumor genome sequencing, and to identify functionally significant contributions of genes that have not attracted notice in genomics studies due to low mutational frequency, or due to changes in activity not associated with mutation. *In vivo* functional screens using transposon mutagenesis of the mouse genome have begun to identify mutations that cooperate with known

cancer driver mutations, such as K-Ras, in specific tumor models [15-17]. Genetic approaches using *Drosophila* models of oncogene cooperation have also been used to identify genes that act together with known cancer drivers in tumor formation [8, 9, 18-20] [21, 22] [2, 23]. The simplicity of the *Drosophila* genome, coupled with the ease of large-scale genetic screens and the high degree of conservation of major signaling pathways with humans, make *Drosophila* an interesting model to identify novel cancer genes and to study the cellular and molecular mechanisms that underlie tumor formation *in vivo* (reviewed in [24-27]).

In *Drosophila*, overexpression of the Epidermal Growth Factor Receptor, EGFR, or Yorkie (Yki, the fly ortholog of the YAP oncoprotein) cause benign tissue over-growth [4, 7, 9]. Combining these with additional genetic alterations can lead to neoplastic transformation and eventually metastasis [8, 9, 21, 22] [28]. Here, we report results of large-scale screens combining UAS-RNAi transgenes with EGFR or Yki expression to identify negative regulators of these growth regulatory networks that can lead to aggressive tumor formation *in vivo*. We also performed an independent screen to identify factors that could suppress EGFR-driven neoplasia. These screens have identified an expanded genomic repertoire of potential tumor suppressors that cooperate with EGFR or Yki. Interestingly, there was limited overlap among the genes that cooperated with EGFR and those that cooperated with Yki.

Results

Overexpression of EGFR or Yki proteins in the *Drosophila* wing imaginal disc produces tissue overgrowth. Under these conditions the imaginal discs retain normal epithelial organization, but grow considerably larger than normal. However, in combination with additional genetic or environmental changes, the tissue can become neoplastic and form malignant tumors [8, 9, 22] [28]. In this context, we carried out large-scale screens using UAS-RNAi lines to identify genes which

would drive hyperplastic growth to neoplastic transformation when down-regulated. To facilitate screening for tumorous growth, we expressed UAS-GFP with UAS-EGFR or UAS-Yki to allow imaginal disc size to be scored in the intact 3rd instar larva (Figure 1A; screen design, examples and quality controls are shown in Supplemental Figure S1).

A large panel of independent UAS-RNAi lines were tested for their effects on tissue growth in the EGFR and Yki expression backgrounds (Figure 1B). Hereafer, the two screens are termed as EGFR screen and Yki screen. Of ~8800 lines tested, 74 interacted with EGFR to produce tumors (~1%), whereas 904 interacted with Yki (~10%). There was limited overlap, with only 21 RNAi lines producing tumors in both screens (Figure 1B). In a parallel screen, we started with neoplastic tumors produced by co-expression of UAS-EGFR and UAS-SOCS36E-RNAi [8] and asked whether including expression of another RNAi transgene could suppress neoplasia (Figure 1A, right panels). Hereafer, this screene is termed SOCS screen. Of ~8900 lines tested, 32 suppressed tumor formation in this assay (Figure 1B). Supplemental Table S1(A) lists the genes identified in these three screens. In previous studies, massive disc overgrowth as in Figure 1(A) was often associated with loss of apically-localized Actin and E-Cadherin: features indicative of Epithelial Mesenchymal Transition (EMT); and with formation of malignant transplantable tumors [8, 9] [22]. Apico-basal polarity and Matrix Metalloprotease 1 (MMP1) expression were assessed for a randomly selected subset of lines from the EGFR and Yki screens to assess neoplastic transformation (Figure S1 and Table S1 – second sheet).

To identify the processes and pathways responsible for the interaction with the screen drivers, we looked for over-representation of biological functions among the screen positives using gene set enrichment analysis and the KEGG, REACTOME, GO and PANTHER databases. Figure 2 presents the results of the enrichment analysis as graphical interaction maps, with similar biological processes color-coded. Edge length represents similarity between genes associated with

significantly enriched terms. Thus, similar terms are closer together and form a community of biological process. The genes in each cluster are shown in Figure 2 and listed in Supplemental Table S2 (has three sheets, once each for EGFR, SOCS and Yki screens).

Genes that potentially modulate EGFR function during growth control

For discs overexpressing EGFR, we observed enrichment of RNAi lines targeting the Hippo pathway, growth signaling, and apoptosis (Figure 2A, B). Many of the genes in the Hippo pathway act as negative regulators of tissue growth, so their depletion by RNAi is expected to promote growth. The Hippo pathway is known to interact with the EGFR pathway to regulate normal developmental growth [4, 5] [6]. The Hippo pathway hits included core elements of the pathway, *hpo*, *wts* and *mats*, which serve as negative growth regulators; the upstream pathway regulators *fat* (an atypical cadherin) and *expanded*; as well as the transcriptional corepressor *grunge*, which is linked to Hippo pathway activity (Table S2). Several of these loci also contributed to the enrichment of terms linked to apoptosis, along with *pten*, a phospholipase that serves as a negative regulator of PI3K/AKT signaling, *protein kinase A-C1*, *Src42A*, the insulin-like peptide, *ilp4*, which are also linked to growth control (Table S2).

For suppression of tumors in discs overexpressing EGFR together with SOCS36E RNAi, we observed enrichment of RNAi lines targeting signaling pathways related to growth, including elements of the AKT/PI3K pathway (Figure 2E, F, Table S2). These pathways may be required for neoplasia in this EGFR driven tumor model. As would be expected, depletion of *Egfr* limited tumor growth. Also enriched was a set of genes involved in protein synthesis (Table S2). This may reflect a need for active cellular growth machinery to support tumor growth. The significance of genes involved in RNA splicing merits further investigation.

Genes that potentially modulate Yki function during growth control

For discs overexpressing Yki, RNAi lines targeting the Hippo pathway and associated growth regulators led to tumor production (Figure 2C, D, Table S2). These include *hpo*, *sav*, *wts*, *mats*, *ft*, *ex* and *gug*. Although this has not been observed previously in *Drosophila*, it is worth noting that overexpression of YAP has been shown to lead to neoplasia in mouse liver and intestinal epithelial models [29, 30]. While most cancers appear to result from activation/inactivation of multiple genes and pathways, sufficient activation of the Hippo pathway can result in neoplasia (Yki in *Drosophila* and YAP in mouse).

The Hippo tumor suppressor pathway is regulated by cell polarity, cell contact, and mechanical forces [31-33] as well as by other growth signaling pathways. Growth signaling pathways involving the *sgg*, *pten*, *PKA-C1*, *TSC1* genes among others, were also identified. Additionally, a number of genes linked to membrane-cytoskeleton interaction and transmembrane transport were found to interact, including Arf and Rab family members. We also noted the enrichment of terms related to lipid and general metabolism. Regulation of lipid metabolism might affect the properties of cellular membranes. An intriguing subgroup contain genes related to glutamatergic signaling, including the vesicular glutamate transporter *VGlut* and the *Eaat* plasma membrane glutamate transporters. The significance of these is unclear.

The large number of Yki interactors could reflect greater sensitivity of the screen. Alternatively, it might indicate a high false positive rate. While this screen was in progress, Vissers et al. [34], reported that some of the RNAi lines from the Vienna *Drosophila* RNAi KK library have the potential to produce false positives in screens based on sensitized Hippo pathway phenotypes. This proved to be due to the presence of a second transgene landing site at 40D that was found in a subset of KK lines, in addition to the 30B landing site [34, 35]. We tested the 40D landing site

strain [34] and found that it did not cause a tumor phenotype under the conditions used for the screen. Nonetheless, we sampled the 40D status for a large subset of our Yki interactors (Table S1, 734/904) and found that 45% of them had insertions at 40D. A small survey comparing KK lines with Trip and GD lines showed that 65% of genes for which the KK line had a 40D site retested positive for interaction with Yki using an independent (non-KK) transgene (15/23). The Yki-interaction screen should therefore be viewed as a more sensitized sampling of potential interactors, compared to the EGFR-interaction screen.

STRING Interactome analyses

To view all genes identified in the three screens as one functional unit (for the fact that they were all growth regulators in one or the other contexts), we made use of STRING v10 [36] to produce protein interaction maps. STRING v10 builds interaction maps by combining experimental data (including protein interaction data) with information about functional associations from text mining. STRING v10 also uses information of co-occurrence, co-expression, gene neighborhood, gene fusion, and does sequence similarity search to predict functional interaction between proteins. An interaction pair supported by multiple lines of evidence has higher confidence score than other pairs.

Figure 3A shows the STRING interaction map for the genes identified as interactors of EGFR. As noted above, Hippo pathway (red) components were prominent among the genes identified as cooperating with EGFR to drive tumor formation. Figure 3(B) shows the interaction map for the genes identified as interactors of Yki. The larger number of hits in this screen results in a more complex interaction map, with multiple interconnected clusters. The Hippo pathway (red) was again prominent in the fly screen. We also noted clusters containing elements of the ubiquitin mediated proteolysis pathway (green) and the PI3K/TOR (blue). As noted above, the higher

sensitivity of this screen leads to the inclusion of weaker interactors, which may add to the complexity of these interaction maps. A focus on the stronger clusters and the interaction between them should guide future studies. Fig. 3(C) shows interaction map for the genes identified as interactors of EGFR in the suppressor screen (in discs overexpressing EGFR together with SOCS36E RNAi). Among fly genes, as expected, we observed suppression of the tumor phenotype when components of EGFR pathway are down regulated.

Human orthologs of the fly genes identified in the three screens

To identify human orthologs for the candidate genes, we used the DRSC Integrative Ortholog Prediction Tool, DIOPT (Version 7.1, March 2018; www.flybase.org). DIOPT scores reflect the number of independent prediction tools that identify an ortholog for a given *Drosophila* gene. Orthology relationships are usually unambiguous when found by most of the 12 independent prediction tools in DIOPT. Table S1 lists the primary human orthologs (highest weighted DIOPT score), as well as the other orthologs with a weighted DIOPT score >2 for each of the hits in the fly screen. The primary human ortholog was used for subsequent analysis. In cases where multiple human orthologs had the same score, all orthologs with highest weighted DIOPT score were used. Out of 73 EGFR positive hits, 46 genes had one or more human orthologs, in total mapping to 50 human genes. Out of 32 SOCS positive hits 30 genes had one or more human orthologs, in total mapping to 31 human genes. Out of 904 YAP positive hits 570 genes had one or more human orthologs, in total mapping to 611 human genes.

To view the human orthologs in a functional context, we performed a gene set enrichment analysis and the KEGG, REACTOME, GO, PANTHER, NCI, MsigDB, BIOCARTA databases. Figure 4 presents the results of the enrichment analyses as graphical interaction maps, with similar biological processes color-coded. Edge length represents similarity between genes associated with

significantly enriched terms. Thus, similar terms are closer together and form a community of biological processes. The genes in each cluster are shown in Figure 4 and listed in Supplemental Table S3. Because the enrichment analysis is highly sensitive to the number of orthologs for each of the fly genes, we used the minimal set consisting of only the primary human orthologs.

Hippo pathway components were enriched among the orthologs cooperating with EGFR to drive tumor formation (Fig 4A, B; Table S3). Two of these, LATS1 and STK3, also contributed to enrichment for a term linked to protein turnover. Regulation of protein turnover is an important mechanism for controlling the activity of a number of Hippo pathway components. For the screen for suppression of tumors in discs overexpressing EGFR together with SOCS36E RNAi, we observed enrichment of orthologs targeting growth signaling pathways, protein synthesis and mRNA splicing (Figure 4E, F, Table S3), similar to what was seen for the fly gene set analysis. We also observed enrichment of pathways related to protein folding and molecular chaperones, in the human gene set. For the Yki screen, the human ortholog set was enriched for terms related to general metabolism, and membrane transport, as well as growth signaling, and other signaling pathways, including genes involved in protein turnover (Fig 4C, D).

Discussion

The Hippo pathway has emerged from this study as the single most important pathway limiting tumor formation in *Drosophila*. Increasing Yki activity by depletion of upstream negative regulators promoted tumor formation in both the EGFR and Yki hyperplasia models. Yki controls tissue growth by promoting cell proliferation and by concurrently inhibiting cell death through targets including *Diap1*, *CycE* and *bantam* miRNA [7, 36-39]. The central role of the Hippo pathway as an integrator of other growth-related signals may also contribute to the abundance of

tumor suppressors associated with Yki-driven growth [1, 2, 26]. Mis-regulation of this pathway also contributes to tumor formation in mouse models [40].

The potential of Yki/YAP expression to drive cellular transformation has been highlighted by studies of primary human cells in culture, which have shown that YAP expression is both necessary and sufficient to confer a transformed phenotype involving anchorage independent growth and the ability to form tumors in xenograft models [41, 42]. We therefore consider it likely that the consequence of Yki overexpression predispose the tissue to transformation, allowing identification of a richer repertoire of cooperating factors. Indeed, YAP overexpression has been causally linked to formation of specific human tumors [43, 44]. The Hippo pathway has also been implicated in tumor formation resulting from cytokinesis failure [45] and this has recently been linked to Yki-mediated regulation of *string (*CDC25*)* expression [46]. The sensitivity of Yki-expressing tissue to tumor formation might be explained by the finding that Yki promotes cell cycle progression at both the G1-S transition (through regulation of *cycE* [7] and at the G2-M transition through regulation of *string*. In contrast, mitogens and growth factors such as EGFR typically induce growth by promoting G1-S, and therefore remain somewhat constrained by the G2-M checkpoint.

While our manuscript was in preparation, another group reported an RNAi screen to identify loci cooperating in tumorigenesis driven by expression in eye discs of the oncogenic activated mutant form of *Ras* [47]. We note that the activated Ras RNAi screen produced over 900 hits, compared with 74 for our EGFR screen, suggesting that the Ras screen was considerably more sensitized. We were surprised to note that there was almost no overlap between the two screens. This suggests that the genetic interactions required to promote tumorigenesis in the context of expression of an activated mutant form of RAS are distinct from those required to promote tumorigenesis in the context of native EGRF overexpression. And perhaps, the differences between

the tissue contexts (eye discs in [47] vs wing discs in our screen). It will be of interest, in future, to learn whether this distinction holds true for factors promoting tumor formation in human cancers that depend on EGFR overexpression vs those dependent on Ras mutants.

To conclude, the results reported here provide an extensive assessment of the genes that can serve as negative regulators of growth that can contribute to the formation of neoplastic tumors *in vivo* in *Drosophila*. In addition to finding genes linked to known growth control pathways, a number of novel connections to Yki and EGFR driven tissue growth have been identified, which merit further investigation in the *Drosophila* genetic model. Exploring the potential relevance of genes identified in this manner to human cancer will involve assessing the correlation of candidate gene expression with clinical outcome across a broad range of cancers (eg [28, 48]), as a starting point to identify biomarkers as well as novel candidate drug targets.

Materials and Methods

RNAi Screens

The KK transgenic RNAi stock library was obtained from the Vienna *Drosophila* RNAi Center (www.vdrc.at) carrying inducible UAS-RNAi constructs on Chromosome II. For each cross, 5 males from the KK transgenic RNAi stock were crossed separately to 10-15 virgins from each of the following three driver stocks: *w**, *ap*-Gal4, UAS-*GFP*/CyO; UAS-*Yki*, *tub*-Gal80^{ts}/TM6B (Yki driver); *w**; *ap*-Gal4, UAS-*GFP*/CyO; UAS-*EGFR*, *tub*-Gal80^{ts}/TM6B (EGFR driver); and *w**; *ap*-Gal4, UAS-*GFP*/CyO; and *w**; *ap*-Gal4, UAS-*GFP*, *Socs36E*^{RNAi}/CyO; UAS-*EGFR*, *tub*-Gal80^{ts}/TM6B (EGFR driver +SOCS36E RNAi).

Virgin female flies were collected over 4-5 days and stored at 18˚C in temperature-controlled incubators on medium supplemented with dry yeast, prior to setting up crosses. Virgin

females were mated to KK stock males (day 1) and the crosses were stored at 18°C for 4 days to provide ample time for mating before starting the timed rearing protocol used for the screen. On day 5, the crosses were transferred into new, freshly yeasted vials for another 3 days at 18°C. On day 8, the adult flies were discarded, and larvae were allowed to develop until day 11, at which time the vials were moved to 29°C incubators to induce Gal4 driver activity. Crosses were aged at 29°C for a further 8-9 days, after which larvae were scored for size and wing disc overgrowth phenotypes for Yki and EGFR driver screen crosses. Flies were scored for suppression of the tumor phenotype for the EGFR driver +SOCS36E RNAi crosses (see Supplemental Fig. S1 for the screen design and workflow).

In order to verify the integrity of the driver stocks during the course of the screen, we examined their expression patterns in conjunction with setting up screen crosses each week. For each driver, 2-3 of the bottles used for virgin collection were induced at 29°C for 24 hours and analyzed using fluorescence microscopy for *apterous*-Gal4 specific expression in wandering 3-instar larvae.

Positive hits form the initial screen were retested by setting up 2 or more additional crosses. The hits were scored as verified if 2 out of 3 tests scored positive. Wandering third instar larvae of confirmed positives were imaged and documented using fluorescence microscopy.

Genomic DNA PCR 40D landing site occupancy test

Genomic DNA from a select number of *Drosophila* KK transgenic RNAi library stocks was isolated following a protocol available at the VDRC (www.vdrc.at). The presence or absence of the KK RNAi transgene at the 40D insertion site on the second chromosome was determined by multiplex PCR using the following primers:

40D primer (C_Genomic_F): 5'-GCCCACTGTCAGCTCTCAAC-3'
pKC26_R: 5'-TGTAAAACGACGGCCAGT-3'

pKC43_R: 5'-TCGCTCGTTGCAGAATAGTCC-3'

PCR amplification was performed using GoTaq G2 Hot Start Green Master Mix kit (Promega) in a 25 µL standard reaction mix and the following program: initial denaturation at 95°C for 2 min, followed by 33 cycles with denaturation at 95°C for 15 sec, annealing at 58°C for 15 sec and extension at 72°C for 90 sec. One final extension reaction was carried out at 72°C for 10 min. Reactions were stored at -20°C prior to gel loading. PCR using these primers generate an approximately 450 bp product in case of a transgene insertion or a 1050 bp product in case of no transgene insertion site at 40D.

Screen Database

Results from the three screening projects were added to a screen management database, www.iiserpune.ac.in/rnai/, including images of positive hits and background information such as RNAi line ID, corresponding gene information from the Flybase etc. The database was developed by Livetek Software Consultant Services (Pune, Maharashtra, INDIA).

Pathway and gene set enrichment analysis

Gene set enrichment analysis was performed using genes that upon down regulation induced tumor formation (EGFR, YKI background) or suppressed tumor formation (EGFR+SOCS background). For *D. melanogaster* enrichment analysis all *D. melanogaster* protein coding genes were used as the "gene universe" together with organism specific datasets. For human ortholog enrichment analysis all human protein coding genes were used as the "gene universe" together with organism specific datasets. The algorithm packages and databases used in analysis are listed in Supplemental Tables S2 and S3. Unless otherwise specified, pathway databases included in these packages were used. The KEGG database was downloaded directly from source on 10.10.2018. Organ system specific

and disease related pathway maps were excluded from this analysis. Minimum and maximum number of genes per pathway or gene set, significant criteria, minimum enriched gene count and annotated gene counts for each test and database are indicated in Supplemental Tables S2 and S3. GO results were filtered for level >2, to eliminate broad high-level categories and <10 to minimize duplication among subcategories. A representative term was selected in the cases were identical set of genes mapped to multiple terms within the same database. After filtering, the top 10 terms from each database were used for clustering analysis.

Pathway and gene set enrichment analysis results were visualized as enrichment map with appropriate layout based on gene overlap ration using igraph. Gene overlap ratio was set as edge width. Edges with low overlap were deleted, filtering threshold was based on a number of "terms" in the results table – from 0 to 50 by 10; increasing filtering thresholds from 0.16 to 0.26 by 0.2. Clusters were detected using "Edge betweenness community" algorithm. Similar biological processes were color-coded.

R packages

clusterProfiler (3.8.1) - [49].

ReactomePA (1.24.0) - [50].

http://pubs.rsc.org/en/Content/ArticleLanding/2015/MB/C5MB00663E.

graphite (1.26.1) - Sales G, Calura E, Romualdi C (2018). graphite: GRAPH Interaction from pathway Topological Environment. R package version 1.26.1.

igraph (1.2.2) - Csardi G, Nepusz T: The igraph software package for complex network research, InterJournal, Complex Systems 1695. 2006. http://igraph.org

Database references

KEGG – [51, 52].

REACTOME – [53]

Panther – [54]

GO – [55].

STRING interaction maps

STRING v10 is a computational tool for protein interaction network and pathway analysis [56]), to identify significant functional clustering among the candidate genes. STRING builds interaction maps by combining experimental data (including protein interaction data) with information about functional associations from text mining. STRING interactome maps were used to search for statistically significant enrichment of KEGG pathways.

Acknowledgements

The professionalism, tireless support and goodwill provided by Snehal Patil, Yashwant Pawar and Bhargavi Naik from the IISER Pune fly facility contributed greatly to the success of the screening projects reported here.

Funding

This work was primarily supported by a Indo-Danish research grant from Department of Biotechnology, Govt. of India to TSS and LSS and from Innovationfund Denmark, Novo Nordisk Foundation NNF12OC0000552 and Neye Foundation to SMC. JC Bose Fellowship and grant from Department of Science & Technology, Govt of India to LSS. We thank other members of all the laboratories for critical input.

Figure legends

Figure 1: tumor formation/suppression visualized in intact larvae

(A) Larvae co-expressed UAS-GFP with the indicated transgenes to permit visualization of the imaginal discs in the intact animal. All samples carried the *ap*-Gal4 driver and UAS-GFP. In addition, they carried either a second copy of UAS-GFP or one of the following: UAS-Yki, UAS-EGFR or UAS-EGFR+UAS-SOCS36E-RNAi.

(B) Table summarizing the number of interacting RNAi lines identified in the three large-scale screens.

Figure 2: Summary of pathway enrichment analysis of fly genes identify in the *in vivo* screens reported here.

(A, C, E) The results of the pathway and gene set enrichment analysis are shown as graphical interaction maps. Each node represents a significantly enriched term or pathway from the GO, KEGG, Reactome and Panther databases (Table S2). Color-coding indicates functionally related groups of terms. Lines indicate genes shared among different terms. (B, D, F) show the individual genes associated with functionally enriched cluster.

(A, B) UAS-EGFR screen

(C, D) UAS-Yki screen

(E, F) UAS-EGFR+UAS-SOCS36E-RNAi screen

Figure 3: STRING interactome analysis of potential interactors of EGFR and YKi in *Drosophila*. STRING analysis was performed with confidence score of 0.7 and MCL clustering value of 2. (A) STRING Interactome of 73 fly genes identified as potential negative regulators in the context of over expression of EGFR. 17 out of those formed molecular clusters (with PPI enrichment value of 0.000482), largest being a cluster of 6 genes, all of which are constitutes of Fat/Hippo pathway (shown in red; FDR-1.39E^{-5}). (B) STRING Interactome of 888 genes of identified as potential negative regulators in the context of over expression of Yki. 228 of those formed a single cluster with PPI enrichment value 1.4E-06. Components of Fat/Hippo pathway (red: FDR-0.00076) and Autophagy genes (blue: FDR-0.0241) are enriched in this cluster. (C) STRING Interactome of 32 fly genes identified as potential oncogenes in the context of SOCS suppression. 27 out of those formed molecular clusters (with PPI enrichment value of 0.0122), largest being a cluster of 14

genes. A smaller cluster comprising of EGFR and DrK were enriched in Dorso-ventral axis formation (shown in purple: FDR-0.0089).

Figure 4: Summary of pathway enrichment analysis of human orthologs

(A, C, E) The results of the pathway and gene set enrichment analysis are shown as enrichment maps. Each node represents a significantly enriched term or pathway from the GO, KEGG, Reactome and PANTHER, NCI, MsigDB, BIOCARTA databases (Table S3). Color-coding indicates functionally related groups of terms. Lines indicate genes shared among different terms. (B, D, F) show the individual genes associated with functionally enriched cluster.

(A, B) UAS-EGFR screen

(C, D) UAS-Yki screen

(E, F) UAS-EGFR+UAS-SOCS36E-RNAi screen

References

1 Harvey, K. F., Zhang, X., Thomas, D. M. 2013 The Hippo pathway and human cancer. *Nat Rev Cancer*. **13**, 246-257. (10.1038/nrc3458)

2 Richardson, H. E., Portela, M. 2017 Tissue growth and tumorigenesis in *Drosophila*: cell polarity and the Hippo pathway. *Curr Opin Cell Biol*. **48**, 1-9. (10.1016/j.ceb.2017.03.006)

3 Herranz, H., Cohen, S. M. 2010 MicroRNAs and gene regulatory networks: managing the impact of noise in biological systems. *Genes Dev*. **24**, 1339-1344. (10.1101/gad.1937010)

4 Herranz, H., Hong, X., Cohen, S. M. 2012 Mutual repression by bantam miRNA and Capicua links the EGFR/MAPK and Hippo pathways in growth control. *Curr Biol*. **22**, 651-657. (10.1016/j.cub.2012.02.050)

5 Reddy, B. V., Irvine, K. D. 2013 Regulation of Hippo signaling by EGFR-MAPK signaling through Ajuba family proteins. *Dev Cell*. **24**, 459-471. (10.1016/j.devcel.2013.01.020)

6 Ren, F., Zhang, L., Jiang, J. 2010 Hippo signaling regulates Yorkie nuclear localization and activity through 14-3-3 dependent and independent mechanisms. *Developmental biology*. **337**, 303-312. (10.1016/j.ydbio.2009.10.046)

7 Huang, J., Wu, S., Barrera, J., Matthews, K., Pan, D. 2005 The Hippo signaling pathway coordinately regulates cell proliferation and apoptosis by inactivating Yorkie, the *Drosophila* Homolog of YAP. *Cell*. **122**, 421-434. (10.1016/j.cell.2005.06.007)

8 Herranz, H., Hong, X., Hung, N. T., Voorhoeve, P. M., Cohen, S. M. 2012 Oncogenic cooperation between SOCS family proteins and EGFR identified using a *Drosophila* epithelial transformation model. *Genes Dev*. **26**, 1602-1611. (10.1101/gad.192021.112)

9 Herranz, H., Weng, R., Cohen, S. M. 2014 Crosstalk between epithelial and mesenchymal tissues in tumorigenesis and imaginal disc development. *Curr Biol*. **24**, 1476-1484. (10.1016/j.cub.2014.05.043)

10 Stratton, M. R. 2011 Exploring the genomes of cancer cells: progress and promise. *Science*. **331**, 1553-1558. (10.1126/science.1204040)

11 Alexandrov, L. B., Nik-Zainal, S., Wedge, D. C., Aparicio, S. A., Behjati, S., Biankin, A. V., Bignell, G. R., Bolli, N., Borg, A., Borresen-Dale, A. L., *et al.* 2013 Signatures of mutational processes in human cancer. *Nature*. **500**, 415-421. (10.1038/nature12477)

12 Kandoth, C., McLellan, M. D., Vandin, F., Ye, K., Niu, B., Lu, C., Xie, M., Zhang, Q., McMichael, J. F., Wyczalkowski, M. A., *et al.* 2013 Mutational landscape and significance across 12 major cancer types. *Nature*. **502**, 333-339. (10.1038/nature12634)

13 Zehir, A., Benayed, R., Shah, R. H., Syed, A., Middha, S., Kim, H. R., Srinivasan, P., Gao, J., Chakravarty, D., Devlin, S. M., *et al.* 2017 Mutational landscape of metastatic cancer revealed from prospective clinical sequencing of 10,000 patients. *Nat Med*. **23**, 703-713. (10.1038/nm.4333)

14 McGranahan, N., Swanton, C. 2017 Clonal Heterogeneity and Tumor Evolution: Past, Present, and the Future. *Cell*. **168**, 613-628. (10.1016/j.cell.2017.01.018)

15 Copeland, N. G., Jenkins, N. A. 2010 Harnessing transposons for cancer gene discovery. *Nat Rev Cancer*. **10**, 696-706. (10.1038/nrc2916)

16 Perez-Mancera, P. A., Rust, A. G., van der Weyden, L., Kristiansen, G., Li, A., Sarver, A. L., Silverstein, K. A., Grutzmann, R., Aust, D., Rummele, P., *et al.* 2012 The deubiquitinase USP9X suppresses pancreatic ductal adenocarcinoma. *Nature*. **486**, 266-270. (10.1038/nature11114)

17 Takeda, H., Wei, Z., Koso, H., Rust, A. G., Yew, C. C., Mann, M. B., Ward, J. M., Adams, D. J., Copeland, N. G., Jenkins, N. A. 2015 Transposon mutagenesis identifies genes and evolutionary forces driving gastrointestinal tract tumor progression. *Nat Genet*. **47**, 142-150. (10.1038/ng.3175)

18 Brumby, A. M., Richardson, H. E. 2003 scribble mutants cooperate with oncogenic Ras or Notch to cause neoplastic overgrowth in *Drosophila*. *Embo J*. **22**, 5769-5779. (10.1093/emboj/cdg548)

19 Pagliarini, R. A., Xu, T. 2003 A genetic screen in *Drosophila* for metastatic behavior. *Science*. **302**, 1227-1231. (10.1126/science.1088474)

20 Brumby, A. M., Goulding, K. R., Schlosser, T., Loi, S., Galea, R., Khoo, P., Bolden, J. E., Aigaki, T., Humbert, P. O., Richardson, H. E. 2011 Identification of novel Ras-cooperating oncogenes in *Drosophila* melanogaster: a RhoGEF/Rho-family/JNK pathway is a central driver of tumorigenesis. *Genetics*. **188**, 105-125. (10.1534/genetics.111.127910)

21 Eichenlaub, T., Cohen, S. M., Herranz, H. 2016 Cell Competition Drives the Formation of Metastatic Tumors in a *Drosophila* Model of Epithelial Tumor Formation. *Curr Biol*. **26**, 419-427. (10.1016/j.cub.2015.12.042)

22 Song, S., Herranz, H., Cohen, S. M. 2017 The chromatin remodeling BAP complex limits tumor-promoting activity of the Hippo pathway effector Yki to prevent neoplastic transformation in *Drosophila* epithelia. *Dis Model Mech*. **10**, 1201-1209. (10.1242/dmm.030122)

23 Wu, M., Pastor-Pareja, J. C., Xu, T. 2010 Interaction between Ras(V12) and scribbled clones induces tumour growth and invasion. *Nature*. **463**, 545-548. (10.1038/nature08702)

24 Gonzalez, C. 2013 *Drosophila* melanogaster: a model and a tool to investigate malignancy and identify new therapeutics. *Nat Rev Cancer*. **13**, 172-183. (10.1038/nrc3461)

25 Herranz, H., Eichenlaub, T., Cohen, S. M. 2016 Cancer in *Drosophila*: Imaginal Discs as a Model for Epithelial Tumor Formation. *Curr Top Dev Biol*. **116**, 181-199. (10.1016/bs.ctdb.2015.11.037)

26 Richardson, H. E., Portela, M. 2018 Modelling Cooperative Tumorigenesis in *Drosophila*. *Biomed Res Int*. **2018**, 4258387. (10.1155/2018/4258387)

27 Sonoshita, M., Cagan, R. L. 2017 Modeling Human Cancers in *Drosophila*. *Curr Top Dev Biol*. **121**, 287-309. (10.1016/bs.ctdb.2016.07.008)

28 Eichenlaub, T., Villadsen, R., Freitas, F. C. P., Andrejeva, D., Aldana, B. I., Nguyen, H. T., Petersen, O. W., Gorodkin, J., Herranz, H., Cohen, S. M. 2018 Warburg Effect Metabolism Drives Neoplasia in a *Drosophila* Genetic Model of Epithelial Cancer. *Curr Biol*. **28**, 3220-3228 e3226. (10.1016/j.cub.2018.08.035)

29 Dong, J., Feldmann, G., Huang, J., Wu, S., Zhang, N., Comerford, S. A., Gayyed, M. F., Anders, R. A., Maitra, A., Pan, D. 2007 Elucidation of a universal size-control mechanism in *Drosophila* and mammals. *Cell*. **130**, 1120-1133. (10.1016/j.cell.2007.07.019)

30 Cai, J., Zhang, N., Zheng, Y., de Wilde, R. F., Maitra, A., Pan, D. 2010 The Hippo signaling pathway restricts the oncogenic potential of an intestinal regeneration program. *Genes Dev*. **24**, 2383-2388. (10.1101/gad.1978810)

31 Wada, K., Itoga, K., Okano, T., Yonemura, S., Sasaki, H. 2011 Hippo pathway regulation by cell morphology and stress fibers. *Development*. **138**, 3907-3914. (10.1242/dev.070987)

32 Halder, G., Dupont, S., Piccolo, S. 2012 Transduction of mechanical and cytoskeletal cues by YAP and TAZ. *Nat Rev Mol Cell Biol*. **13**, 591-600. (10.1038/nrm3416)

33 Aragona, M., Panciera, T., Manfrin, A., Giulitti, S., Michielin, F., Elvassore, N., Dupont, S., Piccolo, S. 2013 A mechanical checkpoint controls multicellular growth through YAP/TAZ regulation by actin-processing factors. *Cell*. **154**, 1047-1059. (10.1016/j.cell.2013.07.042)

34 Vissers, J. H., Manning, S. A., Kulkarni, A., Harvey, K. F. 2016 A *Drosophila* RNAi library modulates Hippo pathway-dependent tissue growth. *Nat Commun*. **7**, 10368. (10.1038/ncomms10368)

35 Green, E. W., Fedele, G., Giorgini, F., Kyriacou, C. P. 2014 A *Drosophila* RNAi collection is subject to dominant phenotypic effects. *Nat Methods*. **11**, 222-223. (10.1038/nmeth.2856)

36 Thompson, B. J., Cohen, S. M. 2006 The Hippo pathway regulates the bantam microRNA to control cell proliferation and apoptosis in *Drosophila*. *Cell*. **126**, 767-774. (10.1016/j.cell.2006.07.013)

37 Nolo, R., Morrison, C. M., Tao, C., Zhang, X., Halder, G. 2006 The bantam microRNA is a target of the hippo tumor-suppressor pathway. *Curr Biol*. **16**, 1895-1904. (10.1016/j.cub.2006.08.057)

38 Tapon, N., Harvey, K., Bell, D., Wahrer, D., Schiripo, T., Haber, D., Hariharan, I. 2002 salvador Promotes Both Cell Cycle Exit and Apoptosis in *Drosophila* and Is Mutated in Human Cancer Cell Lines. *Cell*. **110**, 467.

39 Wu, S., Liu, Y., Zheng, Y., Dong, J., Pan, D. 2008 The TEAD/TEF family protein Scalloped mediates transcriptional output of the Hippo growth-regulatory pathway. *Dev Cell*. **14**, 388-398. (10.1016/j.devcel.2008.01.007)

40 Yu, F. X., Zhao, B., Guan, K. L. 2015 Hippo Pathway in Organ Size Control, Tissue Homeostasis, and Cancer. *Cell*. **163**, 811-828. (10.1016/j.cell.2015.10.044)

41 Hong, X., Nguyen, H. T., Chen, Q., Zhang, R., Hagman, Z., Voorhoeve, P. M., Cohen, S. M. 2014 Opposing activities of the Ras and Hippo pathways converge on regulation of YAP protein turnover. *Embo J*. **33**, 2447-2457. (10.15252/embj.201489385)

42 Nguyen, H. T., Hong, X., Tan, S., Chen, Q., Chan, L., Fivaz, M., Cohen, S. M., Voorhoeve, P. M. 2014 Viral small T oncoproteins transform cells by alleviating hippo-pathway-mediated inhibition of the YAP proto-oncogene. *Cell Rep*. **8**, 707-713. (10.1016/j.celrep.2014.06.062)

43 Shao, D. D., Xue, W., Krall, E. B., Bhutkar, A., Piccioni, F., Wang, X., Schinzel, A. C., Sood, S., Rosenbluh, J., Kim, J. W., *et al.* 2014 KRAS and YAP1 converge to regulate EMT and tumor survival. *Cell*. **158**, 171-184. (10.1016/j.cell.2014.06.004)

44 Kapoor, A., Yao, W., Ying, H., Hua, S., Liewen, A., Wang, Q., Zhong, Y., Wu, C. J., Sadanandam, A., Hu, B., *et al.* 2014 Yap1 activation enables bypass of oncogenic Kras addiction in pancreatic cancer. *Cell*. **158**, 185-197. (10.1016/j.cell.2014.06.003)

45 Ganem, N. J., Cornils, H., Chiu, S. Y., O'Rourke, K. P., Arnaud, J., Yimlamai, D., Thery, M., Camargo, F. D., Pellman, D. 2014 Cytokinesis failure triggers hippo tumor suppressor pathway activation. *Cell*. **158**, 833-848. (10.1016/j.cell.2014.06.029)

46 Gerlach, S. U., Eichenlaub, T., Herranz, H. 2018 Yorkie and JNK Control Tumorigenesis in *Drosophila* Cells with Cytokinesis Failure. *Cell Rep*. **23**, 1491-1503. (10.1016/j.celrep.2018.04.006)

47 Zoranovic, T., Manent, J., Willoughby, L., Matos de Simoes, R., La Marca, J. E., Golenkina, S., Cuiping, X., Gruber, S., Angjeli, B., Kanitz, E. E., *et al.* 2018 A genome-wide *Drosophila* epithelial tumorigenesis screen identifies Tetraspanin 29Fb as an evolutionarily conserved suppressor of Ras-driven cancer. *PLoS Genet*. **14**, e1007688. (10.1371/journal.pgen.1007688)

48 Andrejeva, D., Kugler, J. M., Nguyen, H. T., Malmendal, A., Holm, M. L., Toft, B. G., Loya, A. C., Cohen, S. M. 2018 Metabolic control of PPAR activity by aldehyde dehydrogenase regulates invasive cell behavior and predicts survival in hepatocellular and renal clear cell carcinoma. *BMC Cancer*. **18**, 1180. (10.1186/s12885-018-5061-7)

49 Yu, G., Wang, L. G., Han, Y., He, Q. Y. 2012 clusterProfiler: an R package for comparing biological themes among gene clusters. *Omics*. **16**, 284-287. (10.1089/omi.2011.0118)

50 Yu, G., He, Q. Y. 2016 ReactomePA: an R/Bioconductor package for reactome pathway analysis and visualization. *Mol Biosyst*. **12**, 477-479. (10.1039/c5mb00663e)

51 Kanehisa, M., Sato, Y., Kawashima, M., Furumichi, M., Tanabe, M. 2016 KEGG as a reference resource for gene and protein annotation. *Nucleic Acids Res*. **44**, D457-462. (10.1093/nar/gkv1070)

52 Kanehisa, M., Furumichi, M., Tanabe, M., Sato, Y., Morishima, K. 2017 KEGG: new perspectives on genomes, pathways, diseases and drugs. *Nucleic Acids Res*. **45**, D353-D361. (10.1093/nar/gkw1092)

53 Fabregat, A., Jupe, S., Matthews, L., Sidiropoulos, K., Gillespie, M., Garapati, P., Haw, R., Jassal, B., Korninger, F., May, B., *et al.* 2018 The Reactome Pathway Knowledgebase. *Nucleic Acids Res*. **46**, D649-D655. (10.1093/nar/gkx1132)

54 Thomas, P. D., Campbell, M. J., Kejariwal, A., Mi, H., Karlak, B., Daverman, R., Diemer, K., Muruganujan, A., Narechania, A. 2003 PANTHER: a library of protein families and subfamilies indexed by function. *Genome Res*. **13**, 2129-2141. (10.1101/gr.772403)

55 Ashburner, M., Ball, C. A., Blake, J. A., Botstein, D., Butler, H., Cherry, J. M., Davis, A. P., Dolinski, K., Dwight, S. S., Eppig, J. T., *et al.* 2000 Gene ontology: tool for the unification of biology. The Gene Ontology Consortium. *Nat Genet*. **25**, 25-29. (10.1038/75556)

56 Szklarczyk, D., Franceschini, A., Wyder, S., Forslund, K., Heller, D., Huerta-Cepas, J., Simonovic, M., Roth, A., Santos, A., Tsafou, K. P., *et al.* 2015 STRING v10: protein-protein interaction networks, integrated over the tree of life. *Nucleic Acids Res*. **43**, D447-452. (10.1093/nar/gku1003)

A

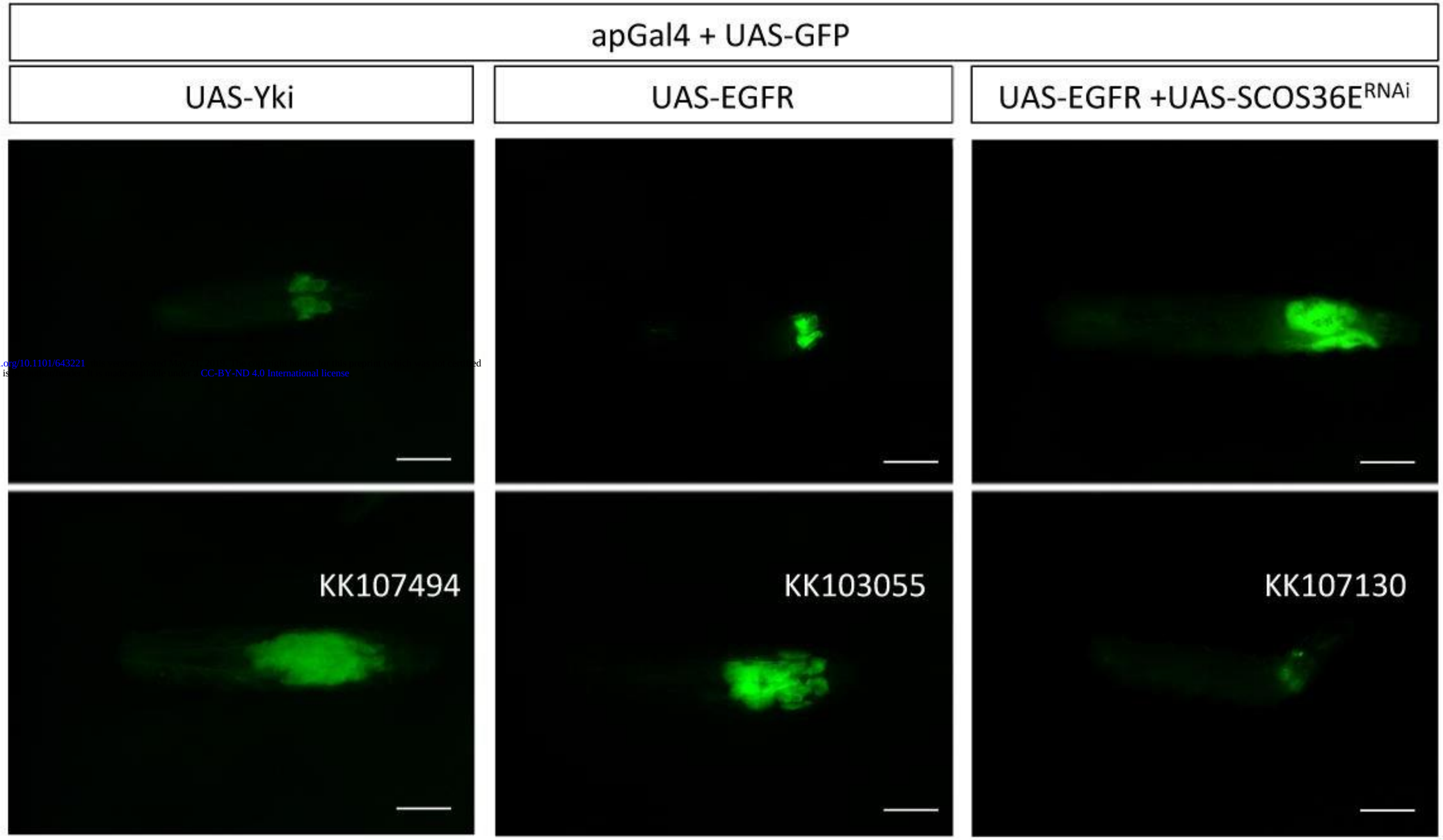

B

	UAS-YKI	UAS-EGFR	UAS-EGFR + SOCS36E RNAi
# Screened	8798	8795	8948
Confirmed Positives	904	74	32
overlap Yki/EGFR	21		
Confirmed Positives with human orthologs	582	48	31
overlap Yki/EGFR	12		

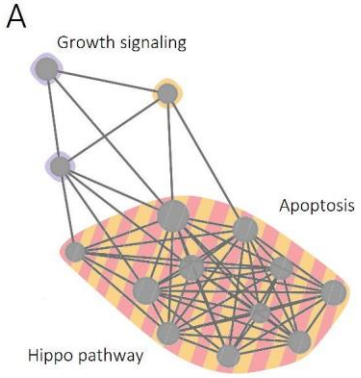
A
Growth signaling
Apoptosis
Hippo pathway

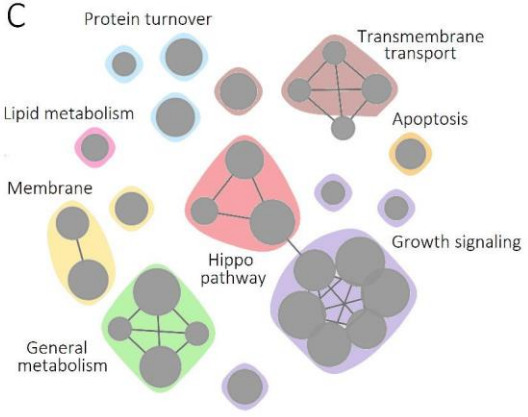
C
Protein turnover
Transmembrane transport
Lipid metabolism
Apoptosis
Membrane
Hippo pathway
Growth signaling
General metabolism

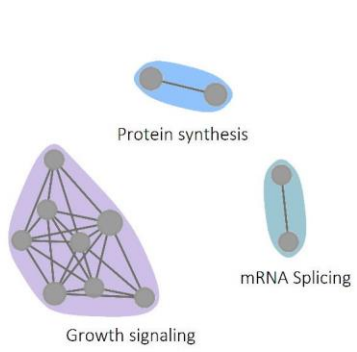
E
Protein synthesis
mRNA Splicing
Growth signaling

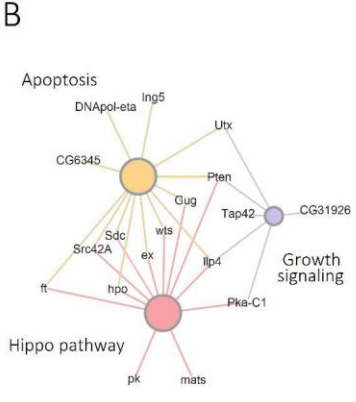
B
Apoptosis
lng5
DNApol-eta
Utx
CG6345
Pten
Gug
Tap42
CG31926
Sdc
wts
Src42A
ex
Ilp4
Growth signaling
ft
hpo
Pka-C1
Hippo pathway
pk
mats

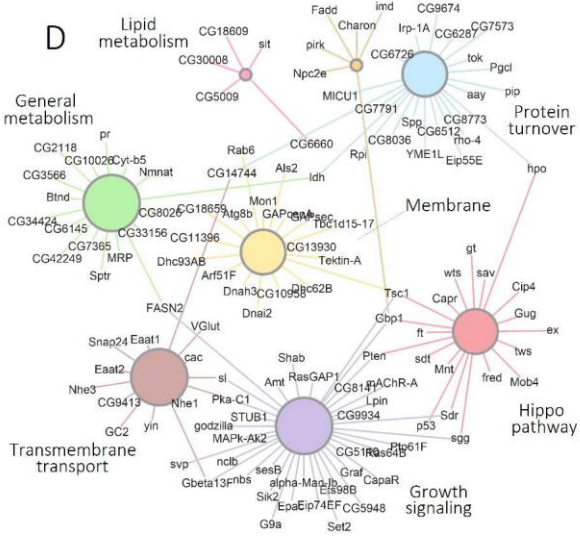
D
Lipid metabolism
CG18609
sit
CG30008
CG5009
Fadd
imd
CG9674
Charon
Irp-1A
CG6287
CG7573
pirk
CG6726
tok
Npc2e
Pgcl
MICU1
aay
pip
CG7791
Spn
CG8773
CG6512
rho-4
CG8036
YME1L
Eip55E
hpo
Protein turnover
General metabolism
pr
CG2118
CG10026
Cyt-b5
CG3566
Nmnat
CG6660
Rpi
Rab6
CG14744
Als2
Idh
Btnd
CG8026
CG18659
Atg8b
GAPcenA
Sec61d15-17
Membrane
CG34424
CG6145
CG33156
CG11396
CG13930
Tektin-A
CG7365
CG42249
MRP
Sptr
Dhc93AB
Arf51F
Dnah3
CG10958
Rbc62B
Dnai2
FASN2
VGlut
Tsc1
Capr
Cip4
Gug
ex
Gbp1
ft
wts
sav
gt
Snap24
Eaat1
Eaat2
Nhe3
CG9413
cac
sl
Nhe1
Pka-C1
STUB1
GC2
yin
godzilla
MAPk-Ak2
Shab
Amt
RasGAP1
mAChR-A
CG8144
Lpin
CG9934
Pten
sdt
Mnt
fred
Mob4
tws
Sdr
p53
sgg
Hippo pathway
Transmembrane transport
svp
nclb
sesB
Gbeta13F
nbs
alpha-Man-Ib
Ptp61F
Ras64B
Graf
CapaR
Ets98B
Sik2
Eip74EF
CG5948
Growth signaling
G9a
Set2

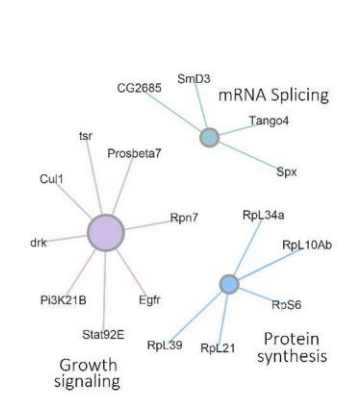
F
CG2685
SmD3
mRNA Splicing
Tango4
tsr
Prosbeta7
Spx
Cul1
Rpn7
RpL34a
drk
RpL10Ab
Pi3K21B
Egfr
RpS6
Stat92E
RpL39
RpL21
Protein synthesis
Growth signaling

A

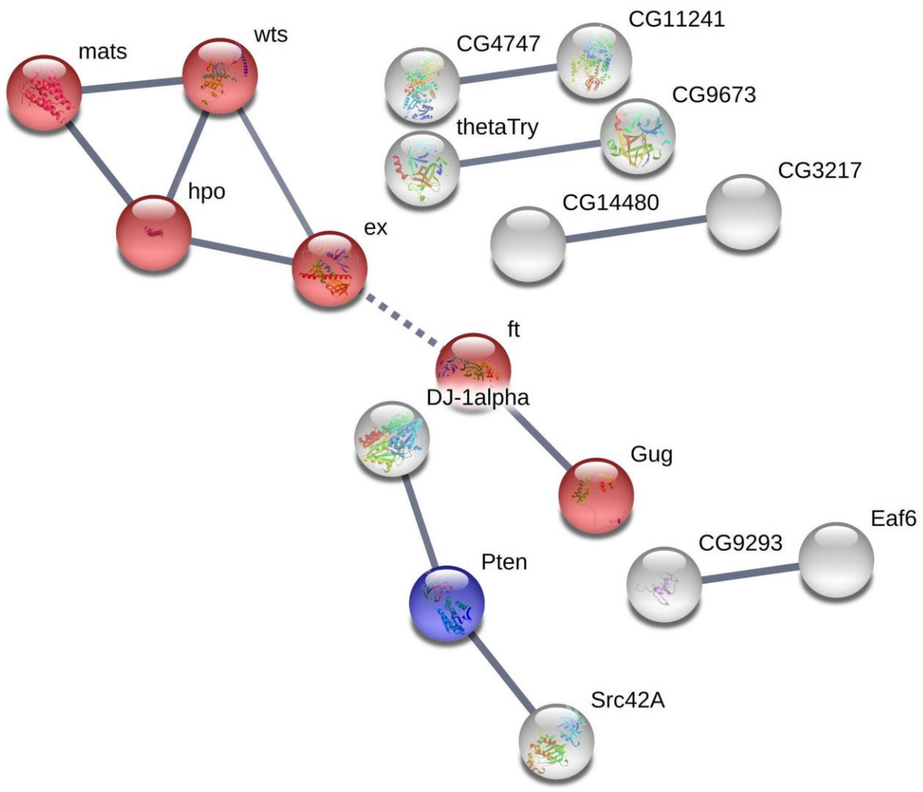

C

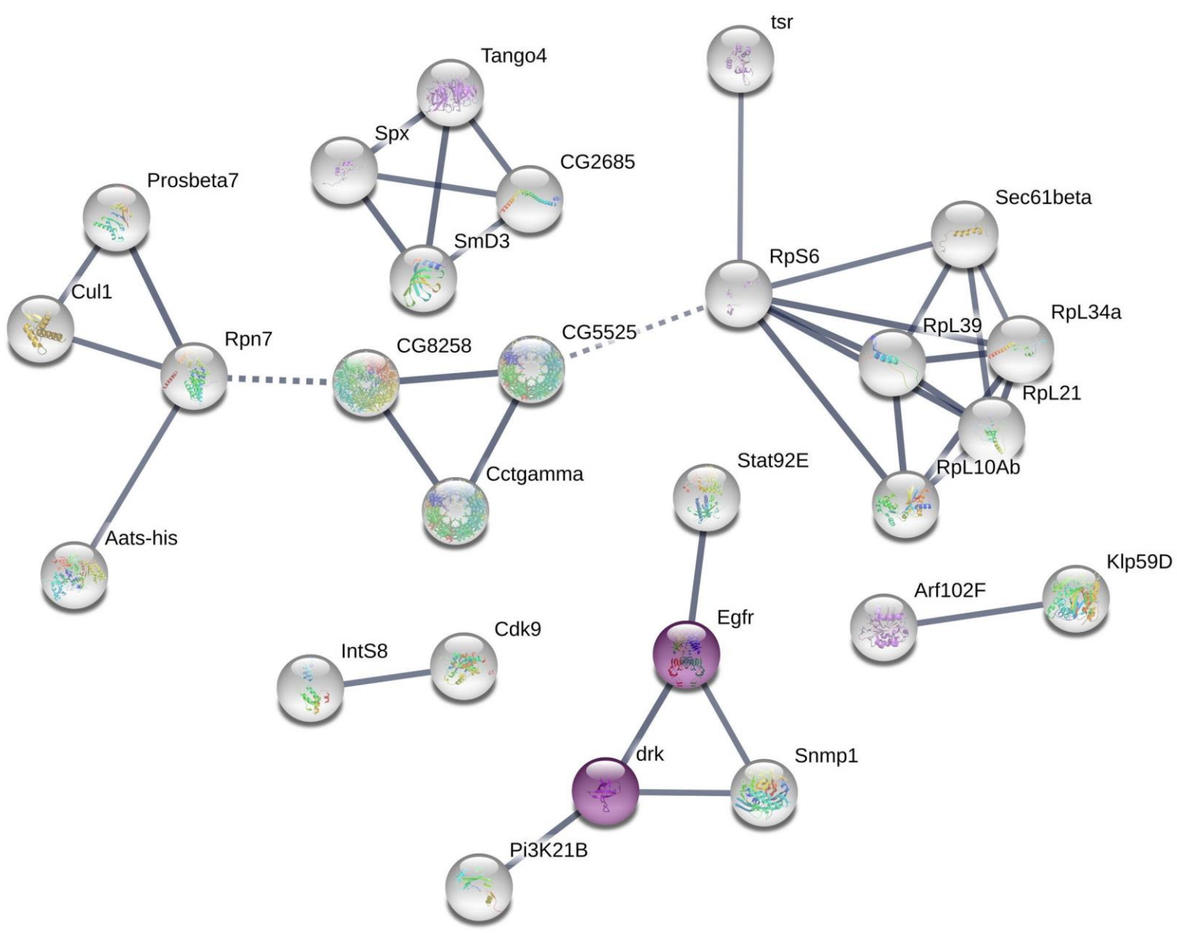

B

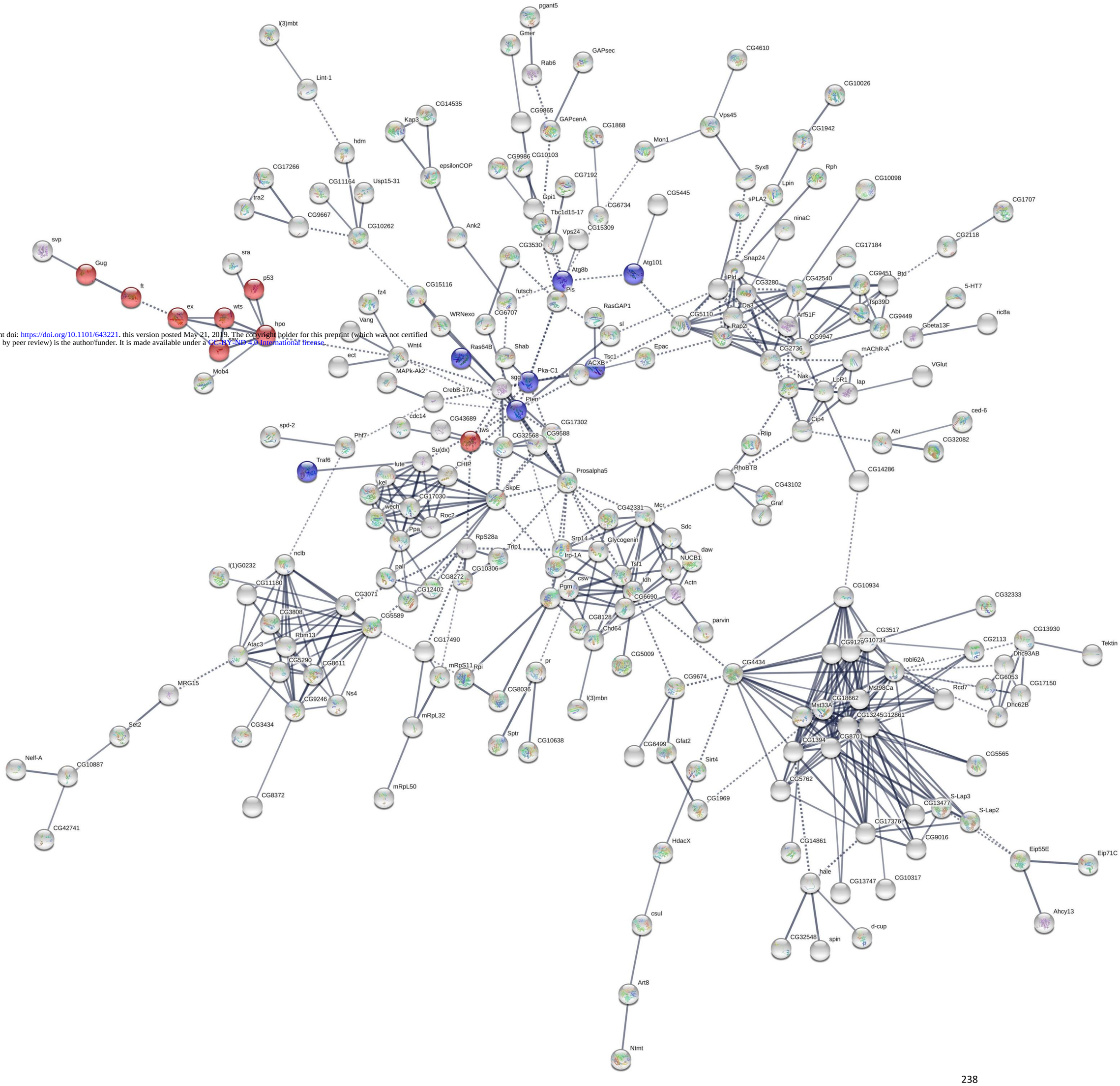

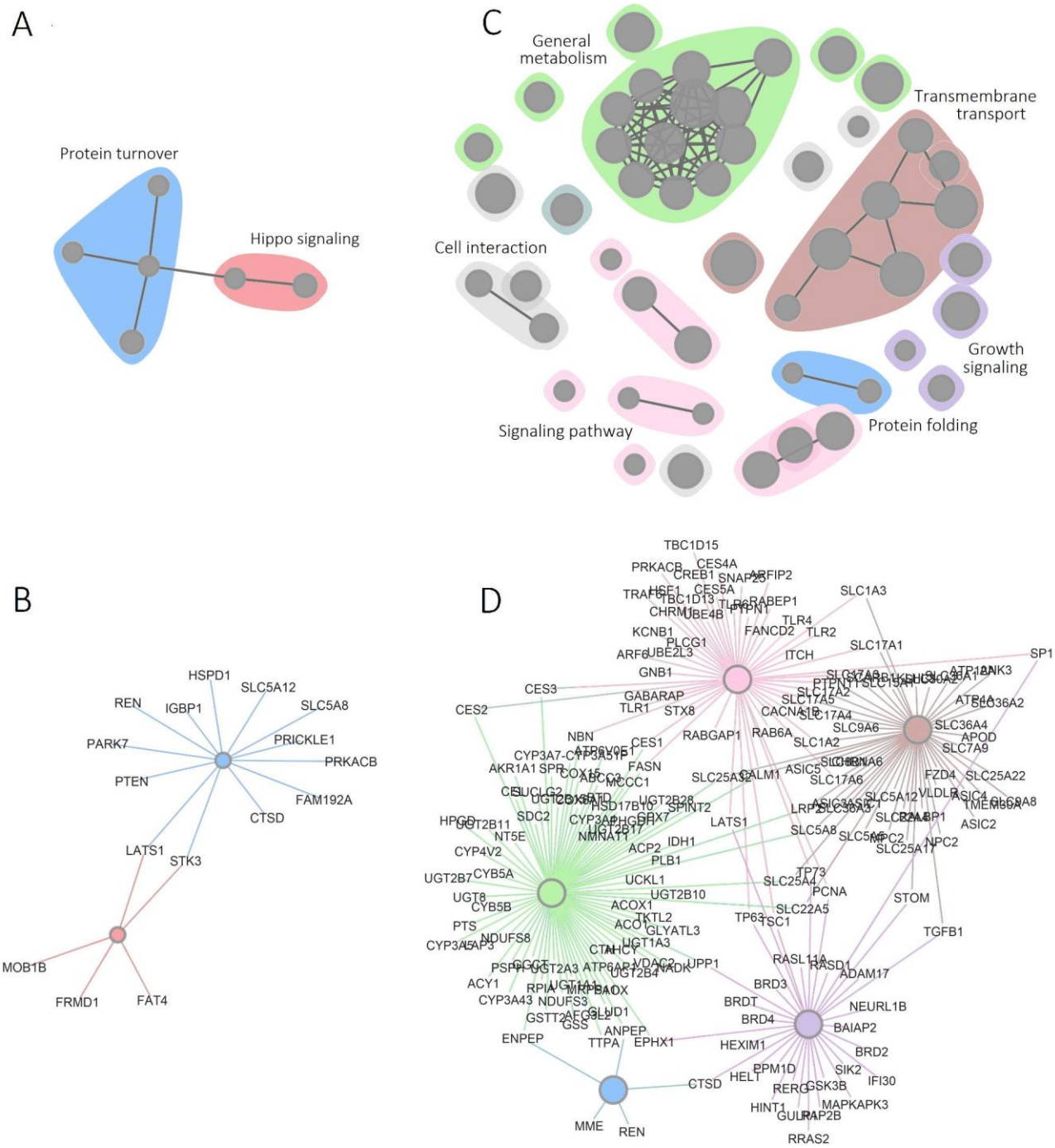

PTPN11/SHP2 negatively regulates growth in breast epithelial cells: implications on tumorigenesis

Madhumita Chakladar[1]*, Madhumathy G Nair[2], Jyothi S Prabhu[2], T S Sridhar[2], Devaki Kelkar[3,4], Madhura Kulkarni[3,4], LS Shashidhara[1,4]

[1]Department of Biology, Indian Institute of Science Education and Research, Pune, India (http://www.iiserpune.ac.in/)

[2]Division of Molecular Medicine, St Johns Research Institute, Bangalore, India (https://www.sjri.res.in/)

[3]Prashanti Cancer Care Centre (https://www.prashanticancercare.org/) and [4]Centre for Translational Cancer Research, Pune, India (https://www.ctcr.in/)

[5] Department of Biology, Ashoka University, Sonipat, India (https://www.ashoka.edu.in/)

*Author of correspondence: madhumita.chakladar@students.iiserpune.ac.in

Author contributions

MC, TSS and LSS conceived, designed and coordinated the study.

MC, MGN, JSP, MK designed various experiments and standardised all protocols. MC carried out all experiments.

MC and DK analysed the TCGA and METABRIC data MC and LSS drafted the manuscript.

All authors gave final approval for publication and agree to be held accountable for the work performed therein.

Abstract

PTPN11/SHP2, a non-receptor protein tyrosine phosphatase is a prominent target of the receptor tyrosine kinase that participates in positive feedback signalling of the human epidermal growth factor receptors and helps in growth and migration. PTPN11/SHP2 is widely believed to be an oncoprotein, although it's possible tumor-suppressor role is also reported. Our analysis of breast cancer metadata shows, PTPN11/SHP2 copy number loss in luminal A subtype is correlated to poor disease-specific survival and late-stage cancer at diagnosis. Analysis of the level 4 Reverse Phase Protein Array (RPPA) data available on the TCGA database resulted in positive correlations between the lower expression levels of constitutively active variant, the phospho-SHP2-Y542, of PTPN11/SHP2 and larger tumor size and lymph node positivity. We experimentally examined possible negative regulation of growth by PTPN11/SHP2 using MCF10A, a normal breast epithelial cell line. Knock-down of PTPN11/SHP2 resulted in increased cell migration, cell shape changes to mesenchymal morphology, and increased survival in cells treated with epirubicin, a DNA-damaging drug. However, it did not alter the rate of cell proliferation. It is possible that PTPN11/SHP2 might function as a tumor suppressor by potentiating proliferating cells with increased cell migration and resistance to apoptosis.

Statement of Significance

Molecules like *PTPN11*/SHP2, among many others that show dual specificity in tumorigenesis in the same tissue depending on the upstream signaling cues, present challenges in the field of targeted drug therapy. This study puts forth the importance of understanding the mechanism of one of the two outcomes and thereby helps better clinical management of a subgroup of cancer.

Introduction

Src homology phosphatase 2 (SHP2) is encoded by the PTPN11 gene. PTPN11/SHP2 has two N terminal SH2 domains, N-SH2 and C-SH2, a middle phosphatase domain, and a C terminal proline-rich tail with tyrosine 542 and 580 which are phosphorylated for catalytic activation of the phosphatase by Src Kinases (Neel, Gu, and Pao 2003; Zhao, Sedwick, and Wang 2015). Characterization of phosphorylation profile regulated by PTPN11/SHP2 activity and its localization has identified 53 different proteins including ERK, P38, and many adhesion kinases (Corallino et al. 2016).

PTPN11/SHP2 is one of the few phosphatases demonstrated to have oncogenic properties. Over-expression of PTPN11/SHP2 is shown to correlate to aggressive clinical manifestations of gastric cancer (Kong et al. 2017), hepatocellular carcinoma (Han et al. 2015), laryngeal carcinoma (Gu et al. 2014), small cell lung cancer (Yang et al. 2017), thyroid cancer (Hu et al. 2015), ovarian cancer (Hu et al. 2017), glioblastoma (Sturla et al. 2011), colorectal cancer (Yu et al. 2011), pancreatic ductal adenocarcinoma (Zheng et al. 2016) and oral cancer (Xie et al. 2014). Its tumorigenic function is known to be associated with the activation of ERK and PI3-AKT pathways (Aceto et al., 2012 and Zhang et al., 2016). A contrasting tumor suppressor role is also reported for PTPN11/SHP2 in hepatocellular cancer (Bard-Chapeau et al., 2011) and oesophageal squamous cell cancer (Qi et al., 2017), which is mediated by the dephosphorylation of pSTAT3.

In the context of breast cancer, while PTPN11/SHP2 expression levels do not correlate to any intrinsic molecular subtype, its overexpression is associated with the poor overall survival in ER-positive-Ki67 low, Luminal A patients and ER-positive-Ki67 high, Luminal B/HER^{-} patients (Muenst et al. 2013). Furthermore, PTPN11/SHP2 is reported to repress let-7 miRNAs in HER2 overexpressing breast epithelial cells (Aceto et al. 2012). Increased co- expression of PTPN11/SHP2 and EGFR is also correlated to basal-like and triple-negative breast cancer (Matalkah et al. 2016). Breast cancer is one of the well-studied cancers, both at

the clinical and the molecular levels. Two major cancer databases, the METABRIC (specific to breast cancer) and TCGA, both house high quality datasets for breast cancer. Using those databases and experimental validation, here we report our results of the study exploring possible tumor suppressor role for PTPN11/SHP2 in the context of breast cancer.

In contrast to earlier reported oncogenic role in breast cancer, our analysis of breast cancer meta data using both TCGA and METABRIC databases indicate a tumor-suppressor role for PTPN11/SHP2. We further experimentally validated this observation using MCF10A, a non-transformed breast epithelial cell line. siRNA mediated knockdown of PTPN11/SHP2 in MCF10A promotes hallmarks of cancer like increased cell migration and decreased chemosensitivity to epirubicin, although it did not affect cell proliferation.

Results

Clinical Correlations of PTPN11/SHP2 copy number changes in Luminal A Subtype: We examined the correlation of PTPN11 copy number status with clinical parameters across the PAM50 subtypes of breast cancer (Bernard et al. 2009). We did not include a subset of patients with claudin-low status for our analysis as it was not defined in the PAM50 classification. We observed a significant association of PTPN11/SHP2 to certain clinical parameters within the Luminal A subtype in the METABRIC database. Copy number loss for PTPN11/SHP2 was correlated to late-stage cancer (Figure 1A) and nodal positivity (Figure 1B), but not to the age of patients at diagnosis (Fig. 1C), or their tumor size (Fig. 1D) and grade (Fig. 1E). More importantly, copy number loss was significantly associated with the poor disease-free survival (Fig. 1F) in Luminal A subtype of the breast cancer.

Clinical Correlation of Phospho (tyrosine 542) PTPN11/SHP2 protein expression in Luminal A subtype

To re-confirm our gene-level observation described above at the protein level, we examined if the correlations between phospho-SHP2 (functionally active form of the protein) and the clinical parameters using the proteome data available in the TCGA breast cancer database. We grouped Luminal A breast cancer patients into two groups, those expressing high (above 3rd quartile) and low (below 1st quartile) levels of phospho-SHP2. Lower levels of expression of phospho-SHP2 protein correlated to larger tumor size (Fig. 2A) and nodal positivity (Fig. 2B), while there was no significant correlation to age (Fig. 2C) of the patients at first diagnosis or metastasis (Fig. 2D) and stage (Fig. 2E) of the cancer. Based on these two observations, we hypothesized that PTPN11/SHP2 may function as a tumor suppressor possibly under specific contexts, perhaps those that are associated specifically with the Luminal A subtype of breast cancer.

Effect of the knockdown of PTPN11/SHP2 on the proliferation of MCF10A cell line Knockdown of PTPN11/SHP2 in luminal A cell line, such as T47D, has been reported to decrease migration rate and EMT (Sun et al. 2017), while inhibition of PTPN11/SHP2 in luminal B cell line, MCF7, decreases cell growth (Li et al. 2014). This is in accordance with the oncogenic function of PTPN11/SHP2. However, as described above we observed that lower levels of phospho-SHP2 are associated with larger tumor size in luminal A subtype of breast cancer patients. We sought to verify possible tumor suppressor role of PTPN11/SHP2 by studying the effects of its loss in the transformation of, otherwise, normal breast epithelial cells. Using normal cells was important to examine the molecular context of its tumor suppressor role unperturbed by hormonal receptor signaling. We silenced PTPN11/SHP2 in MCF10A, a non-transformed breast epithelial cell line. We successfully knocked down PTPN11/SHP2 in

the monolayer culture of MCF10A with two independent siRNAs (hereafter referred as PTPN11/SHP2#si18 and PTPN11/SHP2#si19). We achieved 50-70% depletion of SHP2 protein (Suppl. FigS1A, B) and 80-90% depletion of PTPN11 mRNA expression (Suppl. FigS1C) in transfected MCF10A cells. First, we examined effects on proliferation and survival of MCF10A cells. We used the proliferation marker Ki67 to monitor rate of cell proliferation. We did not observe any significant change in the proliferation index of MCF10A cells due to the knock-down of PTPN11/SHP2 (Fig. 3A, B). We also examined degree of survival of PTPN11/SHP2-depleted cells by MTT assay. We measured cell survival at 72 hours (Day 0), 96 hours (Day 1), 120 hours (Day 2), 144 hours (Day 3) of first transfection. We did not observe any effect on the survival of non-transformed MCF10A breast epithelial cells (Fig. 3C, D).

Effect of PTPN11/SHP2-depletion on cell number and cell size

As lower levels of phospho-SHP2 is correlated to larger tumor size (Fig. 2A), we next examined the effect of knockdown of PTPN11/SHP2 on cell size and cell number. Here too we did not observe any effect (Fig. 3E, F). In Summary, we did not observe any significant change in any of the growth parameters of MCF10A due to the knockdown of PTPN11/SHP2 in MCF10-A cells.

Effect of PTPN11/SHP2-depletion on cell cycle profile

PTPN11/SHP2 is known to regulate cell cycle checkpoints at G1-S transition (Tsang et al. 2012), G2-M phase (Yuan et al. 2005), and transition from metaphase to anaphase (Liu, Zheng, and Qu 2012) upon DNA damage. We did not observe any effect on the cell cycle pattern in MCF10A cells depleted for PTPN11/SHP2 (Fig. 4). We also assessed the effects of the knockdown of PTPN11/SHP2 in the background of induced DNA damage (using epirubicin:

also see below). We did not observe changes in cell cycle patterns upon epirubicin treatment of MCF10A cells in the background of PTPN11/SHP2 knockdown (Suppl. Fig. S2).

Effect of the knockdown of PTPN11/SHP2 on cell migration and invasion

We next assessed the effect of PTPN11/SHP2 knockdown on other hallmarks of cancer such as cell migration using the standard scratch assay and invasion using the transwell invasion assay. We observed that PTPN11/SHP2-depleted cells migrate 25% more in 24 hours of initial scratch (Fig. 5A, B). Interestingly, we also observed a change in cell morphology. Normally confluent monolayer of MCF10A cells appear cobblestone-like, whereas on PTPN11/SHP2- depleted cells acquired mesenchymal or elongated morphology (Fig. 5C). However, we did not observe any change in the invasion capacity (Fig. 5D) of PTPN11/SHP2-depleted cells in either serum-free or the media supplemented with 5% horse serum using both si18 (Figure 5E) and si19 (Fig. 5F).

Effect of the knockdown of PTPN11/SHP2 on epithelial to mesenchymal transition

We examined if the increased cell migration and the mesenchymal morphology of observed in PTPN11/SHP2-depleted MCF10A cells is an indication of epithelial to mesenchymal transition (EMT). We assessed whether depletion of PTPN11/SHP2 affects the expression of mesenchymal markers E-cadherin, N-cadherin, MMP9, Fibronectin and Vimentin. We observed approximately 2-fold increases in MMP9 (Fig. 6A), Vimentin (Fig. 6B) and Fibronectin (Fig. 6C) expression with near significance across both the siRNAs. We did not observe any change in E-cadherin levels (Fig. 6D) and could not detect N-cadherin at the desired molecular size (data not shown). We also examined the levels □-catenin by immunofluorescence, but could not detect any changes either in the nucleus or the cytoplasm

(data not shown). Nonetheless, increased cell migration in the absence of any change in cell proliferation observed in PTPN11/SHP2-depleted cells could be due to increased EMT.

Effect of the knockdown of PTPN11/SHP2 on the sensitivity to chemotherapeutic drugs

PTPN11/SHP2 plays a critical role in cell cycle checkpoint regulation and apoptosis upon DNA damage. PTPN11/SHP2-depletion has been reported to interfere with CHK1 activation and delay in both Cyclin E accumulation and G1-S arrest (Tsang et al. 2012). Moreover, catalytically active PTPN11/SHP2 modulates PLK1 and Aurora B activity to regulate chromosomal alignment, and thereby restoring checkpoint function at metaphase (Liu, Zheng, and Qu 2012). Alternatively, kinase-inactive PTPN11/SHP2 is involved in regulating nuclear Cdc25C translocation to the cytoplasm through 14-3-3β and inducing G2-M arrest (Yuan et al. 2005). PTPN11/SHP2 is also reported to mediate apoptosis via regulating c-ABL and caspases (Morales et al. 2014; Yuan et al. 2003). We examined the response of MCF10A cells to the treatment with DNA-damaging chemotherapeutic drug in the presence and absence of PTPN11/SHP2. We treated cells with chemotherapeutic drugs like carboplatin, epirubicin, and paclitaxel. Carboplatin inhibits replication and transcription and induces DNA breaks and cell death (Jiang et al. 2015). Epirubicin intercalates between DNA and inhibits DNA and RNA synthesis, it induces double-stranded DNA breaks and cell death (Konecny et al. 2001). Paclitaxel interferes with mitotic spindle assembly and chromosomal segregation and cell death (Jordan and Wilson 2004). We determined the Inhibitory Concentration (IC) 50 of these cell cycle and DNA synthesis interfering drugs. We used concentration in range of 100□M to 1000□M for carboplatin, 100nM-100□M for epirubicin, and 10nM-100□M for paclitaxel to optimize the IC50. We observed that MCF10A had high IC50 for carboplatin, while paclitaxel was not effective in at the concentration range tested (Suppl. Fig. S3). IC50 for epirubicin was 1□M (Suppl. Fig. S3) and this drug dose was chosen for subsequent experiments. Ability of

epirubicin to introduce double-stranded DNA breaks in MCF10A cells was confirmed by measuring the levels of phosphorylated (of Serine 139) □-H2AX (Suppl. Fig. S4).

We observed that PTPN11/SHP2-depleted cells show better survival upon epirubicin treatment at 24 hours compared to the normal cells (Fig. 7A, B). We examined if increased viability of PTPN11/SHP2-depleted cells to epirubicin treatment is associated with changes in apoptosis or cell cycle patterns. We observed that PTPN11/SHP2-depleted cells had a 2-fold decrease in early apoptotic cells (Annexin positive), late apoptotic cells (Annexin +PI double- positive) and dead cells (PI-positive) (Fig. 7C, D). However, PTPN11/SHP2-depleted cells did not affect the ploidy or cell cycle pattern when treated with epirubicin (Supplementary Figure 2). Nonetheless, decreased chemosensitivity to epirubicin in PTPN11/SHP2-depleted cells is associated with the inhibition of apoptosis.

In summary, increased cell migration, change in cell morphology, increased EMT and decreased chemosensitivity and apoptosis in response to drug treatment suggest a tumor suppressor role for PTPN11/SHP2, albeit in certain contexts.

Discussion

PTPN11/SHP2, a non-receptor tyrosine phosphatase, participates in positive feedback regulation of EGFR pathway and drive hematologic malignancies and solid tumors including breast adenocarcinoma, prostate adenocarcinoma, lung adenocarcinoma and colorectal cancer (Aceto et al., 2012; Prahallad et al., 2015; Richine et al., 2016; Schneeberger et al., 2015; Zhang et al., 2016). In contrast to its oncogenic role, PTPN11/SHP2, through suppression of the JAK/STAT pathway, seems to function in inhibiting oncogenesis in hepatocellular carcinoma and esophageal squamous cell cancer (Bard-Chapeau et al. 2011; Qi et al. 2017). These observations suggest that PTPN11/SHP2 may function either as an oncogene or a tumor suppressor, perhaps in different cellular and molecular contexts. To verify this, we carried out

a retrospective investigation of publicly available clinical metadata followed by experimental validation of our hypothesis. The oncogenic function of PTPN11/SHP2 has been reported in the backgrounds of HER2, EGFR, WNT and PI3K-AKT in breast cancer (Aceto et al. 2012; Zhao and Agazie 2015; Zhang et al. 2016).

In our analysis of breast cancer data from METABRIC and TCGA datasets, PTPN11/SHP2 does not appear to affect the clinical outcomes of the HER2-driven breast cancer or the TNBC (data not shown). However, we observed putative tumor suppressor function for PTPN11/SHP2 in Luminal A subtype of breast cancer. The copy number loss of PTPN11/SHP2 in Luminal A subtype of METABRIC cohort correlates to late-stage cancer and poor disease-specific survival. Furthermore, lower levels of expression of Phospho- PTPN11/SHP2 in luminal A correlates to larger tumor size and greater lymph node positivity in TCGA dataset. A detailed pathway enrichment analysis of phosphoproteins in TCGA RPPA Level 4 2015 data when correlated to phospho-PTPN11/SHP2 Y542 expression levels could give us insights into the context in which it may function as a tumor suppressor in the luminal A subgroup of patients in TCGA cohort. As PTPN11/SHP2 is a phosphatase, its phosphoprotein expression rather than gene expression and its implications on proteins and phospho-proteins of cancer patients is relevant in the identification of the upstream cues that is responsible for switching between its dual role in tumorigenesis. TCGA level 4 RPPA data provides the expression of a limited number of 225 protein and phosphoprotein data which could be used to understand the context of PTPN11/SHP2 function.

Experimental validation of our clinical results by transient silencing of PTPN11/SHP2 in non-transformed MCF10A showed that knockdown of PTPN11/SHP2 promotes migration, changes in cell shape to mesenchymal morphology and decreased sensitivity to chemotherapeutic drug, epirubicin, by decreasing apoptosis. Mechanistic understanding of the tumor suppressor role of PTPN11/SHP2 from our study suggests regulation of EMT molecules

to limit transformation and migration of breast epithelial cells. We also report the involvement of PTPN11/SHP2 in sensitizing MCF10A cells to chemotherapeutic drugs such as epirubicin by regulating apoptosis. The phosphatase activity of nuclear PTPN11/SHP2, in response to DNA damage, in embryonic fibroblast cells activate c-ABL kinase via its SH3 domain, which in turn stabilizes P73 and allow transcription of target genes including $P21^{Cip1}$ and BAX to initiate apoptosis (Yuan et al. 2003). PTPN11/SHP2 is also reported to mediate Rb/E2F associated apoptosis possibly by caspase8 and caspase3 activation along with PTP-1B and PTEN (Morales et al. 2014). We did not observe any change in BAX (Suppl. FigS5) or caspase 3 expression (data not shown) in PTPN11/SHP2-depleted cells with or without drug treatment. In summary, while PTPN11/SHP2 may activate apoptosis when cells are subjected to severe DNA damage (such as drug treatment), understanding the precise molecular pathway/s needs further analysis. Being a phosphatase, PTPN11/SHP2 may not behave like a classical tumor suppressor. It may function in a dose-dependent manner. Suboptimal levels above wildtype such as gain of copy number could allow it to behave differently, depending on upstream molecular cues/contexts.

Methods

Clinical data analysis

For all analyses, data from METBRIC 2012 and TCGA 2015 was used. METABRIC data was downloaded from cbioportal (Cerami et al. 2012) and TCGA GRCh38 data from the GDC data portal using the GenomicDataCommons R tool (Morgan M, Davis S (2019). *GenomicDataCommons:NIH/NCIGenomicDataCommonsAccess*. (https://bioconductor.org/packages/GenomicDataCommons, http://github.com/Bioconductor/GenomicDataCommons.).

The TCGA RPPA level 4 data was downloaded from FireBrowse (firebrowse.org). The clinical metadata analysis was performed using R (version 3.6.1, platform x86_64-w64-mingw32/x64). Packages used for analysis include survminer_0.4.6, ggpubr_0.2.3, magrittr_1.5, survival_2.44-1.1, forcats_0.4.0, stringr_1.4.0, purrr_0.3.3 8, readr_1.3.1, tidyr_1.0.0, tibble_2.1.3, ggplot2_3.2.1, tidyverse_1.2.1, dplyr_0.8.3. For TCGA RPPA data analysis additional packages Hmisc_4.2-0, Formula_1.2-3, lattice_0.20-38 was used. Kruskal-Wallis, Wilcoxon, and log-rank test were used for statistical analysis, $p<0.05$ was considered significant.

Cell culture

MCF10A cells were harvested in DMEM media (#10566-016, Thermofisher Scientific) with 100units/ml of Penstrep (#15140122). Growth media was supplemented with 5% horse serum (#26050088, GIBCO) and 20ng/ml of EGF (#E9644, Sigma), 0.5ug/ml of hydrocortisone (#H0888-5G, Sigma), 100ng/ml of cholera toxin (#C8052-1MG, Sigma) and 10ug/ml of insulin (# I1882-100MG, Sigma).

Mycoplasma Testing

Cells were routinely checked for mycoplasma contamination and cleared (if any) using LookOutO mycoplasma elimination Kit (#MP0030).

Cell Passaging

Monolayer MCF10A cells from passage 23 to passage 32 were used for all experiments. Media from monolayer cells was aspirated, rinsed with DPBS (3D8537-500ML), and trypsinised for 10-15 mins using 0.05% Trypsin EDTA (# 25300054, Thermofisher Scientific). The cells were incubated at 37^{o}C, 5% CO2; dissociated cells were resuspended in DMEM with 10% horse serum and centrifuged at 2000 RPM, 6mins. Cells were seeded in a 1:4 ratio and they reach confluency of 80-90% by 3-4 days. The cells were cultured for 6 passages at any time and discarded.

siRNA transfection

Cells were seeded at 0.16 million per 6 well and scaled down according to the plate used. 24 hours post-seeding, cells were rinsed in DPBS and grown in serum-free media (growth media without horse serum and pen strep) 24 hours before transfection. Cells were transfected using lipofectamine RNAi max (#13778150, Thermofisher Scientific) and two independent Accell siRNA-PTPN11, Targeted Region: 3'UTR (A-003947-18-0005, denoted as **#18** and A-003947- 19-0010, denoted as **#19**) at 500nM and 1uM concentrations, respectively, in serum-free media. The equimolar concentration of siLACZ was used as control for each. 24 hours post- transfection, the transfection media was aspirated out and cells were replenished with growth media. Following 48 hours of transfection, growth media was aspirated out and cells were rinsed in serum-free media 1 hour before the second shot of transfection. Cells were again transfected and 48 hours post-second transfection all experiments were carried out. All experiments were carried out using both the siRNA, data for si18 is shown. Knockdown efficiency was 60-70% estimated at the protein level. The sequences for the siLACZ used are: LACZ: 5'-CGUACGCGGAAUACUUCGA-3'

3'-GCAUGCGCCUUAUGAAGCU-5'

(dTdT overhang)

RNA isolation and RT-qPCR

Total RNA was isolated using TRIzol reagent (Sigma) and estimated using nanodrop. 500ng RNA was converted to cDNA with superscript III first-strand synthesis for RT-PCR (#1191- 7010). Synthesized RNA was diluted in DNAse free water and mixed with SYBR fast qPCR master mix from Kappa biosystems (KK4601) and processed using the BioRad CFX96 real- time qPCR system. All mRNA quantification of the target gene was optimized to housekeeping control, GAPDH, or an average of housekeeping controls (ACTB, RPLPO, or PUM1) and quantitated using the ΔΔCT method or average RNU. Primer sequences used are as follows:

Gene	Sequence
PTPN11	F: CGGAAAGTGTGAAGTCTCCAG
	R: GCGGGAGGAACATGACATC
GAPDH	F: AATGAAGGGGTCATTGATGG
	R: AAGGTGAAGGTCGGAGTCAA
B-Actin	F: TTCCTGGGCATGGAGTC
	R: CAGGTCTTTGCGGATGTC
RPLPO	F: GGCTGTGGTGCTGATGGGCAAGAA
	R: TTCCCCCGGATATGAGGCAGCAGT
PUM1	F: CCGGAGATTGCTGGACATATAA
	R: TGGCACGCTCCAGTTTC

Cell lysis and Western Blot Hybridization

Cells were washed three times in ice-cold DPBS, followed by addition of cell lysis buffer (RIPA: 20mM Tris (pH=8), 420mM NaCl, 10% glycerol, 0.5% NP40, 0.1mM EDTA, water to add up the volume) and incubated in ice for 40 mins to allow complete lysis. The lysates were collected using a cell scraper and centrifuged at 13,000 RPM, 15mins. The supernatant was collected in labelled tubes and mixed with 1X lamelli buffer and heated at 95 degrees, 5mins. SDS PAGE was run at 70V in stacking gel and at 100V in resolving gel and then transferred to the PVDF membrane for 90mins at 90V. The transferred membrane was blocked in 5% BSA or 5% Milk for 1 hour followed by the addition of primary antibody in 2% BSA or 2% Milk and then incubated overnight at 4 degrees C. Following day, the primary antibody was removed and the membrane was washed thrice with (0.1%) TBST. Secondary antibody conjugated to HRP was added in 1:10,000 dilutions in 2% BSA or 2% milk and incubated for 1hour at room temperature. Secondary antibody incubation was followed by 0.1% TBST wash and developed using an ECL kit (Merck). Densitometry analysis was used for quantitation of protein expression levels using Image J. The expression levels were normalized to housekeeping genes, GAPDH, or β Actin.

Cell Number

PTPN11/SHP2 knocked down cells were trypsinised and centrifuged at 2000 RPM, 6mins. The cell pellets were dissolved in 1ml growth media and counted using a haemocytometer.

Cell Size and Cell Morphology

Immunofluorescence images were captured at 63x oil objective in Leica SP8 confocal microscope. ROI of each cell was calculated for the area using Image J. A total of 100 cells across 3 biological replicates were analysed. At least 60% of the cell population were imaged and analysed for change in morphology.

MTT assay

10ul of 5mg/ml of MTT (#M5655-100MG) was added to 100ul of cells in growth media. Growth media alone as used as blank. We incubated the cells after MTT addition for 3.5 hours at 37ºC and aspirated the media with MTT. Post 3.5 hours, 100ul of DMSO (#D2438-50ml, Sigma) added, kept in a shaker for 5mins and measured absorbance at 570nM and 650nM. **Immunofluorescence microscopy**

Growth media was aspirated and cells were rinsed in DPBS. Cells were fixed with 4% PFA (Sigma) for 10mins. PFA was aspirated and cells were rinsed again in PBS, for 10mins each, repeated thrice. Cells were permeabilised and blocked with 2% FBS in 0.03% PBST (30ul Triton X (Sigma) in 10ml DPBS) for 30mins. Following permeabilization, the primary antibody was diluted in DPBS before adding and incubated overnight at 4 degrees C. Following primary incubation, cells were rinsed in 0.05% PBST (5ul Tween20 (Sigma) in 10ml DPBS) for 10mins each, repeated thrice. Cells were mounted in prolong gold Antifade DAPI or incubated in DAPI (1:1000) for 1 min and washed with DPBS before mounting (#P36931 and D9542).

Wound healing/Scratch assay

Monolayer cells were treated with 10ug/ml of mitomycin C (Sigma M4287) for 2 hours before initial scratch. Cells were wounded using a 10ul sterile micropipette tip. Scratch was rinsed with DPBS, following which growth media were added to wells. Cells were acclimatized at 37ºC for 10mins before recording a 0-hour wound distance. 3 areas per sample were recorded.

24 hours post initial wound, images of the same area recorded for 0-hour were measured with EVOS FL Auto. Wound distance was calculated using ImageJ, an average of 12 data points per sample were used for all analyses. 24-hour wound distance was subtracted from 0-hour wound distance and normalized to 0-hour wound distance (as the initial scratch was not the same across samples) and multiplied by 100 (percentage wound closure). We performed a double normalization by subtracting the percentage wound closure of every sample from its control siLACZ. Data points were plotted in GraphPad prism.

Transwell invasion assay

K913-24 transwell assay kit was used to compare the invasion capacity of PTPN11/SHP2- depleted cells. For invasion assay, we serum-starved PTPN11/SHP2-depleted cells at 72 hours of knockdown (18-24 hours before invasion assay). Cells were then trypsinised and seeded at a concentration of 0.5-1 million cells/collagen-coated wells. 24 hours later, cells that migrated to the lower chamber were assayed using manufacturers protocol.

Flow cytometry and cell cycle analysis

Cells were trypsinised and centrifuged at 2000 RPM, 6mins. The cell pellet was washed with DPBS by gentle vortexing and centrifuged at 2000 RPM, 6mins. The step was repeated twice. Following DPBS wash, cells were fixed in ice-cold 70% ethanol for 30 mins. Post fixation, samples were centrifuged at 2000 RPM, 6mins. The cell pellet was washed with DPBS and centrifuged again at 2000 RPM for 6mins. Cells were treated with RNAse (DS0003) (to remove any RNA contamination) for 5mins in ice. Following incubation, 5ul of Propidium Iodide in a 1million cells/sample was added 5mins before acquisition. The cell cycle profiles were acquired using BD FACS Calibur and BD FACS Celesta. Analysis was performed in BD software.

Apoptosis

Following epirubicin treatment for 24 hours, cells in media supernatant was collected in labelled tubes. Attached cells were trypsinised and collected in the respective tube and centrifuged at 2000 RPM, 6mins, 4°C. Cells were washed with ice-cold DPBS and centrifuged at 2000 RPM, 6mins. Cell pellet was dissolved in ice-cold 90ul 1X Annexin binding buffer and added 5ul of Annexin V and 5ul Propidium iodide. The samples were incubated for 5mins with 0.25mM CaCl2 in dark and imaged and analysed in Operetta, Perkin Elmer.

Antibodies: The following antibodies were used,

Antibody Name	**Catalog number**	**Working Conc.**	**Dilution in**
SHP-2 (D50F2) Rabbit mAb	3397	1:1000	2% BSA
Phospho-SHP-2 (Tyr542) Antibody rabbit mAb	3351	1:1000	2% BSA
Anti-□H2A.X (phospho S139) antibody [9F3]	ab26350	1:10,000	2% Milk
Anti-Ki67 antibody [EPR3610]	ab92742	1:100	DPBS
Anti-MMP9 antibody [EP1254]	ab76003	1:10,000	2% BSA
Purified Mouse Anti-E-Cadherin Clone 36/E-Cadherin (RUO)	610181	1:1000	2% BSA
Purified Mouse Anti-N-Cadherin Clone 32/N-Cadherin (RUO)	610920	1:1000	2% BSA
Purified Mouse Anti-Fibronectin Clone 10/Fibronectin (RUO)	610077	1:1000	2% BSA
□□catenin	#9562S	1:1000/1:500	2% BSA or DPBS
Propidium Iodide - 1.0 mg/mL Solution in Water	P3566	1ul/million cells	DPBS
Annexin V, Alexa Fluor® 488 Conjugate	A13201	5ul/million cells	DPBS
Vimentin	V9 clone, Santacruz	1:1000	2% BSA
□-actin	Santacruz	1:1000	2% BSA
GAPDH	RG000110	1:2500	2% Milk
Secondary Anti-Rabbit Alexa 568	Invitrogen, Molecular probes	1:10,000	DPBS
Secondary Anti-Rabbit Alexa 488	Invitrogen, Molecular probes	1:10,000	DPBS
Secondary Anti-Rabbit HRP	Invitrogen, Molecular probes	1:10,000	2% Milk/BSA
Secondary Anti-Mouse HRP	Invitrogen, Molecular probes	1:10,000	2% Milk/BSA

Statistical Analysis

Column statistics (GraphPad Prism) was used for statistical analysis, $p<0.05$ was considered significant. Unpaired T-Test was used for survival assay. P values are flagged as * ($p<0.05$), ** ($p<0.01$) and *** ($p<0.001$).

Acknowledgements

This work was primarily supported by an Indo-Danish research grant from Department of Biotechnology, Govt. of India to LSS and TSS. JC Bose Fellowship and grant from Department of Science & Technology, Govt of India to LSS. MK is supported by Ramalingswami fellowship from Department of Biotechnology, India. We thank other members of both the laboratories for critical input.

Conflict of interest

We declare “no-conflict-of-interest”.

References

Aceto, Nicola et al. 2012. “Tyrosine Phosphatase SHP2 Promotes Breast Cancer Progression and Maintains Tumor-Initiating Cells via Activation of Key Transcription Factors and a Positive Feedback Signaling Loop.” *Nature Medicine* 18(4): 529–37.

Bard-Chapeau, Emilie A. et al. 2011. “Ptpn11/Shp2 Acts as a Tumor Suppressor in Hepatocellular Carcinogenesis.” *Cancer Cell* 19(5): 629–39.

Bernard, Philip S. et al. 2009. “Supervised Risk Predictor of Breast Cancer Based on Intrinsic Subtypes.” *Journal of Clinical Oncology* 27(8): 1160–67.

Cerami, Ethan et al. 2012. “The CBio Cancer Genomics Portal: An Open Platform for Exploring Multidimensional Cancer Genomics Data.” *Cancer Discovery* 2(5): 401–4.

Corallino, Salvatore et al. 2016. “Alterations in the Phosphoproteomic Profile of Cells

Expressing a Non-Functional Form of the SHP2 Phosphatase." *New Biotechnology* 33(5): 524–36.

Gu, Jia et al. 2014. "SHP2 Promotes Laryngeal Cancer Growth through the Ras/Raf/Mek/Erk Pathway and Serves as a Prognostic Indicator for Laryngeal Cancer." *International Journal of Oncology* 44(2): 481–90.

Han, Tao et al. 2015. "PTPN11/Shp2 Overexpression Enhances Liver Cancer Progression and Predicts Poor Prognosis of Patients." *Journal of Hepatology* 63(3): 651–60. http://dx.doi.org/10.1016/j.jhep.2015.03.036.

Hu, Zhong Qian et al. 2015. "Expression and Clinical Significance of Tyrosine Phosphatase SHP2 in Thyroid Carcinoma." *Oncology Letters* 10(3): 1507–12.

———. 2017. "SHP2 Overexpression Enhances the Invasion and Metastasis of Ovarian Cancer in Vitro and in Vivo." *OncoTargets and Therapy* 10: 3881–91.

Jiang, Shuai et al. 2015. "Paclitaxel Enhances Carboplatin-DNA Adduct Formation and Cytotoxicity." *Chemical Research in Toxicology* 28(12): 2250–52.

Jordan, Mary Ann, and Leslie Wilson. 2004. "Microtubules As a Target For." 4(April). Konecny, Gottfried et al. 2001. "Drug Interactions and Cytotoxic Effects of Paclitaxel in Combination with Carboplatin, Epirubicin, Gemcitabine or Vinorelbine in Breast Cancer Cell Lines and Tumor Samples." *Breast Cancer Research and Treatment* 67(3): 223–33. Kong, Zhi Yuan et al. 2017. "Expression and Clinical Significance of HMGB1 in Gastric Cancer." *Chinese Journal of Cancer Prevention and Treatment* 24(21): 1513–17.

Li, Jun et al. 2014. "Tyrosine Phosphatase Shp2 Mediates the Estrogen Biological Action in Breast Cancer via Interaction with the Estrogen Extranuclear Receptor." *PLoS ONE* 9(7).

Liu, Xia, Hong Zheng, and Cheng Kui Qu. 2012. "Protein Tyrosine Phosphatase Shp2 (Ptpn11) Plays an Important Role in Maintenance of Chromosome Stability." *Cancer Research* 72(20): 5296–5306.

Matalkah, Fatimah, Elisha Martin, Hua Zhao, and Yehenew M. Agazie. 2016. "SHP2 Acts Both Upstream and Downstream of Multiple Receptor Tyrosine Kinases to Promote Basal-like and Triple-Negative Breast Cancer." *Breast Cancer Research* 18(1): 1–14.

Morales, Liza D. et al. 2014. "Protein Tyrosine Phosphatases PTP-1B, SHP-2, and PTEN Facilitate Rb/E2F-Associated Apoptotic Signaling." *PLoS ONE* 9(5): 1–9.

Muenst, Simone et al. 2013. "Src Homology Phosphotyrosyl Phosphatase-2 Expression Is an Independent Negative Prognostic Factor in Human Breast Cancer." *Histopathology* 63(1): 74–82.

Neel, Benjamin G., Haihua Gu, and Lily Pao. 2003. "The 'Shp'ing News: SH2 Domain- Containing Tyrosine Phosphatases in Cell Signaling." *Trends in Biochemical Sciences* 28(6): 284–93.

Prahallad, Anirudh et al. 2015. "PTPN11 Is a Central Node in Intrinsic and Acquired Resistance to Targeted Cancer Drugs." *Cell Reports* 12(12): 1978–85.

Qi, Chen et al. 2017. "Shp2 Inhibits Proliferation of Esophageal Squamous Cell Cancer via Dephosphorylation of Stat3." *International Journal of Molecular Sciences* 18(1).

Richine, B. M. et al. 2016. "Syk Kinase and Shp2 Phosphatase Inhibition Cooperate to Reduce FLT3-ITD-Induced STAT5 Activation and Proliferation of Acute Myeloid Leukemia." *Leukemia* 30(10): 2094–97.

Schneeberger, Valentina E. et al. 2015. "Inhibition of Shp2 Suppresses Mutant EGFR-Induced Lung Tumors in Transgenic Mouse Model of Lung Adenocarcinoma." *Oncotarget* 6(8): 6191–6202.

Sturla, L. M. et al. 2011. "Src Homology Domain-Containing Phosphatase 2 Suppresses Cellular Senescence in Glioblastoma." *British Journal of Cancer* 105(8): 1235–43.

Sun, Xuan et al. 2017. "Shp2 Plays a Critical Role in IL-6-Induced EMT in Breast Cancer Cells." *International Journal of Molecular Sciences* 18(2).

Tsang, Yiu Huen et al. 2012. "Novel Functions of the Phosphatase SHP2 in the DNA Replication and Damage Checkpoints." *PLoS ONE* 7(11).

Xie, Hongjun et al. 2014. "Upregulation of Src Homology Phosphotyrosyl Phosphatase 2 (Shp2) Expression in Oral Cancer and Knockdown of Shp2 Expression Inhibit Tumor Cell Viability and Invasion in Vitro." *Oral Surgery, Oral Medicine, Oral Pathology and Oral Radiology* 117(2): 234–42.

Yang, Xuemei et al. 2017. "Shp2 Confers Cisplatin Resistance in Small Cell Lung Cancer via an AKT-Mediated Increase in CA916798." *Oncotarget* 8(14): 23664–74.

Yu, Shu Jing et al. 2011. "SPARCL1, Shp2, MSH2, E-Cadherin, P53, ADCY-2 and MAPK Are Prognosis-Related in Colorectal Cancer." *World Journal of Gastroenterology* 17(15): 2028–36.

Yuan, Liangping et al. 2003. "Role of SHP-2 Tyrosine Phosphatase in the DNA Damage- Induced Cell Death Response." *Journal of Biological Chemistry* 278(17): 15208–16.

Yuan, Liangping, Wen Mei Yu, Min Xu, and Cheng Kui Qu. 2005. "SHP-2 Phosphatase Regulates DNA Damage-Induced Apoptosis and G 2/M Arrest in Catalytically Dependent and Independent Manners, Respectively." *Journal of Biological Chemistry* 280(52): 42701–6.

Zhang, K. et al. 2016. "Shp2 Promotes Metastasis of Prostate Cancer by Attenuating the PAR3/PAR6/APKC Polarity Protein Complex and Enhancing Epithelial-to- Mesenchymal Transition." *Oncogene* 35(10): 1271–82.

Zhao, S., D. Sedwick, and Z. Wang. 2015. "Genetic Alterations of Protein Tyrosine Phosphatases in Human Cancers." *Oncogene* 34(30): 3885–94.

Zheng, Jiawei et al. 2016. "Expression and Prognosis Value of SHP2 in Patients with Pancreatic Ductal Adenocarcinoma." *Tumor Biology* 37(6): 7853–59.

Figures and Figure Legends

Figure 1

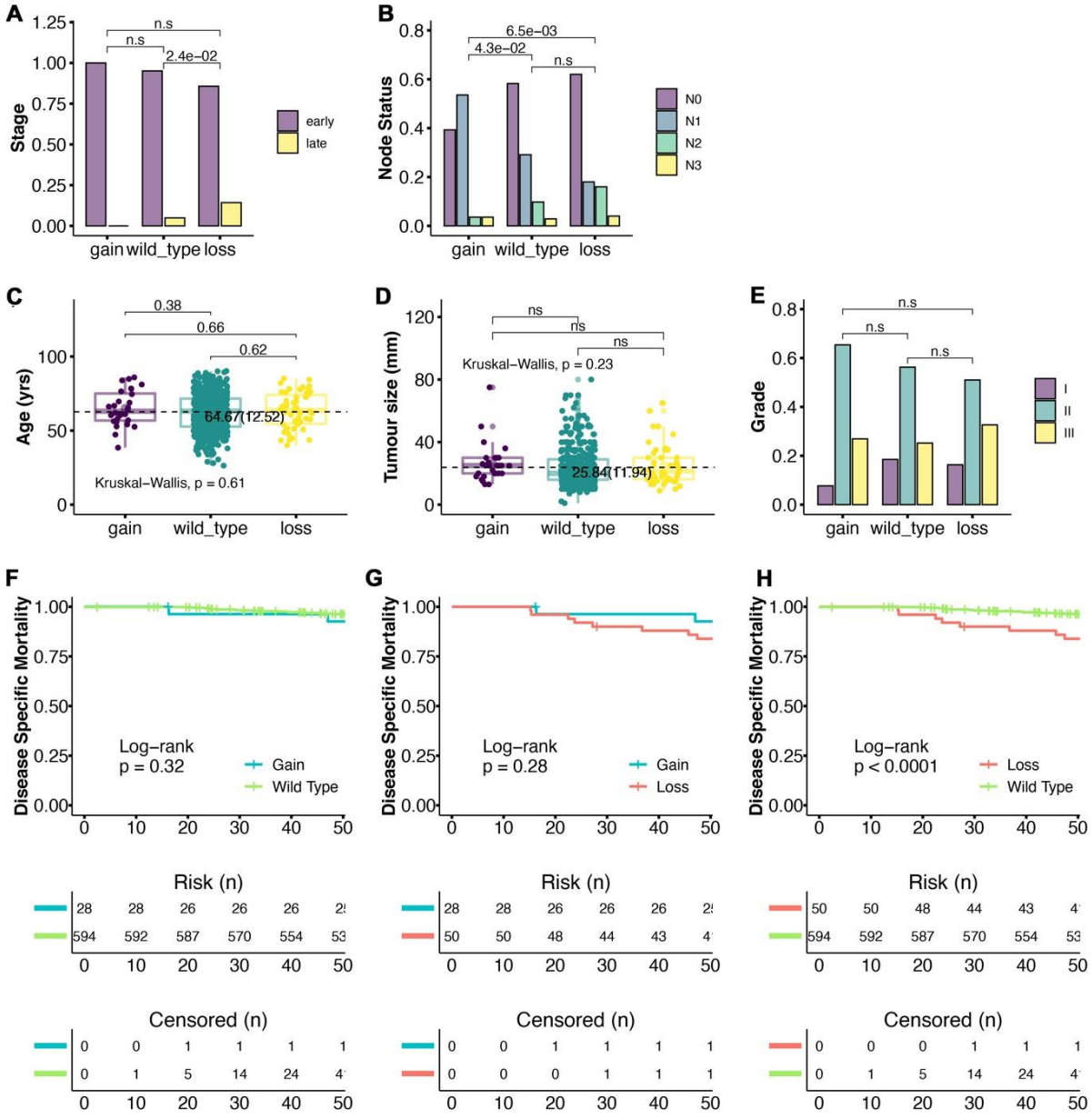

Figure 1: Clinical association of PTPN11/SHP2 copy number changes in Luminal A Subtype of breast cancer. Correlation between the Copy number of PTPN11 and certain clinical parameters were analyzed using the data available in the METABRIC database on Luminal A subtype of breast cancer. (A-E) Statistically significant correlation was observed for late-stage cancer (A) and nodal positivity (B), but not to the age of patients at diagnosis (C), tumor size (D) or the grade (E). In case of nodal positivity, protective role of high copy number

of PTPN11 was obvious when compared to the wildtype or the loss in the copy number. (F-H) Correlations between Copy number differences between gain vs wt (F), gain vs low (G) and low vs wt (H) for the disease-free survival at 4 years of follow up. Loss of copy number is significantly associated with poor disease-free survival (H).

Figure 2

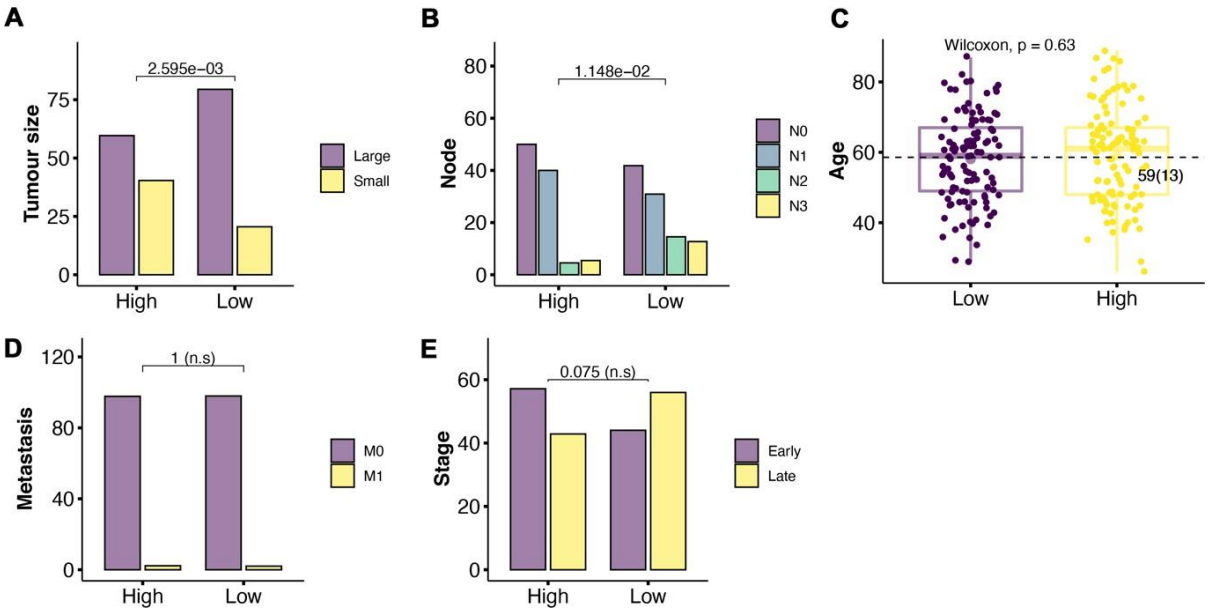

Figure 2: Clinical Correlation between Phospho-PTPN11/SHP2 protein expression and clinical phenotypes of Luminal A patients at diagnosis. We used proteomic data from the TCGA database to examine the correlations between the functionally active phosphor-PTPN11/SHP2 to the clinical manifestations of Luminal A patients of breast cancer. Significant association is observed between Low levels of Phospho- PTPN11/SHP2 and larger tumor size (A) and LN2 and LN3 positivity (B). No such correlations were observed for age (C), metastasis (D) or the stage of the cancer (E).

Figure 3

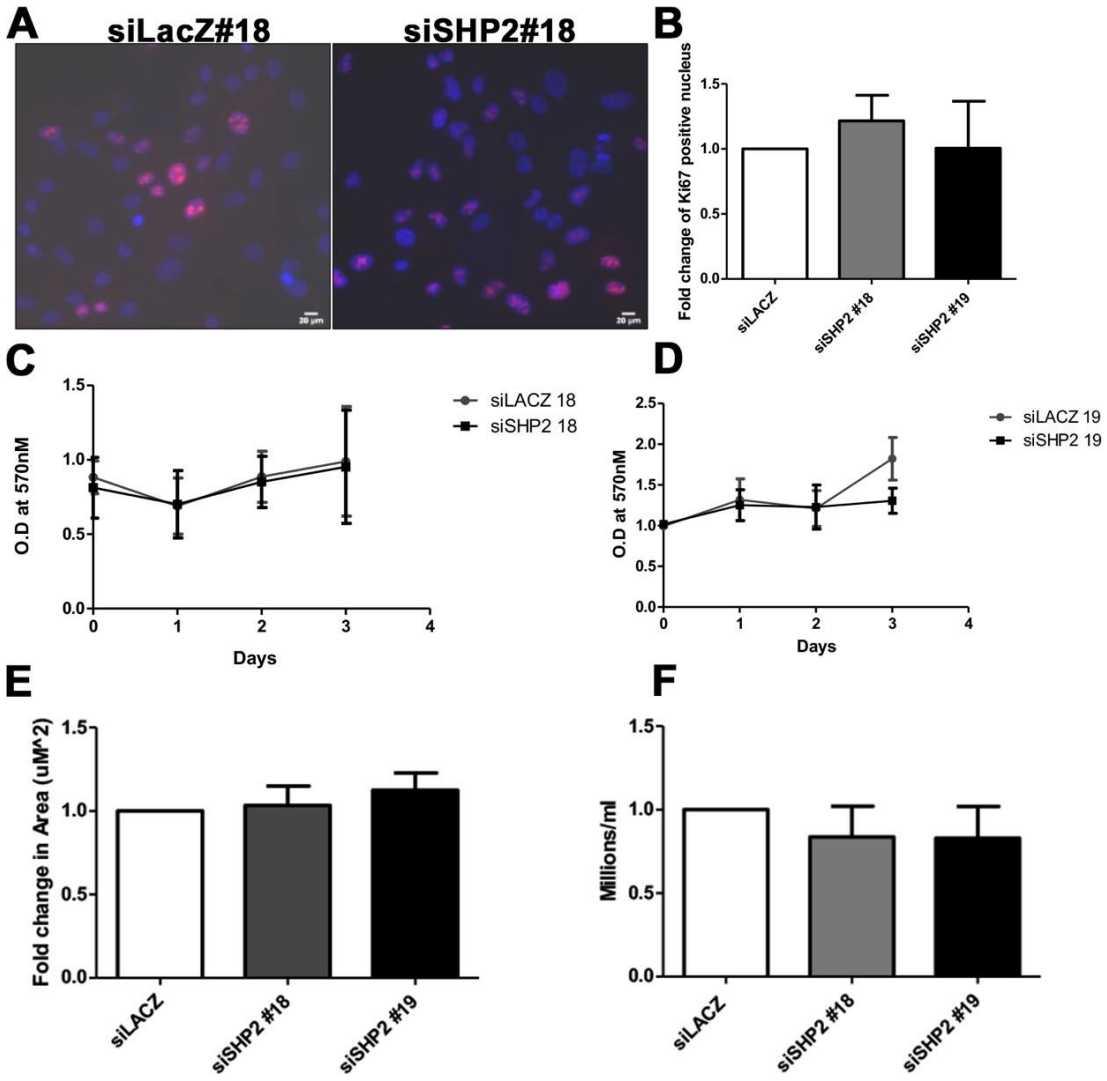

Figure 3: Effect of the knockdown of PTPN11/SHP2 on cell proliferation, survival, size and number. (A-B) Cell proliferation was measured in control and experimental MCF10A cells stained with the proliferation marker Ki67. Representative images of Ki67-stained cells are shown in A, both control (siLacZ#18) and the experimental (siSHP2#18). (B) shows the quantitation of change in the number of Ki67-expressing cells the control and experimental cells. We did not observe any change in Ki67 value. Images and the quantitation are shown for si18, while the observation is reconfirmed with si19 too. (C-D) Cell survival was measured using O.D values normalized to day 0 and plotted for 4 days of growth. For each biological replicate, we had 4 technical replicates. We did not observe any change in cell survival for any

of the 4 days of our assays using both siRNA 18 and 19. (E) Cell size was measured by immunostaining of □-Catenin, an adheren junction protein to mark the borders of the cell. The cell size was quantitated by measuring the area of cells (area in □m^2). At least 100 cells across 5 fields and 3 biological replicates were recorded for quantitation. There was no change observed in cell size. (F) Quantitation of cell number by Hemocytometer count. Here too we did not observe any change due to the knockdown of PTPN11/SHP2.

Figure 4

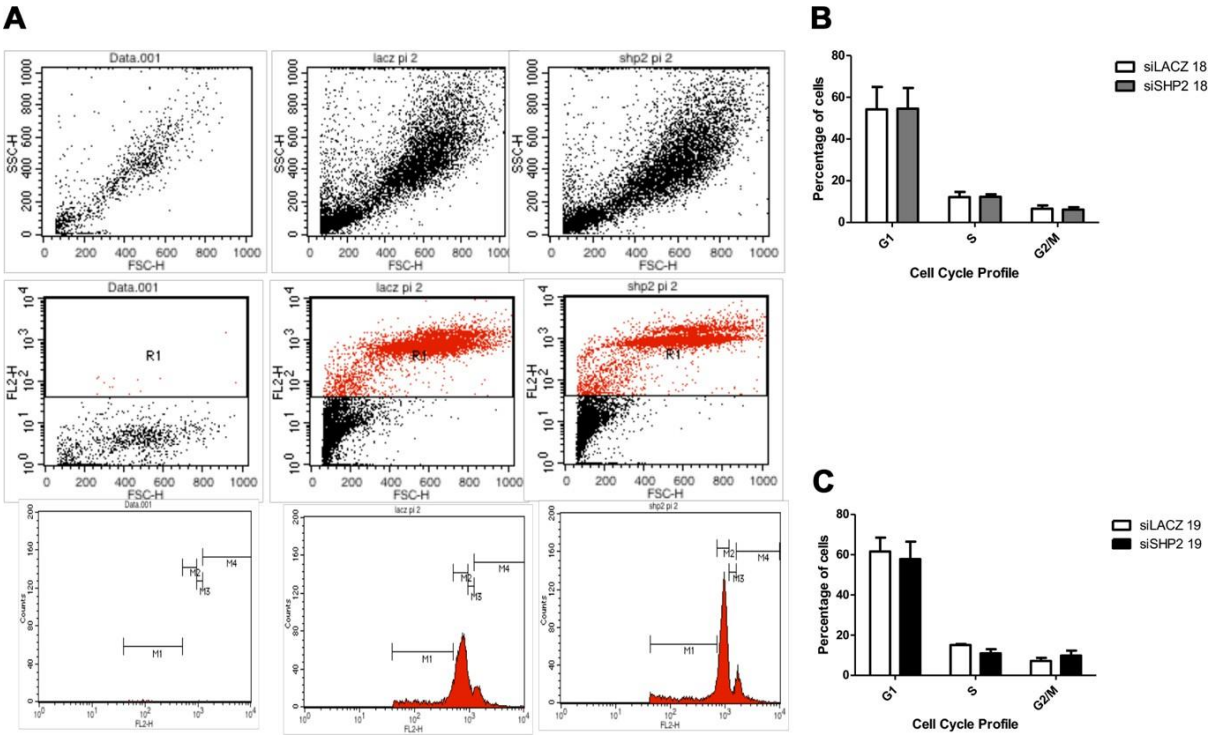

Figure 4: Effect of the knockdown of PTPN11/SHP2 on cell cycle profile of MCF10A cells.

(A) FACS analysis showing cell cycle pattern of control and PTPN11/SHP2-depleted MCF10A cells, with scatter plots showing selected population for analysis and histogram showing cell cycle phases denoted with gate, M. Flow analysis is shown only for si18, however, data was reconfirmed with si19. M1 which is the sub G1 population was not quantitated in our analysis. For the cell cycle pattern, 10,000 cells were recorded by Flow cytometry after PI staining. (B) and (C) show quantitation of cell count in G1 (M2), S (M3), and G2/M (M4)

phases of the cell cycle (N=5). No significant changes are observed for any of the cell cycle phases in PTPN11/SHP2-depleted cells.

Figure 5

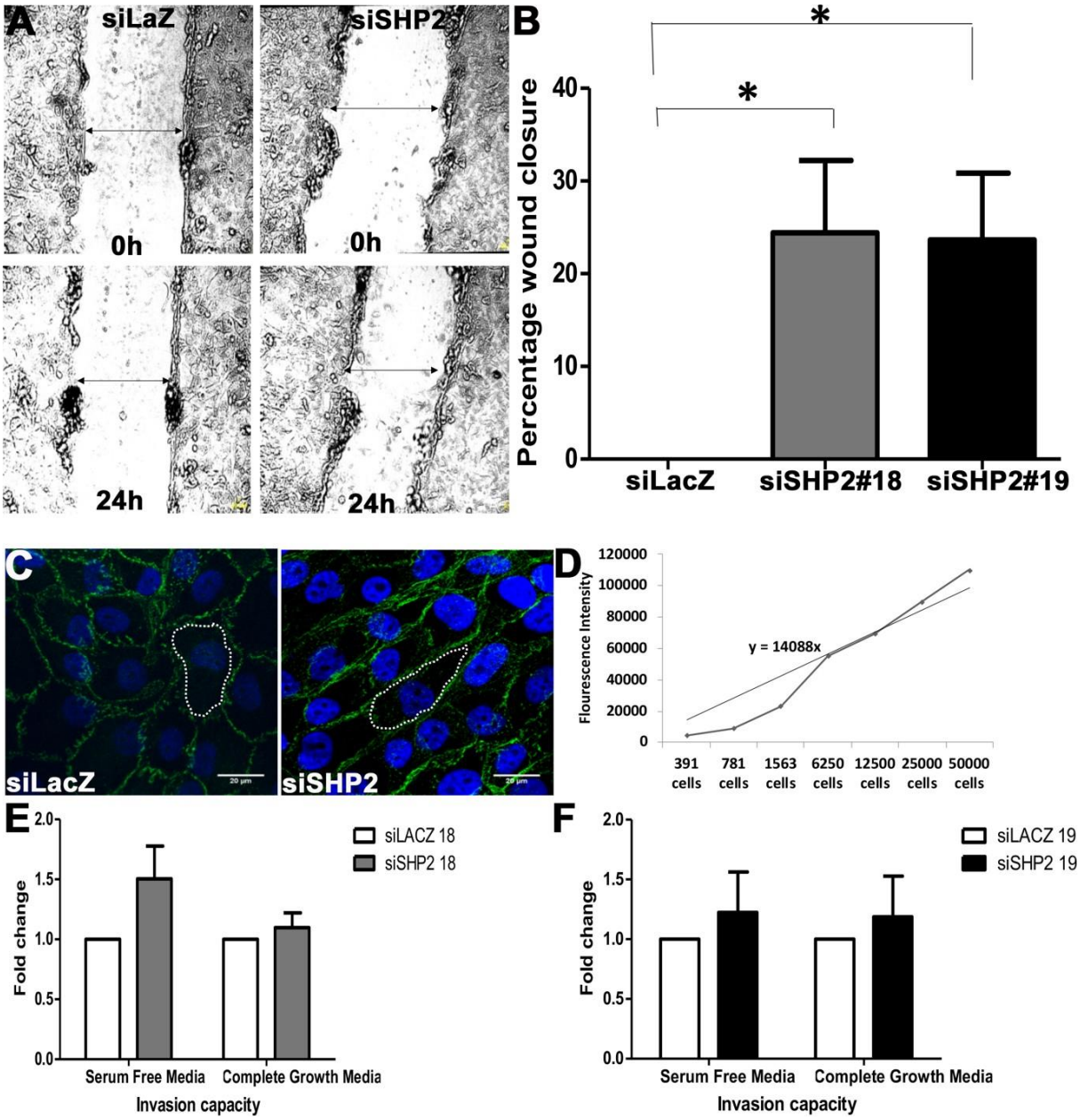

Figure 5: Knockdown of PTPN11/SHP2 increases the rate of cell migration and invasion, which is associated with changed cell morphology. (A) Scratch assay showing the initial wound at 0 hour and gap closure post 24 hours of scratch (shown by arrow) of normal MCF10A cells (siLacZ control) and PTPN11/SHP2-depleted cells (siSHP2). (B) Quantitation of the

percentage wound closure normalized to control. Both siSHP2#18 and 19 show significantly faster would healing. (C) MCF10A cells stained with □-catenin (Green) and DAPI (Blue). White inlet used to show the change in morphology from cobblestone (in siLacZ control cells) to mesenchymal shape (in PTPN11/SHP2-depleted cells). (D) Standard curve showing fluorescence intensity versus cell number for the calibration of the transwell invasion assay Biovison kit. (E, F) The knockdown of PTPN11/SHP2 do not cause any significant changes in the invasion capacity through the matrigel coated transwell.

Figure 6

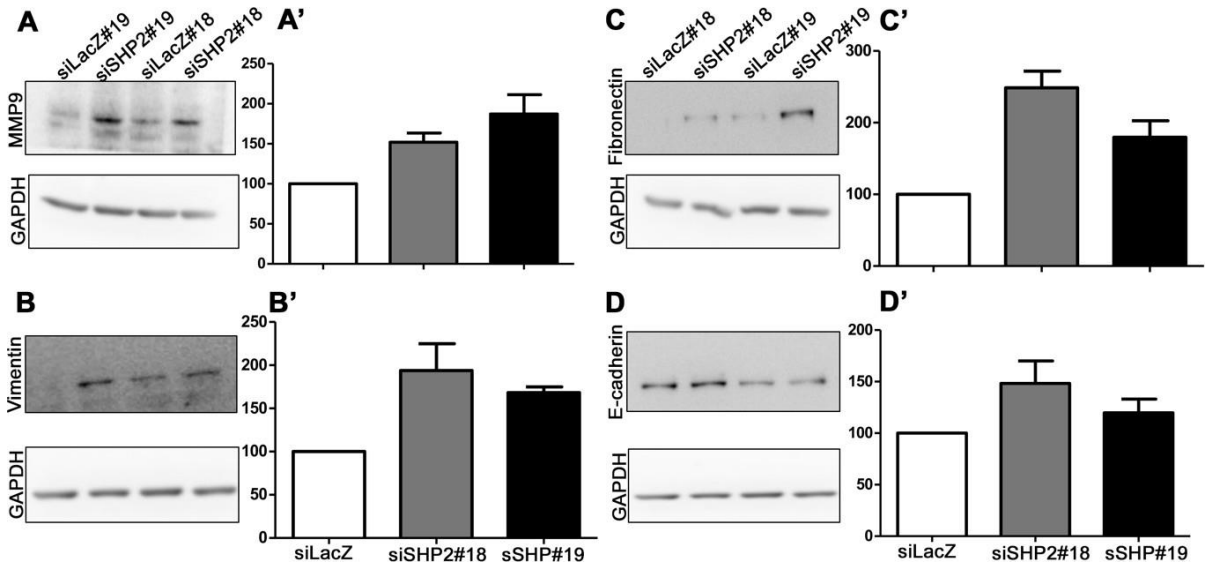

Figure 6: Knockdown of PTPN11/SHP2 enhances the expression of markers of epithelial to mesenchymal transition. Western blot analysis to examine the effect of the knockdown of PTPN11/SHP2 on the expression of MMP9, Vimentin, Fibronectin, and E-cadherin in MCF10A cells. GAPDH was used as loading control. Quantitation of representative blots shows a near significant increase in expression of MMP9 (A), Vimentin (B), and fibronectin (C), but no change in epithelial marker like E-cadherin (D). There were no detectable N- Cadherin levels in both control and PTPN11/SHP2-depleted cells (data not shown).

Figure 7

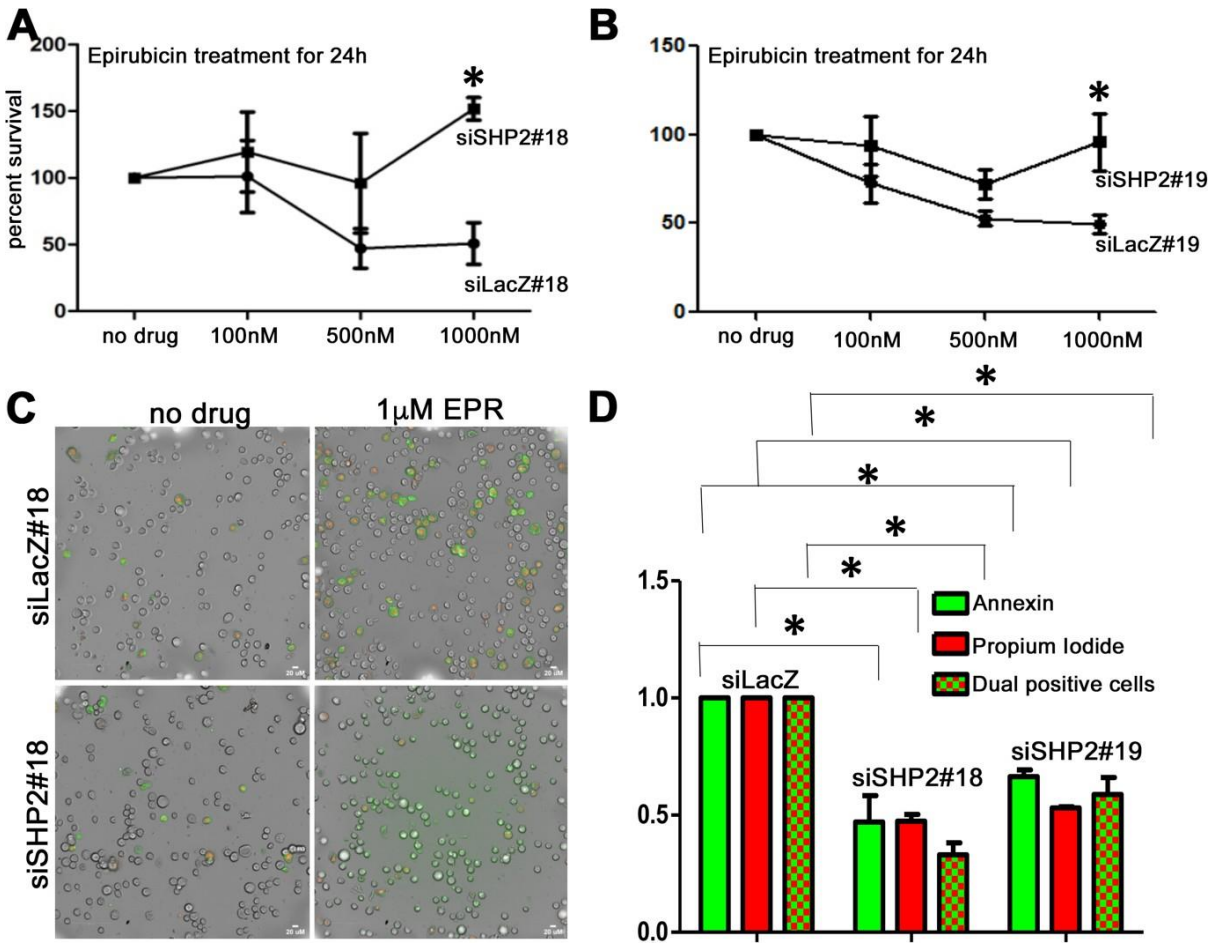

Figure 7: Knockdown of PTPN11/SHP2 reduces sensitivity to chemotherapeutic drugs in MCF10A cells. (A,B) MTT assay showing the dose-response curve upon epirubicin treatment in normal and PTPN11/SHP2-depleted MCF10A cells. We observed an increased survival advantage to PTPN11/SHP2-depleted cells at 1mM concentration of epirubicin. (C, D) Immunofluorescence images showing apoptosis in normal and PTPN11/SHP2-depleted MCF10A cells untreated and treated with 1mM concentration of epirubicin (C) and graphical representation of their quantitative differences (D). PTPN11/SHP2-depleted MCF10A cells show 2-fold decrease in Annexin positive, Annexin+ PI double-positive, and dead PI-positive cells.